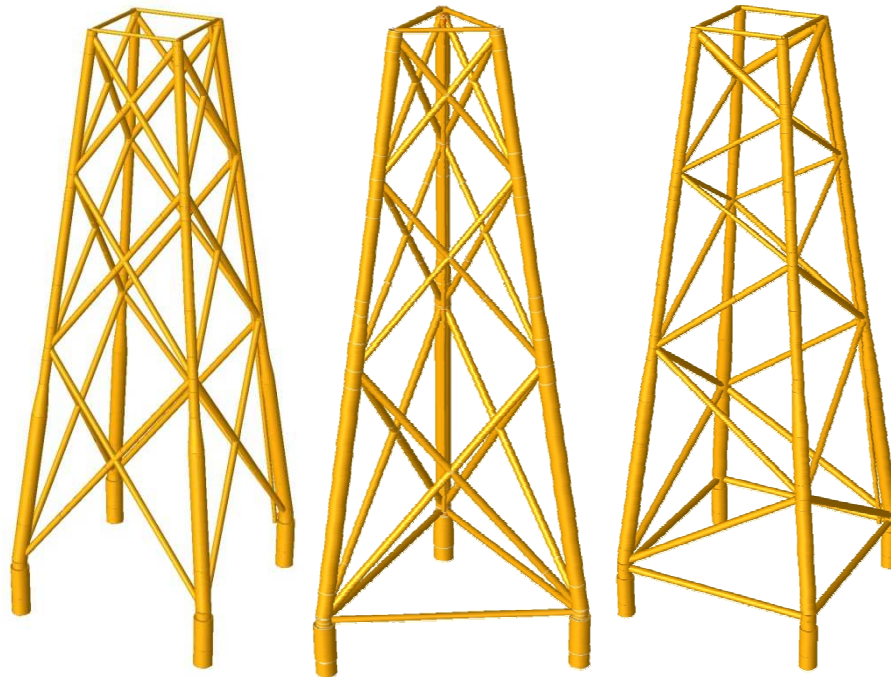

Optimising the Design of a Steel Substructure for Offshore Wind Turbines in Deeper Waters

Frank van Gerven

October 2011



MSc thesis
Delft University of Technology
Faculty of Civil Engineering and Geosciences

Optimising the Design of a Steel Substructure for Offshore Wind Turbines in Deeper Waters

Frank van Gerven
October 14th 2011

Committee:

Prof. Ir. F.S.K Bijlaard
Prof. Ir. C.A. Willemse
Ir. R. Abspoel
Ir. J.N.P.T. Beckers
Ir. S.J.H. Beukers

TU Delft
TU Delft
TU Delft
Hollandia
Iv-Oil & Gas

Abstract

In the need for more green energy a prominent role is reserved for wind energy. Offshore wind energy in deeper waters capitalizes on more efficient wind properties and increased public acceptance compared to onshore wind energy and wind farms close to shore. In the coming years the offshore wind market is expected to evolve rapidly, especially in the deeper water range of thirty to sixty meter. The business case as starting point for this study aims for substructures for these water depths. Based on national government ambitions of The Netherlands, Germany and Norway is accounted for fifty substructures per annum. Monopiles substructures as so far mostly applied are due to stiffness requirements only suitable for water depths until 30 meter. As first reference a jacket type substructure is designed. The goal of this thesis is to reduce the cost of this reference design in total material use and the assembling. Also the transportation and installation of the substructure is taken in consideration.

To reduce installation time is looked at the appliance of suction buckets. Suction buckets are more commonly used in the oil and gas industry and is attempted twice underneath a wind turbine. A brief calculation to determine the dimensions of the suction bucket resulted in large dimensions with a significant weight increase compared to foundation weight of the reference design. Together with several drawbacks during the attempts in practice and theoretical research this resolved that the suction bucket concept is not used in this study as foundation for offshore wind turbines. Instead foundation piles shall be used. Therefore three different piling methods are considered. The main piling method is adverse because the piles have to bridge a large water depth and brings along a complex connection to the substructure in combination with the transition piece. Other two considered methods are the driven piles foundation and installation in sections, where the latter method has the preference. First the foundation piles are installed by making use of a piling template and consequently the substructure is installed in the foundation piles by accurate positioning of the installation vessel. Pertaining to the more conventional driven piles foundation the need for mudmats and leg-mounted sleeves is eliminated, what especially regarding to serial fabrication saves decisive cost.

The reference design and therefore subject to improvement is a four-leg jacket with battered legs. First a step back is taken to reconsider the structural concept of the reference design. Several substructure concepts have passed the review and qualitative weighed against primary criteria in a Multi Criteria Analyse. Apart from the reference design, worth of further investigation were the three-leg battered jacket, the three and four-leg straight jackets and the tripod. Therefore a static in-place analysis was performed, together with a natural frequency check. The natural frequency check was executed to ensure that each design would coincide with the soft-stiff range, between the rotational frequency (1P) and the blade passing frequency (3P) of the turbine. The outcome of the total substructure weight and natural frequency with respect to frequency of wave loading determined the decision to further investigate the battered leg jackets.

For the next design phase a dynamical in-place analysis and a dynamical spectral fatigue damage analysis in the frequency domain is performed. The calculation method for the total fatigue damage due to turbine and wave loading was adjusted compared to the original reference design. A modified method is presented by making use of quadratic summation of equivalent stress ranges of turbine and wave loading. Only interaction between the turbine and wave fatigue is the incorporation of aerodynamic damping by the turbine on wave responses, thereby reducing the stress range.

In relation to the reference design several optimisations have been applied. It was shown that adding a horizontal brace just above mudline level would significantly reduce the bending stresses in the foundation pile, resulting in smaller dimensions of the foundation piles.

Additionally the fatigue damage in the butt welds has been reduced by application of double sided butt welds. The execution of double sided butt welds is justified because of the serial production is chosen to fabricate all tubular components by specialized tubular manufacturers.

Next is considered to adopt other bracing configuration. The usage of K-bracing reduces the total number of members and member intersections resulting in fewer welds. In case of the three-leg (battered) jacket the K-bracing results in large fatigue damage at the connection of the bracing with the leg and is therefore not implemented. Conversely does the four-leg (battered) jacket lend itself for the K-bracing because the internal forces run continuously over all four sides of the jacket.

By performing above mentioned analyses and optimisations finally four designs have been worked out; the reference design (without optimisations), an optimised four-leg jacket, four-leg jacket with k-braces and a three-leg jacket. This is followed by a cost estimation. Therefore is for the four concerned designs the fabrication procedure examined. The total assembling cost of each design is calculated by considering the handling time and the welding volume with corresponding welding time of each weld. Together with the material use the total cost is assessed, from which ensued that most inexpensive design is the four-leg jacket with K-braces followed by the three-leg jacket, the optimised four-leg jacket and finally the reference design.

Transportation of the jacket onshore is done by using Self Propelled Modular Transporters (SPMT's) and for upending a permanent portal crane is suggested. The jacket shall be transported offshore transported by a standard North Sea transport barge. The dimensions of this barge potentially enable the transportation of three four-leg jackets and four three-leg jackets. Depending on the wind farm location this may lead to reduction of one tug and transport barge case of the three-leg jacket.

Further consequence of the three-leg jacket is that a foundation pile less needs to be driven. Thereto is the installation time of the three-leg jacket reduced, resulting in less installation cost.

By combining fabrication, transport and installation cost it is possible to compute an overview for substructures cost in a complete wind farm. Therefore a wind farm of fifty wind turbines is assumed on a random location in the North Sea. The estimated total price of substructure corresponds with the expected twenty percent of the total investment cost in a wind farm. Final conclusion is that the fabrication cost are decisive compared to the installation and transport cost. The four-leg jacket with K-braces turns out to be the most inexpensive design, respectively followed by the three-leg jacket, the optimised four-leg jacket and the reference design. It is expected that the four-leg jacket with K-braces brings total cost reduction of approximately nine percent compared to the reference design.

Acknowledgements

This thesis marks the end of my study Civil Engineering at Delft University of technology. After following the Building Engineering master track, this study was certainly a challenge for me. During the search for a thesis subject Hollandia came on my path, proposing a study in the offshore wind field. After first consultation also Iv Oil&Gas was incorporated in the support of this thesis. The combination of Hollandia as steel constructor and Iv Oil&Gas as consultant and engineering company was interesting and instructive. I am very thankful for the offered guidance of both companies during the past months.

I would like to thank everybody who helped me during graduation in random order and hopefully without forgetting anyone. First I thank the graduation committee; Prof. Ir. F.S.K Bijlaard, Prof. Ir. C.A. Willemse, Ir. R. Abspoel, Ir. J.N.P.T. Beckers, Ir. S.J.H. Beukers for their input and comments during my research project. Drees Brunt and Gerard Bouwman for starting up and find my way at Hollandia. Special thanks to Stefan Beukers for the almost daily support at Iv Oil&Gas. Furthermore, my gratitude goes to my colleagues at Hollandia and Iv Oil&Gas for all the help and the pleasant and enjoyable atmosphere.

Finally, I would like to thank my family and friends, who have been supporting me not only during this thesis, but during my entire study at Delft University of Technology.

Frank van Gerven
Delft, October 2011

Table of Contents

Abstract	i
Acknowledgements	iii
Table of Contents	v
List of Symbols	vii
List of Abbreviations	ix
1. Introduction	1
1.1 Offshore wind energy	1
1.2 Substructures.....	3
1.3 Business case.....	5
1.4 Thesis outline.....	8
2. Design Basis	11
2.1 Basic dynamics.....	11
2.2 Turbine.....	13
2.3 Serial production.....	14
2.4 Site location	15
2.5 Water depth	15
2.6 Design loads	16
2.7 Transition piece	18
3. Suction Bucket	19
3.1 Principle	19
3.2 Dimensions	23
3.3 Evaluation	24
4. Substructure Concepts	25
4.1 Concept designs	25
4.2 Evaluation	28
5. Foundation Connection	31
5.1 Main piling.....	31
5.2 Driving pile foundation	32
5.3 Installation in sections	33
5.4 Evaluation	36
6. Structural Design	39
6.1 Static in-place analysis & natural frequency check	39
6.2 Preliminary designs	41
6.3 Dynamic in-place & dynamic fatigue analysis	47
6.4 Modifications.....	55
6.5 Definitive designs.....	62
6.6 Evaluation	66

7.	Fabrication	67
7.1	Procedure	67
7.2	Cost estimation	69
8.	Transport	73
8.1	Onshore transport.....	73
8.2	Offshore transport.....	77
9.	Installation	81
9.1	Installation procedure	81
9.2	Equipment.....	82
9.3	Substructure Installation	84
10.	Substructures in Offshore Wind Park	87
10.1	Cost overview	87
10.2	Parameter Susceptibility.....	89
11.	Conclusion and Recommendations	91
11.1	Conclusions	91
11.2	Recommendations.....	94
	References	97
	List of Figures	99
	List of Tables	103
Appendix A	Design Parameters	105
Appendix B	Suction Buckets	115
Appendix C	Reference Projects	119
Appendix D	Concept Evaluation	123
Appendix E	Elevation Determination	129
Appendix F	Mode Shapes	131
Appendix G	Structural Analyses Outcome	135
Appendix H	Grout Connection Check	153
Appendix I	Drawing Definitive Designs	155
Appendix J	Fabrication Cost Estimation	157
Appendix K	Installation equipment	159

List of Symbols

$1P$	Rotation frequency of turbine	[Hz]
$3P$	Blade passing frequency of three-bladed turbine	[Hz]
c	Damping coefficient	[Ns/m]
C_m	Added-mass coefficient	[-]
C_d	Hydrodynamic drag coefficient	[-]
d	Water depth	[m]
D_a	Fatigue damage due to aerodynamic loads	[-]
$D_{ah;eq}$	Equivalent fatigue damage due to aerodynamic and hydrodynamic loads	[-]
D_h	Fatigue damage due to hydrodynamic loads	[-]
f_i	Frequency of i -mode	[Hz]
$\Delta\sigma_{a;eq}$	Equivalent stress range due to aerodynamic load	[Mpa]
$\Delta\sigma_{ah;eq}$	Equivalent stress range due to aerodynamic and hydrodynamic loads	[Mpa]
$\Delta\sigma_{h;eq}$	Equivalent stress range due to hydrodynamic loads	[Mpa]

List of Abbreviations

DAF	Dynamic Amplification Factor
FEM	Finite Element Method
HAT	High Astronomical Tide
LAT	Low Astronomical Tide
MCA	Multi Criteria Analysis
MSL	Mean Sea Level
MTO	Material Take Off
OWEC(S)	Offshore Wind Energy Conversion (Systems)
OWT	Offshore Wind Turbine
RNA	Rotor Nacelle Assembly
RPM	Revolutions Per Minute
SCF	Stress Concentration Factor
SLS	Serviceability Limit State
SPMT	Self Propelled Modular Transporter
UC	Unity Check
ULS	Ultimate Limit State
WROV	Water Remotely Operated Vehicle

1. Introduction

Sustainability has become one of the driving forces in government energy policies. In energy supply and more explicitly electrical power supply, demand is growing for green energy. Wind energy is one of the pillars in the green energy philosophy. Of its origin wind power is generated onshore, but last decades offshore wind energy is upcoming.

This thesis holds a design optimisation of a steel substructure for offshore wind turbines in deeper waters. A brief introduction of offshore wind energy is given in section 1.1. Typical components like the substructure are introduced in section 1.1.1 and 1.2. Starting point for this research is the business case in section 1.3 which contains an earlier designed jacket that can serve for a 6MW turbine in a water depth of 60 meter. Further context of this thesis is given in section 1.4.

1.1 Offshore wind energy

The offshore wind energy industry is turning out ever larger numbers of offshore wind turbines every year. Although significant progress has been made in making offshore wind energy more cost-effective, further cost reductions must be achieved to compete on equal terms with other sources of energy.

The application of wind power onshore is restricted due to limited site availability and limited public acceptance. The exploitation of offshore wind resource can become crucial in providing for future green energy needs. Offshore sites are sufficiently available and the sites possess better wind properties making them more efficient for power generation. Offshore wind farm developers know that the performance of wind farms improves greatly in deeper waters, where winds are stronger and steadier. Thereby are wind farms close to shore accused of destruction of the skyline by onshore inhabitants.

Offshore wind technology and practice has come a long way in a short time. About 750 offshore wind farms are constructed, developed or build at this moment (1). The offshore wind market is relative new, but is a rapidly developing business and is continuous evolving. Because of the world wide environmental need for more durable generated energy, the coming year's significant amount of money is invested in the offshore wind market.

An offshore wind park consists of multiple wind turbines, a transformer station and a subsea infrastructure for in-filed transportation and export of produced power.

A wind turbine consists of the following main components: (Section 1.1.1)

- foundation;
- substructure;
- transition piece (optional);
- tower;
- turbine and rotor blades.

1.1.1 Terminology

An overview of the terminology chosen in this thesis is shown in figure 1.1.

Throughout this thesis support structure is used to indicate the entire structure below the Rotor Nacelle Assembly (RNA). The support structure consists of a tower and a foundation structure. The most arguable definition is the boundary between these two and this had lead to miscommunication on various occasions. Contactors prefer to divide the two at a structural boundary, such as the flange at the access platform several meters above sea level, calling the entire subsea structure the foundation. In the more abstract context of a concept study this division is impracticable, as concepts for the submerged structure and the structure in or on the seabed can often be selected separately. For example, a tripod can be combined with both piles and suction buckets.

Therefore will the term foundation be reserved to indicate that element of the structure that is in direct contact with the seabed and for which geotechnical considerations are the design driver. The substructure is the segment underneath the tower, for the most submerged, but also partly above water.

Depending on the type, the substructure is connected to the tower by a transition piece element. The transition piece is responsible for transferring all tower loads to the substructure.

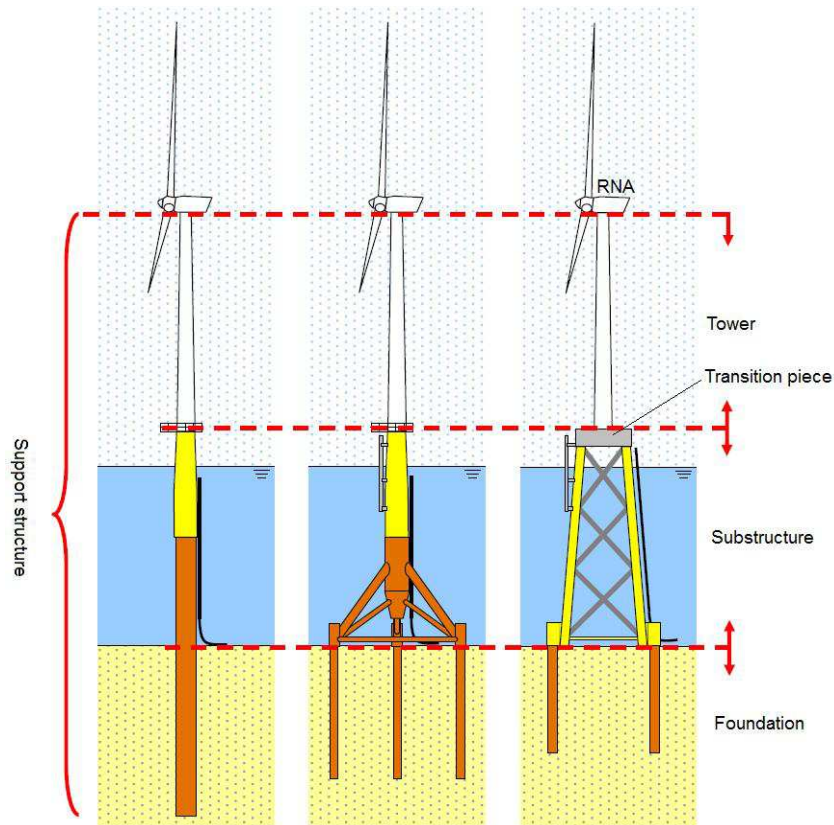


Figure 1.1: Terminology

1.2 Substructures

In search of economic solutions for deeper water already several substructure concepts are known and analysed. These concepts can be divided into five main categories: (Figure 1.2)

- monopile substructure;
- tripod substructure;
- jacket substructure;
- gravity substructure;
- floating substructure.

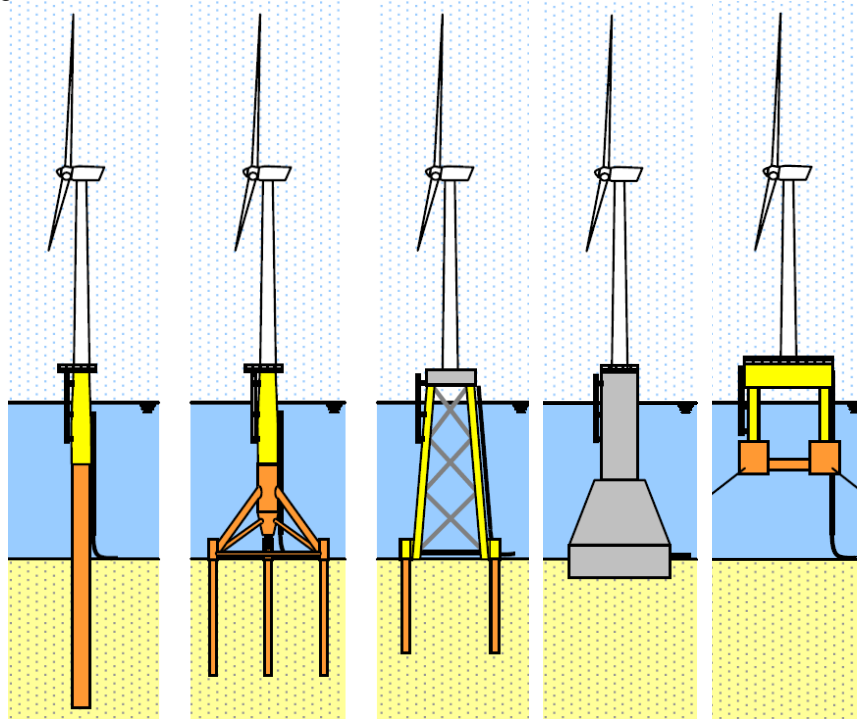


Figure 1.2: From left to right: Monopile, Tripod, Jacket, Gravity Base, Floating substructure (2)

Monopile

The monopile foundation is more or less an extension of the onshore turbine tower below the sea surface and into the seabed. The vertical loads can easily be transferred to the soil through wall friction and tip resistance. The lateral loads, in comparison much larger, are conveyed to the foundation through bending. The loads are subsequently transferred laterally to the soil. To provide enough stiffness the diameter of the monopile foundation has to be large enough. This attracts relative high hydrodynamics loads. For deeper waters, the stiffness and natural frequency requirements will result in such large diameters that it will be impossible to fabricate such a structure, due to limitations on the size of the steel plates that can be produced by steel mills. Difficulties due to limited sizes of pile driving equipment may also be expected.

Tripod

The lower portion of a tripod foundation consists of a framework of relatively slender members, connected to the main tubular by means of a joint section. From the main joint downwards the transfer of loads relies mainly on axial loading of the members. The tripod has a larger base, which gives it a larger resistance against overturning. The piles are also mainly loaded axially. This allows the tripod foundation to be shallower and lighter than the monopile foundation. The main advantage is that the tripod has a larger base, which gives it a larger resistance against overturning. As the base is made up of relatively slender beams, it is transparent, allowing water mass to pass through the structure relatively unobstructed. However, this is not the case for the structure from the main joint upwards. Furthermore, the main joint is a complex element that is susceptible to fatigue and requires much effort in designing and engineering.

Jacket

A jacket structure is made up of three or more legs connected by slender braces, making it a highly transparent structure. Loads are transferred through the members mainly in axial direction. The term 'jacket' has its origin in the oil and gas industry and is used to indicate a spaceframe structure which has the piles driven through the legs. The configuration as shown in figure 1.2 which has the piles driven through pile sleeves at the base of the structure would be termed a 'tower'. However, the term 'jacket' will be maintained to avoid confusion with the turbine tower. The large base offers large resistance to overturning. The space frame structure allows for light and efficient construction. However, each of the joints has to be specially fabricated, requiring many man-hours of welding.

Gravity Base substructure

A Gravity Base Structure (GBS) relies on a low centre of gravity combined with a large base to resist overturning. As the GBS requires a large mass it generally made of concrete as it is much cheaper than steel. The GBS is placed directly on the seabed. It can be equipped with vertical walls that protrude from below the actual base, called skirts, which penetrate into the soil below the base. These skirts increase resistance to base shear and help to avoid scour below the base. The GBS can be extended to the platform level, thereby reducing the number of offshore installation activities, as no separate transition piece needs to be installed.

Floating substructure

A floating structure relies on buoyancy to keep the turbine above the water. To obtain its bearing capacity requires a large submerged volume to generate sufficient buoyancy and a low centre of gravity to maintain stability. The offshore wind turbine can be assembled on the barge floater at an onshore location. The assembly can be towed out to the required location. This concept may be suitable for large scale production as it can easily be adapted to different water depths. The barge type floater's large cross section at the water line makes it sensitive to hydrodynamic loading.

The substructure concepts have different behaviour for various water depths (2).

Monopile concept scores progressively worse for increasing water depth. This is caused by the fact that the monopile diameter has to be increased significantly for deeper waters, because of stiffness and natural frequency requirements. It is found that until 30 meter water depth, the monopile has dimension which are feasible.

Because of the transparent structure and his ability to transfer the forces mainly in axial way, the jacket is perceived to be suitable for various water depths. Disadvantage is however the large number of joints. Therefore in lower water depth it is not as cost-effective as the monopile.

The tripod is seen as a good solution for the 30-60 meter water depth spectrum, because it can be seen as an intermediate solution between the monopile and the jacket. Less number of joints than the jacket type and loads are more transferred axially than the monopile.

The gravity base substructure has the major disadvantage of a large mass and the corresponding complex installation procedure. Creating a large weight is the most cost effective way created by concrete.

Floating structures are expected to perform the best in deeper waters, because it does not depend on water depth and soil conditions. A large submerged volume has to be created, that is in deeper waters beneficial compared to bottom mounted substructures.

1.3 Business case

Preceding of this thesis an internal company research has been done to manufacture steel substructures for offshore wind turbines. It follows that in the near future significant amount of money will be invested in offshore wind turbines. As a part of the business case (Section 1.3.1), a reference design was made for a jacket foundation that is suitable for a water depth of 60 meter (Section 1.3.2).

1.3.1 Offshore wind business case (3)

The wind energy market offers potential business opportunities. This statement is based on the assumption that the market for offshore wind parks follows the ambition of national governments in Germany, the United Kingdom and The Netherlands and that this ambition remains in place for the next 10 to 15 years.

Research (2) indicates that in water depth up to 30 m a monopile substructure and foundation is most effective. In water depth exceeding 60 m a floating substructure is most effective. A jacket and tripod type structure, have the best technical properties for the in between range from 30 m to 60 m. Rotor blades, turbine and tower are components produced by specialist suppliers and are not included in the business case. The jacket/tripod and transition piece are steel structures and typical components that are identified as potential market.

Clients prefer the market to supply integrated services for the design, fabrication and installation of the substructure including the transition piece and the foundation piles. Therefore the scope of the business case and this thesis is the supply of engineering, fabrication and installation of open steel type substructures for water depths ranging between 30 and 60 meter.

Based on recent European study (4), some key figures of the total capital expenditure money in offshore wind energy are as follows.

• investment level per MW installed	3,800,000	euro
• market value per produced MWh	66	euro
government contribution per MWh	114	euro +
total unity cost price per MWh	180	euro

The following elements can be distinguished in terms of capital expenditure for the development of an offshore wind park: Prelims (preparation, permitting, insurance, etc.), project management and engineering, cables, turbines, transformer station and substructure. The chart below shows a typical contribution to the capital expenditure. The orange part is the potential market and takes about 20% of the total cost breakdown.

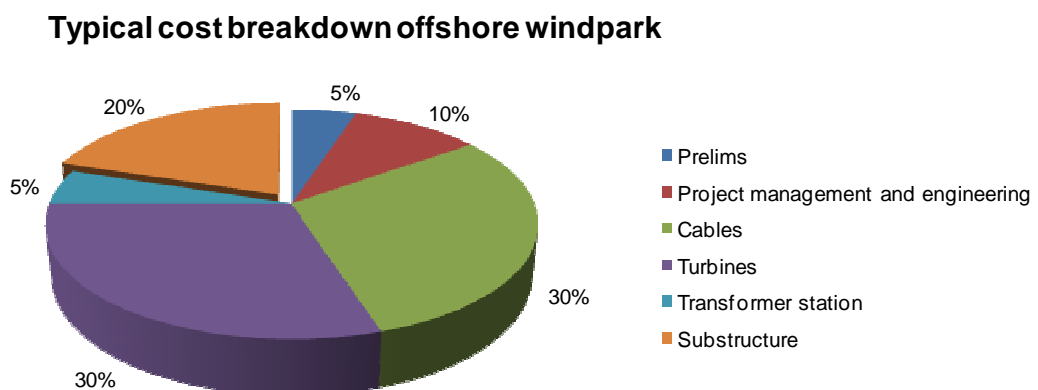


Figure 1.3: Typical cost breakdown offshore wind park(3)

Targets for offshore wind capacity of the governments of German, United Kingdom and the Netherlands in 2020 are respectively: 10,000, 15,000 and 6,000 MW. The cumulative ambition is to install 30,000 MW of capacity before the year 2020 which is approximately 7,500 turbines. Analysis of a market database (1) shows that about 50% of this number, i.e. 3,750 is in the target water depth range between 30 and 60 meter.

An assessment of the potential competitive position in the relevant market has been made by applying a percentage on the future projects. Conclusion is that the potential market share consists of 50 substructures per annum, indicated by the horizontal line in the figure 1.4. The market is broadly for 70% in Germany, 15% in The Netherlands and 15% in the United Kingdom (Figure 1.5).



Figure 1.4: Potential market(3)

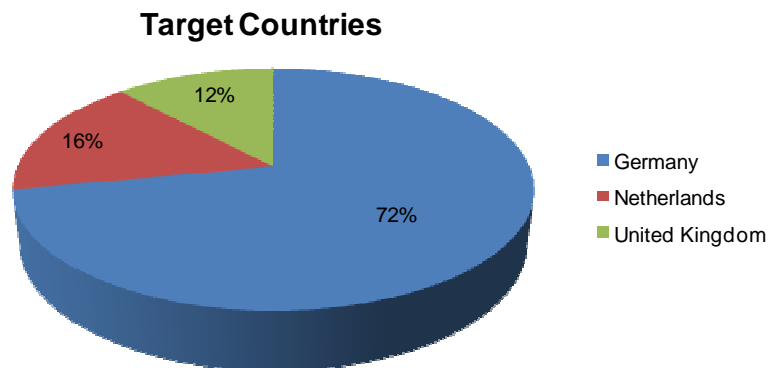


Figure 1.5: Target countries(3)

The large volume of the market and the potential size of each individual order, provides the opportunity to customise the production process and capitalise on repetition effects. In order to comply with the needed capacity of 50 substructure per annum, the existing plant capacity must be increased enormously. Therefore a new set-up customised production process in customised production facility has to make serial production possible.

In order to compete in the tender process, an improvement of the competitive position has to be achieved. This means that the reference substructure design is recommended for further optimisation, leading to cost reduction.

1.3.2 Reference design

The business case includes a design for a jacket as substructure for an offshore wind turbine. This design is seen as the reference design. The objectives stated in section 1.4.1 are based on this reference design.

The reference design is four-leg battered jacket, suitable for a water depth of 60 meter. On top of the tower is placed a 6MW RePower wind turbine, which is expected to be the preferred turbine for these water depths to obtain an efficient and economical design. The base on the seabed is square with sides of 28 meter. The legs converge to a square top with sides of 10 meters. This is the modelled size of the transition piece. On top of the transition piece the tower is modelled given by the turbine manufacturer.

The substructure contains four elevations with diagonal x-bracings for stability and external load transfer. The legs batter and all internal angles are the same and constant throughout the complete structure. The diameter of the diagonal bracings is kept constant in the whole structure, but the wall thickness varies. The diameter of the legs is constant in the upper three elevations and is increased by a conical segment in the bottom elevation.

Total weight of the substructure is 850 ton including 15% contingency.

The foundation is a 50 meter pile underneath each leg, connected by grouting. Dimension of the piles are a diameter of 96 inch with wall thickness of 2 inch.

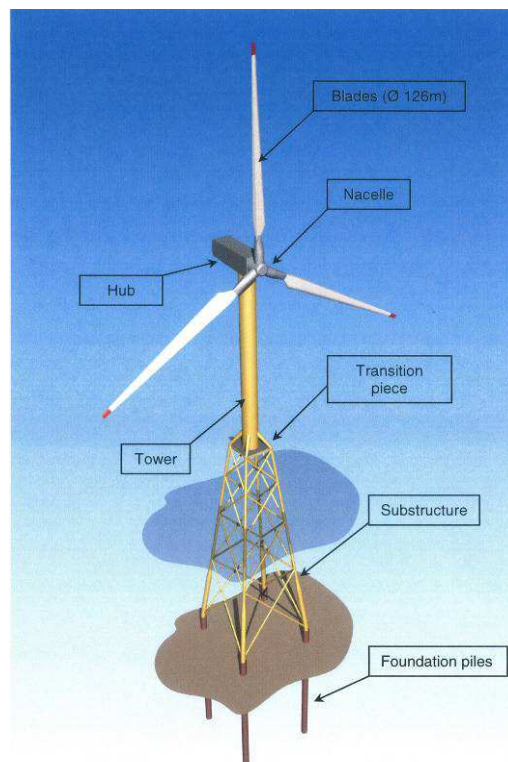


Figure 1.6: Reference design

1.4 Thesis outline

The reference design showed in section 1.3.2 was used as main cost parameter in the business case. The business case recommends further development activities aimed at cost reduction of the substructure. For a long term sustainable market position it is necessary that the design involves competitive manufacturing cost.

Furthermore it requires that the future design fits in the whole process of transport and installation procedure. Therefore it is necessary that apart from the structural design, also the transport and installation cycles are treated. The interaction between all aspects determines the most favourable substructure to gain a good market position.

Further development concerns the aspects of structural design, fabrication, transport and installation. Throughout the project an analysis is made of the design on the best mix of the following criteria:

- weight: total weight of the substructure;
- constructability: fabrication and assembling;
- installability: transport and installation process.

The pursuance for the most favourable design is stated the objectives of this thesis.

1.4.1 Objectives

The reference design is subject of the optimisation and is likewise the starting point. Approaches and thoughts of the reference design are stepping stones and at the same time point for further consideration. Objectives are as follows;

- The modified design must bring a total manufacturing cost reduction compared to the reference design. Goal is a cut back in the total cost combination of material use and substructure assembling.
- The installation of the substructure has to be independent of a particular piece of offshore equipment. If the substructure is relying on one particular vessel, the market price is then highly susceptible to the availability of this vessel. Therefore the installation must be accounted for a variety of available offshore equipment.

1.4.2 Boundary conditions

- The base (footprint) of the jacket needs to be minimized to reduce the required fabrication height and optimise the use and availability of installation equipment. Reduction of the fabrication height means also reduction of the required dimensions of the production facility. This means less required investments in a new production facility. In order to set a limit for the maximum size of footprint is hold on to the dimensions of the standard transportation. In view of minimizing cost, the use of a commonly available transport barge is set as starting point. Therefore a strict limit is set, determined by the dimension of a standard North Sea barge. In bottom line this means that the structure must be able to be transported by a standard transportation barge of 300 x 90 feet (91.4 x 27.4 meter).
- In case the transition piece element is part of the support structure, the designing of the transition piece is not included in the design process. In section 2.7 is gone further into the modelling of the transition piece.

1.4.3 Set-up of the report

In chapter 2 are the choices and parameters displayed that are the basis of this thesis.

The possibility of the application of suction buckets in case of the foundation of the substructure is pondered in chapter 3.

After determination of the foundation principle a number of substructure concepts are taken in consideration by a Multi Criteria Analyse. The outcome of chapter 5 is five substructure concepts which are continued in the design process.

Therefore is in chapter 5 first decided how the substructure is connected to the foundation. There to are the corresponding installation methods considered.

In chapter 6 are the concepts upgraded by a static in-place analysis to preliminary designs. These preliminary designs are weighed on primary criteria and thereby converged to two designs. Subsequently an approach is presented to analyse the fatigue damages due to wave and turbine loading. Together with dynamic in-place analysis four definitive designs are presented.

In chapter 7 respectively the corresponding fabrication procedure and cost estimation are treated.

Chapter 8 deals with the onshore and offshore transportation of the different designs of substructure.

This is followed in chapter 9 by the installation of the substructures and the difference in cost between the designs.

Chapter 7,8 and 9 are all put together in one picture in chapter 10 where the total cost of fabrication, transport and installation enumerated.

From here conclusions and recommendations can be found in chapter 11.

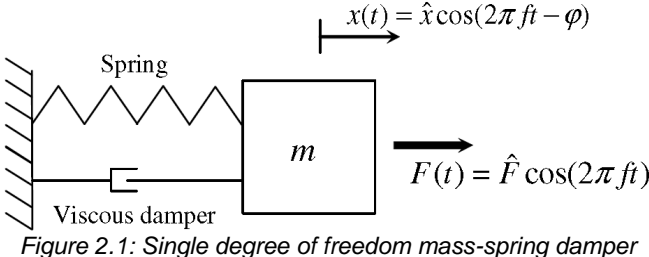
Not all supplementary data is included in the appendices of the report. A disc is attached to the report with all input and output of the SACS software.

2. Design Basis

This chapter indicates various choices and parameters that have been used in this thesis. As much as possible the same parameters as the reference design are used. Otherwise comparable parameters are used. See Appendix A for more detailed information.

2.1 Basic dynamics

Base of the structural dynamics can most conveniently be illustrated by considering a single degree of freedom mass-spring-damper as shown in figure 2.1(5). A complete offshore wind turbine system can be thought of as a number of coupled multi degree-of-freedom mass-spring-damper system.



When a harmonic excitation $F(t)$ is applied to the mass, the magnitude and phase of the resulting displacement x strongly depend on the frequency of excitation f . Three steady state responses can be distinguished as shown in figure 2.2:

- a) quasi-static;
- b) resonance;
- c) inertia dominated.

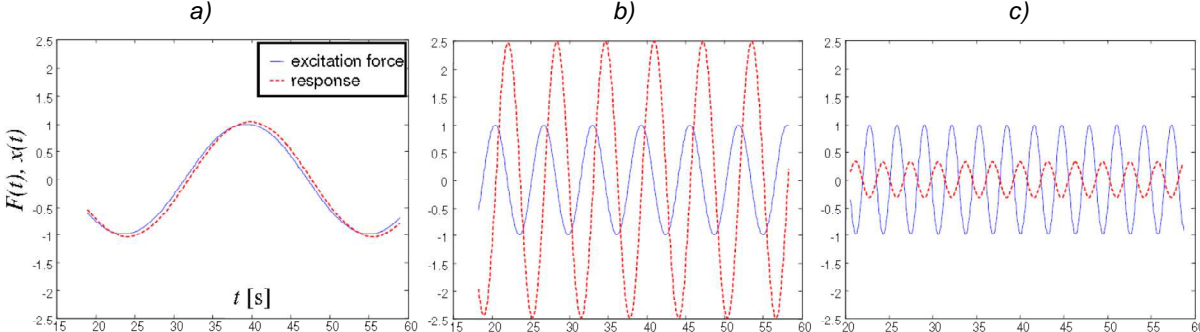


Figure 2.2: a)Quasi-static b)Resonant and c)Inertia dominated response

For frequencies of excitation well below the natural frequencies of the system, the response is quasi-static, as illustrated figure 2.2a. The displacement of the mass follows the time varying force almost instantaneously, as if it was excited by a static load. Figure 2.2b shows a typical response for

frequencies of excitation within a narrow region around the system's natural frequency. A response is produced that is a number of times larger than it would be statically. For frequencies of excitation well above the natural frequency, the mass cannot follow the excitation any more. Consequently the response level is low and almost in counter-phase, as illustrated in figure 2.2c. In this case the inertia of the system dominates the response.

Figure 2.2 illustrates the general fact that, in steady state, a sinusoidal input applied to linear system generates a sinusoidal output at the same frequency, which differs in magnitude and phase. The magnitude and phase modifying property of linear systems can be summarized by a plot of the Dynamic Amplification Factor (DAF) and the related phase lag. The DAF depicts the ratio between the dynamic response magnitude and the static response magnitude due to the same magnitude loading. Figure 2.3 shows the DAF and phase lag plot of the single degree of freedom system depicted in figure 2.1.

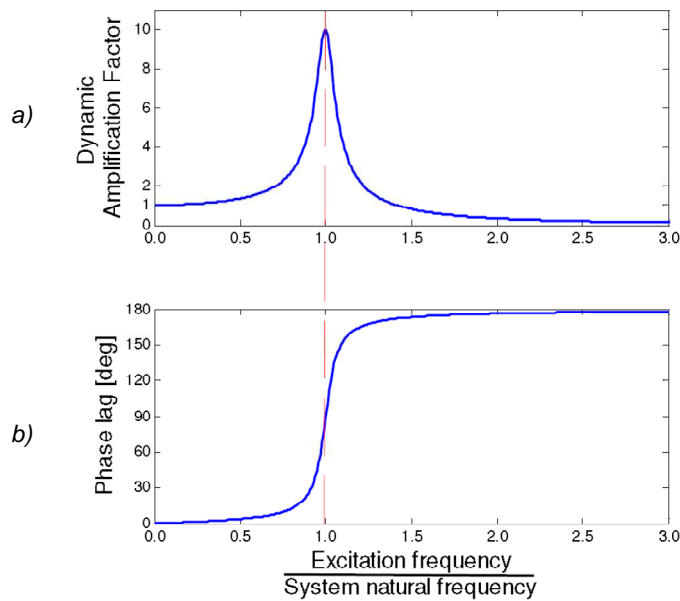


Figure 2.3: a) Dynamic Amplification Factor b) Phase Lag per normalised frequency

The peak in figure 2.3 corresponds to the system's natural frequency. The height of the peak is determined by damping. The frequency and magnitude of excitation are important occurrences that are most of interest for potential fatigue problems. The relation with the wind turbine is discussed in section 2.2.1.

2.2 Turbine

Particularly for the offshore market, wind turbines continue to be proposed and built to ever-greater size. At this moment wind farms with single rate of 6 MW turbines are being built. Also for this thesis a 6 MW turbine shall be used. Loads of the turbine are based on report of the turbine manufacturer and are summarized in appendix A.1 (6). The loads in the document are only an indication for the first iterative steps of the design process and can only be used for conceptual design. So are for example only the extreme turbine loads are given. Besides the turbine properties, the tower dimensions are also defined by the turbine manufacturer. These can be found in appendix A.1.

Table 2.1: Turbine characteristics

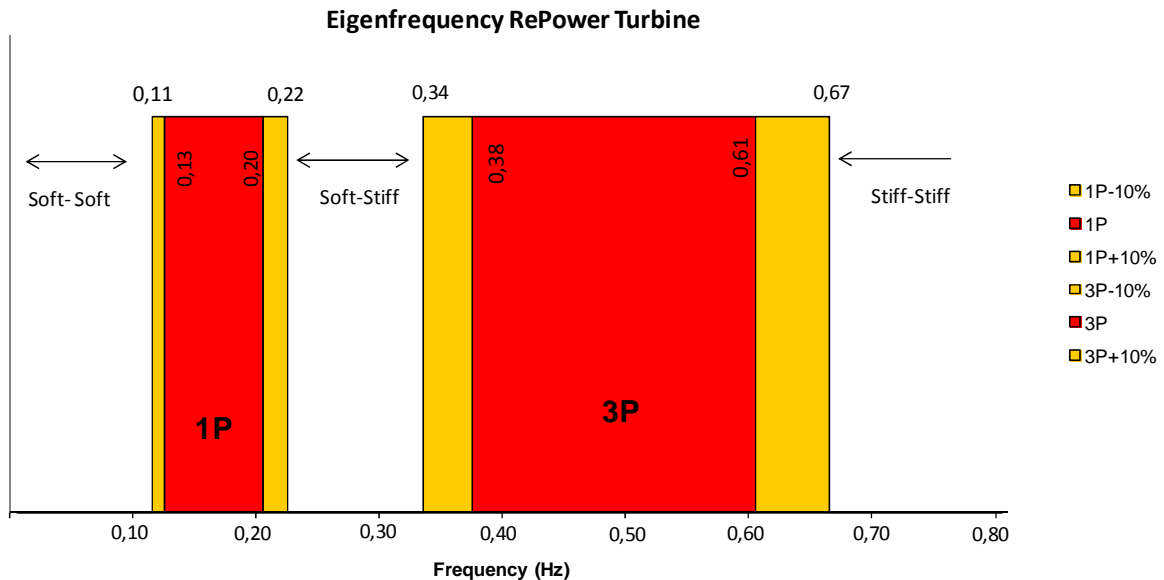
Type	Rated power [MW]	Rotor diameter [m]	Hub height [m]	rpm [1/min]
RePower 6M	6.15 MW	126 m	92	7,5–12,1

2.2.1 Dynamics

An operational wind turbine is subjected to harmonic excitation from the rotor. The rotor's rotational frequency is the first excitation frequency and is commonly referred to as 1P. The range of the rotor speed is given in table above.

The second excitation frequency to consider is the blade passing frequency, often called 3P (for a three-bladed wind turbine) at three times the 1P frequency. The turbine manufacturer advises an additional safety margin of 10% for the lower boundary and upper boundary. Outside additional safety margin the dynamic response due to turbine loading are neglected.

The two frequencies in case of the Repower turbine are plotted in figure 2.4. The horizontal axis represents the frequency and the vertical axis represents an arbitrary response without values. Though higher order excitations do occur, here only 1P and 3P are considered as these are the primary excitations.



To avoid resonance, the substructure should be designed such that its first natural frequency does not coincide with either 1P or 3P excitation. Generally speaking, the natural frequency of a mass-spring system depends on two system properties: mass and stiffness.

$$f_n \sim \sqrt{\frac{k}{m}} \quad (2.1)$$

k = structure stiffness
 m = mass

Looking to the turbine frequency intervals, this leaves three possible intervals. A very stiff structure, with its first natural frequency above 3P is called a stiff-stiff structure; if the first natural frequency falls between 1P and 3P, the structure is said to be soft-stiff while a very soft structure with its first natural frequency below 1P is called a soft-soft structure.

In the case of an offshore wind turbine excitation is due to both wind and waves. For fatigue consideration sea states with a high frequency of occurrence have the largest effect. These are generally relatively short waves. Because waves have various periods, they span wide range in the frequency band. Figure 2.5 shows the turbine loading frequencies with respect to the range of mean wave frequencies that are used for the fatigue analyses later on.

It is clear that when the offshore wind turbine system is designed with a natural frequency less than the rotational frequency (soft-soft) to avoid resonance, it will enter the frequency range where resonance due to wave excitation is important. And because a stiff-stiff design is cost-ineffective, the target of the substructure natural frequency is the upper bound of the soft-stiff region.

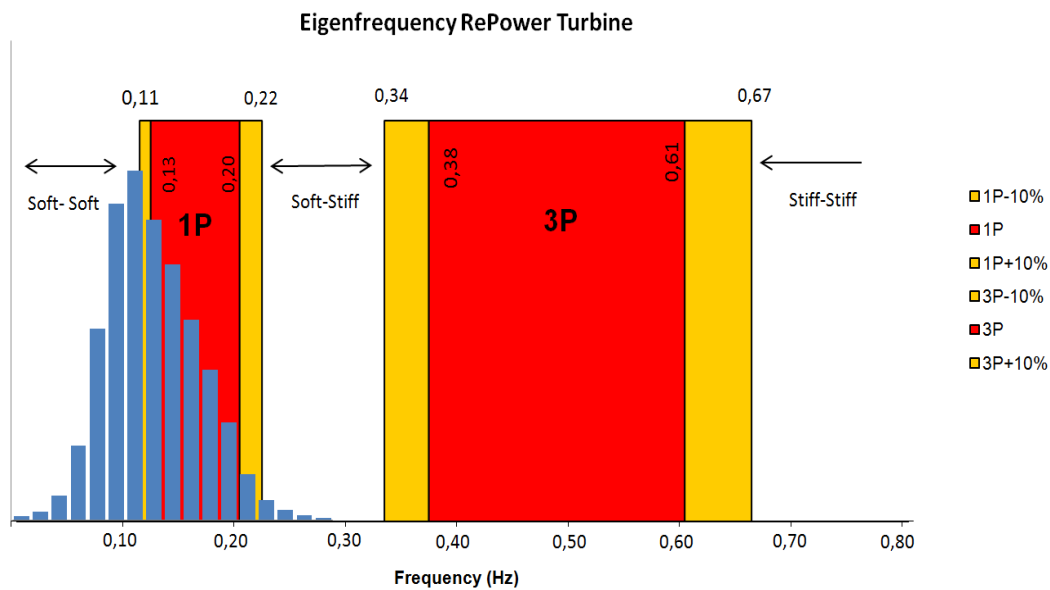


Figure 2.5: Occurrences of wave frequencies with 1P and 3P frequencies of Repower turbine

2.3 Serial production

It must be apprehended that the potential demand for the substructure is on a scale that requires a serial production of substructures. All aspects of the total production cycle should be arranged for large repetition. Investments that normally do not earn enough to repay themselves are now conceivable because they can be written off over a large content.

That's why is assumed that new production line and fabrication yard will be set up, that is devoted to the substructure manufacturing and storing tens of substructures. This is treated in the business case (section 1.3.1, (3)) and is not worked out in this report.

2.4 Site location

For this project no specific location is envisaged. In the business case is stated that the projected market is in Germany, United Kingdom, the Netherlands, Norway, Sweden, Denmark and Belgium. After selection, locations in Germany, United Kingdom and the Netherlands are seen as primary market and therefore a location in the North Sea is logical reference. The jacket substructure should be feasible for multiple locations in the North Sea.

The analyses performed are based on fictive location in the North Sea. Environmental conditions are derived from (7) and (8) and are expected to be representative for locations in the North Sea. However for site specific conditions the designs as presented in this report may have to be adjusted.

Geotechnical soil data is derived from two locations in the North Sea and extracted from existing reports (9) and (10). Geotechnical data is presented in compressed form in appendix A.2.



Figure 2.6: North Sea location

2.5 Water depth

The reference design is made for a water depth of 60 meter. This followed out of the preference to indicate the maximal needed space of the fabrication yard. However, it followed out of the business case that only 8% of the market has a water depth between 45 and 60 meter. This means that 92% of the market lies in the range of 30 to 45 meter (Figure 2.7). In order to adapt substructure water depth to the need of the market is chosen to alter the design water depth to 45 meter.

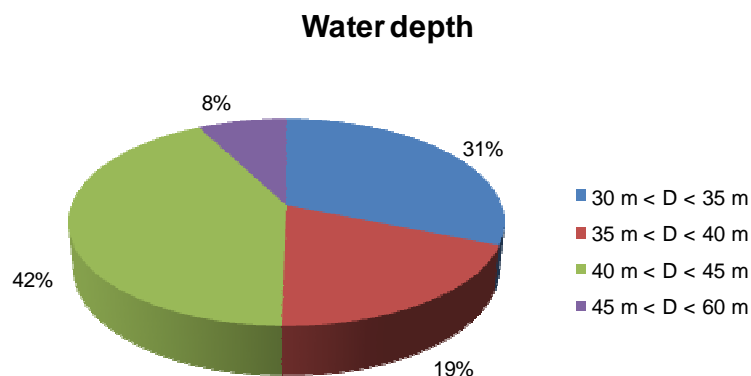


Figure 2.7: Market range of water depth(3)

The reduction of the water depth raises the question to make the base of this design smaller than the 28 meter in the reference design. The underlying idea is that for deeper waters the upper part of the structure can be kept the same while a lower part can be added with a wider base. In this way the substructure can more relative easy adapted for larger water depth. This saves engineering cost and the same fabrication templates can be used for several projects. In case of battered legs the legs can just be extended.

However, reduction of the base width will increase the total loading on the foundation piles. The piles of the reference design already have a large diameter of 96 inch and thickness of 2 inch. Reduction of the base width requires even unwanted bigger piles. This not only detrimental for the total material cost, but also effects the size of the required piling hammer.

Also it is expected that adapting the structure to larger water depth is not achieved by simply adding a lower part to the structure. Because the environmental conditions will change as the location changes,

the design will not remain the same and the engineering part has to be redone. The modifications shall contain structural adjustments and therefore reducing the width base it not considered worthwhile.

How to adapt the substructure to other water depths than 45 meter is not included in this report. The design optimisation is only applicable for the water depth of 45 meter.

2.6 Design loads

In chapter 6 the structural design is addressed. In the first phase only a static in-place analysis has been performed (Section 6.1). Later on a dynamically in-place analyse and a fatigue analyse are done (Section 6.3). All analyses were done with the parameters presented in this section and more detailed in appendix A.3.

2.6.1 Standard

Used standard for load determination and code checking is NEN-EN-ISO 19902 (11). All structural analyses and code checking are performed using the SACS offshore suite version 5.3.

2.6.2 Load combinations

Only extreme loads of the turbine are released by the turbine manufacturer. Based on (6) these loads are combined with the 50-yr extreme wave. That's why only 50-yr environmental data is used in further design phases and classified as extreme load cases for the corresponding load factors.

The load factors are according the ISO standard and are summated in table 2.2.

Table 2.2: Load Factors

Condition Description		Load Factors (NEN-EN-ISO 19902)	
		D	W_e
ULS	Extreme storm with maximum permanent and functional loads	1,1	1,35
ULS	Extreme storm with minimum permanent and functional loads	0,9	1,35
SLS	Extreme storm with maximum permanent and functional loads	1,0	1,0

- D = Dead load including:
- weight of the structure in air;
 - appurtenances weight;
 - weight of permanent equipment (turbine, rotor);
 - weight of marine growth;
 - hydrostatic forces on the structure including buoyancy of steel, entrapped air/fluid and marine growth;
 - the weight of entrapped fluid.
- W_e = Extreme storm, wind, wave and current loading and turbine loadings.

Preferably all combinations of wind and wave with their directions are incorporated in the load combinations. But as the number of load combination is then very large, a reduced number of load cases is used. This is achieved by assuming that wind load and wave load do always occur in the same direction. No misalignment of wave and wind loading is taken in consideration. Further clarification follows in section 6.1.

2.6.3 Loading parameters

Below a summary of the primary parameters is given.

Table 2.3: Summary of primary parameters

Item	Symbol	Units	Value
Extreme wave height	$H_{50\text{-yr}}$	[m]	21.3
Associated wave period	T_{ass}	[s]	14.85
Water elevations	100-yr max (incl. tolerance)	[m]	+6.70
	HAT	[m]	+4.80
	MSL	[m]	+2.40
	LAT	[m]	+0.00
Minimum bottom of steel	BOS	[m]	+22.20
Water depths	Maximum design water level	[m]	51.70
	LAT	[m]	45.00
	Minimum design water level	[m]	43.60
Splash zone (rel. to LAT)	Upper elevation	[m]	+6.80
	Lower elevation	[m]	-2.00
Current (at 100% of water depth)	100	[m/s]	1.122
	60		1.122
	50		1.120
	25		1.074
	10		1.020
	0.05		0.983
	0.01		0.910
Turbine loading	Thrust force	[kN]	1926
	Torsion	[MNm]	17

2.7 Transition piece

The transition piece is the component linking the substructure and the tower (Figure 1.1). Looking ahead to chapter 4 and 6 the transition piece element is point of concern for the structural modelling and designing. But as indicated in section 1.4.2 the design of the transition piece is not included in the outline of this thesis.

The transition piece is however a vital component. The main design criterion of the transition piece is the transfer of the loads from the tower to the substructure. Customary it will have a door to permit access to the turbine tower and will house local switchgear and an emergency refuge.

Base for the transition piece that will be used in this thesis is the transition piece of Alpha Ventus (Figure 2.8) and drawings included in the reference design (Figure 2.9).



Figure 2.8: Transition piece Alpha Ventus

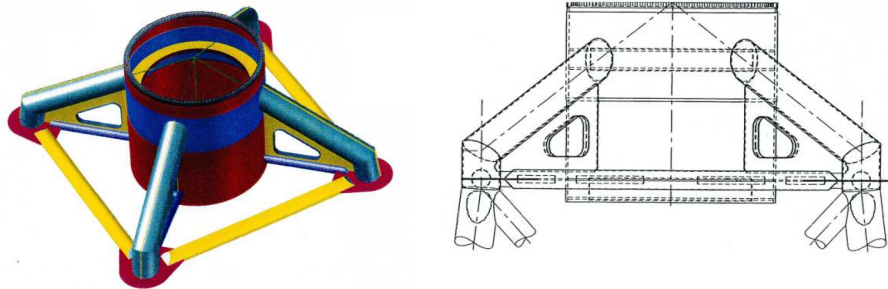


Figure 2.9: Example of a transition piece(3)(7)

Dimensions and weight of the transition piece are based on the reference design (7). Width of the transition piece is 10 meter and total height of 5 meter. The transition piece (125 t) is modelled as dead load over the complete transition piece at level of LAT+25.0m till LAT+30.0m. Figure 2.10 shows the modelling of the transition piece as performed in the software.

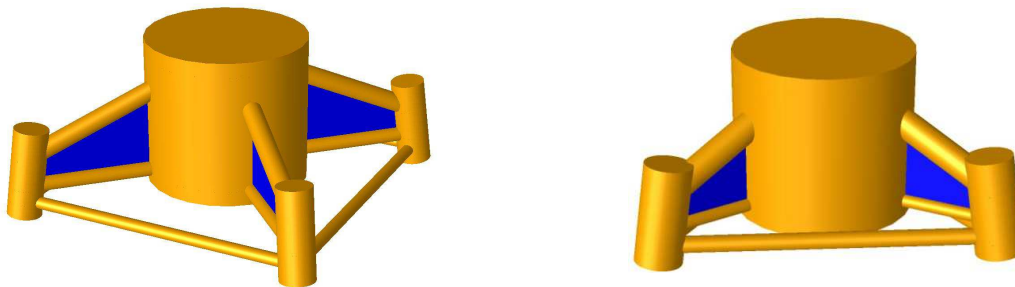


Figure 2.10: Modelling of transition piece

It is recommended that further research is done to the transition piece element. The stiffness properties of all elements affect the dynamically behaviour of the support structure. The transition piece component is the transition between substructure and tower with the turbine as large mass on top. The fact that the tower is a soft structure compared to the substructure makes the transition piece a component with significant influence on the total dynamics. This is further investigated in section 6.5.

3. Suction Bucket

The common practice of driving steel tubular piles in the sea bottom as foundation for the jackets is being increasingly criticized. Offshore pile driving causes noise nuisance and is assumed to affect the local sea life. A 160 dB limit for piling is brought into force in Germany (12). An alternative may be the application of suction caissons which have the form of large buckets placed upside down under the jacket legs.

This chapter goes more deeply into whether or not to apply a suction bucket as foundation for offshore wind turbines. The pile foundation is a much known concept and therefore not further explored.

3.1 Principle

Suction buckets are tubular steel foundations that are installed by sealing the top and applying suction inside the bucket. The hydrostatic pressure difference and the deadweight cause the bucket to penetrate the soil. This installation procedure allows the buckets to be connected to the rest of the substructure before installation, enabling a reduction in steps of the installation procedure.

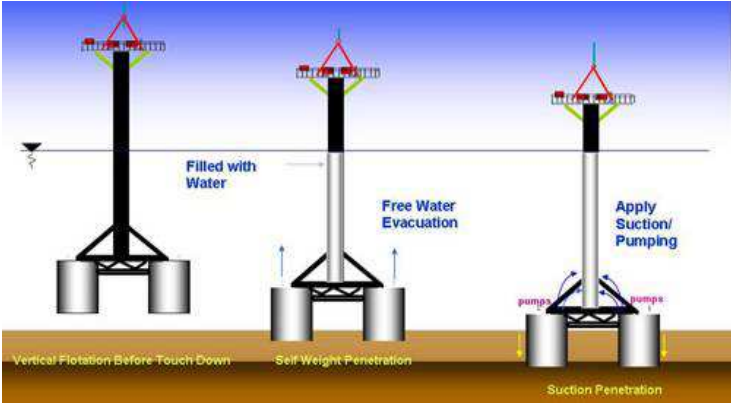


Figure 3.1: Suction bucket installation

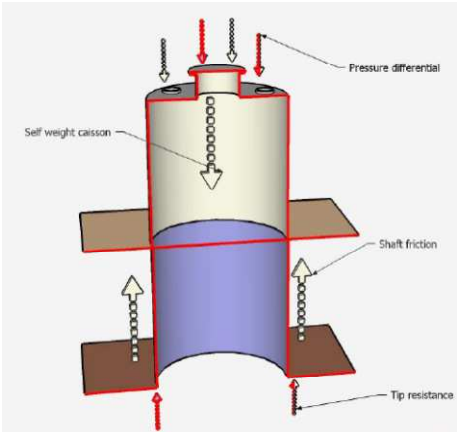


Figure 3.2: Free body diagram

In the first installation phase the suction bucket is lowered onto the seabed. An opened valve on top of the bucket enables water to escape the caisson freely. Next the pump is activated, lowering the pressure inside the caisson. The difference between the caisson pressure and the hydrostatic water pressure causes a distributed force over the top of the anchor directed downward. The bucket penetrates into the seabed partly by self-weight and partly by applied suction.

In principle its behaviour can be considered as a combination of gravity base and pile foundation systems. The penetration resistance results from the skin friction mobilised along the outside and inside surface of the bucket as well as the base resistance at the bucket sleeves toe. The pulling-out resistance is determined by the skin friction and self-weight.

To prevent offshore underwater connections it is assumed that the suction buckets are connected to the substructure onshore. Complex underwater connection would increase again the amount of steps in the installation process and are difficult and expensive connections, which undo the intended advantages of the suction bucket.

3.1.1 Advantages versus disadvantages

Compared to driven pile concept the following advantages and disadvantages are noted.

Advantages

- Installation time reduction is expected due to reductions in installation steps. When the foundation exists of driven piles, the piles and substructure are installed separately. This is in contradiction when suction bucket are used. Then substructure and suction buckets are installed together. No separate installation is necessary and thus the number of steps in the installation process is reduced. This also affects the need for changes in installation equipment. Only one equipment spreading is necessary for the installation.
- The installation process can easily be reversed. Simply putting pressure inside in the suction bucket makes the installation undone. The overpressure creates vertical lifting, what makes it suitable to reuse the whole substructure on other place. This is however more likely to be favourable in case of the traditional oil and gas industry.
- Because no piling driving is needed, the sound pollution is nearly or completely gone. The sound nuisance in environmental area is becoming more and more a point of concern. (e.g. (13)) Especially the installation of a large amount of wind turbine result in a long period of pile driving at sea. Looking at the prospect of the installation of approximately 50 substructures per annum and for example a wind park of 75 wind turbines, then the environmental life is affected for 1.5 year.

Disadvantages

- Because the suction bucket and the substructure are installed in whole, the crane capacity of the installation vessel has to be accounted for the weight of suction buckets. The weight of the suction buckets demand for additional requirements of the installation equipments. Besides the weight the suction buckets also result in a wider base at the bottom of the substructure. Therefore is the required hoisting radius of the complete structure larger due to the appliance of the suction buckets. The inference is that suction buckets demands for extra hoisting capacity in terms capable hoisting load and corresponding radius.
- The dimension of the suction bucket result in an increased total height of the structure that is has to be transported. Due to increased height the centre of gravity is located higher. So naturally the complete structure is more unstable by itself. Transport on an offshore transport barge is more difficult when suction buckets are applied.
- Compared to simple piles as foundation, the suction bucket are more complicated to fabricate. Apart from the amount of material that is used, the amount of labour per ton of steel is far more due to the geometry. Fabrication cost per ton of steel is higher than in case of driven piles.(14)
- Suction buckets are a more high-tech concept, therefore a more vulnerable concept (14). This in contradiction to driven piles, which is a very highly used method for foundations. From the point of risk management, preference is given to the driven pile concept.

3.1.2 Context with oil & gas industry

Suction caissons have been extensively used as anchors, principally in clays, and have also been used as foundations for a small number of offshore platforms in the North Sea. But the loading regimes on offshore turbines differ in respects from those on structures usually encountered in the offshore oil and gas industry.

Typically the substructures in this case are relatively light, but in proportion to the vertical load the horizontal loads and overturning moments are large (15). Looking at the reference design (7) the total amount of horizontal loading (approx. 12MN) is 60% of the total dead load (approx. 22MN). Compared to a conventional platform in the oil & gas industry this percentage is significantly larger. In case of the oil platform of project F3-FA (16) it can be seen that horizontal loading (11MN) is about 13% of the total vertical load (80 MN).

Note that in conditions as might be encountered in the North Sea, the horizontal load from waves is significantly larger than that from the wind. In case of the reference design the horizontal loads were respectively 10 MN and 2 MN. However, because the latter acts at a much higher point (150 m above the foundation) it provides the same order of overturning moment as the wave loading, which act at say 45 m above the foundation. Using these figures the overturning moment of 750 MNm would divide as 300 MNm due to wind and 450 MNm due to waves. Overturning moment caused by wind loading is an important part.

Another important consideration is that, unlike the oil and gas industry where large one-off structures dominate, many relatively small and inexpensive foundations are required for a wind farm development, which might involve anything from 30 to 250 turbines.

3.1.3 Literature study

Relevant reports make clear that the suction bucket concept is feasible for large offshore wind turbines but more research has to be done to handle the problems that rose during the studies. Some of these problems are listed below.

- The installation of a suction bucket foundation is problematical in layered soil, in particular when a non-cohesive soil layer is overlaid by a cohesive soil layer. If in this case no flow can be generated in the non-cohesive layer, only the hydrostatic pressure difference is available. Thus especially in dense sands this might not be sufficient to reach the necessary embedment depth. (17)
- The small difference between the required penetration depth and maximum installable penetration depth of the feasible buckets indicates that nearly the entire potential hydrostatic pressure is required for installation. It has been assumed that the pressure inside the suction bucket can be reduced to zero, although in reality this may cause liquefaction of the soil at the point of critical suction. (18)
- As a wave passes the column of the structure it exerts large horizontal forces, which also cause overturning moments. However, at the same time the wave causes a transient pressure on the seabed, and on the lid of the caisson. Because the caissons are in shallow water these pressures are quite large. The pore water pressure within the caisson is unlikely to change as rapidly as the pressure on the lid, so there will be pressure differential cross the lid of the caisson which result in net vertical forces, and overturning moments on the caisson. (15)
- Following out of (18) and (19) it can be seen that in the same situation the weight of the suction bucket is necessary larger than driven piles foundation in the same situation. Because of the large hydrostatic force that is required for installation, suction buckets commonly have a much lower aspect ratio (length/diameter) than driven piles. Due to the low aspect ratio suction buckets are less suited to comply with the large moments.

- The pile-soil friction for cohesionless soils increases with penetration depth and therefore suction buckets require a larger surface than driven piles. This is only partly compensated by the smaller wall thicknesses that are required for the benign installation procedures of suction buckets. Therefore, a substructure with suction bucket is heavier than substructures with driven piles. (19)

3.1.4 Practical experience underneath wind turbines

The suction bucket is applied successfully only once underneath an offshore wind turbine in Fredrikshavn (20). (Figure 3.3, Appendix B.1). Thereby, so far only two attempts are known, of which one attempt failed during installation because buckling occurred in the suction bucket. It was planned to make a new attempt, but so far no new attempts after 2005 are done. The appliance of suction bucket for offshore wind turbine evokes interest of offshore wind farm developers, but so far the executed tests have mixed outcomes. At this moment no concrete plans are known for the appliance of suction buckets underneath offshore wind turbine substructure. (21)(22)



Figure 3.3: Suction bucket in Fredrikshavn



Figure 3.4: Failed attempt during installation at Wilhelmshaven

3.2 Dimensions

For assessment of the suction bucket dimensions a brief calculation is made. The calculation is a simplified approach, and is only valid for first impression. For better insight in the required dimensions more accurate calculations are necessary. The soil properties of the reference design report are used. In this case the tension loading on the suction bucket is seen as the normative load case. For now the maximum tension load is used, derived from the maximum tension pile load from the reference design rapport (31.6 MN). This also can be derived by considering the push-pull concept in figure 3.6. Dividing the maximum overturning moment (approximately $1.0 \cdot 10^6$ kNm) by the diagonal of the square footprint $\sqrt{28^2 + 28^2} = 39.6\text{m}$ gives the F_{tension} . Using a pile partial resistance factor of 1.25 the required tension capacity is given by $(1.0 \cdot 10^6 / 39.6) \cdot 1.25 = 31.6\text{ MN}$.

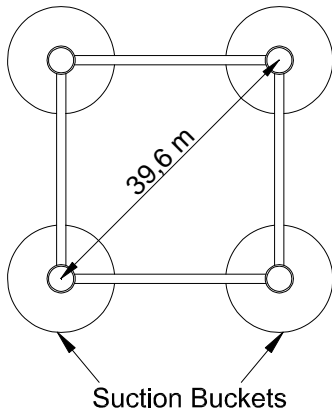


Figure 3.5: Top view suction buckets

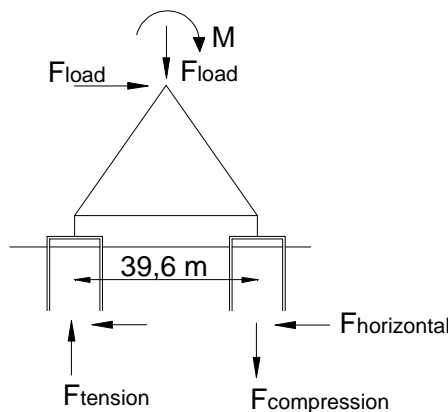


Figure 3.6: Push-pull load concept

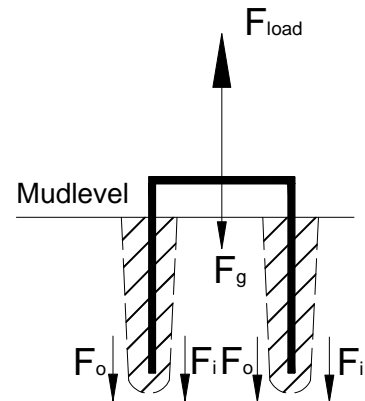
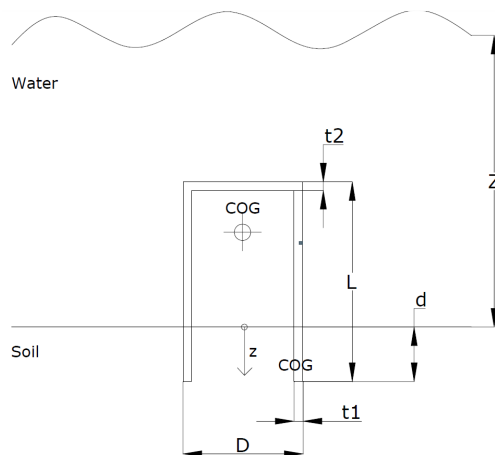


Figure 3.7: Shear failure

The calculation is included in appendix B.2 and is based on the following specifications.

- Suction buckets transfer the gravity loads and the environmental generated overturning moment by a vertical push-pull concept.(Figure 3.6)
- Base shear loads are relative low and insignificant compared to the vertical loads. In this phase base shear is ignored.
- The suction bucket concept fails due to suction bucket / soil interface shear failure along the inner and outer perimeter. (Figure 3.7)

In this calculation the installation phase of the suction bucket is not discussed. Only the operational situation is considered, assuming that the bucket is fully penetrated ($L=d$). This gives the following force balance:



$$\sum F_z = F_g + F_0 + F_i - F_{load} \quad (3.1)$$

- F_{load} = Vertical load force
- F_g = Self weight bucket
- F_0 = Shaft friction outer surface
- F_i = Shaft friction inner surface

Figure 3.8: overview of main parameters

Result of the calculation is those suction buckets have to be applied with the following dimensions:

D= 21 m

L= 18 m

t1=0.08 m

t2=0.09 m

Given $\rho_{\text{steel}}=7850 \text{ (Kg/m}^3\text{)}$ makes a total weight of 860 ton.

The calculation is compared to the project F3-FA where underneath an oil platform suction buckets were applied. Based on (16), the total governing tension load on the suction bucket in this project is approximately 24 MN. Calculation by a company specialized in suction buckets, lead to suction bucket with a diameter of 15 meter and height of 13 meter, resulting in a total weight of 400 ton per suction bucket. From that it can be concluded that the hand calculation in appendix B.2 is probably a conservative approach but is not out of range.

3.3 Evaluation

Out of literature study followed that suction buckets for offshore wind turbines are feasible. But further research has to be done, referring to the problems that appeared during past studies. Only two projects in the offshore wind market tried the suction bucket principle with mixed outcome.

Difference with the oil and gas industry, where the suction bucket is more often applied, is the increased horizontal loading compared to the vertical loading. The overturning moment due to wind loading is significant and has serious effects on the suction bucket.

After a short calculation is followed that based on a four-leg substructure underneath each leg a suction bucket with large dimensions is necessary. With a diameter of 21 meter and a penetrated height of 18 meter the total weight would be about 860 tons. Considering it will be attached to the substructure onshore the total weight of the structure nearly doubled. (Based on reference design weight)

The total weight of the four piles that are designed underneath the reference design is 611 ton. Applying suction caisson would increase the use of material in the foundation and thus the total material cost. Besides this, also the fabrication cost of the buckets is significant higher. The increased structure weight requires an installation vessel with much larger capacities. Therefore the substructure shall be founded on driven piles.

4. Substructure Concepts

In this chapter different concepts of open steel substructures will be considered. The concepts followed out of section 1.2, reference projects (Appendix C), brainstorm session with the involved parties and own development. Starting points are the objectives given in section 1.4. The first section contains the concept definitions, followed by an assessment in the second section. Note that the figures in this chapter are only schematic and do not display a definitive situation.

4.1 Concept designs

1. Jacket

Strictly the term jacket is already referring to certain pile system, including structural design and installation. In this case this is not intended and it must be seen a steel space frame structure as defined in section 1.2. The term tower can also be used, but can cause confusion with the part below the hub. Therefore the term jacket is used.

Type A: 4-leg battered (Figure 4.1)

The four leg battered concept is the reference design. Loads are transferred by four legs to the seabed. The legs are placed battered and are connected on the top to a transition piece. Braces on all sides provide the stability of the structure.

Type B: 3-leg battered (Figure 4.2)

The three leg battered concept is based on the reference design. The principal is the same only this concept consist of three legs to transfer the topside load to the seabed. The three legs form a triangular base plate. The legs again are placed battered and are connected on the top by a transition piece.

Type C: 3-leg straight (Figure 4.3)

Instead of battered legs, this concept has three straight legs as substructure. The three legs are supported by tubular beams that form a wider base. Advantages compared to the battered legs are the less complex connections of the diagonals bracings with the legs. The lower beams will have to deal with a large bending moment obviated by a horizontal placed space frame.

Type D: 4-leg straight (Figure 4.4)

Same principal as type C, only this time four straight legs are applied. The forces in the legs are distributed in the same manor to a lower space frame. From there the loads are transferred to four piles underneath this beam frame.

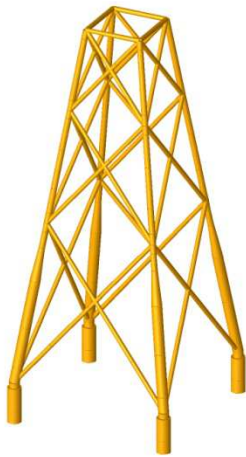


Figure 4.1:
4-leg battered



Figure 4.2:
3-leg battered



Figure 4.3:
3-leg straight jacket



Figure 4.4:
4-leg straight jacket

2. Tri-pod

Type A: conventional tripod (Figure 4.5)

This concept is based on reference projects and is applied more often. This concept relies on fewer, but bigger elements than a jacket type structure. The transference to the seabed is done at three places.

Type B: extended tripod (Figure 4.6)

Based on type A this is a more extended tripod. The presence of the additional diagonal supports gives the opportunity to support the main leg on a higher point and therefore can be dimensioned less heavy.

Type C: split tripod (Figure 4.7)

The split tripod is the modified version of the conventional tripod. The main leg is shortened and is split up in three smaller legs that form the base of the substructure.

Type D: asymmetric tripod (Figure 4.8)

Basic idea behind the asymmetric tripod is advantages in the manoeuvrability during fabrication. During fabrication all other tripod concepts are difficult to place horizontal because the legs are divided all around.



Figure 4.5:
Conventional tripod

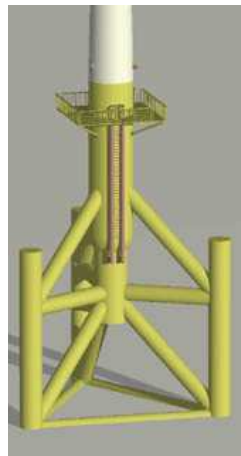


Figure 4.6:
Extended tripod



Figure 4.7:
Split tripod

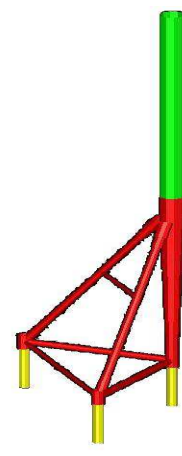


Figure 4.8:
Asymmetric tripod

3. Tripile (Figure 4.9)

The tripile is a known concept of the reference project. This concept is developed by the BARD Company and is already installed at couple of places. Foundation piles are extended to form three legs, which are connected above water by a transition piece.

4. Tetra-pod

Type A: symmetric (Figure 4.10)

Following the path of the tripod, but this time the forces are transferred to four legs to the seabed.

Type B: A-symmetric (Figure 4.11)

In line of tetra-pod type A and the a-symmetric tripod, this concept is a combination of the above-mentioned concepts.

5. Twisted Jacket (Figure 4.12)

The twisted jacket concept consists of a guide structure and four foundation members. The three battered piles, which are arrayed in vertical planes spaced 120° around the central caisson. Keystone Engineering states this design provides more effective use of the axial soil resistance for lateral loads and torsion moments.



Figure 4.9: Tripile

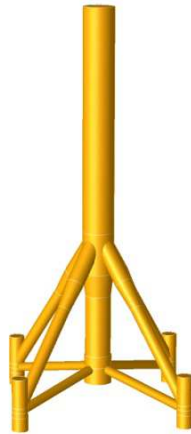


Figure 4.10:
Symmetric tetra-pod

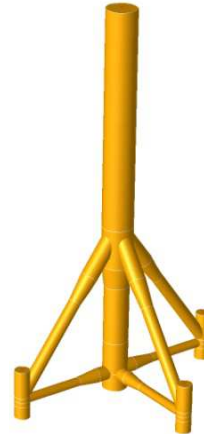


Figure 4.11:
Asymmetric tetra-pod

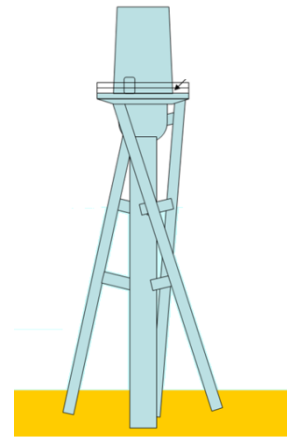


Figure 4.12:
Twisted Jacket

4.2 Evaluation

All the concept designs of are rough designs with their own properties. At this stage in the project, no full quantitative analysis of various aspects of the substructure concepts is performed. Therefore it was decided to perform a qualitative judgement of the support structures, based on own opinion and opinions of involved parties. To make a well considered choice for further developing is made use of a Multi Criteria Analyse (MCA). All concepts are put against the light looking as several criteria, which are of most interest for the total cost of the project. These criteria are seen as the most important properties in the field of design, fabrication, installation and maintenance of the concepts that will define the choice. Some criteria might raise some contradistinctions, but this left as much as possible out of considerations.

The following criteria are evaluated;

Design

- **Mass of the substructure;** The weight of the substructure is a major component of the material cost. The weight of the transition piece and foundation are not included.
- **Footprint;** The footprint defines the base of the substructure. The magnitude and shape of the footprint has consequences for storage on / near the factory plant and transport efficiency.
- **Tower connection;** The concepts have several different types of connection to the tower. In some cases a kind of transition piece is necessary for the connection. Differences in this connection have also effect on the installation.

Fabrication

- **Number of joints;** The number of joints that have to be fabricated are of great deal for the fabrication cost. In this criterion is looked at the expected absolute number of joints.
- **Complexity of the joints;** Besides the number of joints the overall complexity of joints has consequences for the cost.
- **Manoeuvrability;** Look ahead of the ease of handle during fabrication. Large number of manoeuvres that are necessary for fabrication can cause unwanted difficulties.

Installation

- **Lifting;** The lifting procedure during installation largely depends on the weight of the structure. Less heavy structures are easier to install.
- **Foundation;** Installation of the foundation shall require large amount of effort in the total installation process and therefore have a large consequence for the total cost.

Maintenance

- **Number of joints;** The maintenance is mainly the checking for traces of damage at the joints. Inspection normally will be concentrated on the joints. Therefore the number of joints is put as criterion.

Overall

- **Reliability;** Some of the concepts are already in operating state, where other just are concepts on papers. Therefore some of the concepts reliability is already proven, and for others the reliability is still a question.
- **Decommission;** Decommission of the support structure is mandatory and therefore part of the total life cycle cost. That's why is does effect the choice for the substructure and is admitted in the MCA.

Not included is the foundation design itself. It is assumed that for every substructure a suitable location can be chosen. A location has to be chosen that is in the boundary range for a certain type of substructure. At this moment is assumed there will be not large differences between the total foundation costs of the various concepts.

Because some properties are more important than others, weight factors are attributed to each property. In order to determine the relative importance the following table is filled in by all four the participants (Appendix D). In table 4.1 an example is given of a filled in table.

Table 4.1: Example of filled in table to determine weigh factors

nr.	criteria												score		weight factors	
		1	2	3	4	5	6	7	8	9	10	11	absolute	relative		
design																
1	mass		1	1	0	1	1	1	1	1	1	1	1	9	18	1,6
2	footprint	0			0	0	0	1	0	0	1	0	0	2	4	0,4
3	tower connection	0	1		0	0	1	1	0	1	0	0		4	8	0,7
fabrication																
4	number of joints	1	1	1		1	1	1	1	1	1	1	1	10	20	1,8
5	complexity of joints	0	1	1	0		1	1	1	1	1	1	1	8	16	1,4
6	manoeuvrability	0	0	0	0	0		0	0	1	0	0		1	2	0,2
installation																
7	lifting	0	1	0	0	0	1		1	1	0	0		4	8	0,7
8	foundation	0	1	1	0	0	1	0		1	0	0		4	8	0,7
inspection																
9	number of joints	0	0	0	0	0	0	0	0		0	0		0	1	0,1
overall																
10	reliability (proven technology)	0	1	1	0	0	1	1	1	1		1		7	14	1,3
11	decommissioning	0	1	1	0	0	1	1	1	1	0			6	12	1,1
											55	111	10,0			

The table works as follows;

All criteria have been compared to each other and given the value 0 (less important) or 1 (more important). The value 1 means that the criterion in the row is given more priority above the criterion in the column. For instance, mass (nr. 1) is considered of more importance than number of joints (nr. 3), and is therefore given the value 1. If two criteria are being considered of the same importance, they both have been given the value 1.

This has resulted in an absolute score, which defines the distribution of importance. As can be seen in the table, the criteria decommissioning (nr. 11) receives the absolute score 0, which implies that this value is of no importance at all. This is clearly not true, so it is decided to give it a relative score of 1 and to double all the scores of the other criteria. In this way the decommissioning is not neglected, while the mutual proportions remain the same. Finally these relative scores are presented as weight factors, which are used later on in the Multi Criteria Analyses (MCA).

By making use of a MCA, it is possible to give a rate to certain properties of the substructures. In this MCA a rate between 1 and 10 is given to each property. Again this is done by all four participants and the filled in tables are included in Appendix D.

It was noted that results from different contributors showed some significant differences. It showed that it was difficult to express certain effects in a number, but is a way to display the most optimal solutions. Table 4.2 shows the average of the filled-in values of the participants. The outcome is a rank of the variety of substructure concepts.

Table 4.2: Results of Multi Criteria Analyse

design	criteria	jacket				tripod				tetra-pod			
		A: 4-leg battered	B: 3-leg battered	C: 3-leg straight	D: 4-leg straight	A: conventional	B: extended	C: split	D: a-symmetric	triple	A: symmetric	B: A-symmetric	twisted jacket
1	mass of substructure	57,9	13,6	10,9	11,7	8,3	7,4	7,3	6,5	4,0	6,1	5,3	6,2
2	footprint	3,7	4,5	4,5	3,7	4,6	4,6	4,6	3,6	4,4	3,2	3,3	4,6
3	tower connection	4,6	4,1	4,1	4,6	8,0	8,0	8,0	8,0	6,2	8,0	8,0	7,0
fabrication													
4	number of joints	5,0	6,1	6,3	5,3	10,6	9,3	10,6	10,4	10,9	8,6	8,6	9,1
5	complexity of joints	11,3	10,9	11,0	11,3	4,7	5,3	4,3	5,1	4,2	4,6	5,0	9,8
6	manoeuvrability	3,0	3,0	3,2	3,8	1,5	1,4	1,5	2,0	2,2	1,3	1,5	3,1
installation													
7	lifting	8,8	8,4	7,5	7,6	5,4	5,2	5,2	5,4	7,3	5,2	5,2	7,1
8	foundation	8,1	8,1	8,1	7,4	7,2	7,2	6,8	6,8	6,3	6,0	6,4	4,2
inspection													
9	number of joints	0,6	0,8	0,9	0,7	1,6	1,3	1,6	1,5	1,7	1,3	1,3	1,2
overall													
10	reliability (proven technology)	9,3	8,5	8,1	8,1	8,4	6,0	5,4	4,7	6,3	4,4	4,4	3,1
11	decommissioning	2,5	2,5	2,6	2,6	2,4	2,4	2,2	2,3	3,1	2,9	2,9	3,1
Total		114,8	70,4	67,2	66,8	62,6	58,1	57,4	56,2	56,6	51,5	51,8	58,5
Rank		1	2	3	4	5	7	8	10	9	12	11	6

As follows from MCA, the 4-leg battered jacket seems to be the best design. But it can be seen that the scores do not differ much from each other. The reference design is at this stage seen as the optimum solution but is just based on opinions of the participants, a rather subjective approach. This is illustrated in figure 4.13 where the spreading is displayed of score for the twelve concepts of each person. It can be seen that opinions are ambiguous and do not propagate a clear vision what is the best concept.

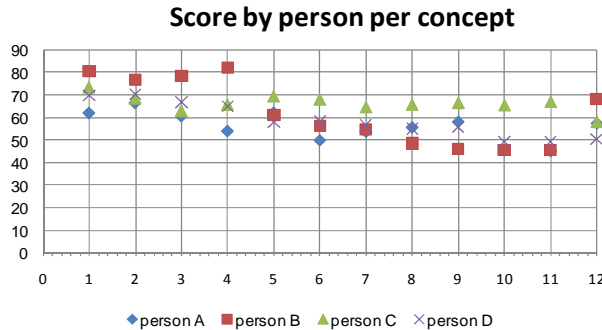


Figure 4.13: Score by person per concept

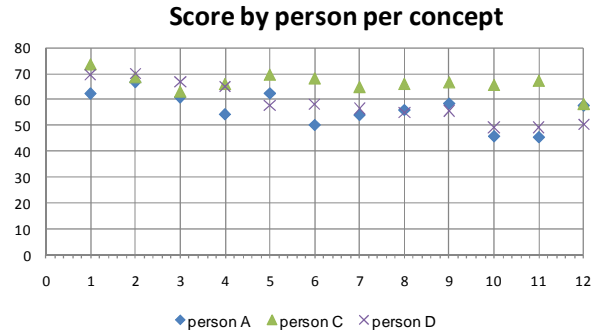


Figure 4.14: Score by person per concept

Because the scores are very close to each other, it is decided to investigate the sensitivity of the opinion of one person on the total outcome of the MCA. Therefore the score of person B is neglected and deleted in the outcome of figure 4.14. Person B is chosen because the corresponding scores are most favourable for the concepts that are in top of the line. The MCA in table 4.3 is the result.

Table 4.3: Results of Multi Criteria Analyse, excluding scores of person B.

		jacket				tripod				tetra-pod			
		A: 4-leg battered	B: 3-leg battered	C: 3-leg straight	D: 4-leg straight	A: conventional	B: extended	C: split	D: a-symmetric	triple	A: symmetric	B: A-symmetric	twisted jacket
design													
1	mass of substructure	13,9	13,9	9,7	9,6	7,5	6,8	7,4	6,8	3,6	6,3	5,2	6,4
2	footprint	4,4	5,5	5,5	4,4	5,8	5,8	5,8	4,6	5,4	3,8	3,9	5,6
3	tower connection	5,3	4,6	4,6	5,3	7,6	7,6	7,6	7,6	5,3	7,6	7,6	6,3
fabrication													
4	number of joints	4,9	6,3	6,7	5,2	10,6	8,8	10,6	10,2	12,0	8,9	8,9	9,6
5	complexity of joints	9,7	9,1	9,3	9,6	5,2	6,0	4,6	5,7	4,5	5,1	5,6	7,7
6	manoeuvrability	1,9	1,9	2,1	2,1	1,4	1,3	1,4	2,1	2,3	1,1	1,5	1,8
installation													
7	lifting	9,4	8,8	7,6	7,7	6,0	5,7	5,7	6,0	8,5	5,7	5,7	7,6
8	foundation	8,4	8,4	8,4	8,4	8,7	8,7	8,1	8,1	7,3	7,1	7,6	3,9
inspection													
9	number of joints	0,7	0,9	1,0	0,8	1,8	1,5	1,8	1,7	2,0	1,5	1,5	1,4
overall													
10	reliability (proven technology)	7,6	6,5	6,0	6,0	6,4	4,2	3,3	3,8	6,0	3,4	3,4	1,8
11	decommissioning	2,4	2,4	2,6	2,6	2,3	2,3	2,0	2,2	3,2	3,0	3,0	3,3
Total		68,4	68,3	63,4	61,6	63,1	58,7	58,3	58,8	60,1	53,4	53,9	55,3
Rank		1	2	3	5	4	8	9	7	6	12	11	10

It turns out that the leaving out the result of this person does have a small effect in the ranking order. Nevertheless are the concepts in top of the line same as first. The differences in score between the concepts are still small. This offers the perspective that other concepts may offer a potential cheaper design. Notice that in both table 4.2 and table 4.3 the jacket type structures are placed in front. The tripod concept is the only concept that is seen as competitive structure.

Further notice remains that the MCA method is based on opinions of persons, and is not directly supported by hard facts.

Because the differences are so small it is decided to go further with the first five concepts. These concepts are further developed in chapter 6 to gain more knowledge and insight in their behaviour. After that a more accurate assessment is possible for further selection.

5. Foundation Connection

In chapter 3 was decided that the substructure would be founded on piles. Next point of consideration is the way the substructure will transfer the load to the foundation piles. A number of solutions are treated hereafter. The first three sections deal with three different principles, after which is worked up to the most economical piling method.

5.1 Main piling

Normally when the term jacket is used in the offshore business, this is directly referring to this option. The piles then are not only function as foundation, but also as part of the complete structural system. The space frame part of the jacket functions structurally mainly as connection between the piles. The jacket contains mud-mats and is placed in right position on the seabed. Piles are guided through the legs and driven in the soil. The piles are connected at the top of the legs to the jacket using shim plates. The fact that the connection is above water makes it less complex, easy accessible and favourable for possible maintenance.

Because a water depth of 45 meter is considered in this case, it follows that the piles have to span the complete height of the jacket. Given that the jacket height is about 75 meter, the piles might have even a length of 100 meter. Because of handling and logistic objections, the installation of a pile has to be done in sections. This demands for offshore welding of extra pile sections to provide the necessary length. Combined use of material in the leg of the jacket and in the pile with this length is very ineffective, making it a very uneconomical choice.

To reduce installation steps it is preferred that the transition piece is installed together with the substructure. The main piling principle does require that the legs are kept open on top. If the legs are kept open on top, this arises extra an extra challenge for a proper connection of the transition piece to the legs. Extra care is needed to prevent damage to the transition piece during the pile driving.

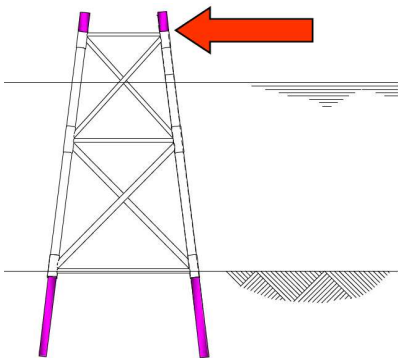


Figure 5.1: Main piling foundation principle(23)

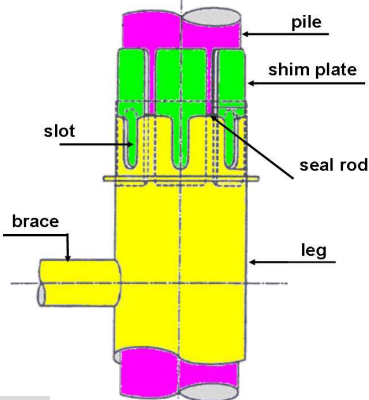


Figure 5.2: Connection of jacket and leg using shim plates(23)

5.2 Driven pile foundation

In the more traditional way of installing a jacket, the piles are driven through sleeves at the bottom of the jacket legs. The piles themselves are hammered into the seabed after the lowering of the jacket on seabed by the use of mudmats. Therefore this foundation connection will here be referred to as the post-piling method.

Typically, the connection between the sleeves and the piles is secured with grouting. The gap between the sleeve and the pile is filled out with a grout material, which prevents the movement of the jacket legs in the sleeves.

The connection can also be secured using swaging, a cold forging process, where the diameter of the pile gets expanded until it establishes a safe connection to the sleeve. Therefore a groove is made in the sleeve, where the pile is pressed into. The pile is expanded using a die or using high pressure water.

Post-piling is seldom used in wind farms. Only in the Beatrice wind farm, where jackets have been used for wind turbines for the first time, was the installation carried out using post-piling. However, in the oil and gas industry post-piling is widely used. This is because the oil and gas industry typically only requires installation of a single structure, whereas wind farms require installation of many similar structures.

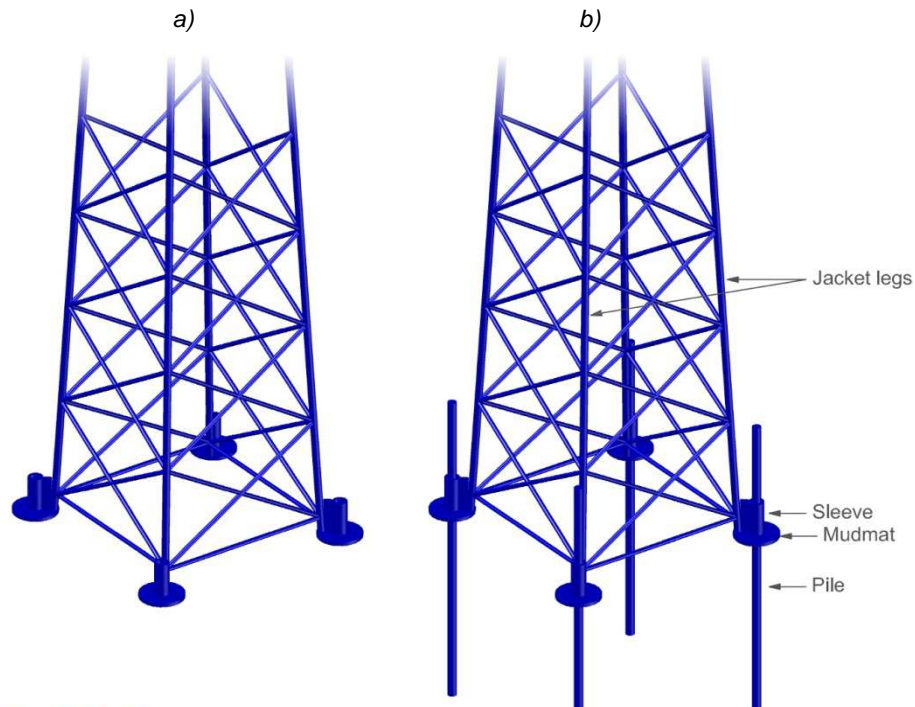


Figure 5.3: Post-Piling a)jacket placement b) pile Driving

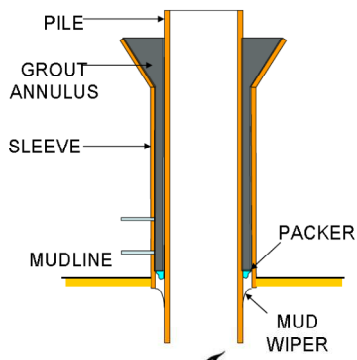


Figure 5.4: Grout connection



Figure 5.5: Swaged connection

Installation work of the foundation piles and positioning of the substructure is done by one installation equipment. Assuming a Heavy Lifting Vessel (section 9.2) is required for the lifting of the complete substructure, this vessel shall also be used for the pile driving. In table 5.1 a brief overview is given for the time that is needed for the installation of one substructure. These working times are based on (24) and own estimation.

Table 5.1: Time assessment of post-piling method

Steps Post-Piling method	Required equipment	Estimated working time
Placing substructure in position	Heavy Lifting Vessel	6 hr
Pile driving	Heavy Lifting Vessel Piling Hammer	24 hr
Move to next location	Heavy Lift Vessel	2 hr

If the supply of sufficient substructures is achieved at the wind park location, than the installation of the multiple substructures is achieved by simple repetition of the above times. This is displayed in the figure below, where installation of two substructures is shown. For now is assumed that a grout connection is applied and that grouting equipment will closely follow in the installation cycle.

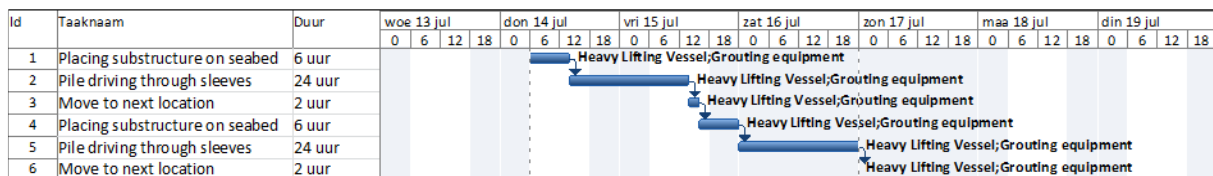


Figure 5.6: Planning of post-piling foundation installing

5.3 Installation in sections

By installation in sections is meant that the foundation piles are installed before the installation of the jacket. Therefore this option is further referred as the pre-piling method. During the pre-piled installation of a jacket, a template is used when hammering the piles into the soil. The template is essential for driving the piles at an accurate distance from each other and for repeated installations it is seen as a relative fast solution.

Seabed variations can be levelled by varying pile stick-up and ensures the standardisation and verticality of jackets. Following after the pile hammering, the piles are measured for its horizontal and vertical position. Alignment in vertical direction is ensured with brackets on the jacket legs.

The measures are taken into account during the fabrication of the jacket so that height deviations between the piles can be levelled out by adjustments to the leg brackets and stabbing guides.

After the piling process and above described survey, the jacket is lowered to the bottom of the sea, where the stabbing guides fit into the piles. The connection between the stabbing guides and the piles typically is made with grouting via an inside pipeline through the legs (Figure 5.9).

Alternative connections with swaging techniques potentially provide new light on the matter. However, swaging via de inside of the legs requires again that the legs are kept open on the top. Connection to the transition piece is then more complicated. Also can the leg diameter variation cause fitting problems for the swaging tools.

Swaging from outside, where the pile is swaged into the groove of a stabbing guide can potentially offer a new method with advantages, because no hardening of the grout has to take place. But so far known, this method has never been applied and there is no equipment on the market that can handle this operation. Previous wind farm projects at Alpha Ventus, Ormonde and Thornton bank the jackets were pre-piled with an inside grouting line.

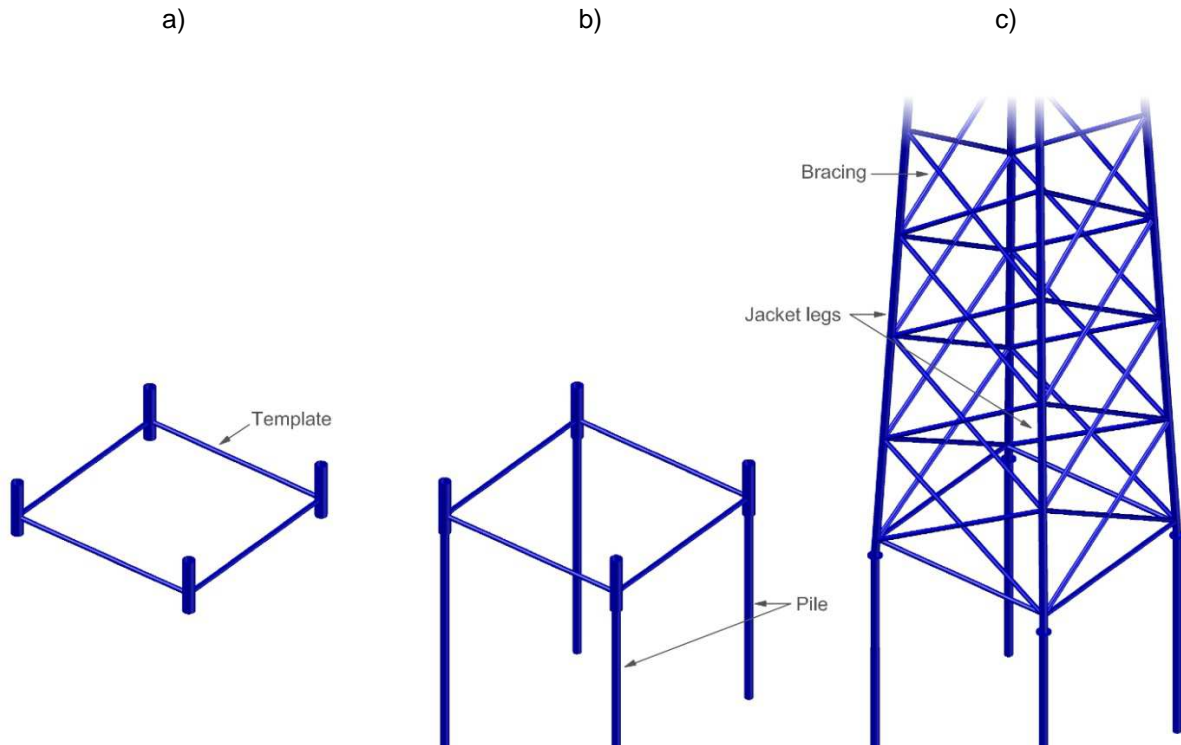


Figure 5.7: Pre-Piling a) Placing Template b) Pile Driving c) Jacket Placement



Figure 5.8: Stabbing of legs in piles

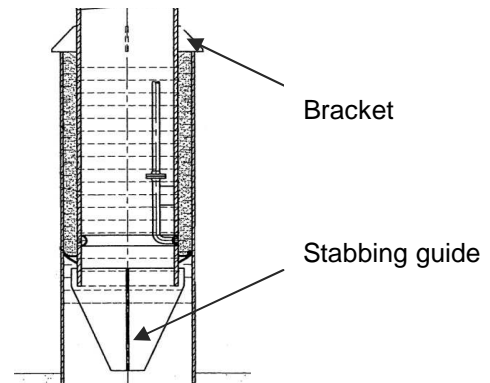


Figure 5.9: Grout connection by inside grouting line

The pre-piled method enables that for the installation of the piles and jackets two different installation vessels can be used. The first vessel will install the foundation piles and the second vessel will install the substructure. Different requirements are valid for both operations. A vessel with less lifting capacity is necessary for installation of the piles resulting in a cheaper day rate. This vessel is here indicated as Auxiliary Vessel and is assisted by survey equipment in form of a Water Remotely Operated Vessel (WROV). (Section 9.2)

The pre-piling method is more demanding on the jacket placing accuracy of the installation vessel compared to the Post-Piling method. But consult at installation companies (25)(26) presented little additional challenges for pre-piling operations using Dynamically Positioning (DP) offshore vessels. It turned out that no positioning difficulties were expected using the Pre-Piling method. The required precise operations were not considered as very special, because the same manoeuvres are done more often installing gas platforms and previous wind farms.

Again a time assessment has been done for the installation process. The working times in table 5.2 characterize the pre-piling method and are based on (24) and own valuation. Notice that for the positioning of the substructure the time is increased to 10 hours compared to the 6 hours in case of the post-piling method.

Table 5.2: Time assessment of Pre-Piling method

Steps Pre-Piling method	Required equipment	Estimated working time
Placing piling template	Auxiliary Vessel WROV	3 hr
Pile driving	Auxiliary Vessel Piling Hammer	24 hr
Pile survey	WROV	3 hr
Sail to next location	Auxiliary Vessel WROV	2 hr
Placing substructure in position	Heavy Lift Vessel	10 hr
Sail to next location	Heavy Lift Vessel	2 hr

The pre-piled method is an installation in sections. Two independent spreadings are incorporated for installation of respectively the piles and the substructure itself. This means that piles can be installed well in advance of the jacket, even in terms of months. Fabrication of jacket can be conducted in parallel with piling operations. Pre-installed piles will take away much of the scheduling risk for the later installation operations.

The planning of two substructures by the pre-piled method is displayed in figure 5.10. Two independent installation cycles can run continuously for installation of multiple wind turbines in a wind farm. In a more sophisticated planning it is plausible that in one wind farm pile installation and substructure installation can be done at the same time in one wind park. For example are the piles installed for turbine number 10 while the substructure is installed for turbine number 2.

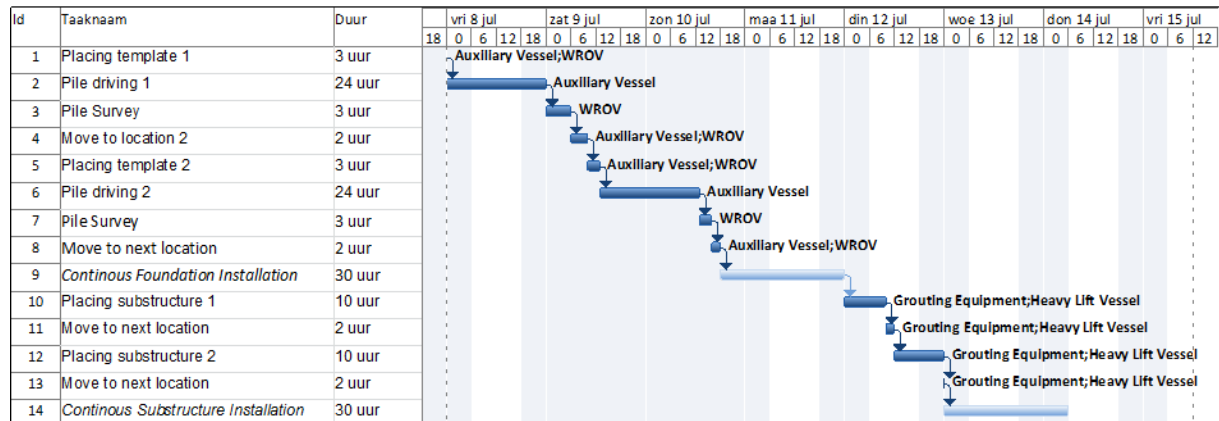


Figure 5.10: Planning of Pre-Piling concept

5.4 Evaluation

As said in the first section, the main piling option results in large increase of total material use. Thereby are also offshore welding activities expected, what results in large labour cost. In increasingly water depths this option is decreasingly favourable. Also can it be expected that the presence of the transition piece forms an obstacle for unhindered pile driving. Therefore is main piling not seen as good option for this purpose.

Considering the post-piling method compared to the pre-piling method the following advantages and disadvantages are obtained:

Advantages

- Purchase of a piling template is unnecessary.
- Less demanding on the jacket placing accuracy of the installation vessel.
- No survey has to be done for pile measurements.

Disadvantages

- All the work activities have to be planned behind each other.
- A larger vessel is also used for lighter work as pile driving.
- Increasingly scheduling risk for the later installation operations.
- Pile sleeves and mudmats have to be mounted on the substructure.

This all is approached in a more quantitative way by the proposed planning in figure 5.6 and figure 5.10 and the corresponding cost expectation of the two methods. Therefore the total weight that is involved in the sleeves and the mudmats in case of the post-piling method is estimated. This is done by looking at three projects in the oil industry with comparable total weight. The weights of the mudmats and sleeves depend on the environmental data and soil data of these particular projects. Therefore the average weight of the three projects is used. The total cost of the mudmats and sleeves are estimated by assuming a total fabrication price of 4 € / kg.

Table 5.3: Weight assessment of sleeves and mudmats

	Project	Weight (t)
Mudmats	K5CU	20
	B13	56
	E17	35
	Average	37
Sleeves	K5CU	138
	B13	175
	E17	120
	Average	144

In case of the pre-piling method the fabrication of a piling template is necessary. The piling template that is used at the Ormonde wind farm had a total weight of 170 ton (27). For here a total weight of 200 ton assumed for again 4 € / kg. Thereby is also assumed that the template can be reused 50 substructures. The purchase of the template can thus be written off over 50 substructures.

Next is the day rate of the used equipment in both methods. In section 9.2 are the day rates and weather windows derived that are given in the table below.

Table 5.4: Day rate estimation

Equipment	Day Rate	Weather Window
Heavy Lifting Vessel	€ 300,000	75%
Auxiliary Piling Vessel	€150,000	60%
Water Remotely Operated Vessel	€ 10,000	
Grouting equipment	€ 50,000	
Piling Hammer	€ 15,000	

Post-piling

In table 5.1 the working times of the Heavy Lifting Vessel is set on 32 hours that is spent for one substructure. Considering a weather window of 75% the total time becomes $32 / 0.75 = 42.6$ hours, equals $42.6 / 24 = 1.8$ days.

The total cost estimation of the post-piling method is gathered in table 5.5.

Table 5.5: Cost estimation post-piling method

Post-piling method	Equipment	Material [t]	Time [days]	Unity price / Day rate [€ / kg , € / day]	Writing-off	Total [k]
Fabrication	Sleeves	37		4		€ 148
	Mudmats	144		4		€ 576
Substructure installation	Heavy Lifting Vessel		1.8	300,000		€ 533
Foundation installation	Piling Hammer		1.8	15,000		€ 27
	Grouting Equipment		1.8	50,000		€ 89
						€ 1,373

Pre-piling

The working time of the Auxiliary Piling Vessel with the WROV and piling hammer is 33 hours (Table 5.2). Considering a weather window of 60% the total time for one substructure becomes $33 / 0.6 = 55$ hours, equals $55 / 24 = 2.3$ days.

Working time of the Heavy Lifting Vessel together with grouting equipment is 12 hours (Table 5.2). Considering a weather window of 75% the total time for one substructure is $12 / 0.75 = 16$ hours, equals $16 / 24 = 0.7$ days.

Total cost estimation of the pre-piling method for one substructure is gathered in table 5.6.

Table 5.6: Cost estimation pre-piling method

Pre-piling method	Equipment	Material [t]	Time [days]	Unity price / Day rate [€ / kg, € / day]	Writing-off	Total [k]
Foundation installation	Auxiliary Vessel		2.3	150,000		€ 344
	Piling Hammer		2.3	14,000		€ 32
	Piling Template	200		4	50	€ 16
	WROV		2.3	10,000		€ 23
Substructure installation	Heavy Lifting Vessel		0.7	300,000		€ 200
	Grouting Equipment		0.7	50,000		€ 33
						€ 648

As can be seen in both tables above, the expectation is that the cost is less in case of the pre-piling method. In this case there is only looked at installation of a single substructure. In case of installation of multiple substructures it is expected that the same trend is perceived. Therefore is chosen for a foundation connection with a pre-piled method.

6. Structural Design

Coming chapter goes further in the structural design of the substructure. Starting points are the design basis of chapter 2 and the concepts evaluation in chapter 4.

The first section expounds the structural analysis that is applied to the concepts. Section 6.2 is the outcome of the analysis in the form of preliminary designs. This is followed by an appraisal on primary criteria.

Section 6.3 goes further into the more extensive analyses that are done to the reference design and improvements to these analyses. Next are modification proposed in section 6.4 for the designs of the substructure. These optimised designs are shown in section 6.5 and called definitive design. However the designs are far from definitive, this term is used to illustrate the design development process.

6.1 Static in-place analysis & natural frequency check

The preliminary designs are based on a static in-place analyse and followed by a natural frequency check, referring to section 2.2.1. The parameters and loads are derived from chapter 2 and Appendix A. As said in 2.6.2 the loading angle of wind and wave are assumed to be in the same direction. Figure 6.1 and figure 6.2 show the attack direction of the loads that are considered for the substructures concepts. In appendix A.3 all the load combination are expounded.

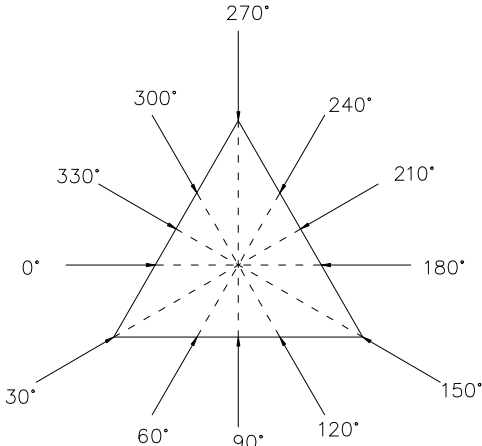


Figure 6.1: Load angle for trilateral substructure

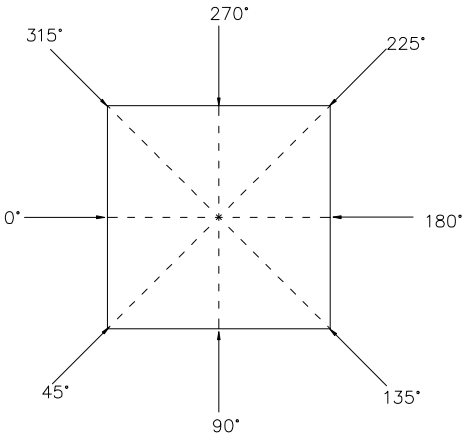


Figure 6.2: Load angle for quadrilateral substructure

Because the preliminary designs are only analysed by a static in-place analyse, a Dynamic Amplification Factor (DAF) is used to estimate the dynamic effects (Section 2.1). A DAF of 1.0625 is applied to the wave and current loading to take into account dynamic amplification including inertia effects. This is based on the calculations done to the reference design (7). No fatigue analysis has been executed in this phase.

In the SACS software the static in-place analysis is performed in one step:

A. Linear static analyse

Loads in the geometric model, including dead loads and turbine loading, is combined with sea state loading in correct load combinations. Interaction with the pile foundation is linearized. Analysis solved by FEM, resulting in member forces, stresses and unity checks.

This analysis is followed by an autonomous analysis to determine the natural frequencies. This is done in three steps.

B. Natural Frequency Check

1. Creating super element

The foundation piles are modelled as super element. In this super element the foundation piles are put in a stiffness matrix for supplement in the FEM software. For the preliminary phase only geotechnical dataset 1 is used.

2. Creation of seastate model

The purpose of step 2 is to integrate the geometrical model with applied environmental loading. Applied dead loads, like transition piece and turbine are transmitted in the geometrical model.

3. Determination of mode shapes

The mode frequency analysis is used for natural frequency and mode shape determination. The foundation supplement of step 1 is integrated in the global stiffness matrix. The equation of motion for an undamped system is:

$$[M]\{\ddot{u}\} + [K]\{u\} = \{0\} \quad (6.1)$$

$[M]$ = Structure stiffness matrix

$[K]$ = Mass matrix

$\{u\}$ = Excitation

For a linear system, free vibrations will be harmonic of the form:

$$\{u\} = \{\varphi\}_i \cos \omega_i t \quad (6.2)$$

$\{\varphi\}_i$ = eigenvector representing the mode shape of the i^{th} natural frequency

ω_i = i^{th} natural circular frequency

t = time

Thus, equation (6.1) becomes:

$$(-\omega_i^2 [M] + [K])\{\varphi\}_i = \{0\} \quad (6.3)$$

This equality is satisfied if either $\{\varphi\}_i = \{0\}$ or if the determinant of $([K] - \omega^2 [M]) = 0$

The first option is the trivial one and therefore not of interest. The second one gives the solution:

$$|[K] - \omega^2 [M]| = 0 \quad (6.4)$$

This is an eigenvalue problem which may be solved for up to n values of ω^2 and n eigenvectors $\{\varphi\}_i$ which satisfy (6.3) where n is the number of degrees of freedom. The eigenvector associated with multiple eigenvalues are evaluated using initial vector deflation by Guyan orthogonalization in the inverse iteration procedure.(28)

Rather than outputting the natural circular frequencies $\{\omega^2\}$, the natural frequencies (f_i) are output:

$$(f_i) = \frac{\omega_i}{2\pi} \quad (6.5)$$

(f_i) = i^{th} natural frequency (cycles per unit time)

The program creates a common solution file containing normalized mode shapes.

$$\{\varphi\}_i^T [M] \{\varphi\}_i = 1 \quad (6.6)$$

6.2 Preliminary designs

In this section the preliminary design are developed. Goal is to display differences between the chosen concepts. At this stage the same design principle are applied as done to the reference design. Later on, in section 6.4 and 6.5 these principles are reviewed and amenable to improvements.

- Maximise the number of similar brace-chord connection with respect to diameters and angles between the legs and braces. From a fabrication point of view this is preferred with respect to the profiling of the braces.
- All structural main steel is in the jacket faces. (no diamond bracings in the elevation)
- X-braces are preferred in the jacket faces.

In concrete this means that all angles between legs and bracings and internal bracing angles are the same in the whole structure. Furthermore the diameters of the bracings are also kept the same for the whole structure. In order to achieve this, the elevation heights are determined by the calculation in Appendix E.

6.2.1 4-leg battered jacket

This design is equivalent with the reference design in geometrical way. This means that all internal angles are the same and base is 28 meter square and the transition piece on top is constructed as a ten by ten component (Figure 6.3). Further is the design water depth adjusted (Section 2.5). Because of the lower water depth, three elevation and three x-braces are applied. As in the reference design the diameter of the leg is changed in the lowest elevation by a conical segment.

6.2.2 3-leg battered jacket

The 3-leg battered jacket is similar to the 4-leg battered jacket only this concept has three legs. All internal angles are the same. The footprint on the seabed is an equilateral triangle with sides of 28 meter and on top of 10 meter. Because the only three legs are applied, the piles underneath the legs are heavier loaded. The legs contain a conical segment in the second elevation. (Figure 6.4)

During development of this concept is turned out that lowest diagonal braces were very heavy loaded. The main reason was not directly the large loads, but the deflection of the foundation piles due to splitting forces. To prevent very large dimensions of the lower bracings extra horizontal braces are added just above mud line level. The large amount of splitting forces was not noticed at the 4-leg jacket because the loads were divided over four legs.

Adding a horizontal brace is at this stage not applied at the 4-leg jacket, but can be an improvement in later stadium. The horizontal brace can later on also be useful for the onshore transport (Section 8.1.3).

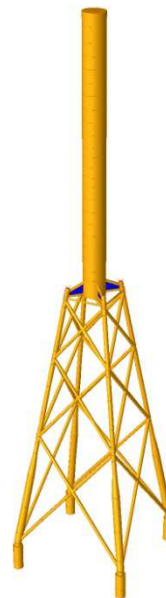


Figure 6.3:
4-leg battered jacket



Figure 6.4:
3-leg battered jacket

6.2.3 3-leg straight jacket

The 3-leg straight jacket is born out of the idea to reduce the complexity of the joints. That's why instead of battered legs, straight legs are applied. As can be seen in figure 6.5 the substructure contains a lower part and upper part. The lower part is an equilateral triangle of 28 meter; the upper part is an equilateral triangle of 14 meter. The upper and lower parts are rotated with respect to each other. The lower part has a height of 10 meter is chosen relative arbitrary. The legs of the upper part have a length of 52.8 meter.

During the development of the 3-leg straight jacket it turned out that a lot of steel was needed to transfer the forces in the upper part to the lower part. Due to the geometry of structure the forces can not follow the sudden widening of the load path to the lower part of the substructure. Therefore a variant was developed for improvement of the results.

In this variant diagonals are added on the outer side of the legs. These are capable to bring over the large horizontal loads to the lower part of the structure. (Figure 6.6)



Figure 6.5:
3-Leg straight jacket

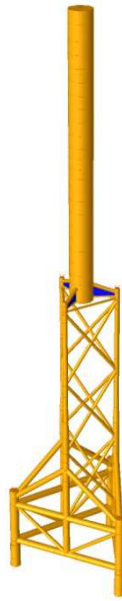


Figure 6.6:
3-Leg straight diagonals jacket



Figure 6.7:
Tripod concept
small base width



Figure 6.8:
Tripod concept
large base width

6.2.4 Tripod

Instead of developing the four leg straight jacket it was decided to develop the tripod concept. Early calculations showed that the four leg straight jacket didn't add any improvement regarding the other jacket concepts. The tripod concept is a different concept with other characteristics which were found more interesting to explore (Figure 6.7 and Figure 6.8).

The tripod concept consists of the triangular base with three diagonal bracing coming to the main leg. The internal angle of the main leg with diagonal bracing is set to 30 degrees because of welding preferences. At the two points where the main leg and other members come together a grouted connection is made. This is favourable to the encountered fatigue damage.

The tripod concept was first set up with a triangle base with 28 meter sides (Figure 6.7). However, because of this base width and the preferred angle of 30 degrees the bracings do not reach to a high point on the main column. This caused very large member sections and above all natural frequencies that were not in range within the boundaries as stated in section 2.2.1.

Therefore is chosen to drop the requirement on the base width and to increase the side width to 45 meter (Figure 6.8). The result is a tripod that satisfies the boundary conditions in term of natural frequency. This is however at the cost of fitting on a standard transport barge.

6.2.5 Results

The preliminary designs presented in previous section have undergone the analyses presented in section 6.1. Three primary results are now considered as primary criteria for further development; self weight of the structure, the natural frequency and the weight of the foundation piles.

Self weight

The most cost-determine property of the substructure is the self weight. The total mass defines the use of material and therefore the material cost. To determine the total weight of the substructure is made use of the material take off function in the software.

Not included in the material take is the secondary steel. Secondary steel contains structures like a seascape ladder, the J-tube and so on. Also not included in this overview are the tower, transition piece, the foundation piles and turbine. This overview only includes the substructure itself.

Table 6.1: Self weight of preliminary designs

Design	Weight [t]
1 4-leg battered	728
2 3-leg battered	722
3 3-leg straight original	1210
4 3-leg straight diagonals	1049
5 Tripod	1306

In table 6.1 can be seen that the battered jackets have the lowest self weight, just as expected in the MCA (Section 4.2). Interesting to see is that the three leg battered jacket contains the same amount of material even with one leg less. Because the loads are less distributed, the members have to be constructed heavier. Looking purely to material use the larger member dimensions undo the advantage of one leg less.

The straight leg original and diagonals jackets are respectively 67% and 45% heavier than the battered concepts. Applying the diagonals do have a positive effect on the self weight, but still the self weight is significant larger. The self weight of the tripod is almost twice as much as the battered jackets, partly due to increased base width.

Natural frequencies

As made clear in section 2.2.1 the natural frequency of the design may not coincide with the rotational frequency of turbine (1P) and the blade passing frequency (3P). If the natural frequency is in the same interval resonance will occur with significant fatigue damage (even failure) as consequence (Figure 2.2).

Figure 6.9 illustrates the natural frequencies of all the preliminary designs that are treated in previous section. The natural frequency is calculated as presented in section 6.1 with 10% weight contingency to account for secondary steel and added weight in next design phase. Below only the first four natural frequencies are displayed, because these are most of interest for interaction with turbine and wave frequencies, the other natural frequencies are larger.

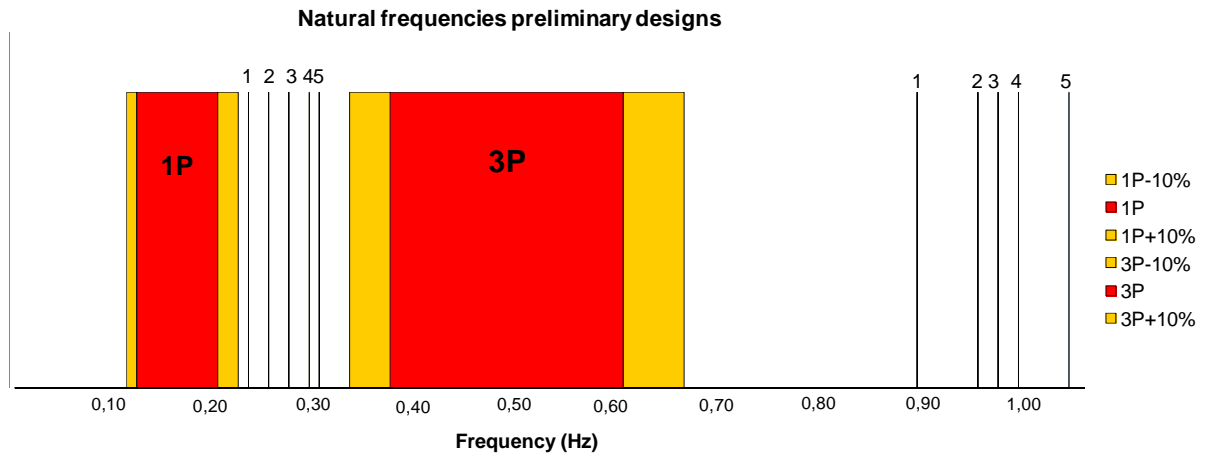


Figure 6.9: Natural frequencies of preliminary designs with respect to turbine loading

Table 6.2: Natural frequencies of the preliminary designs

Design	f_1 [Hz]	f_2 [Hz]	f_3 [Hz]	f_4 [Hz]
1 Tripod	0.235812	0.235820	0.890032	0.890198
2 Three-leg straight original	0.252567	0.252573	0.957920	0.958630
3 Three-leg straight diagonals	0.278221	0.278228	0.970940	0.971603
4 Three-leg battered	0.290115	0.290115	0.996065	0.996705
5 Four-leg battered	0.300959	0.300959	1.044063	1.044063

The disposed natural frequencies of the three-leg jackets raised questions. It was expected that the three-leg jackets would give three equal natural frequencies over the three local principle axis of the jacket. This was not the case though. The reason for this lies in section 6.1, where was said that the eigenvalue problem was solved by the so called Guyan orthogonalization (29). This is meaning that the matrix is solved by two orthogonal eigenvectors. The values given in table 6.2 are the corresponding orthogonal eigenvalues, which are calculated into two orthogonal natural frequencies. The numbers display the mathematical solution rather than what is expected to occur in reality. Though it is checked that one of the given values is actually the natural frequency over a local principle axis of the jacket.

The normalized mode shapes and displacements belonging to above natural frequencies are not reproduced here. Instead is chosen that in section 6.5.1 is dwelled on the corresponding mode shapes of the definitive designs.

The target of all preliminary designs was to fit in the soft-stiff region. This goal is achieved by all preliminary designs. In case of the tripod the earliest design was adapted to not coincide with the frequency of harmonic loading by the turbine.

Except for the ranges of the load frequency of the turbine the wave periods are of important consideration for potential fatigue damage. Figure 6.10 is the same figure as above only then with the relative number of occurrences of the wave frequencies. If the frequency of the design is closer to the frequency of the wave loading this results in a larger excitation (Figure 2.3). This shows that the lower the frequency of the design is the more susceptible for fatigue damage due to waves it is.

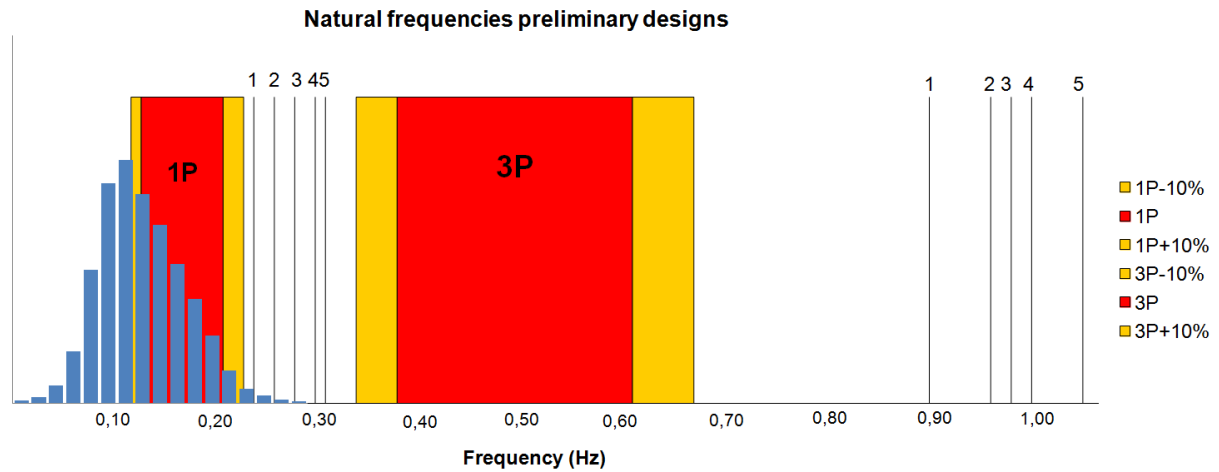


Figure 6.10: Natural frequencies of preliminary designs with respects to wave and turbine loading.

Foundation

Although the substructure weight is probably the most cost determining parameter, the material use in the foundation is of big contribution. In section 4.2 it was assumed that there was no matter of large differences between the concepts. After developing the concepts this can now be checked.

In this phase the pile foundation and soil interaction is only modelled by dataset 1 (Appendix A.2). The first estimation was done by applying piles with a diameter of 96 inch. This is the diameter that was used in the reference design and is one of the largest diameters that are applied in common practice.

The table below indicates the total weight that is now applied in the foundation. In the three leg concepts the piles consist of an upper and lower segment. The upper segment needed an increased wall thickness.

Table 6.3: First estimated foundation pile weight

Design	Length [m]	Nr. of piles	Diameter [in]	Wall thickness [in]	Weight [t]
4-leg battered	50	4	96	2	611
3-leg battered	Upper segment: 15	3	96	3	710
	Lower segment: 55		96	2	
3-leg original	Upper segment: 15	3	96	3	802
	Lower segment: 65		96	2	
3-leg diagonals	Upper segment: 15	3	96	3	802
	Lower segment: 65		96	2	
Tripod	70	3	96	2	642

From this follows that the assumption that the pile foundation would be equal for all concepts is not completely right. Although this table is a good indication, these numbers are very susceptible to the soil data that is implanted. Other soil data will generate a completely other outcome. In section 6.3 also soil dataset 2 is used for better insight in the foundation behaviour.

6.2.6 Evaluation

The results in previous section show that the straight leg concepts (both original and diagonal version) and tripod have a very large self weight. In case of the straight leg jackets the fabrication of less complex joints has to provide a cost reduction that will fade out the increased material cost. A brief assessment distinct that cost reduction due to straight legs will not be enough to clear out respectively 560 ton and 360 ton of the weight difference.

Thereby, looking at the other aspects treated in this chapter there is no advantage found for the straight leg and tripod designs. The natural frequencies are less favourable compared to the other concepts with respect to wave fatigue. Also total foundation weight appeared to be larger. The large self weight will increase the installation cost and will cause more strengthening of the factory site to store all the substructures (something that is left out consideration though).

Then remains both battered concepts. The self weight of the structures is comparable, but the expected weight of the foundation shows a larger foundation weight for the three-leg battered jacket. In next sections this shall be further reviewed.

The natural frequency of four-leg battered concept is slightly favourable for the fatigue of the wave loading, but is closer to natural frequency of the turbine. Considering that the wave loading is larger than the turbine loading the four-leg concept has better behaviour with respect to the fatigue.

Advantage for the three-leg battered concept is the reduced footprint of the structure and moreover a reduction of total number of tubular joints. Because the appliance of one leg less, the total number of joints are reduced by approximately 15%.

On the other hand brings the triangle shape more difficulties regarding the available space on the leg for welding. This can result in unwanted overlap joints of bracings of the three sides.

Hence it is chosen to drop the straight leg concepts and the tripod in favour of both battered concepts. These shall be further developed in next section.

6.3 Dynamic in-place & dynamic fatigue analysis

For further development is gone over to more striking analyses, a dynamic in-place analyse and dynamic fatigue analyse. First a parallel is drawn to methods used for the reference design. After that the applied analysis in this thesis are clarified.

6.3.1 Reference design method

In-place analysis

The original reference design of section 1.3.2 and the preliminary designs of previous section were based on static in-place analyses. Dynamic effects were included in a Dynamic Amplification Factor (DAF). The wind turbine substructure is however a structure susceptible to harmonic wave loading and dynamically turbine loading. The structure natural frequency lies close to the sea state periodic wave load and the period loading due to the turbine. Dynamic responses are inappropriate obviated by applying a DAF. Better approach is then to perform a dynamically analysis. This is done in the further designing. (Section 6.5)

Fatigue analysis

Fatigue failures occur when micro-cracks develop and grow until the material fractures. Such cracks are likely to occur at flaws or inclusions in the material, points of local in homogeneity, and joints with abrupt change in the geometry of the adjacent members. In welded frame structures the welds are be sensitive to fatigue failure.

The fatigue damage is determined using an S-N curve approach combined with appropriate Stress Concentration Factors (SCFs, e.g. for the joints) calculated according Efthymiou. When the S-N curve for the detail under consideration is known, calculation of the stresses that the detail will experience during its lifetime is performed. When all stress variation are known, they can be binned in number of variation n_i per stress range class S_i . Taking the associated maximum allowable number of stress variation N_i for each stress range class S_i from the S-N curve, the Palmgren-Miner rule can be applied. This rule states that the cumulative fatigue damage D_{fat} is equal to the sum of n_i over N_i for all stress range classes.

$$D_{fat} = \sum_i \frac{n_i(S_i)}{N_i(S_i)} \quad (6.7)$$

The Palmgren-Miner rule states that the detail will not fail due to fatigue if $D_{fat} < 1.0$. More fatigue aspects are expounded in appendix A.4.

Total fatigue damage due to wind and wave

The substructure shall experience fatigue damage due to wind and wave loading. Stress response ranges due wind and wave will both determine the total fatigue damage. The method used in the reference design completely separate the fatigue due to wind and wave. The total fatigue damage is calculated simply as a summation of the fatigue damage due to aerodynamic loading (D_a) and the damage due to hydrodynamic loading (D_h). However, in this case the stress response due to combination of aerodynamic and hydrodynamic loading is not considered. The total stress ranges due to both loadings is larger than when the loads are considered separately. Therefore the fatigue damages cannot just simply be added up. These values will generate a too optimistic fatigue lifetime as shall be shown in figure 6.16. A better approach is presented in section 6.3.3.

$$D_{fat} \neq D_a + D_h \quad (6.8)$$

Deterministic versus stochastic

The fatigue analysis performed to the reference design was based on deterministic method. In case of a deterministic method, the ocean environment is described by a series of deterministic individual waves. These are periodic waves with a particular height, period and direction, and an associated number of occurrences. Such periodic waves are merely an abstraction of reality for analysis purposes and do not attempt to produce a realistic representation of the features of wave in a real sea. Therefore the deterministic method is not suitable for application to dynamically structures.

Therefore is chosen to adapt the fatigue method to a probabilistic determination using a dynamically spectral analysis method.

6.3.2 Dynamic in-place analysis

In spectral analysis method, a sea state is represented by a two-parameter wave frequency spectrum. For this thesis is data used that can be founded in appendix A.4. This spectral description provides the most comprehensive representation of the features of wave in real sea. The description contains the random nature as well as the frequency content of a real sea. As a result of this it is able to realistically model the effect of wave frequency on applied wave action and structural response. The spectral procedure is therefore suitable for dynamically responding structures.

For fatigue analysis, a wave spectrum is chosen that is representative of the average distribution of wave energy over wave frequency for a large number of sea states. In this case is chosen for the JONSWAP spectrum.

In total five steps are performed in the FEM software for the analysis.

1. Creating super element

In step 1 the foundation piles are modelled as a super element. In this super element the foundation piles are put in a stiffness matrix for supplement in the FEM software. This has been done for both soil-pile datasets.

2. Creation of sea state model

3. The purpose of step 2 is to integrate the geometrical model with applied environmental loading. The weight combinations defined in order to run analysis for determination of the mode shapes and corresponding dynamic effects.

4. Determination of mode shapes

Goal of step 3 is to extract the mode shapes. The P-delta effect (appendix A.2) is included in determination of the mode shapes. The foundation stiffness matrix is included for extraction of the mode shapes.

5. Generate dynamic (wave) response

Step 4 includes the dynamic (wave) response in the in-place analysis. The included dynamic response is due to 35 mode shapes. The total generated participated mass in all designs was then found to be at least 95%.

6. Static analyses

In step 5 the wave responses are imported in the static analyses to calculate the dynamical internal forces, resulting in stresses and UC's.

6.3.3 Fatigue analysis (30)

To calculate for the fatigue damage in the design process, the offshore wind turbine is subjected to all possible wind and wave combinations and the stresses at relevant locations in the structure are determined. It is recognized that next to operational and idling load cases (non-producing states with unlocked rotor) also turbine start-up and stoppages and pile driving activities contribute to the total fatigue damage. These cases can be analyses separately and added to the total fatigue damage. They are not considered in this thesis.

Preferably all load combination of wind and wave with their direction are incorporated in the fatigue check. But as the number of load is usually very large, it was desired to use a reduced number of load cases. This is achieved by assuming that all loads act in the same direction. This approach is conservative as it leads to an accumulation of fatigue damage in a single location on the circumference of the pile. This is only valid for in the power production state. For idling states wind-wave misalignment may result in higher loads than when wind and waves are aligned. The main reason for this is the lack of aerodynamic damping. (See hereafter in this section).

Frequency domain versus time domain method

To calculate the fatigue damage, several methods exist in the time domain and the frequency domain.

Time domain approach is the generation of random time series from wind and wave spectra in a non-linear unsteady system simulation by time step integration techniques and allocated counting of stress ranges.

Frequency domain approach is the direct application of the environmental spectra in a linear spectral analysis and determination of stress range distribution from the spectral moments.

Application of the integrated, non-linear time domain simulation approach, can potentially lead to more cost-effective and reliable design solution for offshore wind turbine substructures. The high computational effort associated with the fatigue analyses of the simultaneous aerodynamic and hydrodynamic response of the support structure in the time domain is, however, not compatible with the iterative nature of this stage of the design process. Therefore a frequency domain method is used.

Fatigue damage calculation

The core of the fatigue calculation method used in this thesis is the separation of wind and wave response of the substructure. The only interaction between turbine and substructure is the aerodynamic damping. (5)

In (30) a method is demonstrated how the results of separate analyses of wind and wave induced fatigue can be combined in a convenient way which account for the two effects of partial cancellation of wind and wave responses and aerodynamic damping of the wave response. Figure 6.11 compares a simplistic superposition neglecting both aspects, to one the simplified approach for determining the total fatigue damage equivalent. The next paragraphs amplify the used fatigue damage method incorporating the aerodynamic damping and the partial cancellation due to random phase relation between wind and wave response

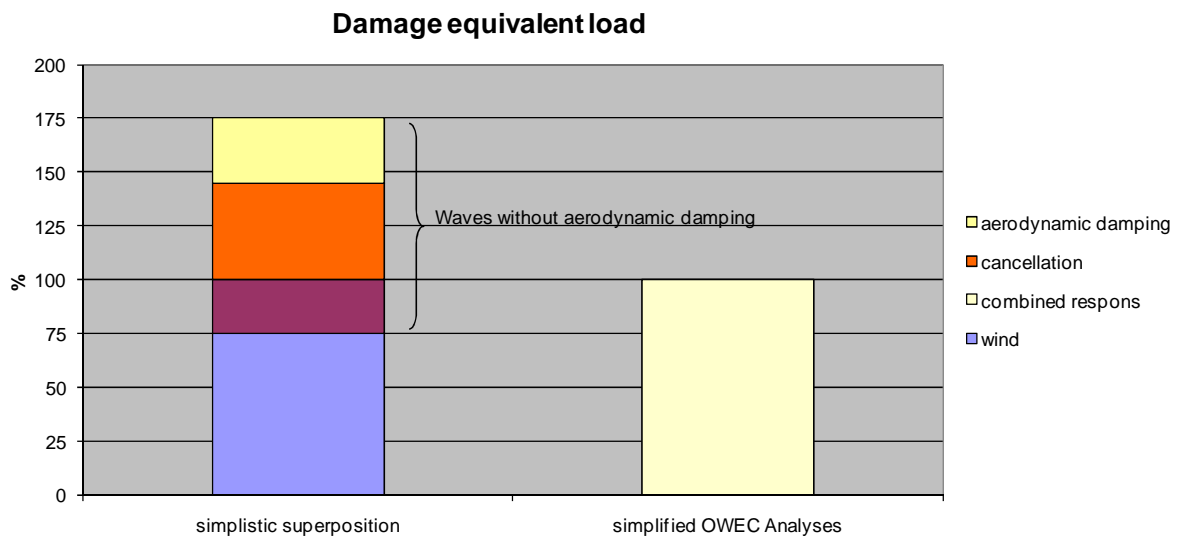


Figure 6.11: Superposition of separate wind and wave fatigue responses (30)

Aerodynamic damping

For an operating RNA the substructure motion and turbine aerodynamics have a significant effect on each other. When the turbine moves forward against the wind, the blades experience an increase in total wind speed. As a result of this increased wind speed, the instantaneous tower top load is increased through basic aerodynamic action of the blades. This load is acting against the tower top motion. For backward motion, the situation is analogous, now resulting in a reduced tower top load, also reducing the tower top motion. This effect known as aerodynamic damping can be incorporated in the model of the substructure as additional viscous damping. (5)(30)(31)(32).

For accurate approach the aerodynamic damping needs to be calculated for all wind speed classes and must be incorporated in the dynamic model of the substructure through an additional damping.

Unfortunately the aerodynamic damping per wind speed is not a generally accepted turbine characteristic that is published in the turbine technical specification sheet. In this thesis for power production cases where wind and wave are aligned, the aerodynamic damping is set at 4% of the

critical damping. The total applied total damping is 4.5%, i.e. 4% of aerodynamic damping and 0.5% of structural damping. (33)

This figure is based on the outcome of methods presented in (5) and (32). The variation of wind speed is neglected.

Figure 6.12 display the overturning moment and the shear wave response due to an added aerodynamic damping to the reference design. The overturning moments and shear are the result of wave loading with a frequency that equals the natural frequency of the substructure. Referring to figure 2.3 the graphs below shows values situated around on the peak of this figure. It can be seen that the static wave response in both cases is the same and the dynamic wave response is reduced.

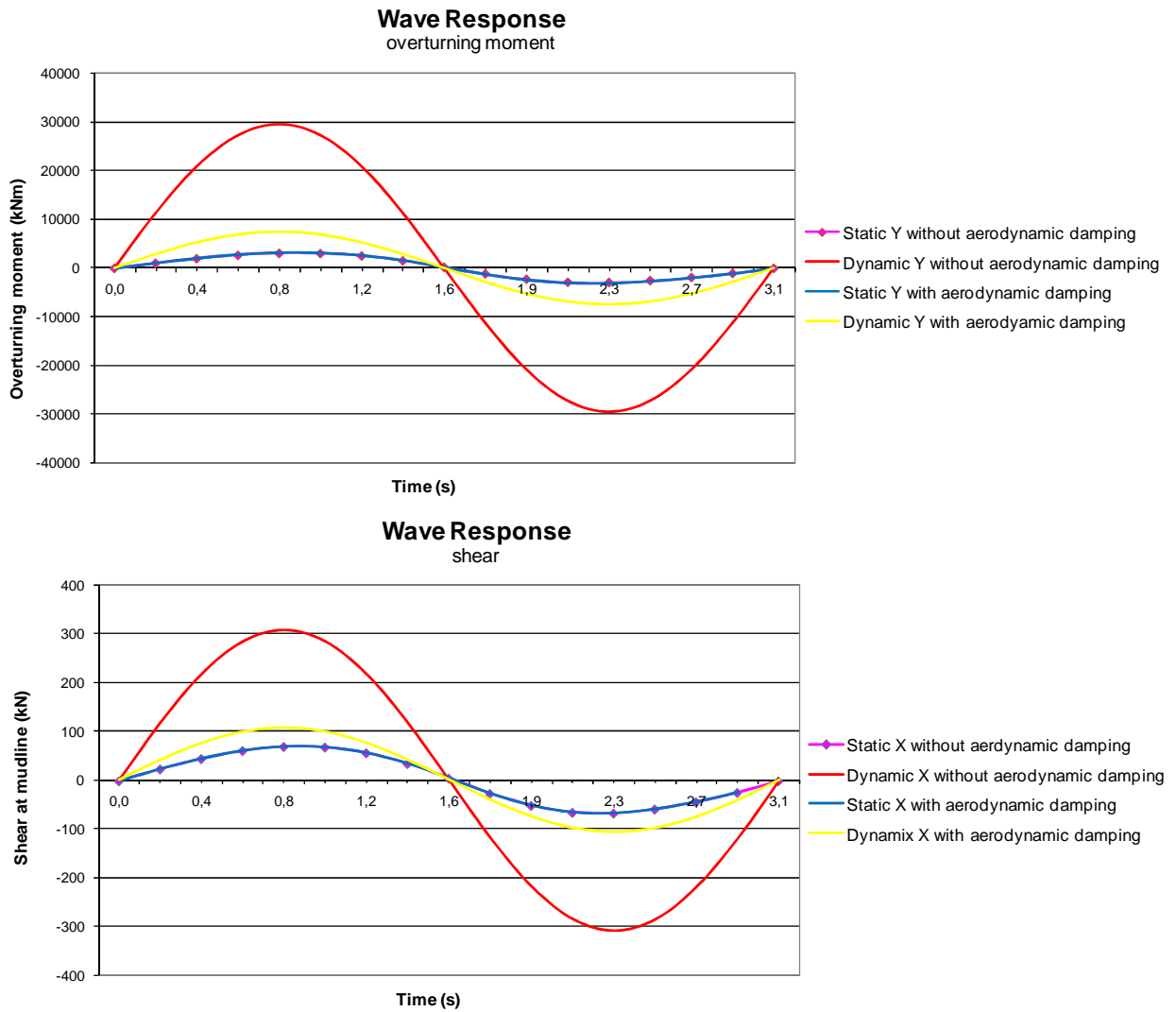


Figure 6.12: Wave response due to aerodynamic damping

As declared in section 6.1 is the natural frequency calculated by solving equation (6.1). This is however based on an undamped system. For a damped system equation (6.1) becomes:

$$[M]\{\ddot{u}\} + [c]\{\dot{u}\} + [K]\{u\} = \{0\} \tag{6.9}$$

As a consequence of additional damping by the turbine it can be questioned if equation (6.9) is a better approach for determination of the natural frequency. The effect of aerodynamic damping on the natural frequency analysis is not further considered here.

Based on (28) it is find that the used software is not using equation (6.9). Other software, like ANSYS (34), has build-in algorithm to incorporate damping effects in het natural frequency analysis.

Superposition of fatigue loading

After establishing the wind and wave contribution to the simultaneous response, the question is how to combine the results of two separate fatigue analyses. Unfortunately, the turbine manufacturer is reluctant to share turbine details and shares only typical bits of information such as damage equivalent loads, a summary of his fatigue analysis procedure, which only can be used for estimating purposes. Nevertheless is in this case the superposition of damage equivalent fatigue stresses identified as most suitable (30).

Damage equivalent fatigue stresses refer to damage equivalent constant amplitude fatigue loads with the same reference number of cycles. These quantities are a compact and characteristic representation of the fatigue loads which are obtained conveniently in the frequency domain.

For S-N curves with a constant slope such an equivalent stress range ($\Delta\sigma_{eq}$) depends only on the slope parameter (Wöhler coefficient μ), the range distribution of cycles ($n^*\Delta\sigma_i$) and an arbitrary reference number of cycles. In this case is chosen for number that is given by the turbine manufacturer ($N_{ref}=2.00E8$). This is based on the total number of rotor revolution during the design life, thus the total number of stress cycles during the design life.

$$N_{ref} = \frac{T_{design\ life}}{T_p} = \sum_j n_j \quad (6.10)$$

The equivalent stress range due to an arbitrary dynamic loading can be determined using the following formula.

$$\Delta\sigma_{eq} = \sqrt[\mu]{\frac{n_{total}}{N_{ref}} \int_0^\infty p(\Delta\sigma) \Delta\sigma^\mu d\Delta\sigma} = \sqrt[\mu]{\frac{1}{N_{ref}} \sum_j \Delta\sigma^\mu * n_j(\Delta\sigma_j)} \quad (6.11)$$

For a bi-linear S-N curve, like in the ISO standard, the equivalent stress range is calculated from the inverse S-N curve $\Delta\sigma(N)$ as function of the damage (D_i).

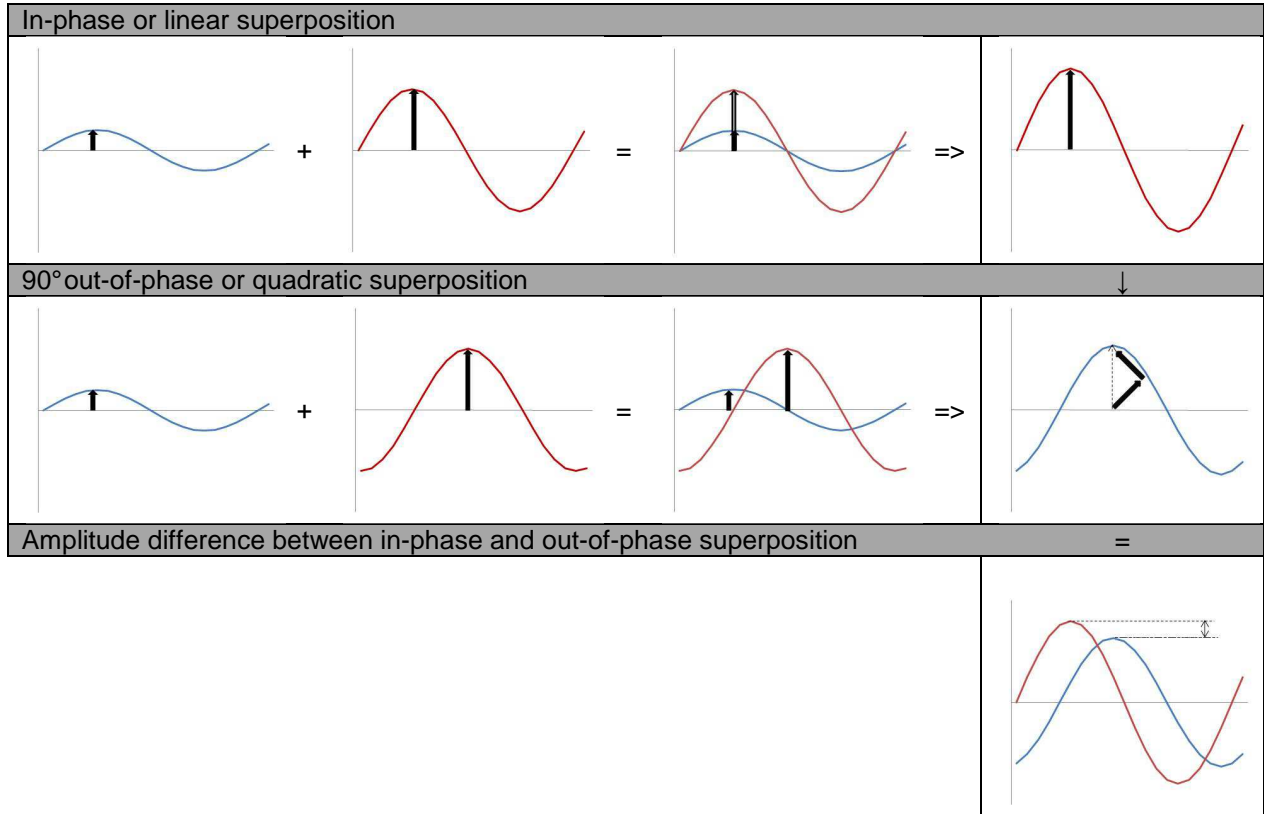
$$\Delta\sigma_{eq;i} = \Delta\sigma\left(\frac{N_{ref}}{D_i}\right) \quad (6.12)$$

In various technical disciplines sometimes damage equivalent, constant amplitude fatigue loads with the same number of cycles are arithmetical combined. If nothing is known on the phase relation, an in-phase superposition summation of the load magnitude provides a conservative estimate for the combined fatigue loading. (Figure 6.11 left and Table 6.4 upper).

An alternative superposition technique that account for the partial cancellation owing to the random phase relation between wind and wave is developed in (30). Here is proven that the 90° out-of-phase superposition or square root of the sum of the squares (quadratic summation) of equivalent stress ranges is valid for determining the total equivalent stress range due to wind and wave. (Figure 6.11 right and Table 6.4 lower)

$$\Delta\sigma_{eq;ah} = \sqrt{\Delta\sigma_{eq;a}^2 + \Delta\sigma_{eq;h}^2} \quad (6.13)$$

Table 6.4: In-phase versus 90° out-of-phase superposition of harmonic signals



By using the S-N curve the corresponding number of stress ranges ($N_{eq;ah}$) can be determined as consequence of the total equivalent stress range $\Delta\sigma_{eq;ah}$. The total equivalent damage is then given by:

$$D_{eq;ah} = \frac{N_{ref}}{N_{eq;ah}} \quad (6.14)$$

The whole process to determine the total fatigue damage due to wind and wave can best be summarized by figure 6.13 t/m figure 6.15.

Figure 6.13: Determining of equivalent stress range due turbine fatigue damage

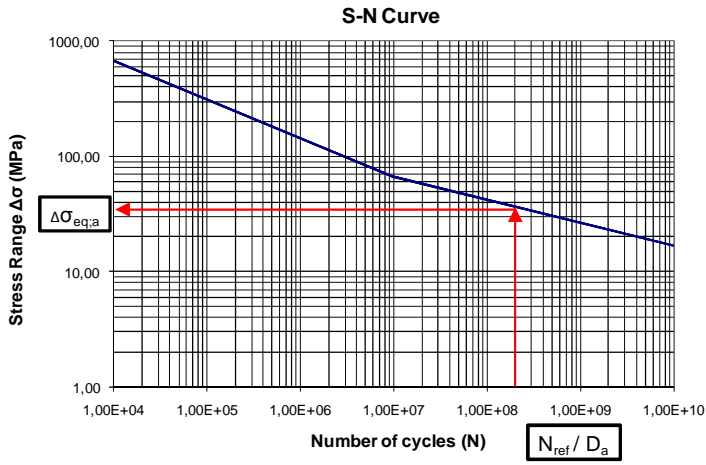
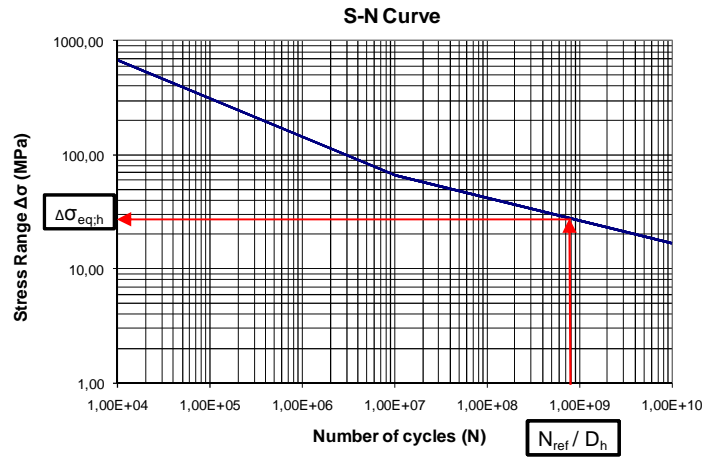


Figure 6.14: Determining of equivalent stress range due to wave fatigue damage



$$\Delta\sigma_{eq;ah} = \sqrt{(\Delta\sigma_{eq;a})^2 + (\Delta\sigma_{eq;h})^2}$$

S-N Curve

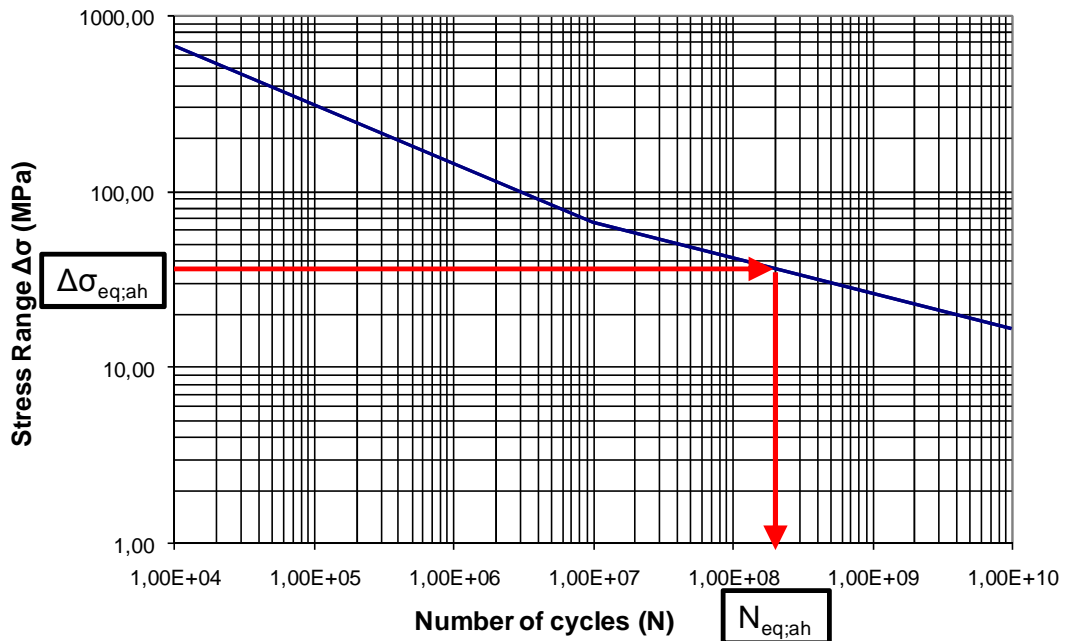


Figure 6.15: Determining equivalent number of stress ranges

$$D_{eq;ah} = \frac{N_{ref}}{N_{ah;eq}}$$

Steps by software

Before the previous explained procedure can take place the damage due to wind and wave separate have to be determined. The turbine and wave fatigue are calculated in autonomous runs.

A. Damage due to wave loading

The first three steps are similar to the analysis of the dynamic in-place analysis (Section 6.3.2).

In step four is the aerodynamic damping incorporated and in step 5 is the fatigue damage calculated.

4. *Generate Dynamic Response*

Step 4 includes the dynamic wave response including the aerodynamic damping. Outcome is the jackets potential structural reaction on waves of different incoming angels and different periods.

5. *Spectral Fatigue Damage analysis*

The scatter diagram included in appendix A.4 is implanted in the last step. Spectrum of JONSWAP is used for distribution of the wave frequencies. The fatigue damage is calculated according the appropriate S-N curves.

B. Damage due to turbine loading

1. *Creation of common file*

Basically are in this phase the equivalent loads of the turbine as given in appendix A.1 implanted in the structural response. Outcome is the potential structural reaction on the turbine loading.

2. *Deterministic fatigue damage analysis*

The number of occurrences of the turbine loading is input. It is chosen to divide the turbine loads equally over the directions given in figure 6.1 or figure 6.2. The fatigue damage is calculated according the appropriate S-N curves.

The total fatigue damage is now superpositioned as presented earlier in this section.

Fatigue approach comparison

As stated section 6.3.1 the determination of the total fatigue damage of the reference design is considered too optimistic. This is graphically shown in figure 6.16. The fatigue damage for tubular joints is shown for the method that is applied to the original reference design and compared to the fatigue calculation as presented in previous paragraphs. From here it is chosen to follow the approach that presented in the past paragraphs.

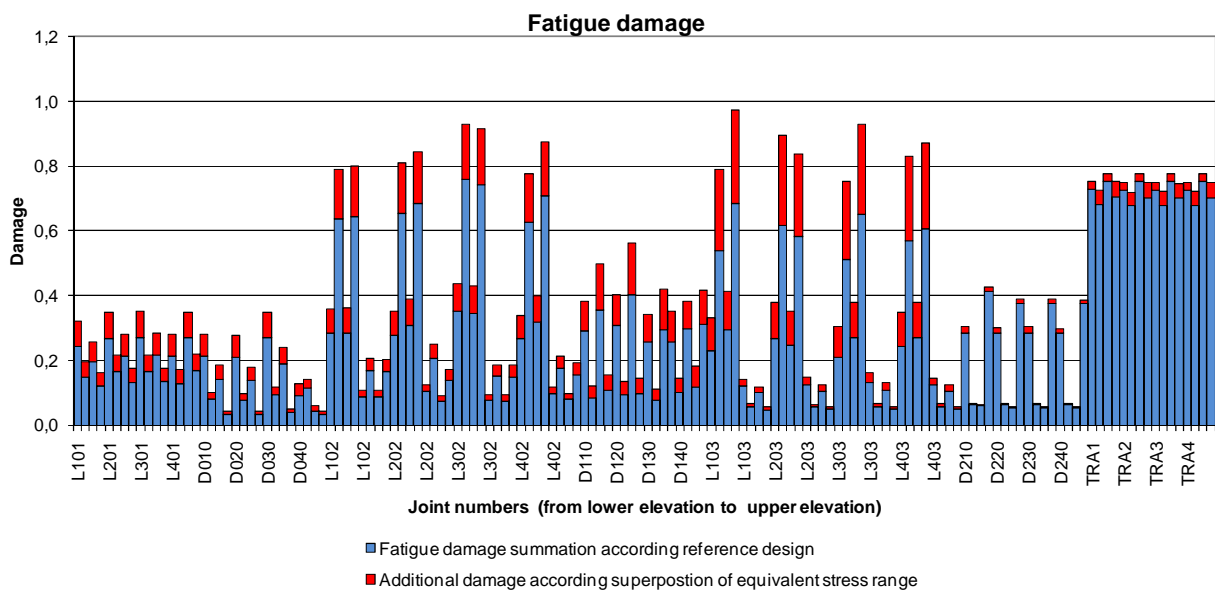


Figure 6.16: Difference between fatigue approaches

6.4 Modifications

In section 6.2 was decided to continue with the three-leg battered jacket and the four-leg battered jacket. Working to the definitive designs several modifications are applied.

Adjustment of the footprint in section 6.4.1 is only applied to the four leg jacket, to fulfil the boundaries conditions as stated in section 1.4.2. Where the rest of the modification in the chapter can be seen as optimisations, this is a necessary adjustment that is also applied to the reference design.

The optimisations are not valid for the reference design itself, because it is desired to make clear the difference between the reference model and the modified models. However a modified design shall be made based on the reference model with the proposed optimisations.

6.4.1 Footprint

In the preliminary design stage geometry of the four-leg (battered) jacket was kept the same as the reference design. No geometrical adjustments were made other than adjusting the total height of the jacket. This however means that this design could not comply with one of the boundary conditions as stated in section 1.4.2. The square footprint with centre to centre distance between the legs of 28 meter does not fit on the defined transport barge. Possible technical adjustments like a special grillage to make this possible are thinkable, but do raise insurance policy issues. Therefore the footprint size has to be reduced to centre to centre distance of 24 meter. This increases the total loads in the piles, because the internal lever arm of the footprint is reduced.

The footprint of the three-leg (battered) structure does not need any adjusted, because they can be rotated in such a way, that they satisfy to fit on the transport barge.

6.4.2 Horizontal brace at mudline level

The battered leg concepts bring along that by vertical loading, like own weight, the legs tend to displace horizontally. The internal force in the legs does have a horizontal vector that is released when the loads are transferred to the piles which are strictly in vertical direction. Horizontal vector has to be taken up by the lower part of the substructure. This can be done by the bracing, but is more effectively done by adding a horizontal brace just above mudline level. The horizontal brace prevents the legs and thus the foundation piles to displace horizontally. This results in less bending moments in piles and legs, and can thus be lighter constructed. This is illustrated by a unity check of the foundation piles with and without the horizontal brace in figure 6.19.

Furthermore is the horizontal brace is opportune in case of the transport of the jacket. This is further elaborated in section 8.1.

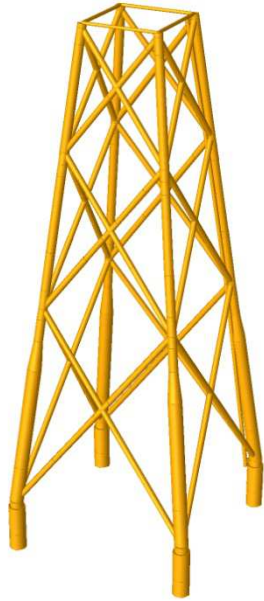


Figure 6.17:
4-Leg jacket without mud level brace

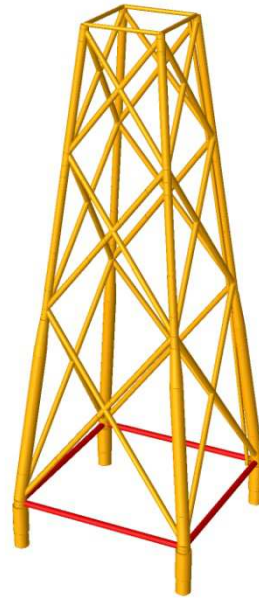


Figure 6.18:
4-Leg jacket with mud level brace

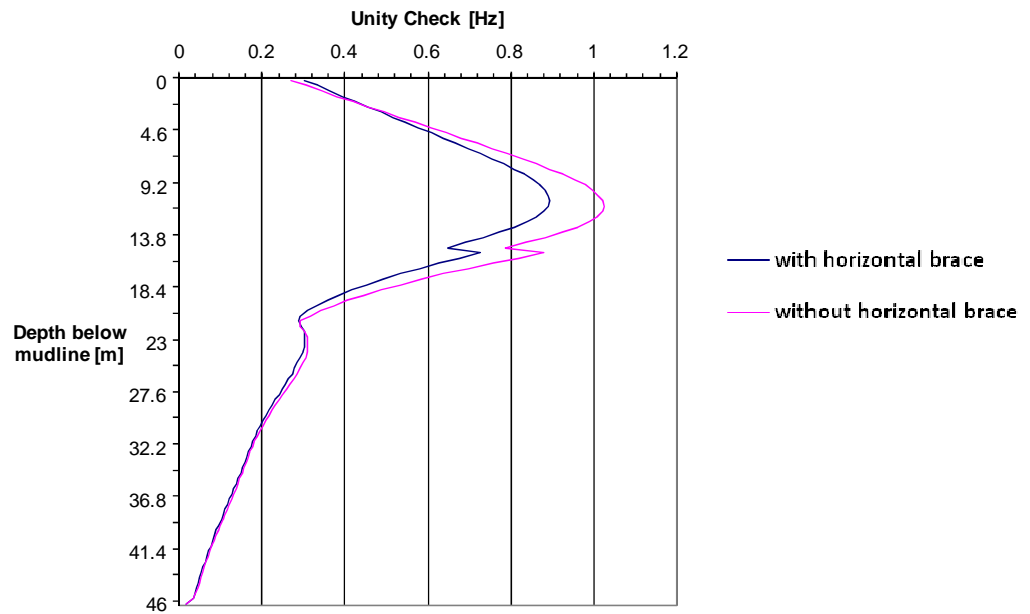


Figure 6.19: Comparison of pile unity check for with or without horizontal brace for soil dataset 2

6.4.3 Other bracing configuration

As stated in the preliminary design phase it was preferred to use x-bracings. This was more or less based on the application in the reference design. Possible optimisation is another bracing configuration. For both concepts the other bracing configurations is considered. Instead of X-bracing, the bracing bay is halved and forms a base for K-joints. Advantage is that an X-joint is avoided, what save at least two welds per elevation of one side. Disadvantage is the increase of the buckling lengths of the bracing elements.

3-leg jacket

An analysis of the modified bracing configuration turned out this configuration does not bring any improvement. The increase of buckling lengths required bigger bracings. Nevertheless was this not the biggest concern. It turned out that the modified bracing configuration was more sensitive for fatigue damage. This is rather logical because the K-bracings of the different sides do not continuous run through the substructure. The load path stops at the leg, for example shown at the joint indicated by the red circle in figure 6.21. That's why joint at the chord of K-bracing is subject of high stress variation during dynamic loading.

Other bracing configuration that able the bracings for continuous load path is impossible in case of three-leg jacket, because of uneven number of sides. Therefore is chosen to stick to the X-braces.



Figure 6.20: 3-Leg jacket with X-braces



Figure 6.21: 3-Leg jacket with K-braces

4-leg jacket

Same strategy to modify the bracing configuration is applied to the 4-leg jacket. In this case the side width is less than in case of the three-leg jacket, 24 meter instead of 28 meter. This means that the increase in buckling length is less governing than in case of the 3-leg jacket. Thereby there are four sides instead of three sides, making it possible to make a continuous path of bracings. See figure 6.23. Consequence is that the legs joints are less subject of stress variations due to dynamic loading and thus less fatigue damage. The internal forces in the bracing can directly be transferred to next set of bracing on the other sides, because of the continuous load path. Indeed the fatigue damage that was occurring at the connection to the legs proved to be less appearing than expected.

Big advantage of this modified design is that fewer welds are necessary, because no intermediate joint is necessary in the bracings. This saves six tubular joint welds per side, compared when X-braces are applied.

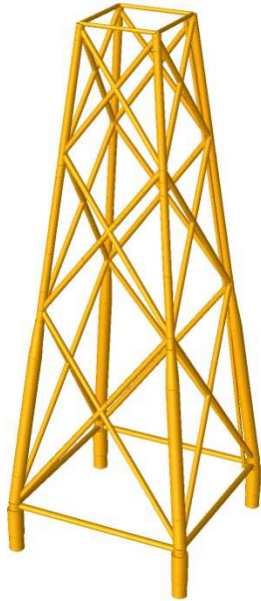


Figure 6.22: 4-Leg jacket with X-braces

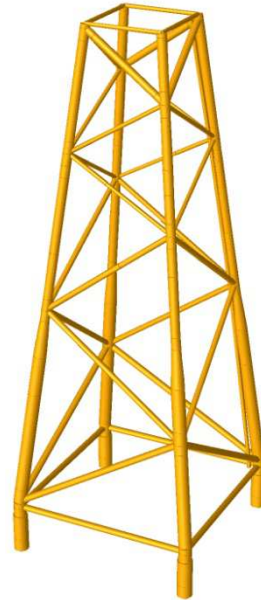


Figure 6.23: 4-Leg jacket with K-braces

6.4.4 Various bracing diameters

In the preliminary design phase the diameter was kept constant in all elevations. Reason was the increase of fabrication simplicity and usage of the same welding templates for all bracings. However in the view of this kind of serial production, this argument is dropped in favour of saving material cost. Templates are subject of wearing and therefore it is not seen as a disadvantage to use multiple templates for the bracings. Therefore the diameter is not constant over the various elevations and optimised to the loading.

6.4.5 S-N Curves

For practical fatigue design, welded joints are divided into several classes, each with a corresponding design S-N curve. All types of joint fall in one of specified classes in a standard depending upon:

- the geometrical arrangement of the detail;
- the direction of the fluctuating stress relative to the detail;
- the method of fabrication and inspection of the detail.

The basic design S-N curve is given as:

$$\log N = \log \bar{a} - m * \log \left(\Delta\sigma * \left(\frac{t}{t_{ref}} \right)^k \right) \quad (6.15)$$

- N = predicted number of cycles to failure stress range $\Delta\sigma$
 $\Delta\sigma$ = stress range
 m = negative inverse slope of the S-N curve
 $\log \bar{a}$ = intercept of log N axis by S-N curve
 t = thickness though which the crack most likely grow
 $t = t_{ref}$ is used for thickness less than t_{ref}
 t_{ref} = reference thickness depending on S-N curve
 k = thickness exponent of fatigue check depending on S-N curve

$$\log \bar{a} = \log a - 2s \quad (6.16)$$

- a = constant relating to mean S-N curve
 s = standard deviation of log N

Tubular joints

For an indistinct reason the reference design used S-N Curves based on the DNV standard. A rather illogical and unpermitted choice given that the in-place analyse was done based on the ISO code. Below are given the differences between the ISO and DNV S-N curves for tubular joints. It can be seen that tubular joints in DNV code are unfavourable compared to the ISO code. No thickness coefficient is applied to the curves below. As put section 2.6.1 the ISO code is followed, which is accompanied which better s-n curves compared to the reference design.

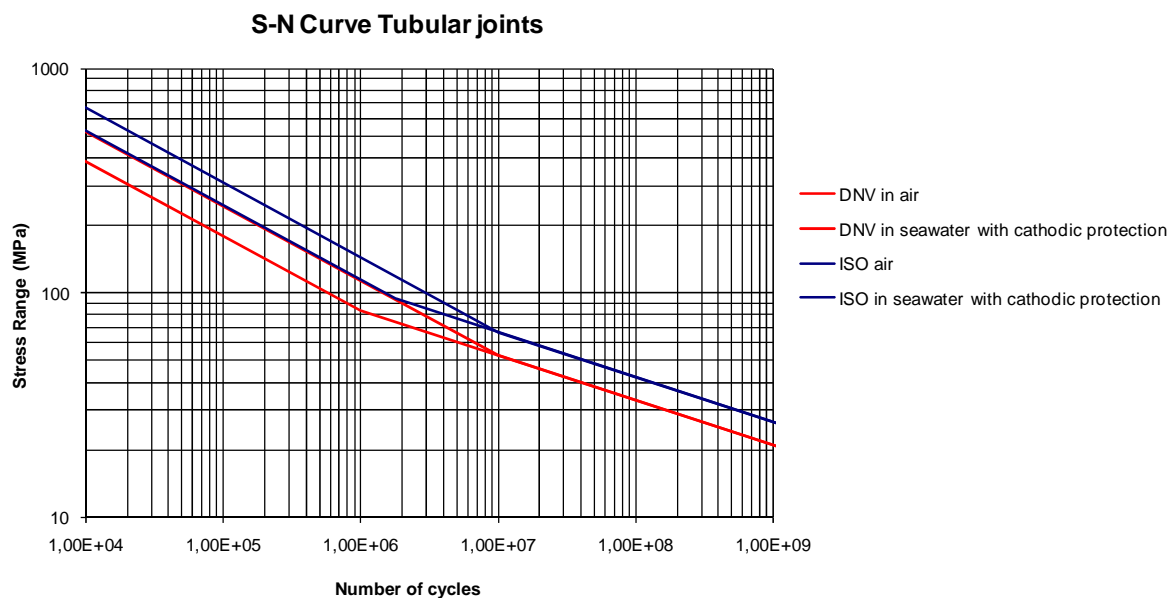


Figure 6.24: S-N curves of DNV and ISO standard

Double sided butt welds

So far it is assumed that all the butt joints were single sided welded. However one of the starting points is that serial production is a key part in fabrication considerations. Therefore it is assumed that all butt welds are welded at the more specialized pipe companies. These specialized companies have equipment that without difficulties can weld butt joints double sided to diameters that are used here (34). The advantage is that this is more favourable for the fatigue damage. The improved S-N curves are shown in figure 6.26.



Figure 6.25: Single sided versus Double sided butt welds

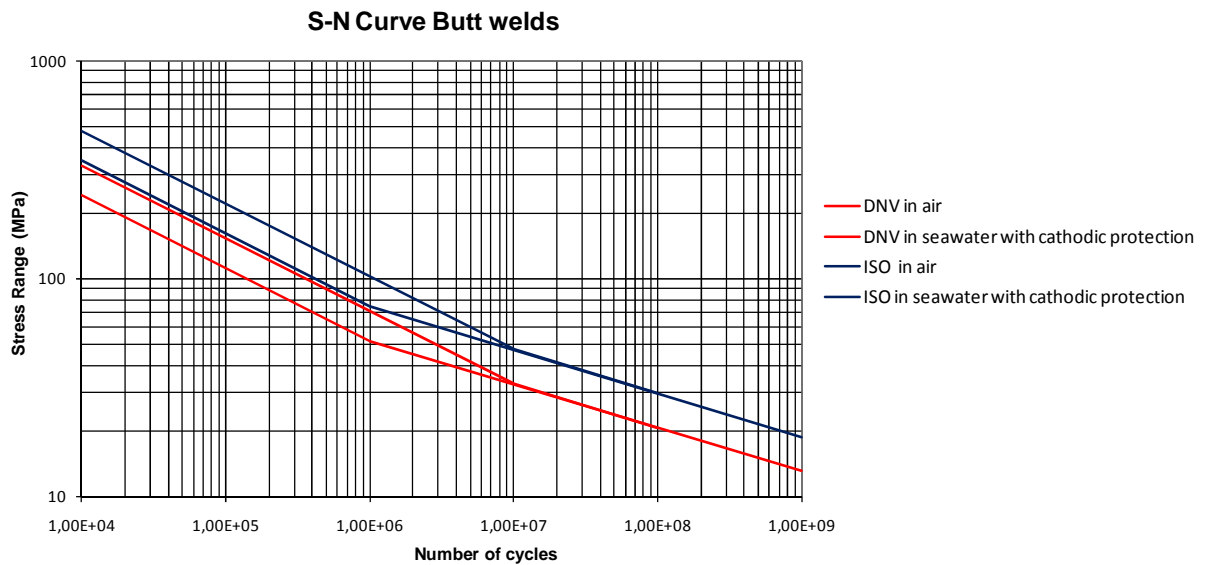


Figure 6.26: S-N curves of DNV single sided weld and ISO double sided weld

Graphs below show the fatigue damage results done by the way as the reference design and the way by the presented modifications. On the horizontal axis the welds are displayed and on the vertical axis the total fatigue damage. The fatigue damage reduction is significant.

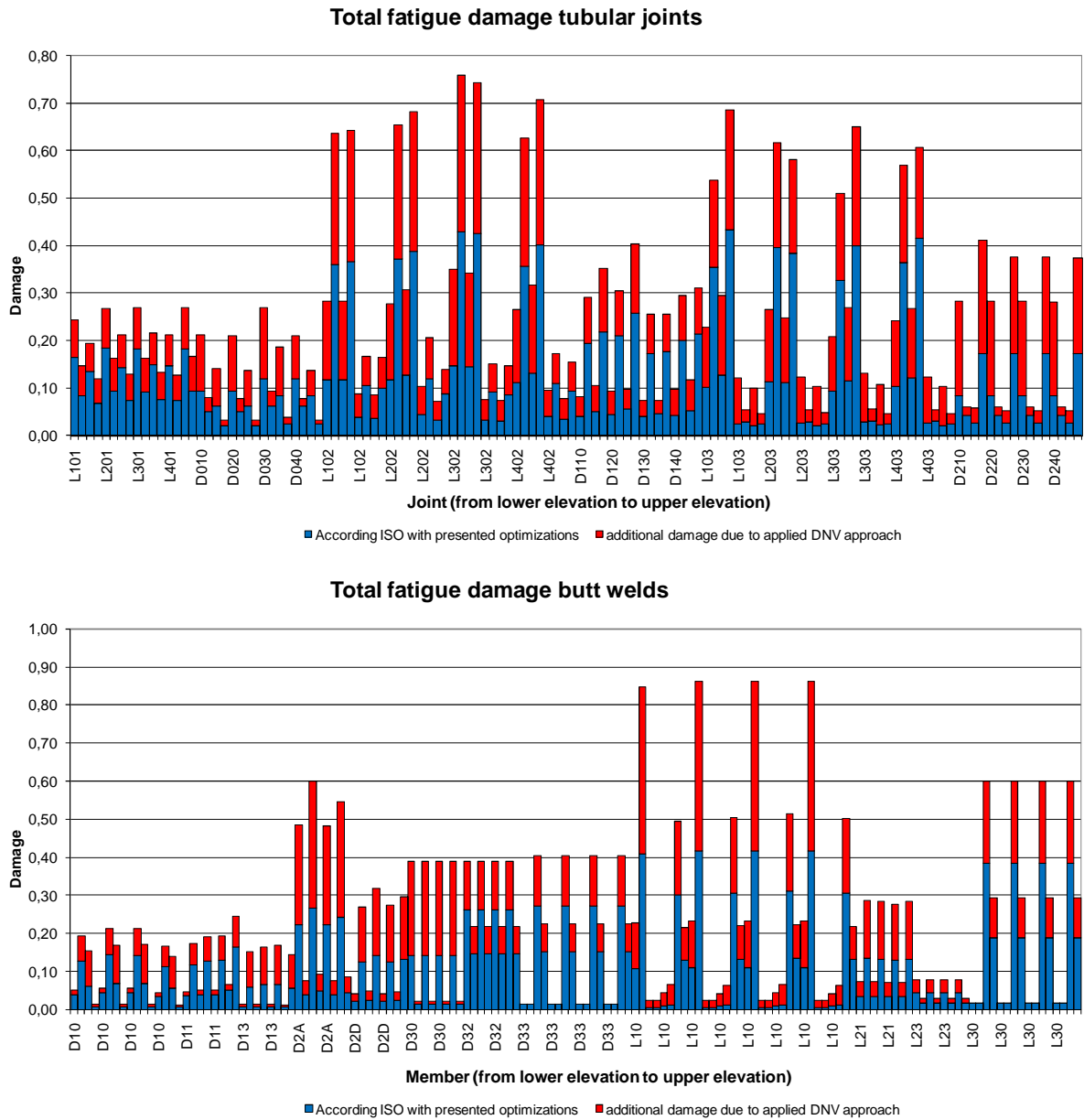


Figure 6.27: Total fatigue damage difference between ISO curves and DNV curves

6.5 Definitive designs

As outcome of section 6.2 to section 6.4 four definitive designs are presented. All four designs have undergone the analyses as described in section 6.3. First design is the reference design where only the footprint is adapted. None of the optimisations are done to this design as this is the reference design and is the base to determine any cost reduction.

Three optimised jackets are presented in figure 6.28. Design number two is the optimised 4-leg jacket with x-braces, followed by four-leg jacket with K-braces and the three-leg jacket.

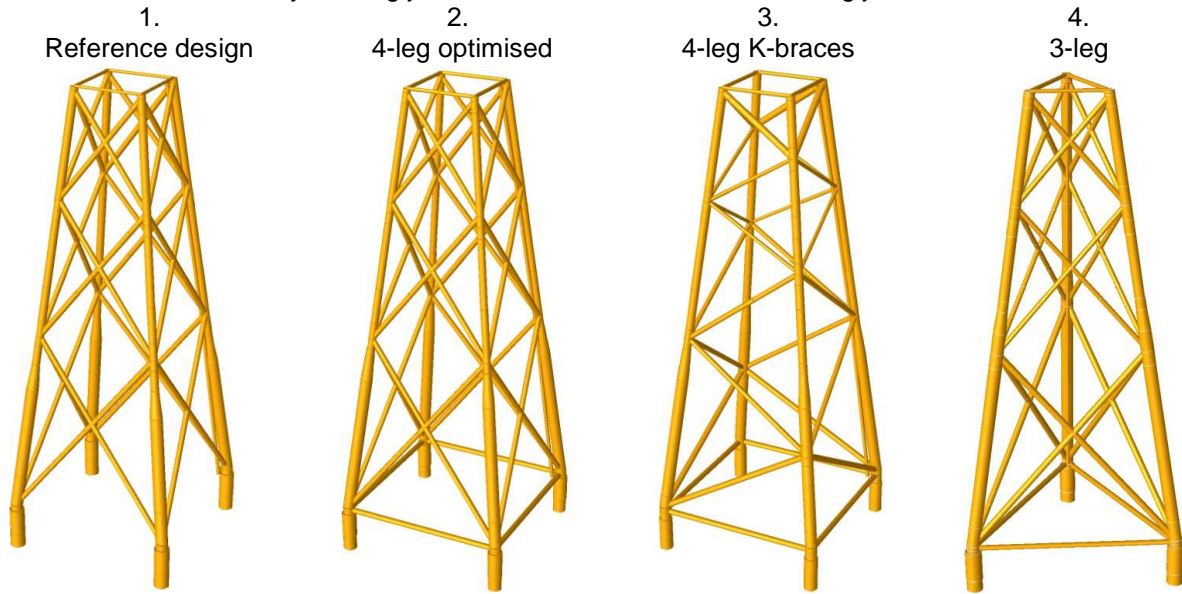


Figure 6.28: Four definitive designs

An abstract of the outcome of the performed analysis is displayed in Appendix G. Example of the performed analysis is the total fatigue damage due to wind and waves. Figure below shows the fatigue damage of both cases of the tubular joints of the lower elevation till the upper elevation of the three-leg jacket design. As expected the main damage in the lower elevation is coming from the wave and in the upper elevation is coming from the turbine.

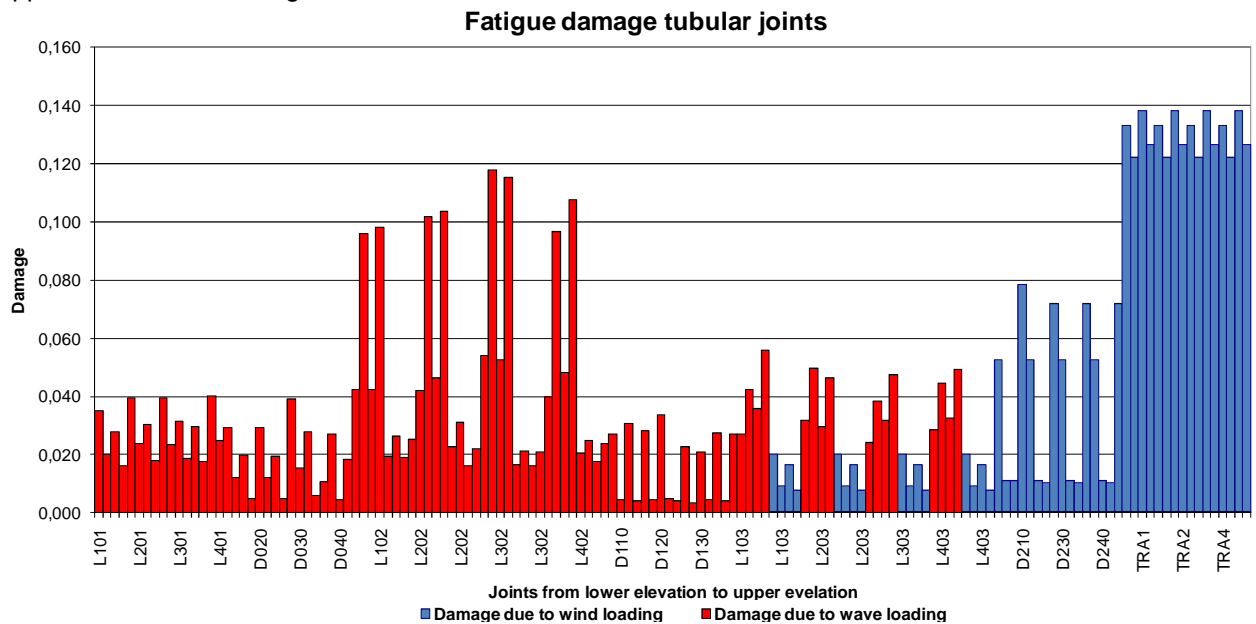


Figure 6.29: Fatigue damage of three-leg jacket

6.5.1 Results

Self Weight

The weights of the substructures are based on a MTO report generated by the software. Compared to the preliminary design phase, the weights have increased. This can be explained by the more extensive and profound analysis performed for this stage. Improvements to the reference design are noticeable and in greater extent for the four-leg K-braces design.

Table 6.5: Self weight definitive designs

Design	Total weight [t]
1 Reference design	777
2 4-leg optimised	752
3 4-leg K-braces	716
4 3-leg	767

Natural frequencies

In the natural frequency analysis a variety of conditions are leading to different natural frequencies, depending on the stiffness and mass properties of the structure considered. These properties are not constant as over time corrosion decrease stiffness, marine growth may accumulate, thereby increasing the mass and water levels may vary leading to different values for added an entrained water mass. For the structure considered, the natural frequency is close to the 3P lower boundary. Therefore it is important to consider the stiffest possible condition, leading to the highest natural frequency.

To this end the natural frequency analysis has been carried out for a foundation with the jacket legs flooded and without consideration of corrosion and marine growth in order to the upper bound natural frequencies, leading to a relatively stiff structure. Soil dataset 2 is used for this calculation.

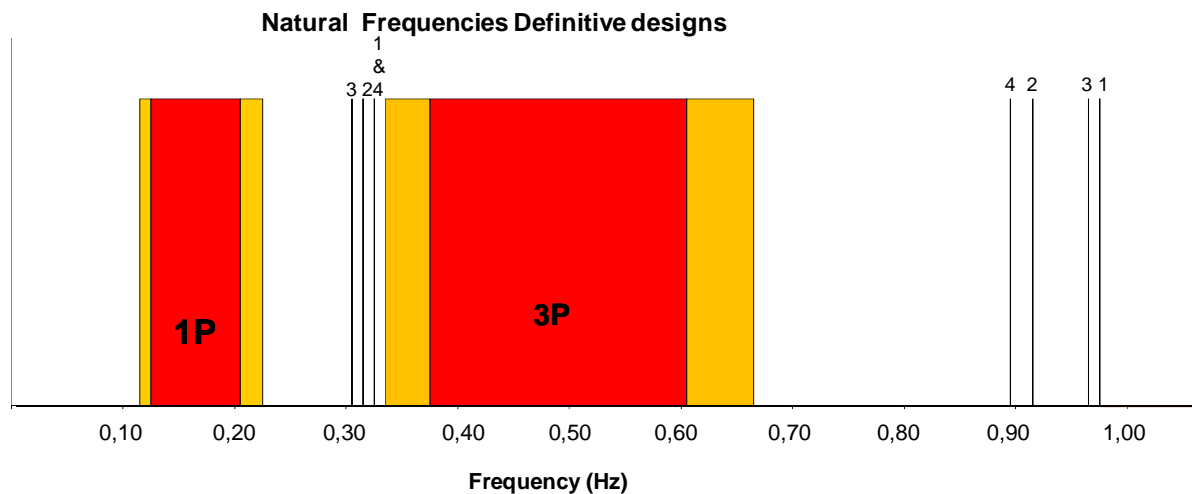


Figure 6.30: Natural frequencies of turbine and definitive design

Table 6.6: Natural frequencies definitive designs

Design	f_1 [Hz]	f_2 [Hz]	f_3 [Hz]	f_4 [Hz]
1 Reference design	0.322656	0.322672	0.972484	0.972643
2 4-leg optimised	0.314198	0.314213	0.914317	0.914445
3 4-leg K-bracing	0.308745	0.314795	0.968765	0.971744
4 3-leg	0.324776	0.324810	0.893537	0.894029

It can be seen that in contrast to the other designs the 4-leg K-bracing design the f_1 is significant different from f_2 and f_3 from f_4 . This can be explained by the asymmetry over 2 sides of the 4-leg K-braces jacket. This is in contrary to the other designs that are symmetrical.

As previously stated in section 6.2.5 the mode shape f_1 to f_4 are the first four solutions of the eigenvalue problem. Whereby f_2 is the orthogonal of f_1 and f_4 the orthogonal of f_3 . For the reference design table 6.7 and figure 6.31 given the mode shapes and corresponding mass participation factors in the global axis of the system. This shows the orthogonality of the mode shapes. Further can be noticed that the first four modes result in mass participation factor of 94% and are therefore the most qualifying mode shape for dynamical analyses. In Appendix F the mode shapes are given for the other designs.

			Mass Participation Factor		Cumulative	
Design	Mode Shape	[Hz]	x	y	x	y
1 Reference design	f_1	0.322656	0.29499		0.29499	
	f_2	0.322672		0.29499	0.29501	0.294951
	f_3	0.972484	0.33296	0.30822	0.62797	0.603180
	f_4	0.972643	0.30841	0.33308	0.93639	0.936262

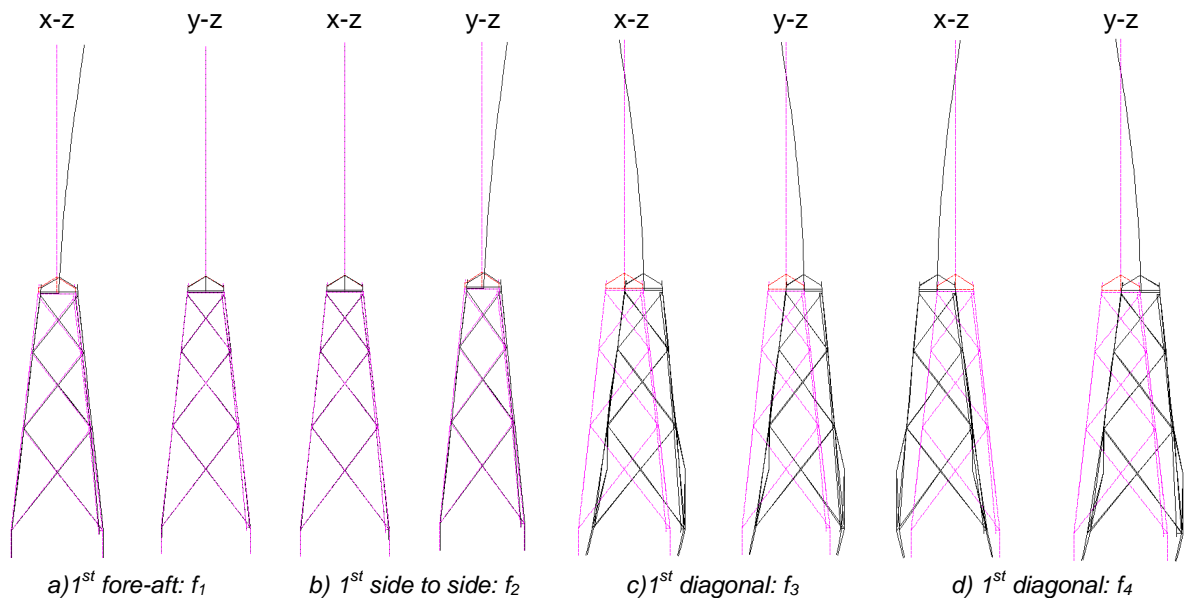


Figure 6.31: First four mode shapes reference design

Modelling of transition piece stiffness

The influence on the dynamics by the stiffness of the transition piece for the reference design is shown in figure 6.32 and figure 6.33. In figure 6.32 the stiffness of the transition piece has been varied plus and minus 30% by changing the Young's Modulus for the elements of the transition piece. The effect on three natural frequencies can hardly be discerned. In figure 6.33 the results for a larger variation of the Young's Modulus are shown. A decrease of the stiffness of the transition piece by a factor 10 results in a decrease of the first natural frequency of 15.0%, a decrease of 1.2% for third mode shape frequency and almost nothing for f_5 . Comparable results are found for the other designs and can be found in Appendix F.

These results show that the transition piece is modelled rather stiff. In reality this structure may be softer, thereby lowering the natural frequencies. It is however expected that it is possible to manufacture a transition piece within the target range as displayed in figure 6.33. A reduction of almost factor 100 will still generate natural frequencies within the chosen boundaries. However, without quantification of the stiffness of a real transition piece no conclusive statements can be made here regarding the accuracy of the modelled transition piece and corresponding fatigue damages. Further research is recommended for the correct stiffness of the transition piece.

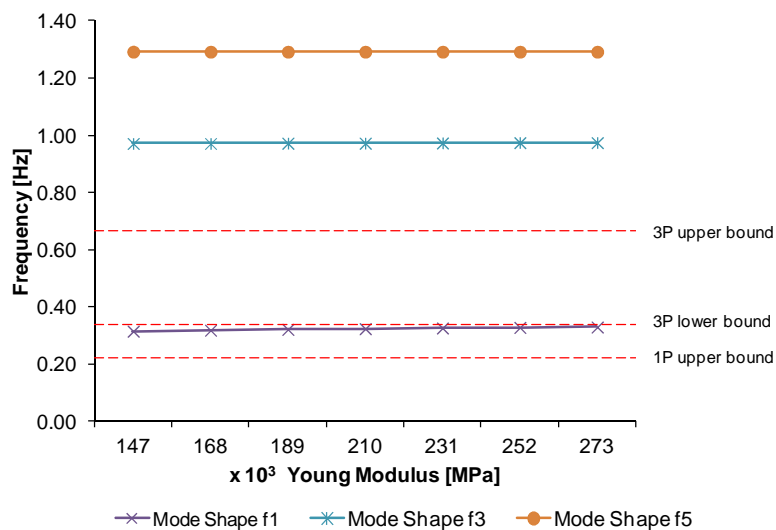


Figure 6.32: influence transition piece stiffness +/- 30% on the natural frequencies

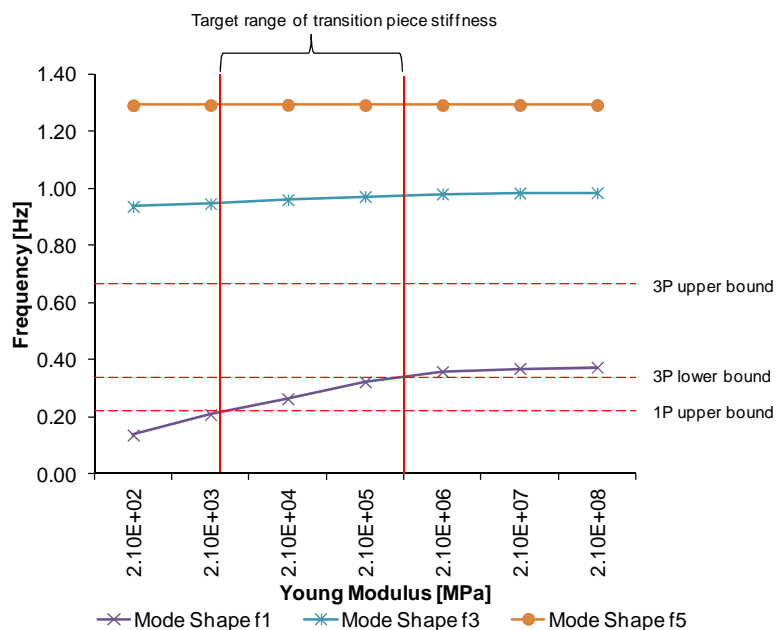


Figure 6.33: Influence transition piece stiffness +/- x1000 on the natural frequencies

Foundation

Two different geotechnical conditions were used for determination of the foundation dimensions. (section 2.4). As expected the soil conditions are of great influence on the foundations dimensions. More details of the soil specifications can be found in Appendix A.2.

Table 6.8: Foundation pile weights

Dataset 1

Design	Length [m]	Nr. of piles	Diameter [in]	Wall thickness [in]	Weight [t]
Reference design	70	4	90	2	797
4-leg optimised	70	4	84	2	748
4-leg K- braces	63	4	84	2	674
3-leg	80	3	90	2	687

Dataset 2

Design	Length [m]	Nr. of piles	Diameter [in]	Wall thickness [in]	Weight [t]
Reference design	45	4	90	2	516
4-leg optimised	45	4	84	2	481
4-leg K-braces	42	4	84	2	449
3-leg	52	3	90	2	447

Compared to the results of the preliminary designs where only dataset 1 was used, the foundation weight for the reference design has increased quite much. This is logical as the footprint has been reduced in section 6.4.1. The foundation of the 3-leg jacket is decreased due to the optimisation pronounced in previous sections.

In chapter 5 is decided to perform the installation in sections. The corresponding pre-piling method is using a grout connection between the jacket leg and the foundation pile. Therefore shear keys are welded on the jacket leg (Figure H.1). For each design this grout connection is designed and checked by the verifications (H.1) t/m (H.6). The complete calculation for the three-leg jacket is included in Appendix H.

Number of tubular joints

Apart from the material cost, the assembling cost is an important cost determining parameter. As first idea of the assembling cost the total amount of tubular joints are given in the table below. The appliance of the K-braces and three legs instead of four legs brings a great reduction of tubular joints. Further assembling issues are considered in next chapter where more meaningful the welding volumes and times are determined.

Table 6.9: Number of tubular joints

Design	Number of tubular joints
1 Reference design	72
2 4-leg optimised	80
3 4-leg K-braces	56
4 3-leg	62

6.6 Evaluation

This chapter brought attention to a better analysis of the substructures. Starting points were the concepts as presented in section 4.2. A static in-place analysis and frequency check resulted in the further research to the three-leg battered and four-leg battered jacket. To this phase a dynamical in-place and dynamical fatigue analysis have been done. After proposed optimisations in section 6.4 the final results of four definitive designs were presented in previous section. It can be seen that the differences between the various jackets are not very large. For better understanding of the deviation between the various designs, they are evaluated in the following chapters where the fabrication, transportation and installation are considered.

7. Fabrication

Subsequent to the structural designing a cost estimation is made of the fabrication of the jackets. The differences between the earlier presented designs are exposed in the total used material, the needed time for assembling and welding. The used values are based on the steel contractor experience and are processed in a simplified calculation for the total cost estimation. First section relates to the fabrication procedure, followed by a cost estimation in the second section.

7.1 Procedure

Because of the highly serial production of the substructure, controlled environmental condition are required for the fabrication. Therefore the fabrication shall be done in a fabrication hall. This contradicts what is often done in the offshore branch, where much jacket fabrication is done outside. Where normally the fabrication is done outside, the assembly of the structure can be done in a vertical way. However, when the assembly is done in a vertical position in a fabrication hall, this would require a massive fabrication hall with height of approximately of 90-100 meter. The investments cost and other technical difficulties make this option impossible to fit in the business case as written. Together with other fabrication issues like safety, lifting of loose parts and manoeuvrability this implies that the assembly of the substructure shall be done in a horizontal position of the substructure.

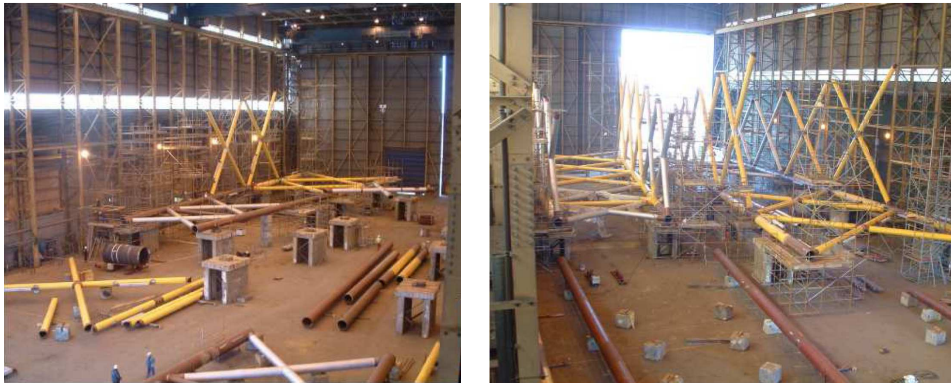


Figure 7.1: Stages in the fabrication of Beatrice jacket

Specialized companies in steel tubular components are far more cost-effective in producing tubular members (34). Therefore is assumed that the standard tubular components are brought in from these specialized companies. Subsequently the tubular members are bevelled for a proper junction between the tubular connections. To secure the right position of tubular members all welding is done by welding templates.

Much of the fabrication cost of the four-leg jackets and the three-leg jacket is affected by the two different assembling procedures. Figure 7.2 shows the two different assembling procedures.

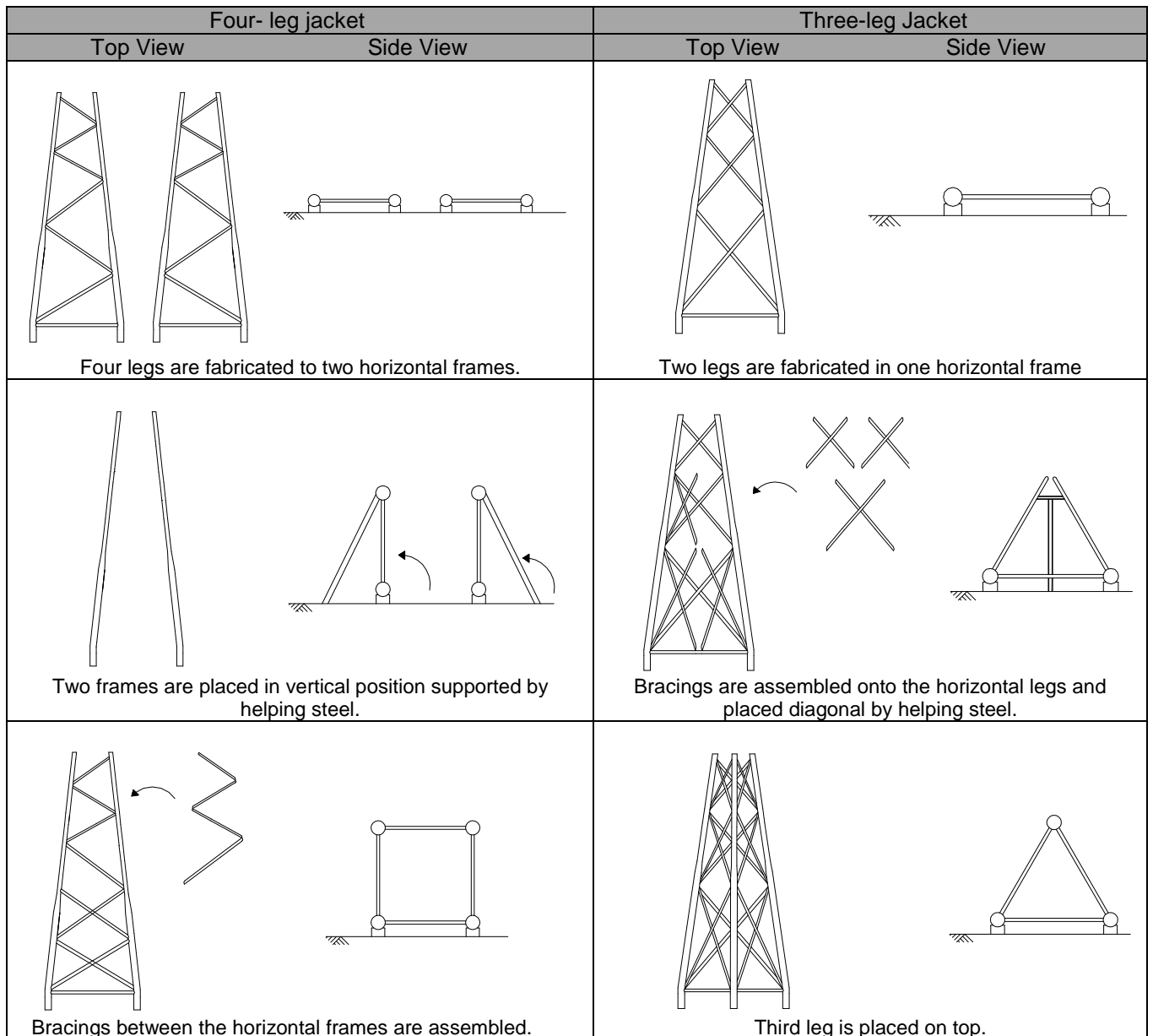


Figure 7.2: Assembling of 4-leg and 3-leg jacket

Disadvantage of the three-leg jacket is that bracings have to be placed in a diagonal way on the legs. This results in increasing amount of labour hours that is spent in handling of the parts. This is one of the aspects processed in next section.

7.2 Cost estimation

The drawings in Appendix I are used for determining the fabrication cost of the reference design, four-leg jacket k-bracing and the three-leg jacket. Thereby are the foundation piles as result of soil dataset 2 used for the cost determination. The used method for the cost determination is a simplified manner to what is normally is done.

Majority of the cost determining items as in table 7.1 are defined as unity price per kilogram of used material. These unity prices are based experience of previous project and considered as a good indication. Naturally these prices are liable to the market and therefore not everlasting valid.

The distinction between the three considered design is made at items assembling, welding and welding investigation.

Table 7.1: Unity Price per part

Item	€/ Kg
Engineering	0,07
Steel Price Jacket	1,17
Steel Price Piles	1,80
Material Transport	0,05
Assembling	1)
Welding	2)
Welding investigation	3)
Scaffolding	0,20
Preservation	0,10
Anodes	0,26
Load out & Intern Transport	0,12
Office	0,23
Beveling	4) 1,75

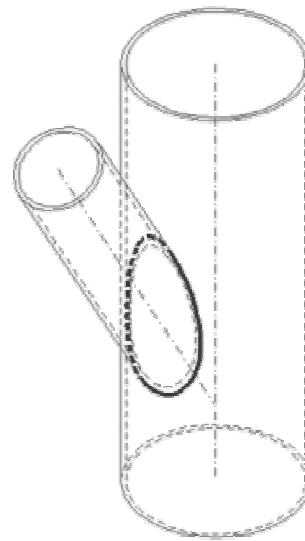


Figure 7.3: Circumference of tubular joint connection

- 1) As pointed out in previous section the assembling of the three-leg jacket is considered more complicated than the four-leg jackets. This is transmitted by changing the estimated hours of handling per ton of steel. In case of the four-leg jacket this is 2 hours / ton. For the three-leg jacket, this is increased to 3 hours/ ton.
- 2) For each design the total welding volume and welding time is calculated. This is depending on the diameter dimensions of the pipes, wall thickness and connection angle (Figure 7.3). For all tubular joints 1/2V with preset angles and gap, fully penetrated, single sided welds are assumed including a surcharge to incorporate losses. The welding capacity in terms of cm^3/hour determines the total amount of welding hours that is necessary. Hereby is for each weld also the position of the welder taken in consideration. If the welding has to be done by using scaffolding this takes extra time and an extra calculation factor is taken into account. That's why the assembling procedure as in figure 7.2 is of great importance in the total welding time. Also the fact that the welding cannot be done simply on a working bench in taken in consideration by a calculation factor. The exact calculation of the welding capacity per hour is not further treated here.
- 3) Just as for the determination of the welding volume, the circumference of the tubular joint connection is calculated. All welding is submitted to welding investigation and therefore the total length of welding in incorporated in the cost estimation.
- 4) Beveling of the pipes is only applied to all bracings and not for the pipes of the legs.

The material use of each design is computed, followed by the total cost estimation per design. As put in section 2.7 a total weight of 125 ton is defined for the transition piece. For now is assumed that the transition piece can be made for the same price per kilogram as the jacket. So the price of the transition piece is related to the price of the jacket.

As herald to chapter 10 it is also estimated what the effect of repeated fabrication is. Therefore is assumed that the engineering item will expire after the first jacket. As logical as it is, this saves 0.07 euro per kilogram. Effects of more efficient fabrication due to repetition are not taken into account. The results are summarized in the table 7.2. More detailed cost estimation is given in Appendix J.

Table 7.2: Cost estimation of designs

Reference Design				1 st jacket		After 1 st jacket	
Item	Weight [t]	Welding [x 1000 hr]	Production [x 1000 hr]	€/ kg	Total [M]	€/ kg	Total [M]
Jacket	755	2.53	6.58	3.45	€ 2.60	3.38	€ 2.55
Piles	570			1.87	€ 1.07	1.80	€ 1.03
Transition Piece	125			3.45	€ 0.43	3.38	€ 0.42
				Total [M]	€ 4.10	€ 4.00	

4-leg jacket optimized				1 st jacket		After 1 st jacket	
Item	Weight [t]	Welding [x 1000 hr]	Production [x 1000 hr]	€/ kg	Total [M]	€/ kg	Total [M]
Jacket	745	2.40	6.39	3.50	€ 2.61	3.43	€ 2.56
Piles	520			1.87	€ 0.97	1.80	€ 0.94
Transition Piece	125			3.50	€ 0.44	3.43	€ 0.43
				Total [M]	€ 4.02	€ 3.92	

4-leg jacket K-braces				1 st jacket		After 1 st jacket	
Item	Weight [t]	Welding [x 1000 hr]	Production [x 1000 hr]	€/ kg	Total [M]	€/ kg	Total [M]
Jacket	688	1.61	5.19	3.36	€ 2.31	3.29	€ 2.26
Piles	489			1.87	€ 0.91	1.80	€ 0.88
Transition Piece	125			3.36	€ 0.42	3.29	€ 0.41
				Total [M]	€ 3.64	€ 3.55	

3-leg jacket				1 st jacket		After 1 st jacket	
Item	Weight [t]	Welding [x 1000 hr]	Production [x 1000 hr]	€/ kg	Total [M]	€/ kg	Total [M]
Jacket	755	2.06	6.89	3.44	€ 2.60	3.37	€ 2.54
Piles	481			1.87	€ 0.90	1.80	€ 0.87
Transition Piece	125			3.44	€ 0.43	3.37	€ 0.42
				Total [M]	€ 3.93	€ 3.83	

Compared to the outcome of section 6.6 the total weights of all designs are decreased. This can be declared because in section 6.6 the weight is based on member going from node to node. In reality this is however not the case as member will end at intersection with another member. Notice that the results above are almost matching with the cost estimation of section 6.6.

It can be seen that the optimisations that have been applied to the reference design are contributing to the reduction of the fabrication costs. The four-leg optimised jacket has less welding time and less total production hours. This is explained by the reduced dimensions of the members of the jacket. Thereby is pile weight reduction further contributing to the cost reduction. The euro per kilogram price is higher than the reference design because more members require beveling.

Worth of noticing is despite the equal amount of weight of the three-leg jacket (compared to the reference design) the expected fabrication cost is lower. Even the increase in total labour hours is resulting in a lower unit price per kg. The increase in production hours is caused by the fact that the three-leg jacket is assumed to have a more complicated assembling (Section 7.1).

Three reasons explain the decrease in cost and can also be derived from the more elaborated overview in Appendix J. First reason is the reduction of the welding volumes and corresponding welding times (Table 7.2) due to the structural design. Furthermore is the reduction of the material in piles a great reduction on the total fabrication cost. Next to this is the number of braces reduced, with the consequence that less diagonals require beveling.

Moreover is the four-leg jacket with K-braces even more advantageous. The total weight of the jacket is reduced and also the amount of welding is in favour of the modified design. Notice that also the total labour hours is reduced significant due to modified bracing in form of K-bracing. Further assessment in view of transport and installation aspects is discussed in chapter 10.

8. Transport

In this chapter the transport aspects of the substructure are considered. The transport part considered here is from the moment the substructure is assembled at the fabrication yard till the moment the substructure is installed at the grid of the wind park.

The total transport can be divided in an onshore part and an offshore part. The onshore part is the transportation on land and in particular on the fabrication yard.

The offshore part is the transportation of the substructure over water from the fabrication yard to the location of the wind park. Considered is the handling of the substructure from the assembly in the fabrication hall to a storage depot at the yard and from the storage depot to the conveyance for offshore transportation.

Transport of the loose parts from part suppliers to the fabrication yard is not further considered.

8.1 Onshore transport

As described above, the onshore transport takes place at the fabrication yard. This can be divided in five phases. There is no significant difference concerning transport aspects between the various jacket designs. Therefore is the following section valid for all designs.

Table 8.1: Transport phases

Phase	Description
1	The substructure is manoeuvred out of the fabrication hall in a horizontal position to the location of phase 2.
2	The substructure is up-ended to a vertical position
3	Transport of substructure in vertical position to the storage area to wait for offshore transport to wind park location.
4	Conveyance to the quay
5	Roll-on the transport barge

In concrete, these five phases include three different kinds of manoeuvres.

Table 8.2: Transport operations

Operation	Description
1	Transport of substructure in horizontal position. (Horizontal transport)
2	Up-ending of the substructure
3	Transport of substructure in vertical position. (Vertical transport)

Phase 1 and 2 are corresponding respectively with operation 1 and 2. Phase 3, 4 and 5 are all considered in operation 3: vertical transport.

Next sections describe the above mentioned operations.

8.1.1 Horizontal transport

Assembly of the substructure in the fabrication hall is in a horizontal position. The whole assembly of the substructure shall be performed on permanent supports that lift the complete structure of the floor. This is necessary for the accessibility of the structure during assembling, but also for the mean of transport. Most suitable solution at this point is to make use of the so-called SPMT (Self Propelled Modular Transporter).

A Self Propelled Modular Transporter (SPMT) is a platform vehicle with a large array of wheels on the bottom. A typical SPMT can have a grid of several dozen computer-controlled wheels, all individually controllable and steerable, in order to evenly distribute weight and steer accurately. Each individual wheel can swivel independently from other wheels, to allow the SPMT to turn, move sideways, or even spin in place.



Figure 8.1: Self Propelled Modular Transporter (SPMT)

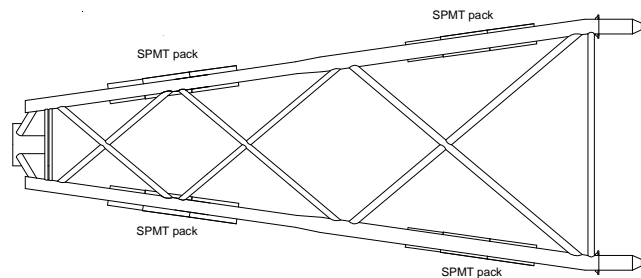


Figure 8.2: Top view of horizontal transport by 4 SPMT packs

With these SPMT it is possible to drive underneath the structure. When the SPMT's are in the right position the can hydraulic push themselves from 1.2 to 1.8 m (35) and then lift the whole substructure from its supports in het assembly hall. Once lifted from their supports, they simply ride the whole to the outside for the next operation.

The SPMT is a modular trailer and can be expanded by modules with sets of 4 or 6 lines. The modules can be coupled to each other in one pack. Each pack needs an additional power pack and can be remotely controlled. The load capacity of each line is 30 ton, so this means that transport of the substructure inclusive transition piece (≈ 900 t) requires 30 lines.

In the case of the horizontal transport of the substructure it is recommended to use a total of four packs, which individually can controlled and steer in their own direction. In figure 8.2 four packs of 2 x 4 lines (≈ 32 lines) are placed under the jacket. No structural calculation is done for this loading condition. Consult at a SPMT company revealed that no difficulties are expected, but pointed out that attention was needed to provide a rigid support on top of the SMPT's to the substructure. This to retain possible movement of the substructure on top of the SPMT, which would cause a statically undetermined system. Additionally calculation is necessary for safe transportation.

8.1.2 Up-ending

As shall become clear in section 8.2 is offshore transportation of the substructure in a vertical position. Thus in the time between leaving the fabrication hall and roll on the transport barge the substructure should be up-ended. Because of restricted weather windows and availability of installation equipment it will be necessary to store a number of substructures on the yard. Therefore it is most logical to up-end the substructure before it shall be store in the storage area. This saves the required space at the storage area.

Several options are available to up-end the substructure. These options are not worked in detail, but generated are the following thinkable solutions;

- The jacket legs are in horizontal direction and can be placed against a solid block on the yard to restrain movement in the horizontal direction. Next step is to attach cable to the jacket, which will be pulled at by winches that are placed on other side of the block. The legs against

the block have to be able to rotate. So some kind of mechanism needs to be developed for this.

The first moment of pulling up the jacket are quite difficult due to short lever arm and will cost a lot of effort. The required size of the winches is large.

Big disadvantage is how to overcome the uncontrolled movement when the point of gravity of the structure is going to the winch side of the rotating point of the lower legs. This uncontrolled movement is causes damage and unsafe situations and can't be prevented by this winch. Another constraint by another device (winch, crane etc.) will be necessary to prevent uncontrolled movements.

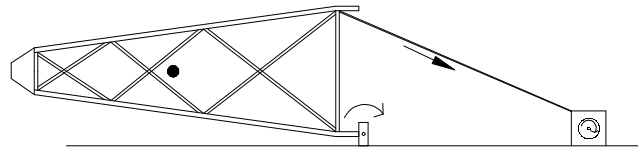


Figure.8.3: Side-view upending by winches

- Second option is to simply lift the substructure by crane(s). The crane(s) will pick up the substructure just above the centre of gravity and a controlled up-ending is possible. An extra crane can be necessary to control the bottom of the jacket. However, onshore crane with the right amount of lifting capacity are not very commonly available and if so, especially in this serial production very expensive. Same can be said to use offshore cranes, like a shear leg vessel. Thereby it is an economical illogical choice to use an offshore crane for onshore serial production activity.

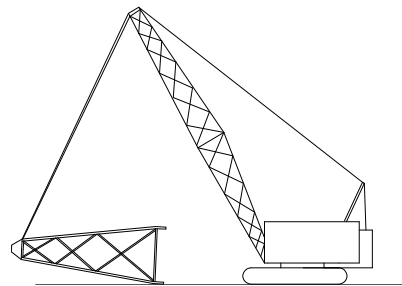


Figure 8.4: Upending by crane

- Third option is to use permanent portal cranes that are installed on the yard. The jacket is placed between two portals. Both portals contain hoisting apparatus. The hoisting lines are attached to both sides of the jacket, above the centre of gravity of the jacket. Also in this case it probably shall be necessary to have an extra crane to control the lower part of the structure. However this crane can be very light and small, because it does not require a lot of hoisting height and doesn't need a lot of lifting capacity because this is taken care by the portal cranes. Big advantage is that this option does not require expensive equipment that has to be chartered. However, instead has to be invested in these permanent portal cranes.

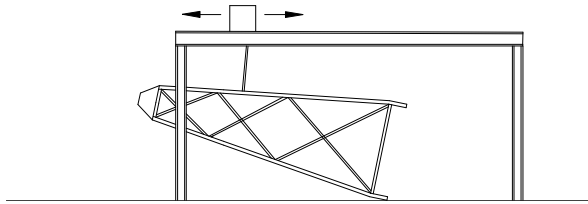


Figure 8.5: Side-view portal crane concept

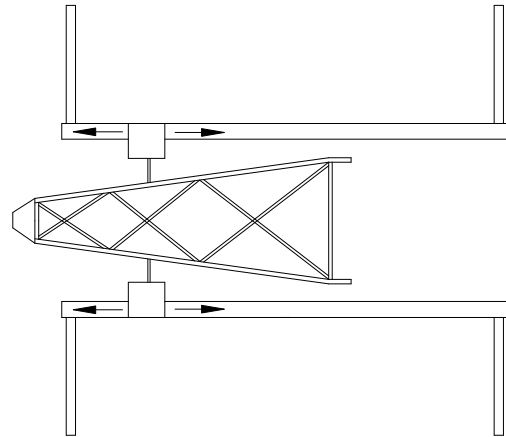


Figure 8.6: Top-view portal crane concept

In broad outline a number of options are presented above for upending of the substructure. Whereby the last presented option sounds the most feasible at this moment. A controlled upending without high day rates of cranes is possible by making use of portal cranes. That's why it appears that this option is the most suitable solution.

8.1.3 Vertical transport

After the structure is upended, the substructure is in vertical position and has to be transported to the storage area. The same SPMT's of that are used for the horizontal transport can be used for the vertical transport. As considered during the design process, between the legs horizontal bracing is added. Besides structural advantages, this can provide opportunity for vertical transport. The SPMT's will ride under the horizontal bracing and then raise themselves to lift the substructure of the ground (Figure 8.7). Then the SPMT's can ride the substructure to the location in the storage area.

Figure 8.8 and figure 8.9 show SPMT packs under the four-leg and three-leg jacket. Four-leg jacket can manage with four packs of 4+4 lines. The three-leg jacket requires three packs of 4+6 lines underneath the mudline bracing. Basic calculation showed that in case of the four-leg jacket this loading condition is not a problem for the mudline bracing. On the other hand is improvement in the handling necessary for the three-leg jacket, since due to large shear forces in the mudline bracing this component will fail. Dynamic influences of moving SPMT's are not considered at this point, but are needed in the future.

After the substructure has been stored, it is transported the quay for rolling the transport barge. The can be done in the same manner as described above. Precise handling is required. According to SPMT's specialized company this is not a problem and can be done.

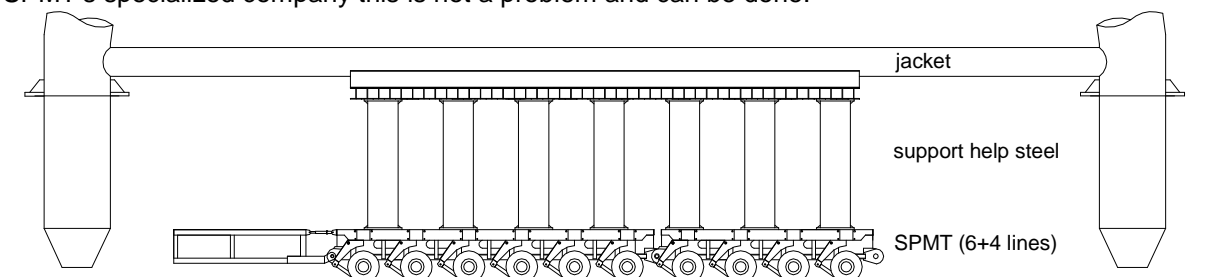


Figure 8.7: SPMT packs under mudline bracing.

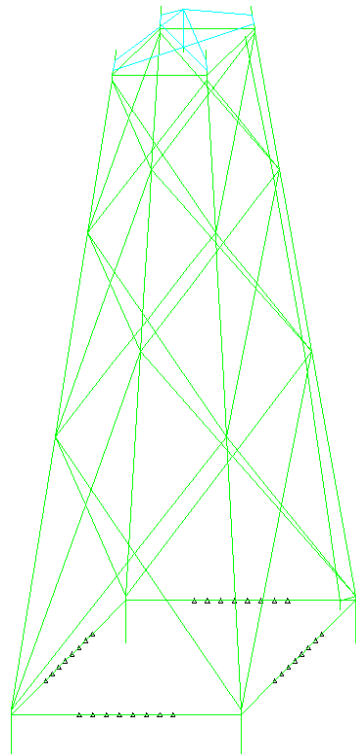
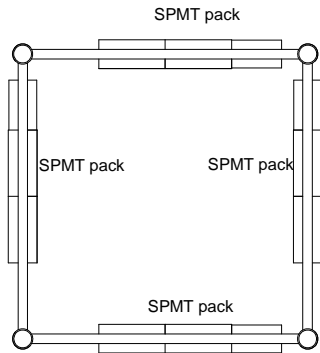


Figure 8.8: SPMT's under 4-leg jacket

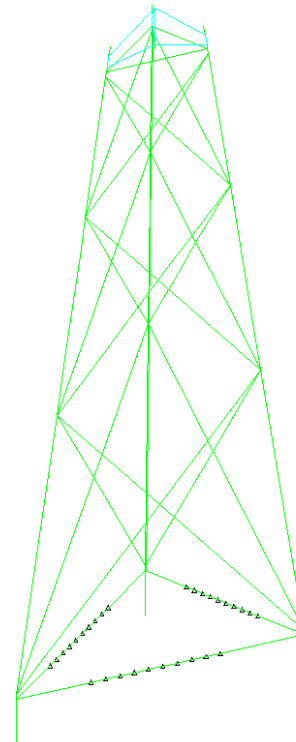
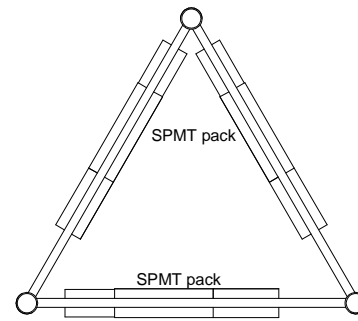


Figure 8.9: SPMT's under 3-leg jacket

8.2 Offshore transport

The substructures are designed to fit on the dimensions of standard North Sea transport barge of 300x90 feet. (91.4 m x 27.4 m) This is the most common size of the transport barge and there easily available on the market, resulting in a low day rate. Day rate of barges with larger dimensions run up fast. The substructures will be rolled on the barge. When the substructures are on the transport barge they will be towed to their location in the North Sea. No governing load conditions for the substructure are expected during the transport to the location offshore.

The loading capacity of the barge is normally by far enough (8000-9000 ton) to carry three or four jackets. A transport barge contains several pump rooms that function as ballast tanks to provide enough stability during various load conditions. This is necessary in case of the jackets are rolled on the barge, during sailing and during lifting the jackets off the barge.

Also is a grillage on the transport barge necessary for prevent the jackets from unwanted displacements during transport.

It can be questioned if the barge can provide enough stability during transport and installation of several jackets. The designed jackets have a total height of 75 meter and total weight of approximately 900 ton. The overturning moment caused by rolling of the barge is large, as a consequence of a high

centre of gravity (approx. 25 meter from bottom) and large self weight. Transport barge suppliers pointed that transport itself is probably not a problem. However lifting the jackets off the barge is not an ambiguous case, referring to safety issues. It can't be granted that the barge provides enough stability to ensure a safe hooking for lifting.

Nevertheless is for this thesis assumed that a transport barge of these dimensions can provide enough stability and that safe installation is taken for granted. Besides this, it is plausible that the barge can be adapted relative easy to satisfy the requirements.



Figure 8.10: Transport of three jackets at Alpha Ventus



Figure 8.11: Transport of four jackets at Ormonde

8.2.1 Jackets transport

In the figure 8.12 below the difference can be seen that in case of a four-leg jacket only three jackets can be transported at a time. In case of a three-leg jacket four jackets can be transported a time. This may lead to cost differences between the three-leg jacket and the four-leg jacket.

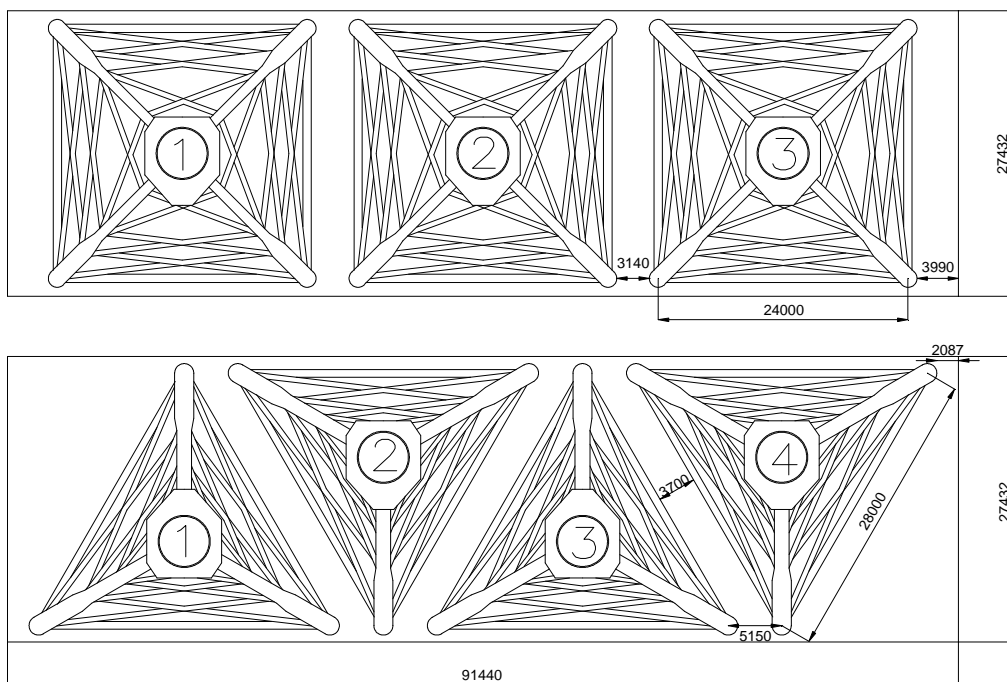


Figure 8.12: Top view of offshore transportation of 3-leg vs. 4-leg jackets.

The only case when a three leg jacket can lead to less transport cost is when less transport barges are needed during a project. Assuming that the Heavy Lifting Vessel will perform installation activities non-stop and regardless of the distance between the wind park location and the loading quay, always at least two transport barges are needed. When all jackets are cleared off the first transport barge, the second barge has to be on the wind park location in order to grant non-stop working of the installation vessel. The first transport barge then can reload new substructures and so on.

When the distance between the wind farm location and the loading quay is becoming larger, this may lead that more than two barges are needed to grant non-stop jacket installation. The corresponding distance where at least three barges are necessary, is smaller in case of the four-leg jacket compared to the three-leg jacket. This is due to the fact that more three-leg jackets fit on a transport barge. (Figure 8.12)

Start from the same estimated working times as in table 5.2 it can be seen that installation of one jacket takes 12 hours. In case of the four-leg jacket one barge is unloaded in $3 \times 12 = 36$ hours. In this time the other transport barge sails back to shore, is reloaded with jackets and sails back to the wind farm location.

Assuming that a transport barge with tug boat reaches a speed of six knots (=11.1 km/h) (36), the distance travelled in this time can be calculated. This distance profiles the distance till when only two barges are needed for non-stop installation by the Heavy Lifting Vessel. This is done in table below for the four-leg and three-leg jacket.

Table 8.3: Estimated distance from quay to wind farm location for appliance of two barges

	4-leg jacket	3- leg jacket
Offshore unloading of barge	$3 \times 12 = 36$ hr	$4 \times 12 = 48$ hr
Reloading of barge at quay	12 hr -	16 hr -
Left over time for two-ways sailing	24 hr	32 hr
Estimated distance	130 km	180 km

From here it can be concluded that between 130 km and 180 km the three-leg jacket needs one transport barge less. In other cases the number is the same.

Table 8.4: Number of required barges

Distance from loading quay to wind farm location	Number of required barges	
	4-leg jacket	3-leg jacket
<130 km	2	2
>130 km <180 km	3	2
>180 km	3	3

In (1) can be found that a number of wind farms are planned with where the distance between wind farm to shore is within the range of 130 km to 180 km. The location to corresponding loading quays is not known, but it follows that it is possible that the three possible designs may result in different cost for offshore transport. In chapter 10 the incorporation of the cost differences is accomplished.

9. Installation

This chapter describes the installation of the jackets. The installation part is expected to bring along a large cost item. Considered in this chapter is the installation of the foundation and the substructure with transition piece. The jacket shall be installed with the transition piece in one lift. Installation of the tower and the RNA is done separately and not further considered.

In section 9.1 the installation process is described. The required equipment and corresponding day rate are treated in section 9.2. Last section is addressed to mark distinctions between the installations of the jackets designs.

9.1 Installation procedure

In chapter 5 the choice was made to use of the so called pre-piling method. The planning presented in section 5.3 is therefore envisioned as the applied installation procedure. The corresponding installation process is described below and seen as the most feasible procedure, but can be subject of modifications. This is however not emphasized here.

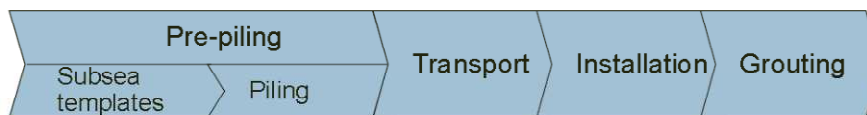


Figure 9.1: Installation procedure

One of the properties of the pre-piling method was the use of two independent spreadings for installation. In the following procedure is referred to an auxiliary vessel, heavy lifting vessel and a WROV. What is meant by this equipment is clarified in the next section.

1. The foundation piles are transported to the offshore location by transport barge and tug.
2. A piling template is placed on the correct location on the seabed by the auxiliary vessel. This template contains mudmats for stability and sleeves through which piles are driven. This template ensures that the piles are driven at the exact correct location and help to guide the foundation pile into the seabed. This guarantees that mutual distance of the piles is exactly as supposed and that the concerned wind turbine is in the exact position within a wind park. Several templates are seen on the market with different designs and systems (Figure 9.2).



Figure 9.2: Two examples of a piling template

3. Next step is to hammer the piles into the soil. The piles are lifted from a transport barge by the auxiliary vessel and guided in the template on the seafloor. The slot of the template provides vertical stability for the piles and the piling hammer can be lowered on top of the pile. The piles are driven in the seafloor by subsea hammers to the required depth.
4. The template can be removed and reused for installation of the next wind turbine.
5. Following on pile hammering a survey is done by a WROV to measure the piles position. The position has to be on the exact location and on the required depth. Hereby the installation tolerances of both vessels have to be taken in consideration. Small differences between the piles dept can be overcome by small adaption of the brackets on the bottom of the legs. If necessary the soil plug has to be removed for a clean connection between pile and leg of the jacket. This is however not expected because the pile head can be designed high enough above the seafloor that prevents a soil plug at the grouted connection.

The piling process continues at the next wind turbine location.

6. The jackets are transported to sea on transport barges and tug boats (section 8.2).
7. The jackets are lifted off the transport barge and positioned on the foundation piles. This is done by a heavy lifting vessel. The jacket installation requires accurate positioning by the heavy lifting vessel. To simplify the exact positioning of the jacket, stabbing guides are attached below the legs. These spikes are extensions of the legs and reduce in diameter when going lower. One of the stabbing guides is made longer than the stabbing guides to ease the stabbing of the jacket. Leg of this guide is put first into a pile head, where after it is more easy to positing other seekers in the pile.

The jacket installation continues at the next wind turbine location.

8. Next step is to pump grout between the pile and the leg. Inside the legs pipelines are laid to pump the grout from above to the space between the leg and the pile. After this hardening of the grout takes place and the jacket is secured to the foundation piles.

The grouting continues at the next wind turbine location.

9.2 Equipment

Transport barge & tug

Chosen transport barge is the 300 x 90 ft pontoon. These are commonly available and therefore have a low day rate. The transport barges are not self propelled and need a tug.

Auxiliary Vessel

The vessel indicated as auxiliary vessel is the piling vessel that installs the foundation piles. First it is used for lifting and placing of the piling template. Subsequently the foundation piles are in the template sleeves, where after the hammer is placed on top of het pile head.

The following weights are based on respectively based on reference projects, own calculation and information of hammer suppliers;

- Template 200 ton
- Pile 230 ton
- Hammer 200 ton

This means that the total required lifting capacity is with a minimum of 200 ton. Required corresponding radius is most determined by the template and is approximately 15 meter.

Relative small equipment can be used for these installation activities and is commonly available on the market. But applying small crane vessels will result in a relative small weather window. This results that the installation time will increase because increasingly heavy weather condition enforces small

vessel to stop their activities. In the amount of serial work like a large wind park this can result in undesired planning issues.

Heavy Lifting Vessel

The heavy lifting vessel will act as the jacket installer. The hoisting capacity has to be around 900 ton at a radius of 20 meters. Radius is determined on the half of the foot base (14 meter in case of three-leg jacket), the estimated distance from the crane to the edge of the vessel and some spare room.

Roughly can be said that the crane needs a hoisting height of 75-80 meter. This is based on the substructure height and extra height necessary for connection equipment between the crane and the substructure. Besides the required hoisting capacity, the work calls for accurate positioning and therefore large crane vessel with dynamic positioning systems are required.

On the market are also jack-up barges that are capable of doing the job. Jack-up barge are a steady platform that can also perform accurate positioning. However bad weather conditions easily stall the whole operations, because jacking is then not possible.

In Appendix K an overview is given of possible installation equipment that can do the job. At this moment a lot of equipment is developed dedicated to the offshore wind market. It is expected that coming years more vessels arrive on the market capable of installation of jackets in deeper waters.

Water Remotely Operated Vehicle (WROV)

The WROV is used for all underwater operations such as pile measurements and further installation activities. WROV's are unoccupied, manoeuvrable and operated by a person aboard a vessel. They are linked to the ship by a group of cables that carry electrical power, video and data signals back and forth between the operator and the vehicle. Most WROV's are equipped with at least a video camera and lights. Additional equipment is commonly added to expand the vehicle's capabilities.



Figure 9.3: WROV

Grouting equipment

Soon after installation of the jacket, another vessel will arrive with grouting equipment on board. This is pumped to the grouting lines in the jacket legs. These grouting lines are standard fabricated in each jacket leg.

Next is to determine the day rate of the used equipment. The day rates are highly susceptible to the market. The availability of and the demand for installation vessels have a great influence on the day rates. The offshore market and certainly the offshore wind market is in a very whimsical phase. There is a lot in the pipeline and nobody knows exactly what is going to happen in the market.

The day rates given in table 9.1 are used and based on own estimation, (24) and (37). Besides the day rate, the operational conditions under which the installation vessels can continue their work activities are assumed.

Table 9.1: Day rate estimation

Equipment	Day Rate	Operational conditions
Heavy Lifting Vessel	€ 300,000	< 2.0 Hs
Auxiliary Piling Vessel	€ 150,000	< 1.5 Hs
Water Remotely Operated Vessel	€ 10,000	
Grouting equipment	€ 50,000	
Piling Hammer	€ 15,000	
Transport barge	€ 15,000	
Tug	€ 25,000	

The operational conditions result in a weather window under which the respective vessel can undertake their installation operations. The weather windows in figure 9.4 (37) are assumed and incorporated in the total installation times. It must be noted that these figures are largely depending on local conditions at the chosen location at sea. Considering the heavy lifting vessel and the auxiliary piling vessel the weather windows are determined on respectively 75% and 60%.

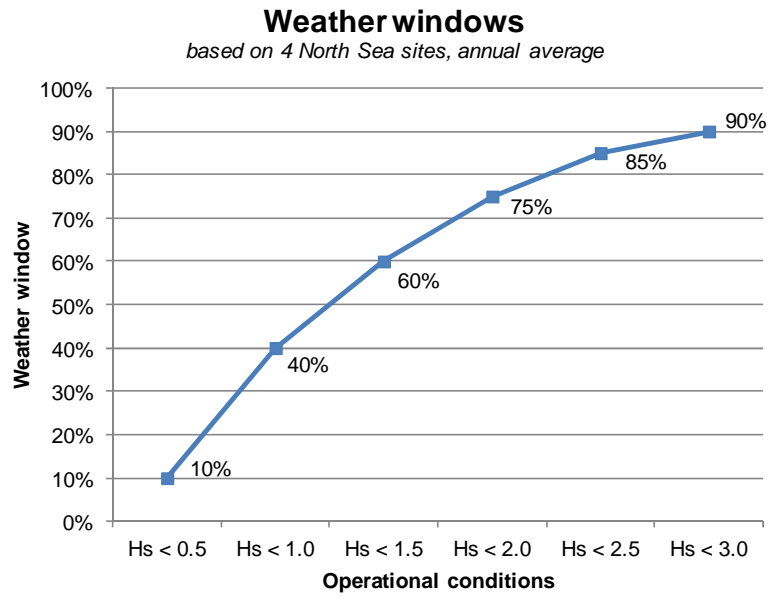


Figure 9.4: Weather windows

9.3 Substructure Installation

The different designs of the jackets do not have major influence on the installation cycle. The only distinct difference between the four-leg jacket and the three-leg jacket is the number of foundation piles that have to be driven, respectively four and three. Therefore is the first estimation that foundation installation time of the 3-leg jacket is reduced by ¼ of the time.

Table 9.2: Assessment of working times

Steps	Required equipment	4-leg jacket	3-leg jacket
		Estimated time	
Placing piling template	Auxiliary Vessel WROV	3 hr	3 hr
Pile driving	Auxiliary Vessel Piling Hammer	24 hr	18 hr
Pile survey	WROV	3 hr	3 hr
Sail to next location	Auxiliary Vessel WROV	2 hr	2 hr
Placing substructure in position	Heavy Lift Vessel	10 hr	10 hr
Sail to next location	Heavy Lift Vessel	2 hr	2 hr

The planning as presented in section 5.3 is still valid for the four-leg jacket and therefore not given here. Except for the piling time the planning of the three-leg jacket is similar (Figure 9.5). Let it be clear that an arbitrary number of hours are given to the continuous pile driving activities and jacket installation activities. This is depending on the scale of the wind park.

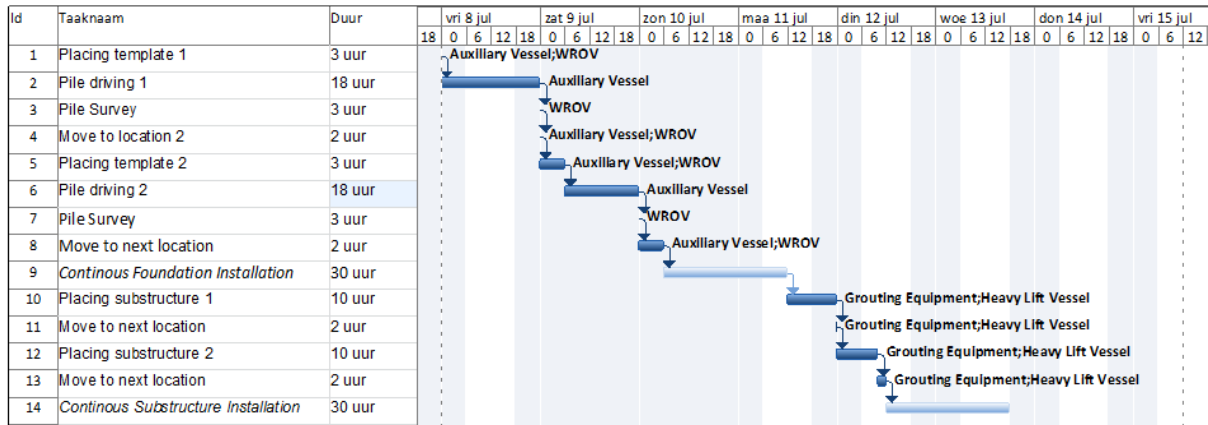


Figure 9.5: Installation planning 3-leg jacket

In the tables below are the total installation cost given for respectively the four-leg and three-leg jacket. The working times of table 9.2 and corresponding weather window are used for the computation of the total installation cost in the same way as in section 5.4.

Table 9.3: Installation cost of 4-leg jacket

Four-leg jacket	Equipment	Material [t]	Time [days]	Unity price / Day rate [€ / kg, € / day]	Writing-off	Total [k]
Foundation installation	Auxiliary Vessel		2.3	€ 150,000		€ 344
	Piling Hammer		2.3	€ 14,000		€ 32
	Piling Template	200		€ 4	50	€ 16
	WROV		2.3	€ 10,000		€ 23
Substructure installation	Heavy Lifting Vessel		0.7	€ 300,000		€ 200
	Grouting Equipment		0.7	€ 50,000		€ 33
						€ 648

Table 9.4: Installation cost of 3-leg jacket

Three-leg jacket	Equipment	Material [t]	Time [days]	Unity price / Day rate [€ / kg, € / day]	Writing-off	Total [k]
Foundation installation	Auxiliary Vessel		1.9	€ 150,000		€ 281
	Piling Hammer		1.9	€ 14,000		€ 26
	Piling Template	200		€ 4	50	€ 16
	WROV		1.9	€ 10,000		€ 19
Substructure installation	Heavy Lifting Vessel		0.7	€ 300,000		€ 200
	Grouting Equipment		0.7	€ 50,000		€ 33
						€ 576

From here it follows that installation of the three-leg jacket save a considerable amount of money due to the fact that one pile less has to be driven.

10. Substructures in Offshore Wind Park

The final result of past chapters comes together in the fabrication, transportation and installation of the substructure in an offshore wind park. As stated in section 1.4 is the goal to find the best mix of these components. Section 10.1 gives a full cost overview of three considered jackets. In section 10.2 is an anticipation given of some parameter susceptibility.

10.1 Cost overview

For a full cost overview a wind park of 50 wind turbines is assumed in the North Sea. In table 10.1 and table 10.2 the total installation and transport cost are set out for the 50 substructure. For the transportation of the foundation piles is assumed that at all times two transport barges are needed. As treated in section 8.2.1 the transport cost are depending on the distance from the loading quay to the offshore location. This determines how many barges are needed for the jacket transportation. Either two or three required barges are processed in the tables below.

Table 10.1: Total installation and transport cost four-leg jacket for 50 jacket wind park

Four-leg jacket	Equipment	Unit [t / nr.]	Time [days]	Unity price / Day rate [€ / kg , € / day]	Total [M]
Foundation installation	Auxiliary Vessel		114.6	150,000	€ 17.2
	Piling Hammer		114.6	14,000	€ 1.6
	Piling Template	200		4	€ 0.8
	WROV		114.6	10,000	€ 1.1
	Transport barge	2	114.6	40,000	€ 9.2
Substructure installation	Heavy Lifting Vessel		33.3	300,000	€ 10.0
	Grouting Equipment		33.3	50,000	€ 1.7
	Transport barge	2 v 3	33.3	40,000	€ 2.7 € 4.0 +
					€ 44.2 € 45.6

Table 10.2: Total installation and transport cost three-leg jacket for 50 jacket wind park

Three-leg jacket	Equipment	Unit [t / nr.]	Time [days]	Unity price / Day rate [€ / kg , € / day]	Total [M]
Foundation installation	Auxiliary Vessel		93.8	150,000	€ 14.1
	Piling Hammer		93.8	14,000	€ 1.3
	Piling Template	200		4	€ 0.8
	WROV		93.8	10,000	€ 0.9
	Transport barge	2	93.8	40,000	€ 7.50
Substructure installation	Heavy Lifting Vessel		33.3	300,000	€ 10.0
	Grouting Equipment		33.3	50,000	€ 1.7
	Transport barge	2 v 3	33.3	40,000	€ 2.7 € 4.0 +
					€ 38.9 € 40.3

Above cost are interesting facts but as fabrication cost of the three-leg jacket are higher (Section 7.2) it is to be seen if the installation cost can fade away the increase in fabrication cost.

As stated in section 1.3.1 and according (4) the total investment level per MW installed is €3.8 million. A total wind park of 50 wind turbines of 6 MW, as the turbine in this case, brings a total installation of 300 MW. Total capital expenditure then becomes 300 x €3.8 million = €1.14 billion.

In section 1.3.1 was also declared that it is expected that 20% of this number would belong to the substructure.

Table 10.3 shows the complete picture of fabrication, transportation and installation of the three considered jackets. As it is depending on the distance to the loading quay, this is also assimilated in the table. In the table is also included the percentage of capital expenditure in the substructure as part of the total wind park.

Table 10.3: Total cost of designs for 50 jackets in a offshore wind park

Total cost [M]	Distance	Reference design	4-leg optimized	4-leg K-braces	3-leg
Fabrication		€ 200.1	€ 196.2	€ 177.8	€ 191.7
Installation & Transport	<130 km	€ 44.2	€ 44.2	€ 44.2	€ 38.9
	>130 km <180 km	€ 45.6	€ 45.6	€ 45.6	€ 38.9
	>180 km	€ 45.6	€ 45.6	€ 45.6	€ 40.3
Total	<130 km	€ 244.3	€ 240.4	€ 222.0	€ 230.6
	>130 km <180 km	€ 245.6	€ 241.8	€ 223.3	€ 230.6
	>180 km	€ 245.6	€ 241.8	€ 223.3	€ 232.0
% of total estimated cost of total wind park	<130 km	21.4%	21.1%	19.5%	20.2%
	>130 km <180 km	21.5%	21.2%	19.6%	20.2%
	>180 km	21.5%	21.2%	19.6%	20.3%
% cost difference with respect to reference design	<130 km		-1.6%	-9.1%	-5.6%
	>130 km <180 km		-1.6%	-9.1%	-6.2%
	>180 km		-1.6%	-9.1%	-5.6%

By table 10.3 it is verified that about 20% of the estimated capital expenditure of €1.14 billion is for the expense of the substructure.

From here it follows that the four-leg jacket with K-braces emerges as substructure with the lowest cost. Compared to the reference design also the three-leg jacket is more advantageous in terms of cost.

The advantage of the reduction in installation cost is however insufficient to pay it out compared to the four-leg jacket with K-braces.

10.2 Parameter Susceptibility

The results presented in previous section are based on the parameters that are fixed during the study. Next to this, is in the table below a view given of the effect of changing parameters on the choice of substructure. The consequences are based on perception and not based on any numbers.

Table 10.4: Parameter susceptibility

Parameter	Consequence
Water depth < 45 m	<p>If the water depth will decrease, it will become less subject of the hydrodynamic loading and relative more to turbine loading. The jackets as proposed in this study are well capable of dealing with the hydrodynamic loading as they are very transparent.</p> <p>Going to lower water depth this is a less requisite property. Other substructures like tripod and in even lower water depths the monopile are in sight.</p> <p>Between the proposed jackets of this thesis no other differences than in table 10.3 are expected. The K-braces still keep their advantages in terms of reducing the fabrication cost.</p>
Water depth > 45 m	<p>The reverse of above is the case here. Hydrodynamic loading is more and more the parent loading. More transparent substructure is then advantageous. A step further is the floating substructure. Till floating substructure is becoming a more economical choice, the proposed jackets are expected to the most cost-effective.</p>
Transition piece stiffness	<p>As stated in 6.2.5 the modelled transition piece is a stiff element. Effects of the transition piece have been investigated in this thesis. If the transition piece is fabricated with less stiffness, the natural frequency decreases. Much is depending on the final design of the transition piece. But it is believed that a transition piece with the same stiffness properties can be fabricated without much difficulty.</p> <p>If not the same stiffness can be achieved, it is expected that especially the jacket with K-braces has to suffer more from fatigue damages. The traditional X-braces are then more advantageous, because they have a better distribution of the stress variations.</p>
Variation in site location	<p>As the three-leg jacket is only transferring the loads to three foundation piles, it is believed that different site locations can be detrimental for the three-leg jacket.</p>
Base width	<p>In this thesis is chosen to hold on to a strict base due to transportation limitations and reduction of required fabrication height. In case of the tripod, this already turned out that this can make quite some difference. However, the estimation is that increasing the base width shall not make a lot of difference in the total picture.</p>

11. Conclusion and Recommendations

Goal of this thesis was to make an economical optimisation of a steel substructure for an offshore wind turbine in deeper waters. Deeper waters were specified by the business case to water depths of 30 to 60 meters. Therefore a water depth of 45 meter was assumed in this thesis. No offshore wind parks have been implemented at these water depths so far. It is however expected that wind parks in the future are being located further offshore with deeper water as consequence. Conclusions of this thesis are presented in section 11.1. Several recommendations for further study are given in section 11.2.

11.1 Conclusions

The outcomes of this study are based on assumptions, literature study and performed analyses as presented in this report. Environmental conditions such as soil and wave data are acquired from existing projects in the North Sea with similar water depth. The turbine data is based on a concise loading report of the RePower turbine and is only valid for first designs.

As the substructure is part of the complete support structure (Figure 1.1) two other main components, tower and transition piece, are predefined. The tower is predefined by the turbine manufacturer (Table A.1). The transition piece is taken from a reference project but needs further verification (Figure 6.33).

From practice and earlier studies much knowledge is gained about steel substructure for offshore wind turbines. The following is obtained by means of literature study.

- For water depth range of 30 to 60 meters, open steel spaceframe as tripods and jackets are based on economics the most suitable structural concepts. Other substructure concepts like monopiles and floating substructures are better solutions for respectively smaller and larger water depths.
- Suction buckets are not a cost effective foundation of the substructure. Despite the advantage of reduction of installation steps, research emerged disadvantages and difficulties during installation process and operational state of the suction bucket. Apart from mixed outcome of practical experience, large dimensions of the suction bucket are foreseen. Compared to driven piles an increase of weight and fabrication cost is expected. Furthermore shall the installation require equipment with larger capacity. Therefore are piles a more cost effective solution for the foundation.

The structural calculation behind the original reference design as proposed in the business case was analysed. For a more proper analysis the static in-place analyse is adjusted to a dynamical in-place analysis and the deterministic fatigue method is replaced by a dynamic spectral fatigue method.

- The approach used in the original reference design for determination of the total fatigue damage due to aerodynamic and hydrodynamic loading is too optimistic (Figure 6.16). A more applicable approach for calculation of the total fatigue damage due to turbine loading and wave loading is applied. The reference design is modified, based on quadratic superposition of equivalent stress ranges. Thereby an additional damping is assumed due to aerodynamic effects of the turbine.

The following optimisations have been conducted to the reference design.

- The working times of the installation vessel have been estimated considering two installation methods. Installation in sections (pre-piling method) is found to be advantageous for the installation of multiple substructures. Based on comparable jackets, the elimination of mudmats and leg-mounted sleeves and reductions of anodes brings along a substantial cost reduction. More accurate jacket placement of this method with respect to the driven pile installation (post-piling method) is not expected to bring difficulties. Usage of two smaller installation spreadings reduces risks in time management of the installation process.
- Adding a horizontal brace just above mudline level results in significant reduction of the foundation pile weights. Splitting forces in the legs are efficiently spread by the horizontal brace and thereby reducing the bending moments in the piles.
- Because of the highly serial fabrication it is chosen that tubular members are fabricated by specialized tube manufacturers. Here it is feasible to weld double sided butt welds. The double sided butt welds brings along a better fatigue damage assessment, so increasing the life period.

By the followed design process four different designs have been worked out. Objective as stated in section 1.4.1 is to reduce the total fabrication cost. Furthermore is the cost estimation taken to a next level by also estimating the transport and installation costs of the different designs. Next to the modified reference design, a four-leg optimised jacket, a three-leg jacket and a four-leg jacket with K-braces were proposed. Each design was evaluated in terms of costs for fabrication, transport and installation.

- Except for welding items, the fabrication cost items were assessed by making use of unity prices per kilogram based on previous executed projects. All three designs are expected to bring a cost reduction compared to the reference design. Despite the similar total weight of the three-leg jacket the expected fabrication costs are lower than the reference design. This is mainly caused by the reduction of the welding time and the reduction of the material in piles. The estimation is that the four-leg jacket with K-braces is favourable. Because the large reduction of amount of members, the corresponding welding and assembling times a fabrication cost reduction of approximately 11% is expected.
- Transport onshore does not bring any big differences between the jacket types. For offshore transport all jackets are designed to fit on a standard North Sea transport barge. In case of the three-leg jacket, the number of transported jackets that can be transported on one barge is increased from three to four. Furthermore it is assumed that the barge is capable for installation of multiple jackets from one barge. Depending on the sailing distance of the barge for the three-leg jacket and midrange distances one barge less is needed for continuous jacket installation.

- The installation of the jackets is given by the pre-piling method. Distinction between the three-leg and the four-leg jackets are the number of piles that have to be driven. Using working time estimations and expectation of corresponding weather windows a cost reduction of approximately 11% is expected for the three-leg jacket (Table 10.2).
- The cost items of fabrication, transport and installation have been assembled in one picture assuming a wind park of 50 substructures. Based on literature study it was expected that 20% of the total wind park cost is of the expense of the substructure. The outcome of the summation of the cost of jacket fabrication, transportation and installation corresponds with this estimation.

The total cost assessment (Table 10.3) of the four considered jackets made clear that the 4-leg optimised jacket is estimated to bring a cost reduction of almost 2%. Followed by the three-leg jacket where a cost reduction around 6% is expected. The four-leg jacket with K-braces turned out to be most favorable design, expecting a cost reduction around 9% compared to the reference design.

11.2 Recommendations

The following recommendations are made as results of this study.

- Further going structural analysis for the new designs are necessary as not all required checks have been performed. Concerned analyses include vortex induced vibration, boat impact and transport analysis. The designs presented in this thesis are only based on dynamic in-place analysis and a dynamic fatigue damage assessment.
- Only a water depth of 45 meter is considered in this thesis. Similar optimisation studies as this can be done to determine the most economic choices for other water depths.
- More accurate calculation of the required dimensions of the suction buckets is necessary for less conservative results. The hand calculation as in chapter 3 is only appropriate for first assumptions. If the total weight of the suction bucket can be reduced, this offers new insights and other possibilities in the integral design.
- A time domain approach for calculation of the fatigue damage is recommended for further design phases. Loads and the used frequency domain method in this report are only good for first design phases. Lack of data by the turbine manufacturers is a common heard obstacle for acquiring the necessary information and is also encountered during this thesis.
- At this moment the transition piece is modelled as a rather stiff element (section 6.5.1). The structural design is based on reference projects and the dimensions are based on first calculation in (7). Further research is necessary to determine the influence of the transition piece design on the loading effects and to the design itself.
- The effect of the aerodynamic damping in the natural frequency analysis is not incorporated. Further research is recommended if extension of the aerodynamic damping is necessity for improvement of the natural frequency analysis. If so, this may result not only in a modified natural frequency check, but also in new results of the fatigue damage calculation.
- The impact of the used soil dataset on the natural frequency is not analysed. In the definitive design phase only soil dataset 2 used. It is recommended to investigate the influence of the soil data on the natural frequency and the fatigue damage calculation.
- The pre-piling method is now using a grouting as connection between the leg and the substructure. The swaging method (Figure 5.5) can however bring new light on the case. Swaging is now and then used in the post-piling method pushing the pile in grooves of the sleeves. In case of pre-piling it seems more complicated to using swaging from inside, thereby pushing jacket leg into grooves in the piles. (the wall thickness of the pile is smaller) Therefore it can be considered to develop a new kind of swaging tool that invert the swaging movement. Then swaging can take place from outside to inside, plastically straining the pile head into grooving in the jacket leg.
- At this moment is assumed that the transport barge is suitable for the transport and installation of three or even four jackets. However, if this can be done in reality remains to be seen. Further investigation is recommended to the transport and especially the installation of multiple substructures from one barge.

References

1. **4C Offshore Limited.** www.4coffshore.com. [Online]
2. **Vries, W.E. de.** *Assessment of bottom-mounted support structure types with conventional design stiffness and installation techniques for typical deep water sites.* s.l. : Upwind, 2007.
3. **Brunt, Drees.** *Business Case Offshore Wind.* s.l. : Hollandia, 5 november 2010.
4. **Ministerie van Economische zaken.** *Eindrapport Windenergie op zee.* s.l. : Taskforce Windenergie op Zee, mei 2010.
5. **Tempel, Jan van der.** *Design of Support Structures for Offshore Wind Turbines.* Delft : Offshore Engineering & DUWIND, 2006. ISBN 90-76468-11-7.
6. **REpower systems.** *REpower 5M/6M Offshore Wind Turbine generic offshore loads V-5.1-OG-00.00-A-G-EN.* 29 march 2010. Confidential.
7. **KCI.** *OWT jacket foundation design, preliminary In-place and fatigue analysis.* Schiedam : s.n., 2010. HOL-10106-0000-R-S-04001-01.
8. **PhyseE ltd.** *Metocean data for B13 southern North Sea, engineering reference document.* 8 march 2010. C310_10-R402-1D.
9. **IGB ingenieurgesellschaft MBH.** *Report on Design basis, Northern Sea, German Bight.*
10. **Fugro.** *General Technical Report, Metocean Condition E17, North Sea.*
11. **NEN-EN-ISO 19902.** December 2007.
12. **Dr. Ivan Østvik.** *Pre-piling for offshore wind foundations-advantages and practical considerations.* s.l. : NORWIN, 6 april 2011.
13. *Assessing underwater noise levels during pile-driving at an offshore windfarm and its potential effects on marine mammals.* by **Helen Bailey, Bridget Senior, Dave Simmons, Jan Rusin, Gordon Picken, Paul M Thompson.** s.l. : Marine Pollution Bulletin, Vol. 2010.
14. *The bucket foundation.* **Bakmar, Cristian LeBlance.** s.l. : Offshore technology, Dong Energy, 12 may 2009.
15. *Suction caissons for wind turbines.* **Guy T. Houlsby, Lars Bo Ibsen, Byron B. Byrne.** London : Tylor & Francis group, 2005. ISBN 041539063.
16. **Iv-Oil & Gas.** *In-place analyse Venture F3-FA.* Papendrecht : s.n., 21-4-2010. FA-IV-S-RP-01-003.
17. **Lesny, Kerstin.** *Foundation for Offshore Wind Turbines.* Essen, Germany : AALEX Buchproduktion GmbH, 2010. ISBN 978-3-86797-042.
18. **Zaaijer, M.B.** *Suction bucket foundation.* s.l. : DOWEC, 2002.
19. *Comparison of monopile, tripod, suction bucket and gravity base design for a 6 MW turbine.* **Zaaijer, Michiel B.** Delft : DOWEC.
20. **Lars Bo Ibsen, Morten Liingaard, Soren A. Nielsen.** *Bucket foundation, a status.* 2005.
21. *Stiff prices for a firm base.* **Smidt, Stefan.** s.l. : Neue Energy, october 2005.
22. *40,0000 NW by 2020.* **Renewable Energy World.** 3 januari 2008.
23. **Willemse, Prof. C.A.** *Bottom founded structures, quasi-static-behaviour. presentation part of course: Bottom founded structures.* Delft : s.n., 2009.
24. **S.A. Herman, H.J.T Kooijman.** *Installation alternatives for DOWEC.* november 2002.
25. **Olthof, Fre.** *correspondence on transport and installation of jackets.* *Heerema Marine Contractors.* 22 april 2011.
26. **Verhoeven, Tom.** *correspondence on transport and installation of jackets.* *Seaway Heavy Lifting.* 23 maart 2011.
27. *Piling Template for Ormonde Wind Farm.* **TWD bv.** Schiedam : s.n., 2011.
28. **SACS.** help document.
29. **Ray W. Clough, Joseph Penzien.** *Dynamics of structure.* 1975. ISBN 0-07-011392-0.

30. **Kühn, Martin.** *Dynamics and Design Optimisation of Offshore Wind Energy Conversion Systems.* Delft : DUWIND, 2001. ISBN 90-76468-07-9.
31. **Fischer, Tim.** *Final report Task 4.1, project UPwind.* Stuttgart : Upwind, 2011.
32. **Schmidt, B.** *Aerodynamic Damping of Offshore Wind Turbines.* s.l. : Technische Universität Darmstadt, february 2008.
33. **Vries, Wybren de.** *Final Report WP4.2: Support Structure Concepts for Deep Water sites.* Delft : UpWind, 2011.
34. **Cees de Rooij, Hollandia.** *correspondence welding techniques.*
35. **Mammoet.**
<http://www.mammoet.com/LinkClick.aspx?fileticket=pK99c6Fl6nY%3d&tabid=691&mid=491>. [Online]
36. **Mark J. Kaiser, Brian Snyder.** *Offshore Wind Energy Installation and decommissioning Cost Estimation in the U.S. Outer Continental Shelf.* s.l. : Energy Research Groep, november 2010.
37. **Ballast Nedam Offshore.** *Installation of offshore wind support structures.* 29-9-2010.
38. **Slot, Andre van der.** *correspondence on transport and upending of jackets.* s.l. : Mammoet bv.

List of Figures

Figure 1.1: Terminology.....	2
Figure 1.2: From left to right: Monopile, Tripod, Jacket, Gravity Base, Floating substructure (2).....	3
Figure 1.3: Typical cost breakdown offshore wind park(3).....	5
Figure 1.4: Potential market(3).....	6
Figure 1.5: Target countries(3).....	6
Figure 1.6: Reference design.....	7
Figure 2.1: Single degree of freedom mass-spring damper.....	11
Figure 2.2: a)Quasi-static b)Resonant and c)Inertia dominated response.....	11
Figure 2.3: a) Dynamic Amplification Factor b) Phase Lag per normalised frequency.....	12
Figure 2.4: Loading frequency of turbine.....	13
Figure 2.5: Occurrences of wave frequencies with 1P and 3P frequencies of Repower turbine.....	14
Figure 2.6: North Sea location.....	15
Figure 2.7: Market range of water depth(3).....	15
Figure 2.8: Transition piece Alpha Ventus.....	18
Figure 2.9: Example of a transition piece(3)(7).....	18
Figure 2.10: Modelling of transition piece.....	18
Figure 3.1: Suction bucket installation.....	19
Figure 3.2: Free body diagram.....	19
Figure 3.3: Suction bucket in Frederikshavn.....	22
Figure 3.4: Failed attempt during installation at Wilhelmshaven.....	22
Figure 3.5: Top view suction buckets.....	23
Figure 3.6: Push-pull load concept.....	23
Figure 3.7: Shear failure.....	23
Figure 3.8: overview of main parameters.....	23
Figure 4.1: 4-leg battered.....	26
Figure 4.2: 3-leg battered.....	26
Figure 4.3: 3-leg straight jacket.....	26
Figure 4.4: 4-leg straight jacket.....	26
Figure 4.5: Conventional tripod.....	26
Figure 4.6: Extended tripod.....	26
Figure 4.7: Split tripod.....	26
Figure 4.8: Asymmetric tripod.....	26
Figure 4.9: Tripile.....	27
Figure 4.10: Symmetric tetra-pod.....	27
Figure 4.11: Asymmetric tetra-pod.....	27
Figure 4.12: Twisted Jacket.....	27
Figure 4.13: Score by person per concept.....	30
Figure 4.14: Score by person per concept.....	30
Figure 5.1: Main piling foundation principle(23).....	31
Figure 5.2: Connection of jacket and leg using shim plates(23).....	31
Figure 5.3: Post-Piling a)jacket placement b) pile Driving.....	32
Figure 5.4: Grout connection.....	32
Figure 5.5: Swaged connection.....	32
Figure 5.6: Planning of post-piling foundation installing.....	33

Figure 5.7: Pre-Piling a) Placing Template b) Pile Driving c) Jacket Placement	34
Figure 5.8: Stabbing of legs in piles	34
Figure 5.9: Grout connection by inside grouting line	34
Figure 5.10: Planning of Pre-Piling concept	35
Figure 6.1: Load angle for trilateral substructure	39
Figure 6.2: Load angle for quadrilateral substructure	39
Figure 6.3: 4-leg battered jacket	41
Figure 6.4: 3-leg battered jacket	41
Figure 6.5: 3-Leg straight jacket	42
Figure 6.6: 3-Leg straight diagonals jacket	42
Figure 6.7: Tripod concept small base width	42
Figure 6.8: Tripod concept large base width	42
Figure 6.9: Natural frequencies of preliminary designs with respect to turbine loading	44
Figure 6.10: Natural frequencies of preliminary designs with respects to wave and turbine loading. ..	45
Figure 6.11: Superposition of separate wind and wave fatigue responses (30)	49
Figure 6.12: Wave response due to aerodynamic damping	50
Figure 6.13: Determining of equivalent stress range due turbine fatigue damage	53
Figure 6.14: Determining of equivalent stress range due to wave fatigue damage	53
Figure 6.15: Determining equivalent number of stress ranges	53
Figure 6.16: Difference between fatigue approaches	54
Figure 6.17: 4-Leg jacket without mud level brace	56
Figure 6.18: 4-Leg jacket with mud level brace	56
Figure 6.19: Comparison of pile unity check for with or without horizontal brace for soil dataset 2	56
Figure 6.20: 3-Leg jacket with X-braces	57
Figure 6.21: 3-Leg jacket with K-braces	57
Figure 6.22: 4-Leg jacket with X-braces	58
Figure 6.23: 4-Leg jacket with K-braces	58
Figure 6.24: S-N curves of DNV and ISO standard	59
Figure 6.25: Single sided versus Double sided butt welds	60
Figure 6.26: S-N curves of DNV single sided weld and ISO double sided weld	60
Figure 6.27: Total fatigue damage difference between ISO curves and DNV curves	61
Figure 6.28: Four definitive designs	62
Figure 6.29: Fatigue damage of three-leg jacket	62
Figure 6.30: Natural frequencies of turbine and definitive design	63
Figure 6.31: First four mode shapes reference design	64
Figure 6.32: influence transition piece stiffness +/- 30% on the natural frequencies	65
Figure 6.33: Influence transition piece stiffness +/- x1000 on the natural frequencies	65
Figure 7.1: Stages in the fabrication of Beatrice jacket	67
Figure 7.2: Assembling of 4-leg and 3-leg jacket	68
Figure 7.3: Circumference of tubular joint connection	69
Figure 8.1: Self Propelled Modular Transporter (SPMT)	74
Figure 8.2: Top view of horizontal transport by 4 SPMT packs	74
Figure 8.3: Side-view upending by winches	75
Figure 8.4: Upending by crane	75
Figure 8.5: Side-view portal crane concept	76
Figure 8.6: Top-view portal crane concept	76
Figure 8.7: SPMT packs under mudline bracing.	76
Figure 8.8: SPMT's under 4-leg jacket	77
Figure 8.9: SPMT's under 3-leg jacket	77
Figure 8.10: Transport of three jackets at Alpha Ventus	78
Figure 8.11: Transport of four jackets at Ormonde	78
Figure 8.12: Top view of offshore transportation of 3-leg vs. 4-leg jackets	78
Figure 9.1: Installation procedure	81
Figure 9.2: Two examples of a piling template	81
Figure 9.3: WROV	83
Figure 9.4: Weather windows	84
Figure 9.5: Installation planning 3-leg jacket	85
Figure B.1: Suction bucket in Frederikshavn	115
Figure B.2: Failed attempt during installation at Wilhelmshaven	116
Figure B.3: Shear failure	117

Figure B.4: Circle of Mohr.....	117
Figure B.5: Overview of main parameters.....	118
Figure C.1: Horizontal placement of jacket in fabrication hall	119
Figure C.2: Installing Beatrice Jacket.....	119
Figure C.3: Transport of Alpha Ventus jacket	119
Figure C.4: Transport of tripods.....	120
Figure C.5: Installation of tripod.....	120
Figure C.6: BARD's tripile.....	121
Figure C.7: Triple installation.....	121
Figure F.1 :First four mode shapes optimised 4-leg jacket	132
Figure F.2: Transition piece stiffness influence on natural frequencies	132
Figure F.3: First four mode shapes 4-leg K-braces.....	133
Figure F.4: Transition piece stiffness influence on natural frequencies	133
Figure F.5: First four mode shapes 3-leg jacket.....	134
Figure F.6: Transition piece stiffness influence on natural frequencies	134
Figure G.1: Member groups in jacket face	136
Figure G.2: Joint numbers	136
Figure G.3: Fatigue damage tubular joints due to wind and wave.....	138
Figure G.4: Total fatigue damage tubular joints	138
Figure G.5: Fatigue damage butt welds due to wind en waves	139
Figure G.6: Total fatigue damage butt welds	139
Figure G.7: Member groups in jacket face	140
Figure G.8: Joint numbers	140
Figure G.9: Fatigue damage tubular joints due to wind and wave.....	142
Figure G.10: Total fatigue damage tubular joints	142
Figure G.11: Fatigue damage butt welds due to wind and wave	143
Figure G.12: Total fatigue damage butt welds	143
Figure G.13: Member groups in jacket face	144
Figure G.14: Joint numbers.....	144
Figure G.15: Fatigue damage tubular joints due to wind and wave.....	146
Figure G.16: Total fatigue damage tubular joints	146
Figure G.17: Fatigue damage butt welds due to wind and wave	147
Figure G.18: Total fatigue butt welds	147
Figure G.19: Member group in jacket face.....	148
Figure G.20: Joint numbers.....	148
Figure G.21: Fatigue damage tubular joints due to wind and wave.....	150
Figure G.22: Total fatigue damage tubular joints	150
Figure G.23: Fatigue damage butt welds due to wind and wave	151
Figure G.24: Total fatigue damage butt welds	151
Figure H.1: Grout connection	153

List of Tables

Table 2.1: Turbine characteristics	13
Table 2.2: Load Factors.....	16
Table 2.3: Summary of primary parameters.....	17
Table 4.1: Example of filled in table to determine weigh factors	29
Table 4.2: Results of Multi Criteria Analyse	29
Table 4.3: Results of Multi Criteria Analyse, excluding scores of person B.	30
Table 5.1: Time assessment of post-piling method.....	33
Table 5.2: Time assessment of Pre-Piling method.....	35
Table 5.3: Weight assessment of sleeves and mudmats	36
Table 5.4: Day rate estimation.....	37
Table 5.5: Cost estimation post-piling method	37
Table 5.6: Cost estimation pre-piling method.....	37
Table 6.1: Self weight of preliminary designs.....	43
Table 6.2: Natural frequencies of the preliminary designs	44
Table 6.3: First estimated foundation pile weight.....	45
Table 6.4: In-phase versus 90° out-of-phase superposition of harmonic signals	52
Table 6.5: Self weight definitive designs	63
Table 6.6: Natural frequencies definitive designs.....	63
Table 6.7: Mode shapes Reference design.....	64
Table 6.8: Foundation pile weights.....	66
Table 6.9: Number of tubular joints	66
Table 7.1: Unity Price per part.....	69
Table 7.2: Cost estimation of designs	70
Table 8.1: Transport phases.....	73
Table 8.2: Transport operations	73
Table 8.3: Estimated distance from quay to wind farm location for appliance of two barges	79
Table 8.4: Number of required barges	79
Table 9.1: Day rate estimation.....	83
Table 9.2: Assessment of working times.....	84
Table 9.3: Installation cost of 4-leg jacket	85
Table 9.4: Installation cost of 3-leg jacket	85
Table 10.1: Total installation and transport cost four-leg jacket for 50 jacket wind park.....	87
Table 10.2: Total installation and transport cost three-leg jacket for 50 jacket wind park.....	87
Table 10.3: Total cost of designs for 50 jackets in a offshore wind park	88
Table 10.4: Parameter susceptibility	89
Table A.1: Tower sections	105
Table A.2: Masses of turbine and blades	106
Table A.3: Turbine loads	106
Table A.4: Fatigue damage equivalent loads	106
Table A.5: Marine growth profile	107
Table A.6: Main parameters overview	108
Table A.7: Material Properties	108
Table A.8: Geotechnical data Dataset 1	110
Table A.9: Geotechnical data dataset 2	110
Table A.10: Fatigue safety factors.....	113

Table A.11: Scatter Diagram	114
Table D.1: Concept criteria.....	123
Table F.1: First 4 mode shapes optimised 4-leg	132
Table F.2: First 4 mode shapes 4-leg jacket K-braces.....	133
Table F.3: First four mode shapes 3-leg jacket.....	134
Table G.1: Pile maximum axial capacity summary dataset 1.....	136
Table G.2: Pile maximum axial capacity summary dataset 2.....	136
Table G.3: Member group summary	137
Table G.4: Joint Can summary.....	137
Table G.5: Pile maximum axial capacity summary dataset 1.....	140
Table G.6: Pile maximum axial capacity summary dataset 2.....	140
Table G.7: Member group summary	140
Table G.8: Joint can summary.....	141
Table G.9: Pile maximum axial capacity summary dataset 1.....	144
Table G.10: Pile maximum axial capacity summary dataset 2.....	144
Table G.11: Member group summary	145
Table G.12: Joint can summary.....	145
Table G.13: Pile maximum axial capacity summary dataset 1.....	148
Table G.14: Pile maximum axial capacity summary dataset 2.....	148
Table G.15: Member group summary	149
Table G.16: Joint Can summary.....	149
Table K.1: Jack-Up barges	159
Table K.2: Crane vessels	159

Appendix A Design Parameters

A.1 Turbine Data

The following data is adopted from the RePower report. (6).

Introduction

- The loads in this document are only an indication for the first iterative steps of the design process.
- This are loads for conceptual design of substructure and foundation

RePower 5M / 6M turbine

- 5M and 6M: minimal rotor speed: 7.5 RPM
maximal rotor speed: 12.1 RPM
- Dynamic characteristics of combined system foundation, tower and 5M/6M turbine.
minimum first natural frequency: 0.22Hz
maximum first natural frequency: 0.34 Hz

Tower height

The following tower sections are defined by the turbine manufacturer.

Table A.1: Tower sections

Member section	Elevation bottom [m]	Elevation top [m]	Segment length [m]	Diameter [mm]	Wall thickness [mm]
T14	30.000	32.200	2.20	5500	50
T14	32.200	35.140	2.94	5500	50
T13	35.140	38.080	2.94	5500	32
T12	38.080	41.020	2.94	5500	31
T11	41.020	43.970	2.95	5500	30
T10	43.970	46.920	2.95	5500	28
T09	46.920	49.870	2.95	5500	26
T08	49.870	52.820	2.95	5500	25
T07	52.820	55.020	2.20	5500	24
T06	55.020	57.350	2.33	5500	23
T05	57.350	59.680	2.33	5500	22
T05	59.680	61.880	2.20	5500	22
T04	61.880	64.830	2.95	5500	21
T03	64.830	67.780	2.95	5500	20
T03	67.780	70.730	2.95	5500	20
T03	70.730	73.680	2.95	5500	20
T02	73.680	76.630	2.95	5500	19
T01	76.630	79.580	2.95	5500	18
T01	79.580	82.530	2.95	5500	18
T01	82.530	85.480	2.95	5500	18

Masses

For this thesis the 6M turbine with RE61.5 blades are chosen.

Table A.2: Masses of turbine and blades

Turbine		5M			6M		
		Mass[t]	X _{cogL} [m]	Z _{cogL} [m]	Mass[t]	X _{cogL} [m]	Z _{cogL} [m]
Rooter blade	LM 61.5	444.5	1.17	2.54	453.5	1.12	2.53
	RE 61.5				465.5	1.25	2.56

Tower & foundation loads

Only extreme load is extracted from several calculations and can be used for preliminary designs.

Table A.3: Turbine loads

	5M en 6M	6M
	LM 61,5 rotor blade	RE 61.5 rotor blade
Resulting thrust force $F_{res;Tb}$	± 2.3 MN	± 2.6 MN
Torsion $F_{res;tb}$	± 21 MNm	± 23 MNm

- These loads are inclusive a load factor of 1.35.
- It is proposed that these tower bottom loads are combined with the 50-yr extreme wave. This is because at least some of the load cases which may be governing include the 50-yr wave.

Fatigue loads

The fatigue load are given for two sites as damage equivalent loads for $N=2.00E8$ at tower bottom. As can be seen, only damage equivalent loads for site with 30 meter water depth are given. Due to lack of other reliable data is decided to use this data for the site with 45 meter water depth.

Table A.4: Fatigue damage equivalent loads

		5M site A	6M site A	5M site B	6M site B
	unit	Jacket	Jacket	Monopile	Monopile
F _x	kN	125	134	195	247
F _y	kN	115	131	268	302
F _z	kN	60	67	61	89
M _x	kNm	6208	7465	16900	18998
M _y	kNm	6946	7756	12170	15417
M _z	kNm	2880	3138	3760	4517
Water depth		30	30	15	15
Hub height		92	92	84	84
V mean		10.15	10.15	9.3	10

A.2 Environmental data & Loading parameter

Environmental Data

The parameters used in the report of the reference model are used as guiding principle as often as possible.

Turbine, wave and current data

For the extreme conditions the following design data shall be applied for the global design of the substructure:

- 50-yr return period maximum wave height with associated period;
- 100-yr return period one hourly mean current;
- Maximum turbine loads by appendix A.1.

Design water levels

The maximum design water levels during extreme condition are composed out of:

- 100-yr return storm surge;
- Spring tidal amplitude;
- Water depth tolerance of +0.5 meter.

The minimum design water levels during extreme condition are composed out of:

- 100-yr return storm surge;
- Spring tidal amplitude;

Splash zone

The splash zone is defined as the zone between the following elevations:

Upper elevation: HAT +2 meter;
Lower elevation: LAT -3 meter.

Minimum air gap

Because the offshore wind turbine can be considered unmanned, the abnormal 10,000-yr return period does not have to be considered for the normative air gap. The minimum air gap is defined as the distance between LAT and BOS of the transition piece and is determined by the water level occurring at the 100 year return period storm. This water level is composed out of:

- 100-yr return period crest wave elevation;
- 100-yr return storm surge;
- Spring tidal amplitude;
- Water depth tolerance of 0.5 meter;
- 1.5 meter extra gap to account for platform settlements, possibility of extreme waves.

Marine growth

The marine growth profile as depicted in the table below shall be used for the design.

Table A.5: Marine growth profile

Depth (ref LAT) [m]	Marine growth [mm]
+2.0	125
0.0	125
-6.0	50
Seabed	50

Intermediate values shall be interpolated. The dry density of marine growth shall be taken as 1400 kg/m³.

Results

This results in the following overview.

Table A.6: Main parameters overview

Item	Symbol	Units	Value
Extreme wave height	$H_{50\text{-yr}}$	[m]	21.3
Associated wave period	T_{ass}	[s]	14.85
Water elevations	100-yr max (incl. tolerance)	[m]	+6.70
	HAT	[m]	+4.80
	MSL	[m]	+2.40
	LAT	[m]	+0.00
Minimum bottom of steel	BOS	[m]	+22.20
Water depths	Maximum design water level	[m]	51.70
	LAT	[m]	45.00
	Minimum design water level	[m]	43.60
Splash zone (rel. to LAT)	Upper elevation	[m]	+6.80
	Lower elevation	[m]	-2.00
Current (at 100% of water depth)	100	[m/s]	1.122
	60		1.122
	50		1.120
	25		1.074
	10		1.020
	0.05		0.983
	0.01		0.910

Material

The steel grade used for the primary structure is high tensile steel, S355 in EN 10225. In case through thickness properties are required this will be indicated on the drawings. The yield stress depends on the wall thickness (WT) as listed below.

Table A.7: Material Properties

Steel	Thickness [mm]	Min. Yield Stress [N/mm ²]
S355	$t \leq 16$	355
	$16 \leq t \leq 40$	345
	$40 \leq t \leq 63$	335
	$63 \leq t \leq 100$	325

Loading effects

Appurtenance loads

The following loads will be modelled with regards to the appurtenances;

- Anodes are modelled by increasing the hydrodynamic coefficients of members to which anodes are attached by 7%. The mass of the anodes are included in the non-modelled dead load case.
- The J-tube is modelled in the SACS software by adding a pipe of 508mm. The mass of J-tube is expected to be included in the contingency.
- The boat landing is modelled by increasing the hydrodynamic coefficients of one leg of the jacket. Location is just below the LAT to the transition piece. The weight of the boat landing is expected to be included in the contingency.

Corrosion Protection

Below the splash zone are protected by sacrificial anodes. Total required mass of the anodes is assumed to be 35 ton. The members in the splash zone are designed with a corrosion allowance of 0.5 mm/year. With a design life time of 25 years, this means a wall thickness reduction of 1/2" and diameter reduction of 1". In the fatigue analyses the corrosion is reduced by 50%.

Hydrostatic loads

Hydrostatic load for hydrostatic member checks will be generated by the SACS software.

Extreme Wave and current loads

The combined wave and current load on the substructure shall be calculated using Morison's equation in conjunction with Stream Function wave theory of the appropriate order.

The following principles will be applied to the evaluation of wave loading:

- Current loading is applied in accordance with Wave loading cases are generated for the extreme (50-yr) return period storm in which the following variables are investigated:
 - Wave period (T_{ass})
 - Wave direction (0° - 360°)
 - Water depth (min and max design water level)
- Each wave shall pass the structure in 72 steps resulting in 72 results regarding the hydrodynamic forces acting on the substructure. The phase angle of the wave resulting in a maximum overturning load relative to the mud line shall be used as design load case.
- The combination of above resulting in the maximum wave loading shall be designated as the design wave load case.
- Basic hydrodynamic coefficients for tubulars are chosen as follows;

○ Smooth tube	Drag coefficient (C_d)=0.70	Mass coefficient (C_m)=1.6
○ Rough tube	Drag coefficient (C_d)=1.05	Mass coefficient (C_m)=1.2
- Wave kinematics factor of 0.91 will be used.
- No current blockage factor will be used.
- Current velocity profile will be non-linearly stretched to the surface and wave and current velocities will be added vectorially before applying Morrison's equation.
- Member diameters will be increased by marine growth thickness as defined in Table A.5.

P-delta effect

For members having large axial forces the P-delta effect will result in lateral stiffening effects. For the substructure legs the compressive axial force causes a decrease of lateral stiffness.

The SACS program performs an initial run to assess the axial internal loads. Then the lateral stiffness of the model is modified due to the P-delta effect and the model is reanalysed with modified stiffness.

Member and Joint design*General*

Member forces and moments derived from the global analysis for design loading combinations will be checked for member strength and stability, hydrostatic collapse and tubular joint strength. Generally all member and joints will be checked against the requirements of the ISO standard. All code checks will be performed on the corroded section properties of the members when applicable.

Tubular Joint checks

ISO guidelines and checks are performed for all nodes where applicable. SACS automatically define joint as T, Y, X, K or KT depending on geometry and load path consideration. A minimum acceptable gap, between the surfaces intersections of adjacent braces with a node can, shall be taken to be 75 mm.

Vortex Shedding Design

Substructure members and appurtenances will not be checked regarding vortex induced vibrations in this phase of design.

Wave slam

Wave slam loadings are not determined in this phase of the design.

Geotechnical Data

Dataset 1

Geotechnical data is derived from Geotechnical report for project E17 (10).

Table A.8: Geotechnical data Dataset 1

Ground Model	Depth Top-Bottom [m]	γ [kN/m ³]	δ [deg]	c_u [kPa]	q_c [Mpa]
Sand	0.0	19.5	15		0.5
	3.4				7.0
Clay	3.4	18.5		50	1.0
	5.4			50	1.0
Clay	5.4	21.5		125	3.0
	10.0			300	10.4
Sand	10.0	20.0	25		10.4
	13.5		25		16.0
Sand	13.5	21.0	30		32.0
	28.0		30		62.0
Sand	28.0	21.0	30		38.0
	32.9		30		48.0
Sand	32.9	20.0	25		30.0
	36.5		25		30.0
Sand	36.5	21.0	30		42.0
	43.5		30		42.0
Clay	43.5	20.0		300	6.0
	45.0			500	12.0
Sand	45.0	20.0	25		42.0
	47.2		25		42.0
Clay	47.2	20.0		100	2.0
	48.3			100	2.0
Sand	48.3	21.0	35		60.0
	54.8		35		76.0
Sand	54.8	21.0	30		42.0
	57.0		30		42.0
Sand	57.0	21.0	35		80.0
	81.0		35		80.0
Key: δ : soil-pile interface friction angle γ : unit weight of ground			c_u : undrained shear strength q_c : CPT cone resistance		

Dataset 2

Geotechnical data is derived from (9), North Sea, German Bight.

Table A.9: Geotechnical data dataset 2

Axial pile behaviour

Layer	Soil	Z [m]	γ' [kN/m ³]	δ [deg]	f_{lim} [kPa]	N_q	q_{lim} [MPa]
1	Sand	3,20	10,0	20.0	0	12	0.0
2	Sand	5,50	10.0	25.0	100	20	0.0
3	Sand	21.90	10.5	30.0	125	40	0.0
4	Sand	60.90	11.0	35.0	160	50	12.0

Lateral pile behaviour

Layer	Soil	Z [m]	γ' [kN/m ³]	δ [deg]	p_{lim} [kPa]	k [MN/m ³]
1	Sand	3,20	10,0	32.5	2.0	15
2	Sand	5,50	10.0	35.0	5.0	22
3	Sand	21.90	10.5	37.5	10.0	31.5
4	Sand	44.00	11.0	40.0	16.0	43.5

A.3 Loading Combinations

A.4 Fatigue analysis

General

A selection of main critical welds is made to analyse. These welds are:

- All circumferential butt welds in the legs.
- All circumferential butt welds in the braces.
- All welds at tubular joint connections for the legs and diagonal braces.
- All welds at tubular joint connection for the X braces.

Construction items which are not analysed:

- tower;
- transition piece;
- piles;
- stubs between the J-tube and legs.

Fatigue safety factors

The minimum service lifetime is set to 25 years with a fatigue safety factor as depicted in the table below. All joints are typed a critical failure joints. Joint in the splash zone are not inspectable, the rest are inspectable.

Table A.10: Fatigue safety factors

Location	Inspectable	Not Inspectable
Failure non critical	2	5
Failure critical	5	10
Splash Zone	n/a	10

Stress Concentration Factors

SCF's for nodal joints will be generated automatically using facilities within SACS. The procedure for calculating stress concentration factors for unstiffened T, K, Y tubular joints will be as follows;

- Load path classification of joints as K, X and T/Y is undertaken automatically by the SACS software. The load path SCF will be determined as the weighted average of K, X, T/Y percentages.
- Use Efthymiou's parametric formulae for calculation of axial, in-plane bending and out-of-plan SCF's for T/Y and X joints.
- Normally SCF's will be calculated for the actual parameters applicable to the joint. However, where parameters are outside the applicable range for the formula, SCF's will be calculated for the actual joint parameters and the parameters at the range limit and the maximum of these values will be used.
- SCF's will be calculated at eight points around the brace, SCF's at quarter points will be calculated by interpolation between crown and saddle SCF's.
- A minimum of SCF of 1.5 is applied for tubular joints.

Scatter Diagram

The following data is obtained by (8).

Table A.11: Scatter Diagram

		Spectral Peak Period (s)																												
Lower Bound	Upper Bound	0	1	2	3	4	5	6	7	8	9	10	11	12	13	14	15	16	17	18	19	20	21							
		1	2	3	4	5	6	7	8	9	10	11	12	13	14	15	16	17	18	19	20	21	22							
Significant Wave Height (m)	11.5	12.0																						0	0					
	11.0	11.5																							0	0				
	10.5	11.0																							0	0				
	10.0	10.5																							0	0				
	9.5	10.0															2		1						3	3				
	9.0	9.5														1	1								2	5				
	8.5	9.0													5	6	6									17	22			
	8.0	8.5													8	5	3										16	38		
	7.5	8.0												3	18	12	4											37	75	
	7.0	7.5										1	14	40	17	3	1												76	151
	6.5	7.0									1	4	67	71	19	2	1												165	316
	6.0	6.5										36	140	38	9														223	539
	5.5	6.0									3	4	165	133	32	10	1	1											349	888
	5.0	5.5									5	69	382	154	35	6	3												654	1542
	4.5	5.0									3	9	344	570	110	26	9												1071	2613
	4.0	4.5								10	69	995	512	112	25	7	3				1								1734	4347
	3.5	4.0						1	11	669	1446	427	121	26	8	8	3												2720	7067
	3.0	3.5						10	82	1939	1855	307	89	21	11	3					1		1						4319	11386
	2.5	3.0					2	17	895	3483	1327	290	74	24	4	1	1	2											6120	17506
2.0	2.5				1	26	155	3360	3513	1049	318	64	20	5	2	1												8514	26020	
1.5	2.0				10	80	1390	5415	2687	1132	333	69	20	1	1													11138	37158	
1.0	1.5			2	50	471	4798	4732	2233	903	246	41	8	2	4			2						1				13493	50651	
0.5	1.0		2	54	209	2861	4881	2484	1040	392	110	38	16	9	5	2			1									12104	62755	
0.0	0.5		8	57	256	1426	1533	471	187	65	18	1	4	3														4029	66784	
		0	0	10	113	526	4866	12785	17463	15837	9582	3719	1230	437	143	51	12	5	3	0	1	0	1				Sum			
		66784	66784	66784	66774	66661	66135	61269	48484	31021	15184	5602	1893	653	216	73	22	10	5	2	2	1	1					Cumulative Sum		

Appendix B Suction Buckets

B.1 Reference Projects

The concept of the suction bucket foundation was developed in the classical offshore technology and has already been used there frequently. This concept is however comparatively new as a foundation for an offshore wind energy plant, which is subject to very complex loading situations. There are 2 occasions known where a suction bucket served as foundation for a wind turbine.

Frederikshavn, Denmark

A fully operation 3.0 MW offshore wind turbine was installed on a prototype of the bucket foundation in Frederikshavn in October 2002 (18). The wind turbine is a part of an offshore research test field consisting of four 2-3 MW wind turbines next to the harbour of Frederikshavn in the northern part of Denmark. The research program deals with foundation of offshore wind turbines in general, but the ongoing projects are related to the development of bucket foundations.

The prototype in Frederikshavn was designed with a diameter of 12 meters and a skirt length of 6 meters. The water depth is 4 meters, and as the sitting is in a basin, no wave and ice loads are applied. The steel construction weight is 140 tons. The actual installation period lasted 12 hours, where the soil penetration period lasted 6 hours, using a computer system to perform the inclination guidance and control of the suction pressure and penetration rate.

The prototype has been equipped with a monitoring system that measures the modal space of the foundation and the wind turbine. Output-only analysis has been used to analyse the structural behaviour of the wind turbine in various operational conditions. The analysis has shown highly damped mode shapes of the foundation/wind turbine system, which the present aero-elastic codes for wind turbine design are insufficient to model. Further studies are to be carried out with respect to soil-structure interaction.



Figure B.1: Suction bucket in Frederikshavn

Wilhelmshaven, Germany

During 2005 an attempt to install a rotor diameter of 114 meter with a tubular steel tower on top of a suction bucket foundation in shallow water of the coast of Hooksiel, Wilhelmshaven failed.

The bucket was designed for a 5MW Enercon turbine. The bucket had a diameter of 16 meter and the skirt length was 15 m.

The decision to cancel sinking operation was taken after buckling occurred in the suction bucket.

Some soil mechanic experts think that the foundation condition might have been falsely calculated. Rumours are also circulating that fractures arose in the material, negating the vacuum and ultimately causing the bucket to shift. (19)

But according the companies involved the installation barge floated sideways and collided with the bucket during the installation process. The impact left a dent of about 80 mm in the skirt and initiated buckling after 7 m penetration. (20)



Figure B.2: Failed attempt during installation at Wilhelmshaven

B.2 Suction bucket calculation

In this calculation the installation is not discussed. Only the operational situation is considered, assuming that the bucket is fully penetrated.

Design criteria

- In the design load the (submerged) weight of the bucket is not yet included.
- Based on suction bucket / soil interface failure.
- Suction buckets transfer the gravity loads and the environmental generated overturning moment by a vertical push-pull concept. The base shear is distributed equally to the buckets.
- Base shear loads are relative low and insignificant compared to the vertical loads. In this phase base shear is ignored.

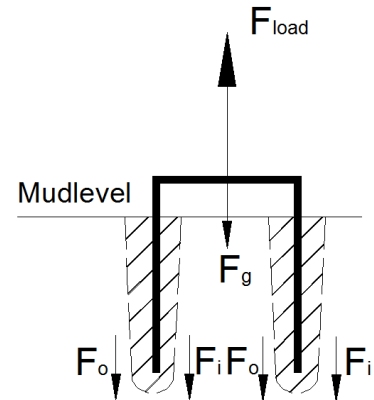


Figure B.3: Shear failure

Failure concept

- The suction bucket concept fails due to shear failure along the inner and outer perimeter. The inner shear failure is due to the large diameter, but it should be demonstrated that the internal plugs bearing capacity supersedes the shear load.

Force balance

The active forces are:

- Vertical load force (F_{load})
- Self weight bucket (F_g)
- Shaft friction outer surface (F_o, τ_o)
- Shaft friction inner surface (F_i, τ_i)

$$\sum F_z = F_g + F_o + F_i - F_{load}$$

For now active earth pressure is considered.

Shaft friction outer surface

$$\tau_o = c + \sigma'_{h;min} \cdot \tan \varphi_e = c + K_a \cdot \tan \varphi_e$$

$$\varphi_e \approx \frac{2}{3} \cdot \varphi_i$$

$$K_a = \frac{1 - \sin(\varphi_e)}{1 + \sin(\varphi_e)}$$

$$F_o = \iint \tau_{min} \cdot dA = \pi \cdot D \int_0^d \tau_{min} dZ = \frac{1}{2} \cdot \pi \cdot D \cdot K_a \cdot \tan \varphi_e \cdot (\gamma_{soil} - \gamma_{water}) \cdot d^2$$

Shaft friction inner surface

$$F_i = \min \left\{ \begin{array}{l} F_o \\ W_{soil} = \frac{1}{4} \cdot \pi \cdot D^2 \cdot (\gamma_{soil} - \gamma_{water}) \cdot d^2 \end{array} \right.$$

Load capacity

$$F_{load} \leq W + F_o + F_i$$

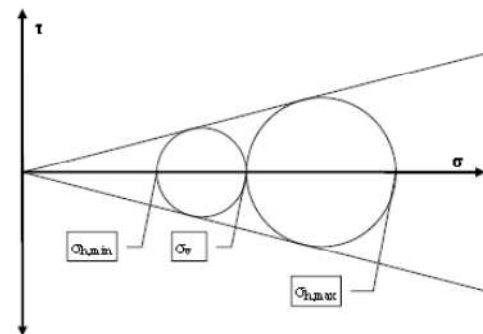


Figure B.4: Circle of Mohr

As in the reference design the following soil properties are used.

Medium Dense sand

$$\varphi_i = 37^\circ$$

$$\gamma_{soil} = 20kN / m^3$$

$$c = 0$$

Water

$$\rho_{water} = 1030kg / m^3$$

$$\gamma_{water} = 10kN / m^3$$

The following suction bucket is defined.

$$D = 21m$$

$$d = 18m$$

$$t_1 = 0.08m$$

$$t_2 = 0.09m$$

$$\rho_{steel} = 7850kg / m^3 \Rightarrow \gamma_{steel} = 9.81 \cdot (7850 - 1030) / 1000 = 66.9kN / m^3$$

Self weight bucket

$$F_g = (D \cdot \pi \cdot L \cdot t_1 + \frac{1}{4} \cdot D^2 \cdot \pi \cdot t_2) \cdot \gamma_{steel} = (21 \cdot \pi \cdot 18 \cdot 0.08 + \frac{1}{4} \cdot 21^2 \cdot \pi \cdot 0.09) \cdot 66.9 = 8441kN$$

Outer surface friction

$$\varphi_e = \frac{2}{3} \cdot \varphi_i = \frac{2}{3} \cdot 37 = 24.66^\circ$$

$$K_a = \frac{1 - \sin(37^\circ)}{1 + \sin(37^\circ)} = 0.2485$$

$$F_0 = \frac{1}{2} \cdot \pi \cdot 21 \cdot 0.2485 \cdot \tan(24.66^\circ) \cdot (20 - 10) \cdot 18^2 = 12074kN$$

Inner surface friction

$$F_i = \min \left\{ \begin{array}{l} F_0 = 12074kN \\ W_{soil} = \frac{1}{4} \cdot \pi \cdot 21^2 \cdot (20 - 10) \cdot 18 = 62695kN \end{array} \right. = 12074kN$$

The maximum tension load on the suction bucket can be:

$$F_{load} \leq 8441 + 12074 + 12074 = 32589kN$$

This calculation shows that a suction bucket with a diameter of 21 meter and a penetrated height of 18 meter is capable to restrain pulling out. The following remarks have to be made:

- Using an internal friction angle of 37° indicates very dense sand in the seabed layer. That is rather optimistic for the North Sea. It has to be questioned which earth pressure is the right one, but in this calculation the most optimistic value is chosen.
- At this moment is assumed that the suction caisson reacts as a deep piled foundation. Other option is to look at it as a shallow foundation. The opinion among experts is divided and further evaluation is suggested, but is beyond the scope of this thesis.
- Scour effects are neglected in this calculation.

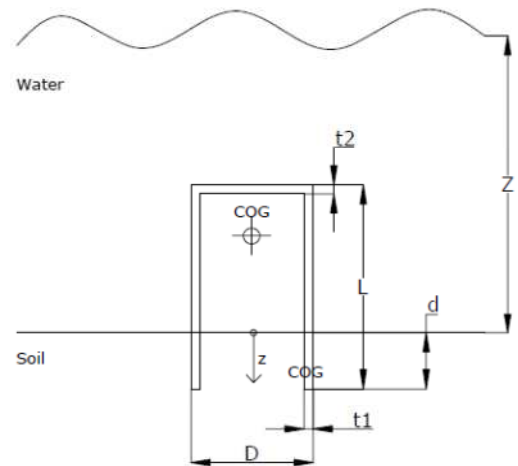


Figure B.5: Overview of main parameters

Appendix C Reference Projects

Jackets

The Beatrice Wind Farm Demonstration Project

Early in 2005 a detailed review of the potential substructure designs was undertaken. A four legged lightweight lattice structure derived from oil and gas technology was utilized. These were set on the seabed on mud mats and levelled and then anchored to the seabed using four driven piles.

Each wind turbine installation required two lifts. First, the substructure jacket was set down onto the seabed and secondly the tower, turbine and blades mated to the jacket as one unit.

The tower, turbine and blades were assembled on top of a 'soft landing' module at the quayside and lifted onto the installation vessel. Installation of the Demonstrator turbines took place in the summers of 2006 and 2007.

- The cost of the total project was €41 million.
- Location is 23 kilometres from shore, in a water depth of approximately 45 meters.
- jacket height (including transition piece): 70 meters
- Total weight: jacket and associated equipment: 760 ton.

Alpha Ventus

The Alpha Ventus wind farm consist of twelve turbines of which six turbines are 5 megawatt (MW) Areva Multibrid (M5000) and six turbines are REpower 5M. The turbines stand in 30 m of water. The REpower turbines are installed onto jacket foundations and the Areva turbines are installed onto tripod-style foundations.

The concepts of the jacket are based on the Beatrice project, two years earlier. As such, the concept had already proven feasible. The steel structures are supported by four driven piles. The piles were installed prior to the jacket structures. Thereby the six jackets could be made identical.



Figure C.1: Horizontal placement of jacket in fabrication hall



Figure C.2: Installing Beatrice Jacket



Figure C.3: Transport of Alpha Ventus jacket

Tripod*Alpha Ventus*

Besides the jacket substructures in the Alpha Ventus wind farm, also Tripod substructures are installed. The tripods for the AREVA Multibrid wind turbines were installed in the spring of 2009. The 45 meter tall and more than 700 ton heavy tripods. The three legs of the tripods were each “nailed” separately to the seabed using an approximately 40-metre long pile, then subsequently balanced and sealed into their final position by pouring concrete into the pile sleeve. This work was completed on 1 June 2009. After their installation, the bottom tower segments of all six turbines were secured to the substructure with steel flanges. By September 2009, all six turbines were completed in this manner. The completed wind turbines rise to a height of 90 meters over the surface of the sea to a rotor blade tip of 148 meters. If one were to measure the height from the seabed, the turbines would reach an actual total height of 178 meters. The triangular area of the tripods covers an area of 255 square meters



Figure C.4: Transport of tripods



Figure C.5: Installation of tripod

Tripile

BARD offshore 1

The BARD Offshore 1 wind turbine farm is located in the North Sea, about 100km north-west of the German island of Borkum. This wind turbine farm consists of 80 wind turbines of the BARD 5MW turbines.

The Bremen-based company developed a patented concept for the foundation of the wind turbines: the BARD Tripile. The high wind turbine rests on three main pilings that are each 90m in length. Depending on the ground quality, these piles are driven 30 to 45m into the sea bed using a template. Their position is accurately determined using a satellite controlled navigation system. The height of these pilings above the water surface is also automatically determined to an accuracy of 3 to 4cm. Above the water surface, these three pilings are connected to each other by a cross piece on which the turbine mast stands. All necessary connections can be constructed above the water surface. That is why all installation activities can be performed above the water surface.

Once the supporting cross piece is level, it is locked in place together with the piles by a 5m high grouting and 13cm thick ring against the wall of both the supporting cross piece and the piles.

- Weight of foundation pile: 400 t
- Weight of support cross piece: 500 t
- Height of foundation piles: 90 m
- Water depth: 40 m



Figure C.6: BARD's tripile



Figure C.7: Tripile installation

Appendix D Concept Evaluation

The way to assess the concepts on base of the set criteria is defined in the table below. Next pages show the assessment of the concept in the same table form.

Table D.1: Concept criteria

Design			
1	Mass of substructure	What magnitude is the mass expected to be compared to other concepts?	Very small = 10 Very large = 1
2	footprint	What magnitude is the footprint expected to be compared to other concepts?	Very small = 10 Very large = 1
3	Tower connection	How complex is the connection to the tower? How much effort is required for the connection to the tower?	Not complex / very little = 10 Very complex / very much = 1
Fabrication			
4	Number of joints	How much time is required to fabricate the welds of the support structure components?	Very little time = 10 A lot of time = 1
5	Complexity of the joints	How complex is a joint? Are the weld locations easily accessible?	Very simple / yes = 10 Very complex / no = 1
6	Manoeuvrability	How easy is the substructure to handle during fabrication?	Very easy = 10 Very difficult = 1
Installation			
7	Lifting	How much time and effort is required to lift the components in place?	Very little / very easy = 10 Very much / very difficult = 1
8	Foundation	How much time and effort is required to install the foundation and to connect the substructure to the foundation?	Very little / Very easy = 10 Very much / Very difficult = 1
Maintenance			
9	Number of joints	How much time is required to inspect joints?	Very little time = 10 A lot of time = 1
Overall			
10	Reliability	Is it a proven concept? Is it applied before?	Very proven concept / common applied = 10 Non proven concept / not applied = 1
11	Decommissioning	How much effort is required for decommission?	Very little effort = 10 A lot of effort = 1

Assessment by Frank van Gerven

nr.	criteria	score											absolute	relative	weight factors		
		1	2	3	4	5	6	7	8	9	10	11					
design																	
1	mass		1	1	1	1	1	1	1	1	1	1	1	1	10	20	1,7
2	footprint	0		1	0	0	1	1	1	1	1	1	1	1	7	14	1,2
3	tower connection	0	0		0	0	1	1	0	1	1	1	1	1	5	10	0,9
fabrication																	
4	number of joints	0	1	1		0	1	1	1	1	1	1	1	1	8	16	1,4
5	complexity of joints	0	1	1	1		1	1	1	1	1	1	1	1	9	18	1,6
6	manoeuvrability	0	0	0	0	0		0	0	1	1	1	1	1	3	6	0,5
installation																	
7	lifting	0	0	0	0	0	1		1	1	1	1	1	1	5	10	0,9
8	foundation	0	0	1	0	0	1	1		1	1	1	1	1	6	12	1,0
inspection																	
9	number of joints	0	0	0	0	0	0	0	0		0	1	1	1	1	2	0,2
overall																	
10	reliability (proven technology)	0	0	0	0	0	1	0	0	1		1	1	1	3	6	0,5
11	decommissioning	0	0	0	0	0	0	0	0	0	0		1	1	0	1	0,1
													57	115	10,0		

design	1 jacket				2. Tri-pod				3. tetra-pod				jacket				tripod				tetra-pod					
	A: 4-leg battered	B: 3-leg battered	C: 3-leg straight	D: 4-leg straight	A: conventional	B: extended	C: split	D: a-symmetric	4. triple	A: symmetric	B: A-symmetric	5. twisted jacket	Weight-factor	A: 4-leg battered	B: 3-leg battered	C: 3-leg straight	D: 4-leg straight	A: conventional	B: extended	C: split	D: a-symmetric	triple	A: symmetric	B: A-symmetric	twisted jacket	
1	mass of substructure	8	9	6	5	5	3	4	4	1	4	3	6	1,7	13,9	15,7	10,4	8,7	8,7	5,2	7,0	7,0	1,7	7,0	5,2	10,4
2	footprint	6	8	8	6	8	8	8	5	8	4	3	7	1,2	7,3	9,7	9,7	7,3	9,7	9,7	9,7	6,1	9,7	4,9	3,7	8,5
3	tower connection	6	7	7	6	8	8	8	8	3	8	8	5	0,9	5,2	6,1	6,1	5,2	7,0	7,0	7,0	7,0	2,6	7,0	7,0	4,3
fabrication																										
4	number of joints	3	4	4	3	8	5	8	8	9	6	6	7	1,4	4,2	5,6	5,6	4,2	11,1	7,0	11,1	11,1	12,5	8,3	8,3	9,7
5	complexity of joints	6	6	7	7	3	4	2	4	5	3	4	7	1,6	9,4	9,4	11,0	11,0	4,7	6,3	3,1	6,3	7,8	4,7	6,3	11,0
6	manoeuvrability	6	7	7	6	5	4	5	8	9	4	6	5	0,5	3,1	3,7	3,7	3,1	2,6	2,1	2,6	4,2	4,7	2,1	3,1	2,6
installation																										
7	lifting	7	7	5	5	5	4	4	5	9	4	4	7	0,9	6,1	6,1	4,3	4,3	4,3	3,5	3,5	4,3	7,8	3,5	3,5	6,1
8	foundation	6	7	7	6	7	7	7	7	5	6	6	2	1,0	6,3	7,3	7,3	6,3	7,3	7,3	7,3	7,3	5,2	6,3	6,3	2,1
inspection																										
9	number of joints	3	4	4	3	8	5	8	8	9	6	6	7	0,2	0,5	0,7	0,7	0,5	1,4	0,9	1,4	1,4	1,6	1,0	1,0	1,2
overall																										
10	reliability	9	5	4	4	9	1	1	1	8	1	1	2	0,5	4,7	2,6	2,1	2,1	4,7	0,5	0,5	0,5	4,2	0,5	0,5	1,0
11	decommissioning	6	7	7	6	7	7	7	7	4	5	5	5	0,1	0,5	0,6	0,6	0,5	0,6	0,6	0,6	0,6	0,3	0,4	0,4	0,4
total		66	71	66	57	73	56	62	65	70	51	52	60	10,0	60,7	66,8	60,9	52,7	61,6	49,4	53,2	55,1	57,9	45,2	44,9	57,0
Rank															4	1	3	9	2	10	8	7	5	11	12	6

Assessment by Jan Beckers

nr.	criteria	score											absolute	relative	weight factors
		1	2	3	4	5	6	7	8	9	10	11			
design															
1	mass		1	1	0	1	1	1	1	1	1	1	9	18	1,6
2	footprint	0		0	0	0	1	0	0	1	0	0	2	4	0,4
3	tower connection	0	1		0	0	1	1	0	1	0	0	4	8	0,7
fabrication															
4	number of joints	1	1	1		1	1	1	1	1	1	1	10	20	1,8
5	complexity of joints	0	1	1	0		1	1	1	1	1	1	8	16	1,4
6	manoeuvrability	0	0	0	0	0		0	0	1	0	0	1	2	0,2
installation															
7	lifting	0	1	0	0	0	1		1	1	0	0	4	8	0,7
8	foundation	0	1	1	0	0	1	0		1	0	0	4	8	0,7
inspection															
9	number of joints	0	0	0	0	0	0	0	0		0	0	0	1	0,1
overall															
10	reliability (proven technology)	0	1	1	0	0	1	1	1	1		1	7	14	1,3
11	decommissioning	0	1	1	0	0	1	1	1	1	0		6	12	1,1
													55	111	10,0

design	1 jacket				2. Tri-pod				3. tetra-pod				weight-factor	jacket				tripod				tetra-pod				
	A: 4-leg battered	B: 3-leg battered	C: 3-leg straight	D: 4-leg straight	A:conventional	B: extended	C: split	D: a-symmetric	4. triple	A: symmetric	B: A-symmetric	5. twisted jacket		A: 4-leg battered	B: 3-leg battered	C: 3-leg straight	D: 4-leg straight	A:conventional	B: extended	C: split	D: a-symmetric	triple	A: symmetric	B: A-symmetric	twisted jacket	
1	mass of substructure	10	9	7	8	4	5	4	3	2	2	2	1	1,6	16,2	14,6	11,4	13,0	6,5	8,1	6,5	4,9	3,2	3,2	3,2	1,6
2	footprint	4	3	3	4	5	5	5	5	6	6	6	7	0,4	1,4	1,1	1,1	1,4	1,8	1,8	1,8	1,8	2,2	2,2	2,2	2,5
3	tower connection	3	3	3	3	8	8	8	8	8	8	8	8	0,7	2,2	2,2	2,2	2,2	5,8	5,8	5,8	5,8	5,8	5,8	5,8	5,8
fabrication																										
4	number of joints	4	5	5	4	6	6	6	6	7	6	6	7	1,8	7,2	9,0	9,0	7,2	10,8	10,8	10,8	10,8	12,6	10,8	10,8	12,6
5	complexity of joints	8	8	8	8	5	5	5	5	2	3	3	4	1,4	11,5	11,5	11,5	11,5	7,2	7,2	7,2	7,2	2,9	4,3	4,3	5,8
6	manoeuvrability	8	7	7	9	5	5	5	5	4	3	3	9	0,2	1,4	1,3	1,3	1,6	0,9	0,9	0,9	0,9	0,7	0,5	0,5	1,6
installation																										
7	lifting	8	8	8	6	4	4	4	4	7	4	4	8	0,7	5,8	5,8	5,8	4,3	2,9	2,9	2,9	2,9	5,0	2,9	2,9	5,8
8	foundation	6	7	7	6	8	8	8	8	5	5	5	2	0,7	4,3	5,0	5,0	4,3	5,8	5,8	5,8	5,8	3,6	3,6	3,6	1,4
inspection																										
9	number of joints	4	6	6	4	8	8	8	8	10	9	9	10	0,1	0,4	0,5	0,5	0,4	0,7	0,7	0,7	0,7	0,9	0,8	0,8	0,9
overall																										
10	reliability	10	10	10	10	8	7	7	7	8	6	6	3	1,3	12,6	12,6	12,6	12,6	10,1	8,8	8,8	8,8	10,1	7,6	7,6	3,8
11	decommissioning	6	6	6	6	5	5	5	5	8	7	7	8	1,1	6,5	6,5	6,5	6,5	5,4	5,4	5,4	5,4	8,6	7,6	7,6	8,6
total		71	72	70	68	66	66	65	64	67	59	59	67	10,0	63,1	63,6	60,4	58,6	52,4	52,8	51,2	49,5	47,0	41,7	41,7	41,8
Rank															2	1	3	4	6	5	7	8	9	11	11	10

Assessment by Nico Noorlander

nr.	criteria											score		weight factors		
		1	2	3	4	5	6	7	8	9	10	11	absolute		relative	
design																
1	mass		1	1	1	1	1	1	1	1	1	1	1	10	20	1,8
2	footprint	0		0	0	0	0	0	0	1	0	0		1	2	0,2
3	tower connection	0	1		0	0	1	1	1	1	0	0		5	10	0,9
fabrication																
4	number of joints	0	1	1		0	0	1	1	1	0	1		6	12	1,1
5	complexity of joints	0	1	1	1		1	1	1	1	1	1		9	18	1,6
6	manoeuvrability	0	1	0	1	0		0	1	1	0	1		5	10	0,9
installation																
7	lifting	0	1	0	0	0	1		0	1	0	1		4	8	0,7
8	foundation	0	1	0	0	0	0	1		1	0	1		4	8	0,7
inspection																
9	number of joints	0	0	0	0	0	0	0	0		0	0		0	1	0,1
overall																
10	reliability (proven technology)	0	1	1	1	0	1	1	1	1		1		8	16	1,4
11	decommissioning	0	1	1	0	0	0	0	0	1	0			3	6	0,5
												55	111	10,0		

design	1 jacket				2. Tri-pod				3. tetra-pod				weight-factor	jacket				tripod				tetra-pod					
	A: 4-leg battered	B: 3-leg battered	C: 3-leg straight	D: 4-leg straight	A:conventional	B: extended	C: split	D: a-symmetric	4. triple	A: symmetric	B: A-symmetric	5. twisted jacket		A: 4-leg battered	B: 3-leg battered	C: 3-leg straight	D: 4-leg straight	A:conventional	B: extended	C: split	D: a-symmetric	triple	A: symmetric	B: A-symmetric	twisted jacket		
1	mass of substructure	9	7	8	10	6	5	4	3	3	3	3	1,8	16,2	12,6	14,4	18,0	10,8	9,0	7,2	5,4	5,4	5,4	5,4	5,4		
2	footprint	9	8	7	10	5	5	5	5	8	8	8	0,2	1,6	1,4	1,3	1,8	0,9	0,9	0,9	0,9	1,4	1,4	1,4	1,4		
3	tower connection	3	3	3	3	10	10	10	10	10	10	10	0,9	2,7	2,7	2,7	2,7	9,0	9,0	9,0	9,0	9,0	9,0	9,0	9,0		
fabrication																											
4	number of joints	5	5	5	5	10	10	10	10	7	7	7	1,1	5,4	5,4	5,4	5,4	10,8	10,8	10,8	10,8	7,6	7,6	7,6	7,6		
5	complexity of joints	10	10	10	10	2	2	2	2	2	2	10	1,6	16,2	16,2	16,2	16,2	3,2	3,2	3,2	3,2	3,2	3,2	3,2	16,2		
6	manoeuvrability	7	7	7	10	2	2	2	2	2	2	8	0,9	6,3	6,3	6,3	9,0	1,8	1,8	1,8	1,8	1,8	1,8	1,8	7,2		
installation																											
7	lifting	10	10	10	10	5	5	5	5	5	5	8	0,7	7,2	7,2	7,2	7,2	3,6	3,6	3,6	3,6	3,6	3,6	3,6	5,8		
8	foundation	10	10	10	6	4	4	4	4	5	4	4	0,7	7,2	7,2	7,2	4,3	2,9	2,9	2,9	2,9	3,6	2,9	2,9	5,0		
inspection																											
9	number of joints	5	5	5	5	10	10	10	10	7	7	7	0,1	0,5	0,5	0,5	0,5	0,9	0,9	0,9	0,9	0,6	0,6	0,6	0,6		
overall																											
10	reliability (proven technology)	10	10	10	10	10	8	8	5	5	5	5	1,4	14,4	14,4	14,4	14,4	14,4	11,5	11,5	7,2	7,2	7,2	7,2	7,2		
11	decommissioning	5	5	5	5	5	5	5	5	5	5	5	0,5	2,7	2,7	2,7	2,7	2,7	2,7	2,7	2,7	2,7	2,7	2,7	2,7		
total		83	80	80	84	69	66	65	61	59	58	58	10,0	77,7	74,0	75,6	79,5	58,4	53,7	51,9	45,8	43,5	42,8	42,8	65,5		
Rank														2	4	3	1	6	7	8	9	10	11	11	5		

Assessment by Stefan Beukers

nr.	criteria	score										absolute	relative	weight factors		
		1	2	3	4	5	6	7	8	9	10				11	
design																
1	mass		1	1	1	1	1	0	0	1	1	1	8	16	1,4	
2	footprint	0		0	0	0	1	0	0	1	1	1	4	8	0,7	
3	tower connection	0	1		1	1	1	0	0	1	1	1	7	14	1,3	
fabrication																
4	number of joints	0	1	0		1	1	0	0	1	1	1	6	12	1,1	
5	complexity of joints	0	1	0	0		1	0	0	1	1	1	5	10	0,9	
6	manoeuvrability	0	0	0	0	0		0	0	0	0	1	1	2	0,2	
installation																
7	lifting	1	1	1	1	1	1		1	1	1	1	10	20	1,8	
8	foundation	1	1	1	1	1	1	0		1	1	1	9	18	1,6	
inspection																
9	number of joints	0	0	0	0	0	1	0	0		0	1	2	4	0,4	
overall																
10	reliability (proven technology)	0	0	0	0	0	1	0	0	1		1	3	6	0,5	
11	decommissioning	0	0	0	0	0	0	0	0	0	0		0	1	0,1	
												55	111	10,0		

nr.	criteria	1 jacket				2. Tri-pod				3. tetra-pod				weight-factor	jacket				tripod				tetra-pod			
		A: 4-leg battered	B: 3-leg battered	C: 3-leg straight	D: 4-leg straight	A: conventional	B: extended	C: split	D: a-symmetric	4. triple	A: symmetric	B: A-symmetric	5. twisted jacket		A: 4-leg battered	B: 3-leg battered	C: 3-leg straight	D: 4-leg straight	A: conventional	B: extended	C: split	D: a-symmetric	triple	A: symmetric	B: A-symmetric	twisted jacket
design																										
1	mass of substructure	8	8	5	5	5	5	6	6	4	6	5	5	1,4	11,5	11,5	7,2	7,2	7,2	7,2	8,6	8,6	5,8	8,6	7,2	7,2
2	footprint	6	8	8	6	8	8	8	8	6	6	8	8	0,7	4,3	5,8	5,8	4,3	5,8	5,8	5,8	5,8	4,3	4,3	5,8	5,8
3	tower connection	6	5	5	6	8	8	8	8	6	8	8	7	1,3	7,6	6,3	6,3	7,6	10,1	10,1	10,1	10,1	7,6	10,1	10,1	8,8
fabrication																										
4	number of joints	3	4	5	4	9	8	9	8	10	7	7	6	1,1	3,2	4,3	5,4	4,3	9,7	8,6	9,7	8,6	10,8	7,6	7,6	6,5
5	complexity of joints	9	7	6	7	4	5	4	4	3	7	7	7	0,9	8,1	6,3	5,4	6,3	3,6	4,5	3,6	3,6	2,7	6,3	6,3	6,3
6	manoeuvrability	7	5	8	9	4	5	4	7	9	4	4	6	0,2	1,3	0,9	1,4	1,6	0,7	0,9	0,7	1,3	1,6	0,7	0,7	1,1
installation																										
7	lifting	9	8	7	8	6	6	6	6	7	6	6	6	1,8	16,2	14,4	12,6	14,4	10,8	10,8	10,8	10,8	12,6	10,8	10,8	10,8
8	foundation	9	8	8	9	8	8	7	7	8	7	8	5	1,6	14,6	13,0	13,0	14,6	13,0	13,0	11,4	11,4	13,0	11,4	13,0	8,1
inspection																										
9	number of joints	3	4	5	4	9	8	9	8	10	7	7	6	0,4	1,1	1,4	1,8	1,4	3,2	2,9	3,2	2,9	3,6	2,5	2,5	2,2
overall																										
10	reliability (proven technology)	10	8	6	6	8	6	1	4	7	4	4	1	0,5	5,4	4,3	3,2	3,2	4,3	3,2	0,5	2,2	3,8	2,2	2,2	0,5
11	decommissioning	1	1	8	8	10	10	1	6	7	10	10	8	0,1	0,1	0,1	0,7	0,7	0,9	0,9	0,1	0,5	0,6	0,9	0,9	0,7
total		71	66	71	72	79	77	63	72	77	72	74	65	10,0	73,4	68,4	62,9	65,8	69,4	67,9	64,6	65,8	66,4	65,4	67,0	58,0
Rank															1	3	11	8	2	4	10	7	6	9	5	12

Appendix E Elevation Determination

Determination of SACS joint coördinates

battered legs concepts

Definiton of design parameters.
b: width of base
t: width of topside
D: water depth
d: begin of leg
BOS: Bottom of Steel (transition piece)

$$b := 24$$

$$t := 10$$

$$D := 45$$

$$d := 7.2$$

$$\text{BOS} := 25$$

$$\text{height} := \text{BOS} + D - d$$

Calculation of batter angle

$$\text{batter} := \frac{\frac{(b-t)}{2}}{\text{height}}$$

$$\text{batter} = 0.111$$

The calculation is a iterative procedure.
Arbiratry begin values for difference between elevation heights are chosen.
hx is the elevation heigh for elevation x

$$h1 := 30$$

$$h2 := 5$$

$$h3 := 15$$

Design parameters are defined:
x: are x coördinates of at elevation heights

$$x1 := b$$

$$x2 := (x1 - h1 \cdot \text{batter})$$

$$x3 := x2 - h2 \cdot \text{batter}$$

$$x4 := t$$

Setting the concerned equations for five variables.
Equations define that all angle is the construction are the same.

Given

$$\frac{h1}{x1 + x2} - \frac{h2}{x2 + x3} = 0$$

$$\frac{h2}{x2 + x3} - \frac{h3}{x3 + x4} = 0$$

$$h1 + h2 + h3 = \text{height}$$

$$\frac{x1 - x2}{h1} = \frac{(x2 - x3)}{h2}$$

$$\frac{(x2 - x3)}{h2} = \frac{(x3 - x4)}{h3}$$

Generating output

$$\begin{pmatrix} h1 \\ h2 \\ h3 \\ x2 \\ x3 \end{pmatrix} = \text{Find}(h1, h2, h3, x2, x3)$$

$$h1 = 27.248$$

$$h2 = 20.352$$

$$h3 = 15.201$$

$$x1 = 24$$

$$x2 = 17.926$$

$$x3 = 13.389$$

$$x4 = 10$$

check

$$h := h1 + h2 + h3$$

$$h = 62.8$$

Check if all angles are the same and compute the angles.

$$a := \frac{h1}{x1 + x2} = 0.65$$

$$b := \frac{x1 - x2}{h1} = 0.223$$

$$\frac{h2}{x2 + x3} = 0.65$$

$$\frac{(x2 - x3)}{h2} = 0.223$$

$$\frac{h3}{x3 + x4} = 0.65$$

$$\frac{(x3 - x4)}{h3} = 0.223$$

$$360 \cdot \frac{\text{atan}(a)}{2 \cdot \pi} = 33.02$$

$$360 \cdot \frac{\text{atan}(b)}{2\pi} = 12.567$$

$$x := 90 - \frac{\text{atan}(a)}{2 \cdot \pi} \cdot 360 - \frac{\text{atan}(b)}{2 \cdot \pi} \cdot 360 = 44.412$$

Defining the coördinates

$$z0 := -D + d = -37.8$$

$$\frac{x1}{2} = 12$$

$$\frac{-x1}{2} = -12$$

$$z1 := -D + d + h1 = -10.552$$

$$\frac{x2}{2} = 8.963$$

$$\frac{-x2}{2} = -8.963$$

$$z2 := -D + d + h1 + h2 = 9.799$$

$$\frac{x3}{2} = 6.694$$

$$\frac{-x3}{2} = -6.694$$

$$z3 := -D + d + h1 + h2 + h3 = 25$$

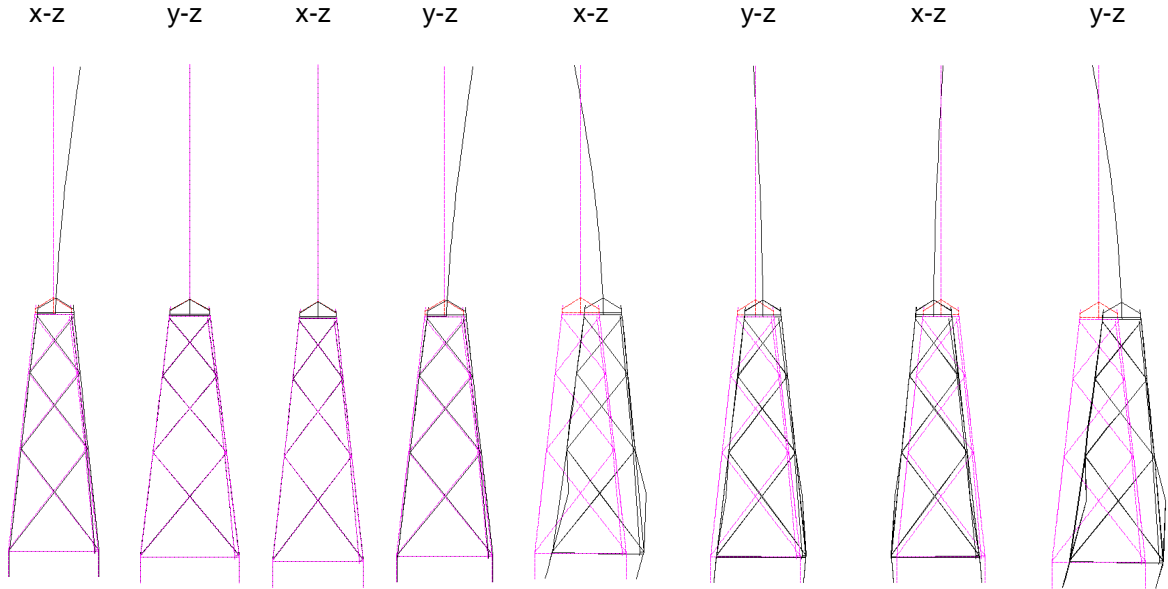
$$\frac{x4}{2} = 5$$

$$\frac{-x4}{2} = -5$$

Appendix F Mode Shapes

Table F.1: First 4 mode shapes optimised 4-leg

				Mass Participation Factor		Cumulative	
Design	Mode Shape	(Hz)		x	y	x	y
2 Optimised 4-leg jacket	f ₁	0.314198		0.30603		0.30603	
	f ₂	0.314243			0.30597	0.30606	0.305990
	f ₃	0.914317		0.57335	0.06485	0.87942	0.370846
	f ₄	0.914445		0.06496	0.57337	0.94438	0.944218



a) 1st fore-aft: f₁ b) 1st side to side: f₂ c) 2nd fore-aft: f₃ d) 2nd side to side: f₄

Figure F.1 :First four mode shapes optimised 4-leg jacket

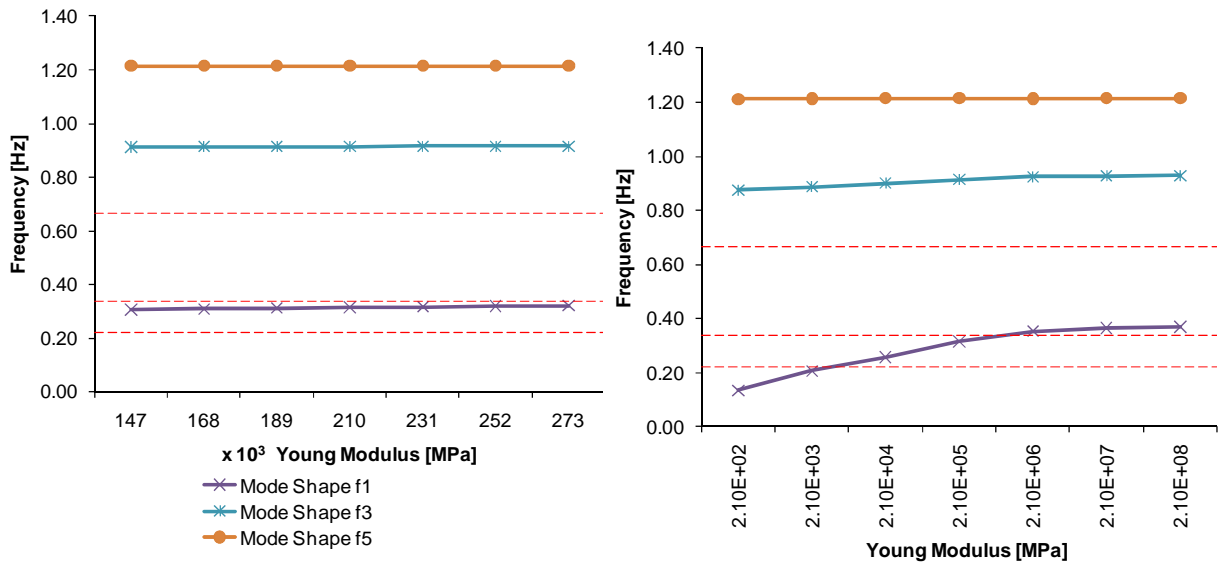


Figure F.2: Transition piece stiffness influence on natural frequencies

Table F.2: First 4 mode shapes 4-leg jacket K-braces

Design	Mode Shape	(Hz)	Mass Participation Factor		Cumulative	
			y	x	y	
3 4-leg jacket K-braces	f ₁	0.308745	0.15475	0.15410	0.15475	0.154102
	f ₂	0.314795	0.15595	0.15660	0.31071	0.310702
	f ₃	0.968765	0.32319	0.31775	0.63390	0.628452
	f ₄	0.971744	0.32206	0.32738	0.95597	0.955583

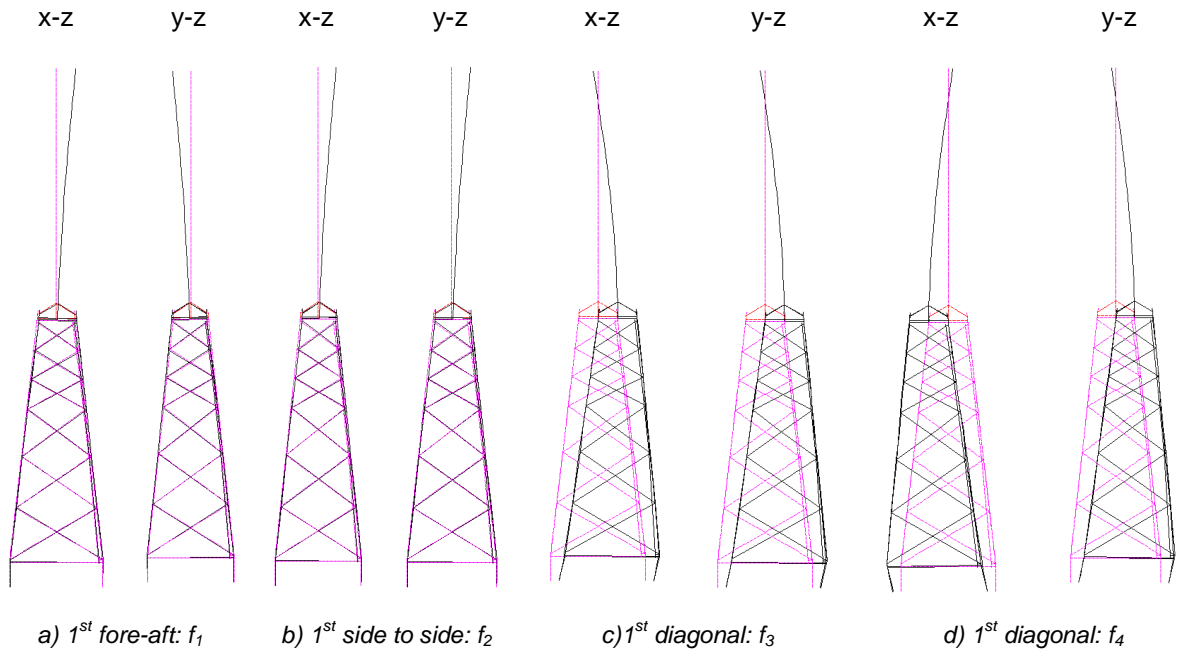


Figure F.3: First four mode shapes 4-leg K-braces

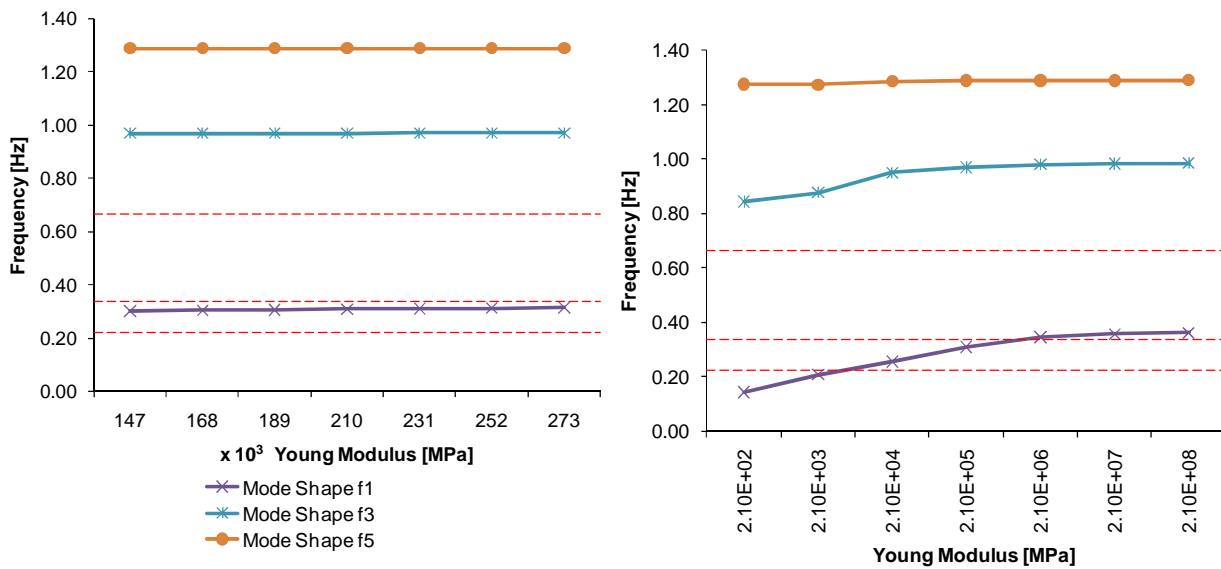


Figure F.4: Transition piece stiffness influence on natural frequencies

Table F.3: First four mode shapes 3-leg jacket

Design	Mode Shape	(Hz)	Mass Participation Factor		Cumulative	
			x	y	x	y
4 3-leg jacket	f ₁	0.324776	0.32679		0.32679	
	f ₂	0.324810		0.32669	0.32680	0.326710
	f ₃	0.893537	0.61736	0.0012	0.94416	0.0.32798
	f ₄	0.894029	0.0012	0.61723	0.94542	0.94521

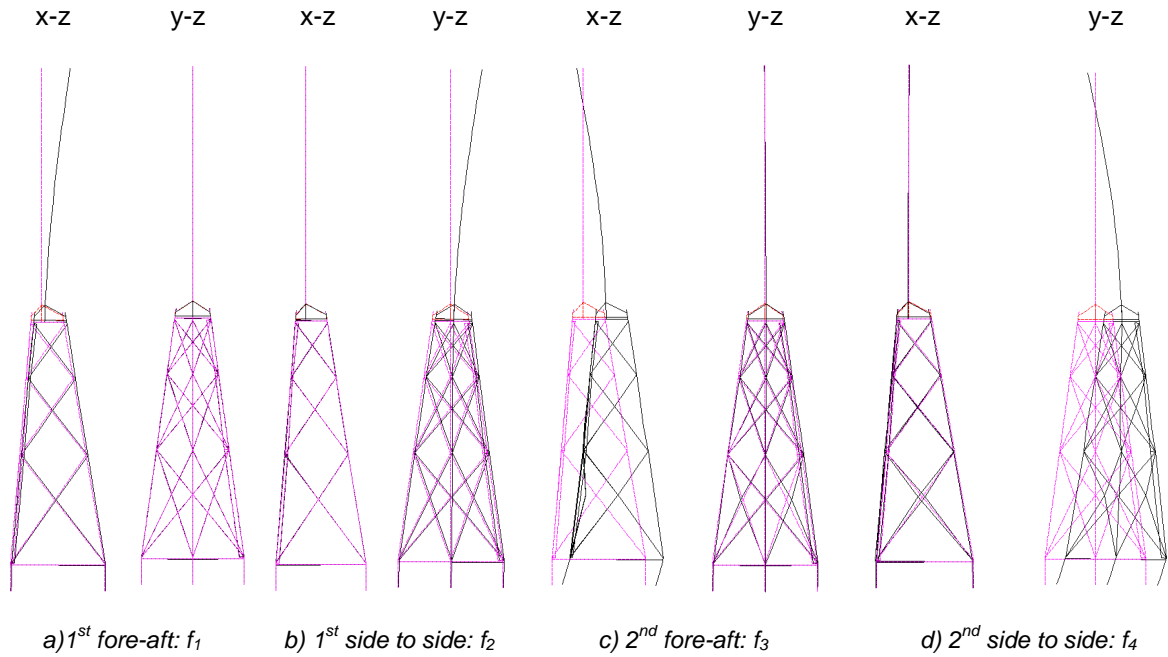


Figure F.5: First four mode shapes 3-leg jacket

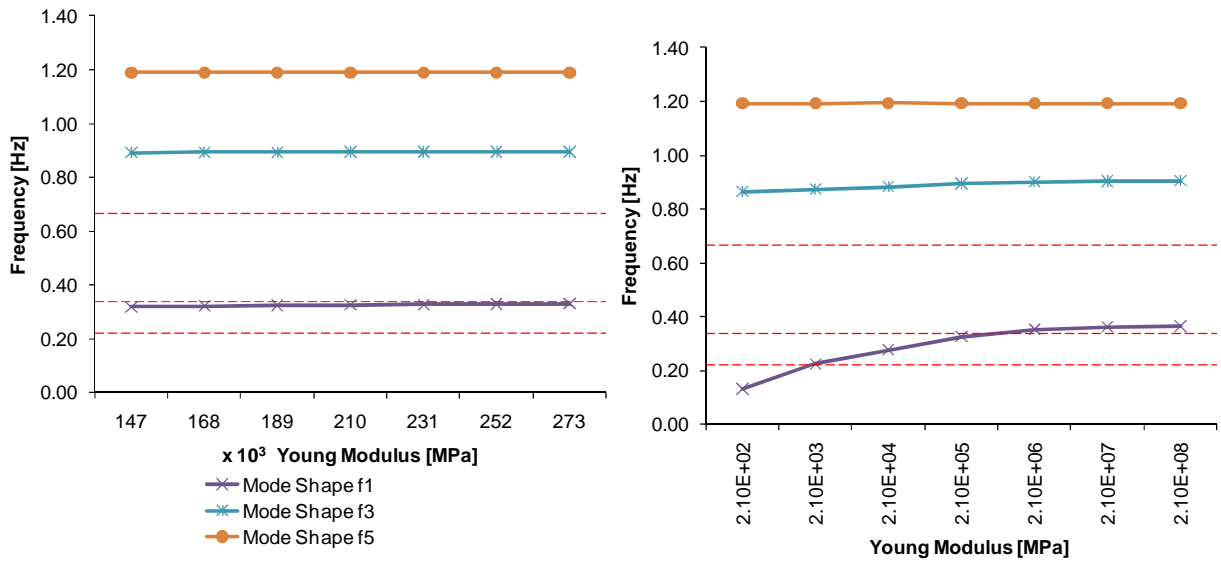


Figure F.6: Transition piece stiffness influence on natural frequencies

Appendix G Structural Analyses Outcome

G.1 Reference design

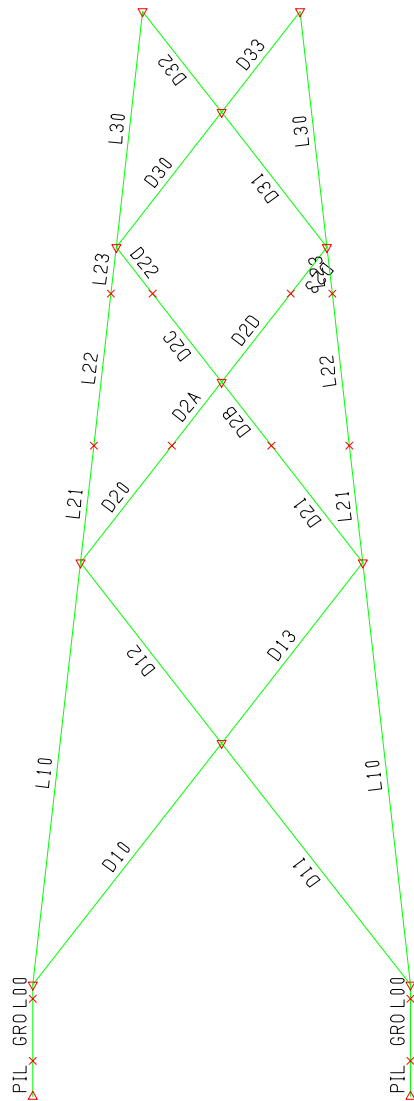


Figure G.1: Member groups in jacket face

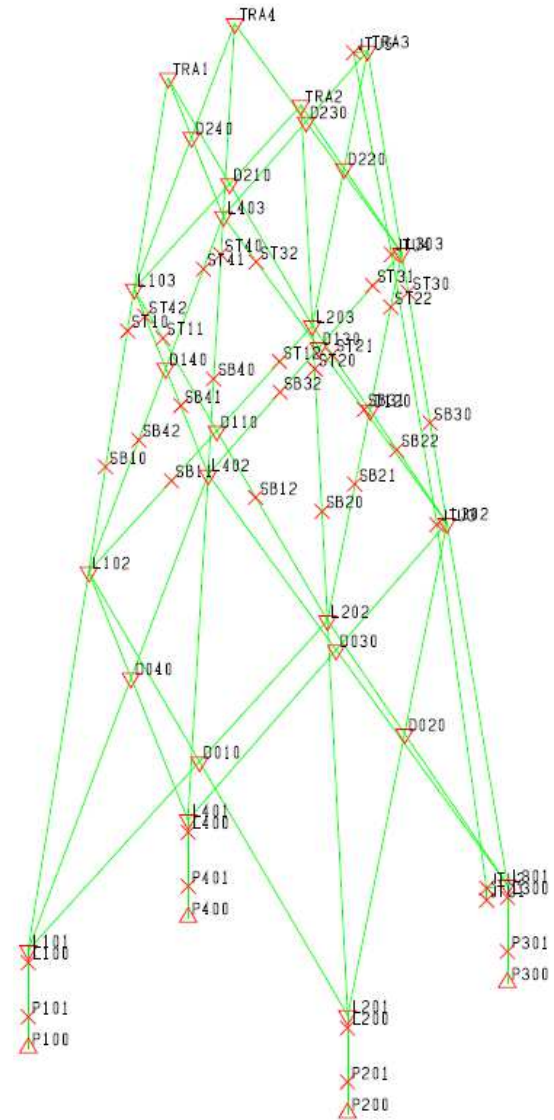


Figure G.2: Joint numbers

Table G.1: Pile maximum axial capacity summary dataset 1

PILE GRP	***** PILE *****	***** COMPRESSION *****							***** TENSION *****					***** *MAXIMUM* *****			
		O.D.	THK.	WEIGHT	PEN.	CAPACITY	MAX.	CRITICAL CONDITION	CAPACITY	MAX.	CRITICAL CONDITION	*****					
													(INCL. WT)		LOAD	LOAD SAFETY	(INCL. WT)
P100	PL1	228.60	5.08	1922.3	70.0	-46918.1	-31238.6	-31238.6	UR16	1.50	32840.3	24514.0	24514.0	UL32	1.34	1.12	UL32
P200	PL1	228.60	5.08	1922.3	70.0	-46918.1	-31306.5	-31306.5	UR18	1.50	32840.3	24554.3	24554.3	UR34	1.34	1.12	UR34
P300	PL1	228.60	5.08	1922.3	70.0	-46918.1	-30918.3	-30918.3	UR12	1.52	32840.3	24150.8	24150.8	UL36	1.36	1.10	UL36
P400	PL1	228.60	5.08	1922.3	70.0	-46918.1	-31307.3	-31307.3	UR14	1.50	32840.3	24555.0	24555.0	UL38	1.34	1.12	UL38

Table G.2: Pile maximum axial capacity summary dataset 2

PILE GRP	***** PILE *****	***** COMPRESSION *****							***** TENSION *****					***** *MAXIMUM* *****			
		O.D.	THK.	WEIGHT	PEN.	CAPACITY	MAX.	CRITICAL CONDITION	CAPACITY	MAX.	CRITICAL CONDITION	*****					
													(INCL. WT)		LOAD	LOAD SAFETY	(INCL. WT)
P100	PL1	228.60	5.08	1235.8	45.0	-62866.0	-31344.4	-31344.4	UR16	2.01	31803.5	24176.8	24176.8	UL32	1.32	1.14	UL32
P200	PL1	228.60	5.08	1235.8	45.0	-62866.0	-31377.0	-31377.0	UL18	2.00	31803.5	24169.2	24169.2	UR34	1.32	1.14	UR34
P300	PL1	228.60	5.08	1235.8	45.0	-62866.0	-31010.5	-31010.5	UR12	2.03	31803.5	23799.8	23799.8	UL36	1.34	1.12	UL36
P400	PL1	228.60	5.08	1235.8	45.0	-62866.0	-31378.4	-31378.4	UR14	2.00	31803.5	24170.1	24170.1	UL38	1.32	1.14	UL38

Table G.3: Member group summary

GRUP ID	CRITICAL MEMBER	LOAD COND	MAX. UNITY CHECK	DIST FROM END M	* APPLIED STRESSES *			*** ALLOWABLE STRESSES ***				CRIT COND	EFFECTIVE LENGTHS		CM * VALUES *	
					AXIAL	BEND-Y	BEND-Z	AXIAL	EULER	BEND-Y	BEND-Z		KLY	KLZ	Y	Z
					N/MM2	N/MM2	N/MM2	N/MM2	N/MM2	N/MM2	N/MM2		N/MM2	M	M	
D10	L201-D020	UL17	0.94	0.0	-96.68	-160.04	22.02	207.48	283.36	435.99	435.99	ACBI	19.8	15.8	0.85	0.85
D11	L401-D030	UR35	0.94	19.8	-134.89	120.37	15.61	237.94	397.37	422.89	422.89	ACBI	19.8	15.8	0.85	0.85
D12	D030-L302	UR16	0.76	14.8	-108.25	-77.95	-132.68	266.34	636.03	422.89	422.89	ACBI	14.8	11.8	0.85	0.85
D13	D030-L402	UL18	0.78	14.8	-106.99	-80.66	142.16	266.75	641.53	422.55	422.55	ACBI	14.8	11.8	0.85	0.85
D20	L202-SB21	UL11	0.67	0.0	-36.37	70.53	-214.55	221.49	326.45	422.55	422.55	ACBI	11.8	20.6	0.85	0.85
D21	L402-SB32	UR13	0.67	0.0	-36.66	69.05	211.58	221.49	326.45	422.55	422.55	ACBI	11.8	20.6	0.85	0.85
D22	L203-ST21	UR11	0.46	0.0	-31.31	56.55	-134.37	221.49	326.45	422.55	422.55	ACBI	8.8	20.6	0.85	0.85
D23	L403-ST32	UL13	0.64	0.0	-43.21	70.03	168.09	223.01	331.93	393.66	393.66	ACBI	8.8	20.6	0.85	0.85
D2A	SB21-D120	UL11	0.58	3.7	-51.08	-48.75	129.24	221.06	324.93	396.91	396.91	ACBI	11.8	20.6	0.85	0.85
D2B	SB32-D130	UR13	0.55	3.1	-51.62	-38.13	-118.16	216.51	309.72	396.91	396.91	ACBI	11.8	20.6	0.85	0.85
D2C	D130-ST31	UR13	0.52	0.0	-48.05	-74.09	-97.92	216.51	309.72	396.91	396.91	ACBI	8.8	20.6	0.85	0.85
D2D	D120-ST22	UL11	0.50	1.5	-47.36	-61.51	98.78	218.60	316.53	396.91	396.91	ACBI	8.8	20.6	0.85	0.85
D30	L403-D240	UR05	0.34	0.0	47.41	-59.42	-51.37	328.57	1173.49	393.66	393.66	TN+BN	11.0	11.0	0.85	0.85
D31	L303-D220	UL02	0.33	11.0	48.16	72.62	-21.22	338.10	1159.64	402.42	402.42	TN+BN	11.0	11.0	0.85	0.85
D32	D220-TRA2	UR25	0.20	8.2	-18.09	11.33	-62.25	313.64	1700.95	439.56	439.56	ACBI	8.2	6.6	0.85	0.85
D33	D230-TRA4	UL27	0.20	8.2	-18.34	12.20	64.90	322.73	1700.95	452.30	452.30	ACBI	8.2	6.6	0.85	0.85
GR0	P201-L200	UL18	0.40	4.0	-40.30	80.50	-70.84	313.64	*****	401.79	401.79	ACBI	4.0	4.0	0.85	0.85
L00	L200-L201	UL18	0.81	0.9	-73.70	173.93	-152.56	295.45	*****	410.72	410.72	ACBI	0.9	0.9	0.85	0.85
L10	L201-L202	UL18	0.93	5.0	-90.27	-255.90	-15.48	270.65	836.83	408.51	408.51	ACBI	27.6	27.6	0.85	0.85
L21	L102-SB10	UL16	0.67	2.5	-100.83	134.80	5.09	276.34	806.43	432.12	432.12	ACBI	20.6	20.0	0.85	0.85
L22	SB10-ST10	UL06	0.78	0.0	-164.16	64.83	2.40	273.25	744.78	399.74	399.74	ACBI	20.6	20.0	0.85	0.85
L23	ST30-L303	UL02	0.45	1.5	-104.84	-33.92	-6.34	278.40	853.62	432.12	432.12	ACBI	20.6	20.0	0.85	0.85
L30	L103-TRA1	UR06	0.37	13.4	-86.00	8.74	-34.00	291.29	1346.19	436.76	436.76	ACBI	15.4	15.4	0.85	0.85
P1L	P200-P201	UL18	0.45	2.3	-90.02	45.34	-41.92	304.55	*****	392.66	392.66	ACBI	2.3	2.3	0.85	0.85

Table G.4: Joint Can summary

JOINT	***** ORIGINAL *****				***** DESIGN *****			
	DIAMETER (CM)	THICKNESS (CM)	YLD STRS (N/MM2)	UC	DIAMETER (CM)	THICKNESS (CM)	YLD STRS (N/MM2)	UC
D030	76.200	4.445	335.000	0.953	76.200	4.445	335.000	0.953
D020	76.200	4.445	335.000	0.941	76.200	4.445	335.000	0.941
D040	76.200	4.445	335.000	0.922	76.200	4.445	335.000	0.922
D010	76.200	4.445	335.000	0.918	76.200	4.445	335.000	0.918
D130	73.660	2.540	345.000	0.761	73.660	2.540	345.000	0.761
D110	73.660	2.540	345.000	0.745	73.660	2.540	345.000	0.745
D140	73.660	2.540	345.000	0.724	73.660	2.540	345.000	0.724
D120	73.660	2.540	345.000	0.689	73.660	2.540	345.000	0.689
L402	116.840	5.715	335.000	0.578	116.840	5.715	335.000	0.578
L102	116.840	5.715	335.000	0.578	116.840	5.715	335.000	0.578
L302	116.840	5.715	335.000	0.576	116.840	5.715	335.000	0.576
L202	116.840	5.715	335.000	0.574	116.840	5.715	335.000	0.574
D220	76.200	3.175	345.000	0.455	76.200	3.175	345.000	0.455
D210	76.200	3.175	345.000	0.452	76.200	3.175	345.000	0.452
D230	76.200	3.175	345.000	0.447	76.200	3.175	345.000	0.447
D240	76.200	3.175	345.000	0.442	76.200	3.175	345.000	0.442
L201	182.880	7.620	325.000	0.422	182.880	7.620	325.000	0.422
L401	182.880	7.620	325.000	0.418	182.880	7.620	325.000	0.418
L301	182.880	7.620	325.000	0.403	182.880	7.620	325.000	0.403
L101	182.880	7.620	325.000	0.396	182.880	7.620	325.000	0.396
L203	116.840	5.080	335.000	0.290	116.840	5.080	335.000	0.290
L403	116.840	5.080	335.000	0.284	116.840	5.080	335.000	0.284
L103	116.840	5.080	335.000	0.275	116.840	5.080	335.000	0.275
L303	116.840	5.080	335.000	0.273	116.840	5.080	335.000	0.273
TRA4	116.840	5.715	335.000	0.209	116.840	5.715	335.000	0.209
TRA1	116.840	5.715	335.000	0.204	116.840	5.715	335.000	0.204
TRA2	116.840	5.715	335.000	0.203	116.840	5.715	335.000	0.203
TRA3	116.840	5.715	335.000	0.196	116.840	5.715	335.000	0.196

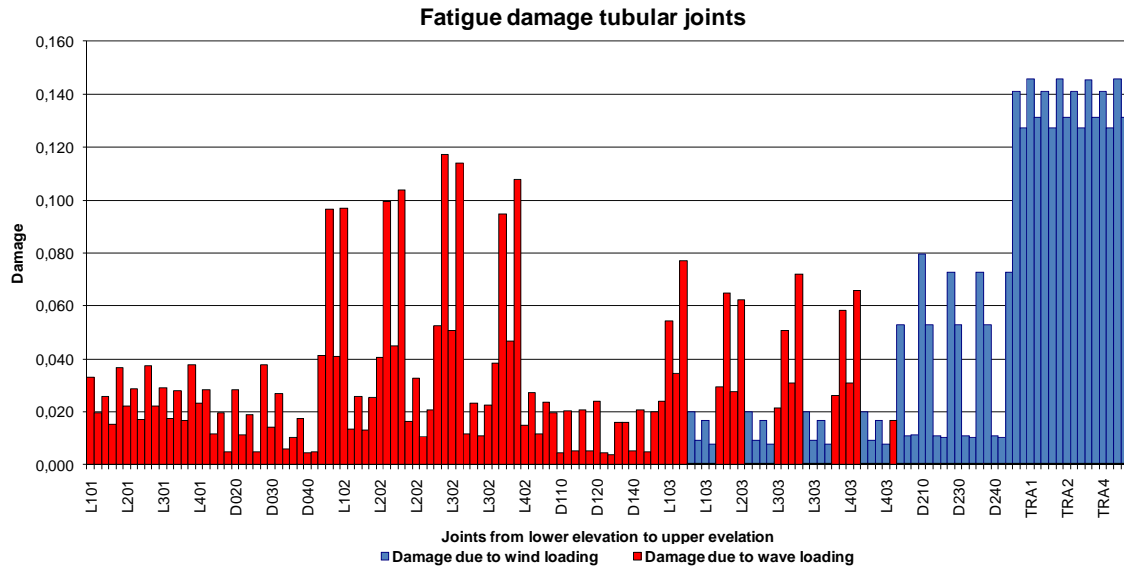


Figure G.3: Fatigue damage tubular joints due to wind and wave

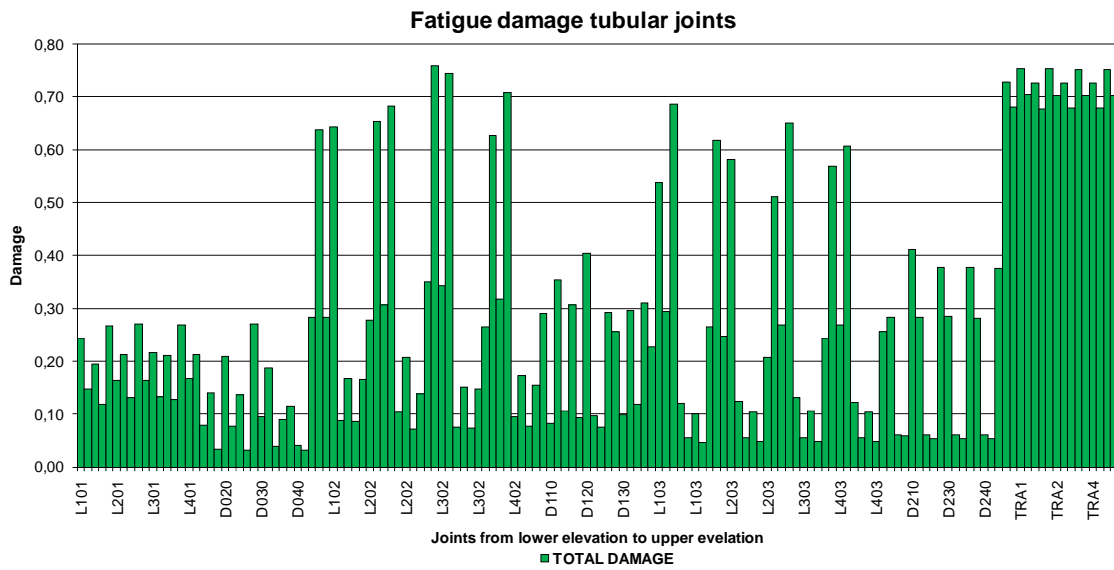


Figure G.4: Total fatigue damage tubular joints

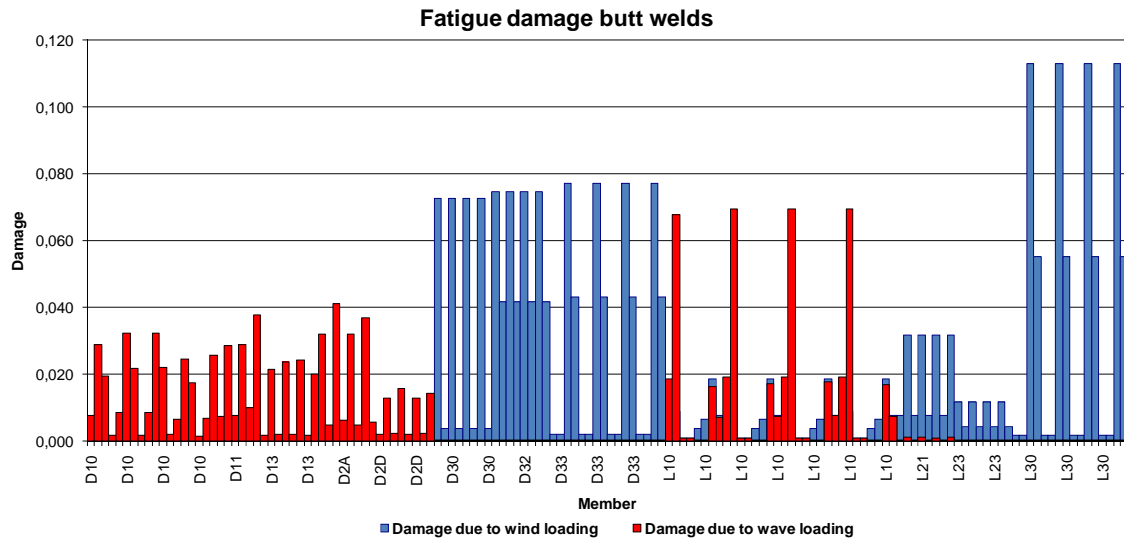


Figure G.5: Fatigue damage butt welds due to wind en waves

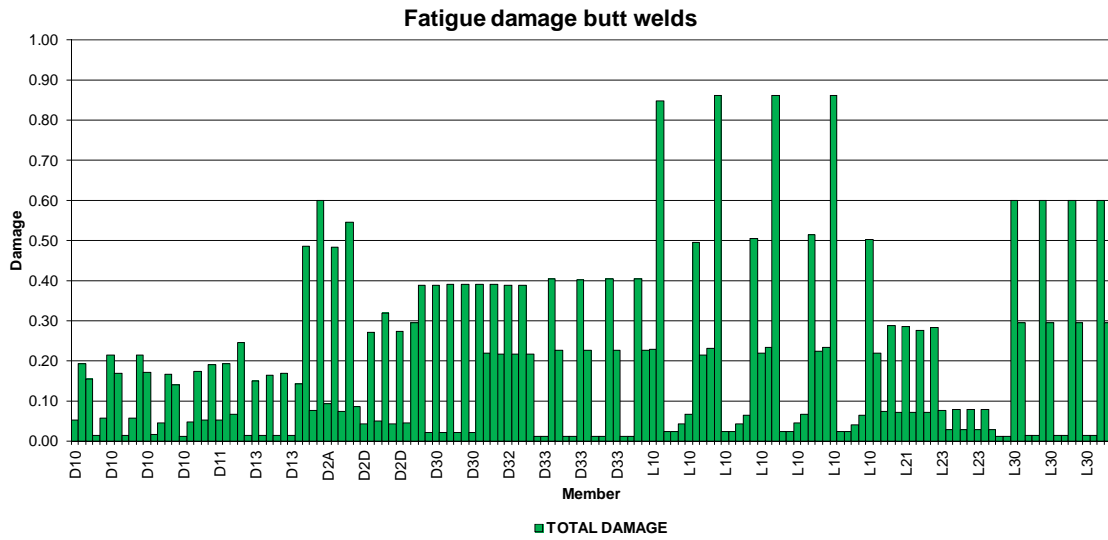


Figure G.6: Total fatigue damage butt welds

G.2 4-leg jacket optimised

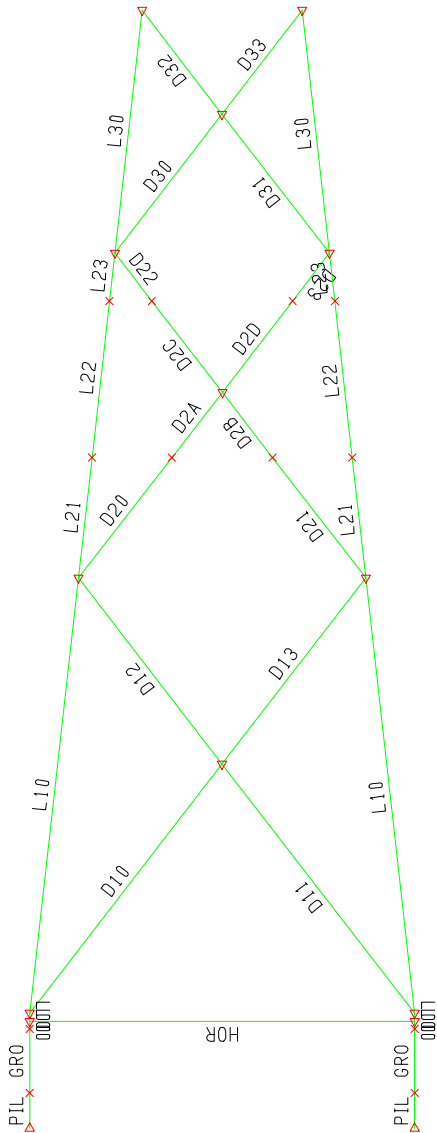


Figure G.7: Member groups in jacket face

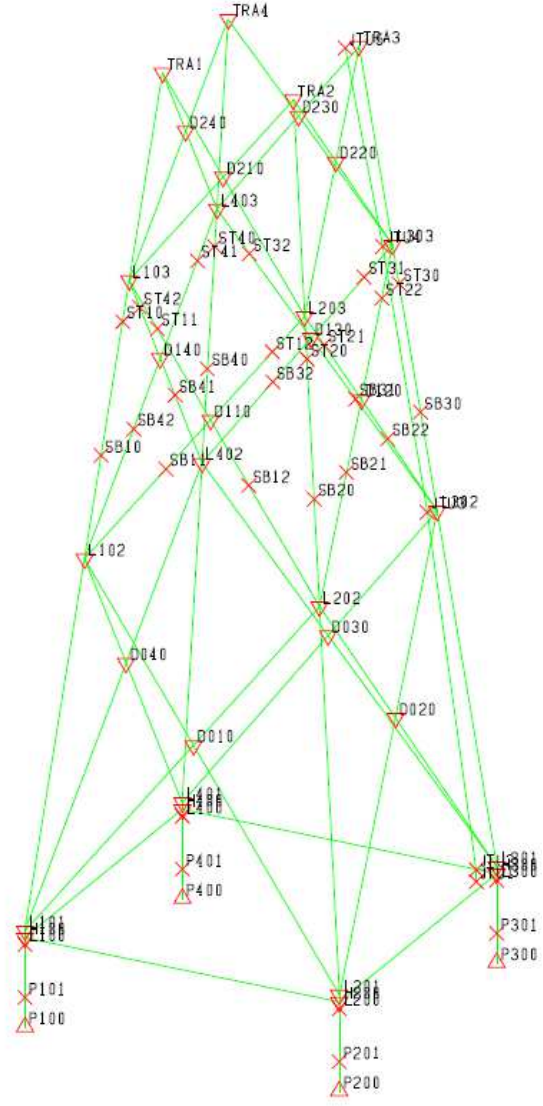


Figure G.8: Joint numbers

Table G.5: Pile maximum axial capacity summary dataset 1

PILE GRP	***** PILE *****				***** COMPRESSION *****				***** TENSION *****								
	PILEHEAD		WEIGHT	PEN.	CAPACITY	MAX.	CRITICAL CONDITION		CAPACITY	MAX.	CRITICAL CONDITION		*MAXIMUM*				
	O.D.	THK.	KN	M	(INCL. WT)	LOAD	LOAD	LOAD SAFETY	(INCL. WT)	LOAD	LOAD	LOAD SAFETY	UNITY LOAD				
P100	PL1	213.96	5.08	1796.4	70.0	-42708.7	-31167.5	-31167.5	UL16	1.37	30733.8	24967.3	24967.3	UR32	1.26	1.22	UR32
P200	PL1	213.96	5.08	1796.4	70.0	-42708.7	-31213.8	-31213.8	UL18	1.37	30733.8	25020.4	25020.4	UR34	1.26	1.22	UR34
P300	PL1	213.96	5.08	1796.4	70.0	-42708.7	-30919.8	-30919.8	UL12	1.38	30733.8	24651.9	24651.9	UR36	1.27	1.20	UR36
P400	PL1	213.96	5.08	1796.4	70.0	-42708.7	-31213.6	-31213.6	UR14	1.37	30733.8	25019.6	25019.6	UL38	1.26	1.22	UL38

Table G.6: Pile maximum axial capacity summary dataset 2

PILE GRP	***** PILE *****				***** COMPRESSION *****				***** TENSION *****								
	PILEHEAD		WEIGHT	PEN.	CAPACITY	MAX.	CRITICAL CONDITION		CAPACITY	MAX.	CRITICAL CONDITION		*MAXIMUM*				
	O.D.	THK.	KN	M	(INCL. WT)	LOAD	LOAD	LOAD SAFETY	(INCL. WT)	LOAD	LOAD	LOAD SAFETY	UNITY LOAD				
P100	PL1	213.36	5.08	1177.1	46.0	-58575.8	-31610.7	-31610.7	UL16	1.85	30779.8	24690.6	24690.6	UR32	1.25	1.20	UR32
P200	PL1	213.36	5.08	1177.1	46.0	-58575.8	-31664.7	-31664.7	UL18	1.85	30779.8	24716.9	24716.9	UR34	1.25	1.20	UR34
P300	PL1	213.36	5.08	1177.1	46.0	-58575.8	-31280.9	-31280.9	UL12	1.87	30779.8	24343.4	24343.4	UR36	1.26	1.19	UR36
P400	PL1	213.36	5.08	1177.1	46.0	-58575.8	-31664.3	-31664.3	UR14	1.85	30779.8	24716.1	24716.1	UL38	1.25	1.20	UL38

Table G.7: Member group summary

GRUP ID	CRITICAL MEMBER	LOAD COND	MAX. UNITY CHECK	DIST FROM END	* APPLIED STRESSES *			*** ALLOWABLE STRESSES ***				CRIT COND	EFFECTIVE LENGTHS		CM * VALUES *	
					AXIAL	BEND-Y	BEND-Z	AXIAL	EULER	BEND-Y	BEND-Z		KLY	KLZ	Y	Z
					N/MM2	N/MM2	N/MM2	N/MM2	N/MM2	N/MM2	N/MM2		M	M		
D10	L201-D020	UL17	0.98	0.0	-101.98	-158.70	-14.46	207.15	282.49	435.99	435.99	ACBI	19.8	15.8	0.85	0.85
D11	L401-D030	UR15	0.96	0.0	-101.57	-154.53	13.70	207.07	282.28	435.99	435.99	ACBI	19.8	15.8	0.85	0.85
D12	D030-L302	UR35	0.90	0.0	-149.75	124.05	-9.93	266.75	641.53	410.16	410.16	ACBI	14.8	11.8	0.85	0.85
D13	D020-L302	UL37	0.85	1.5	-150.84	104.86	10.82	267.14	646.93	410.16	410.16	ACBI	14.8	11.8	0.85	0.85
D20	L402-SB41	UL11	0.86	0.0	-24.07	-53.23	310.21	322.731011	.62	402.42	402.42	ACBI	11.8	10.6	0.85	0.85
D21	L202-SB12	UR13	0.81	0.0	-23.94	-49.66	-291.40	322.731011	.62	402.42	402.42	ACBI	11.8	10.6	0.85	0.85
D22	L203-ST21	UR15	0.62	0.0	-20.71	-72.37	213.10	322.731810	.68	402.42	402.42	ACBI	8.8	7.9	0.85	0.85
D23	L403-ST32	UL17	0.66	0.0	-20.85	-73.55	-229.23	322.731810	.68	402.42	402.42	ACBI	8.8	7.9	0.85	0.85
D2A	SB31-D130	UL17	0.77	3.7	-39.38	23.24	-234.01	318.171048	.08	365.55	365.55	ACBI	11.8	10.6	0.85	0.85
D2B	SB22-D120	UR15	0.61	3.1	-39.36	19.02	178.40	318.17	960.35	365.55	365.55	ACBI	11.8	10.6	0.85	0.85
D2C	D110-ST11	UR12	0.65	0.0	-73.17	88.98	125.23	318.171718	.92	365.55	365.55	ACBI	8.8	7.9	0.85	0.85
D2D	D130-ST32	UL17	0.66	1.5	-36.59	52.60	-190.96	318.171785	.43	365.55	365.55	ACBI	8.8	7.9	0.85	0.85
D30	L203-D220	UL01	0.34	0.0	-40.27	-1.68	-84.47	322.731028	.43	385.54	385.54	ACBI	11.0	8.8	0.85	0.85
D31	L303-D220	UL22	0.35	11.0	43.44	75.35	-37.40	338.101016	.22	385.54	385.54	TN+BN	11.0	11.0	0.85	0.85
D32	D240-TRA4	UR04	0.30	6.7	-26.94	91.13	-6.54	313.641783	.33	433.45	433.45	ACBI	8.2	6.6	0.85	0.85
D33	D210-TRA2	UL08	0.30	6.7	-27.20	91.50	6.08	313.641783	.33	433.45	433.45	ACBI	8.2	6.6	0.85	0.85
GR0	P401-L400	UR14	0.36	4.0	-43.00	-57.91	71.44	313.64*****		405.95	405.95	ACBI	4.0	4.0	0.85	0.85
H0R	H300-H200	UL17	0.75	24.0	10.38	-308.84	-6.00	328.57	272.51	427.69	427.69	TN+BN	24.0	24.0	0.85	0.85
L00	H400-L400	UR14	0.79	0.0	-85.97	-128.93	-158.93	295.45*****		410.22	410.22	ACBI	0.5	0.5	0.85	0.85
L10	L101-L102	UR16	0.82	27.6	-140.79	151.45	-11.70	286.701588	.89	425.83	425.83	ACBI	27.6	27.6	0.85	0.85
L21	L102-SB10	UL16	0.69	2.5	-124.82	91.56	8.23	267.98	658.92	433.45	433.45	ACBI	20.6	20.6	0.85	0.85
L22	SB10-ST10	UR06	0.83	0.0	-198.48	27.51	-3.59	264.77	615.59	408.05	408.05	ACBI	20.6	20.6	0.85	0.85
L23	ST10-L103	UL06	0.51	1.5	-129.92	5.27	-9.75	268.94	673.02	433.45	433.45	ACBI	20.6	20.6	0.85	0.85
L30	L103-TRA1	UR16	0.46	13.9	-101.92	-19.53	-46.37	286.911125	.70	435.99	435.99	ACBI	15.4	15.4	0.85	0.85
P1L	P400-P401	UR14	0.62	2.2	-135.94	-41.52	52.62	304.55*****		377.13	377.13	ACBI	2.2	2.2	0.85	0.85

Table G.8: Joint can summary

JOINT	***** ORIGINAL *****				***** DESIGN *****			
	DIAMETER (CM)	THICKNESS (CM)	YLD STRS (N/MM2)	UC	DIAMETER (CM)	THICKNESS (CM)	YLD STRS (N/MM2)	UC
D030	76.200	3.810	345.000	0.993	76.200	3.810	345.000	0.993
D020	76.200	3.810	345.000	0.945	76.200	3.810	345.000	0.945
D040	76.200	3.810	345.000	0.932	76.200	3.810	345.000	0.932
D010	76.200	3.810	345.000	0.929	76.200	3.810	345.000	0.929
H400	172.720	6.985	325.000	0.835	172.720	6.985	325.000	0.835
H200	172.720	6.985	325.000	0.847	172.720	6.985	325.000	0.847
H300	172.720	6.985	325.000	0.852	172.720	6.985	325.000	0.852
H100	172.720	6.985	325.000	0.835	172.720	6.985	325.000	0.835
L302	106.680	5.080	335.000	0.571	106.680	5.080	335.000	0.571
L102	106.680	5.080	335.000	0.568	106.680	5.080	335.000	0.568
L402	106.680	5.080	335.000	0.560	106.680	5.080	335.000	0.560
L202	106.680	5.080	335.000	0.554	106.680	5.080	335.000	0.554
D210	71.120	2.540	345.000	0.460	71.120	2.540	345.000	0.460
D220	71.120	2.540	345.000	0.460	71.120	2.540	345.000	0.460
D230	71.120	2.540	345.000	0.453	71.120	2.540	345.000	0.453
D240	71.120	2.540	345.000	0.446	71.120	2.540	345.000	0.446
L201	172.720	6.985	325.000	0.443	172.720	6.985	325.000	0.443
L401	172.720	6.985	325.000	0.439	172.720	6.985	325.000	0.439
L301	172.720	6.985	325.000	0.421	172.720	6.985	325.000	0.421
L101	172.720	6.985	325.000	0.406	172.720	6.985	325.000	0.406
D110	73.660	3.175	345.000	0.406	73.660	3.175	345.000	0.406
D130	73.660	3.175	345.000	0.395	73.660	3.175	345.000	0.395
D140	73.660	3.175	345.000	0.377	73.660	3.175	345.000	0.377
D120	73.660	3.175	345.000	0.370	73.660	3.175	345.000	0.370
L403	106.680	4.445	335.000	0.358	106.680	4.445	335.000	0.358
L203	106.680	4.445	335.000	0.347	106.680	4.445	335.000	0.347
L103	106.680	4.445	335.000	0.346	106.680	4.445	335.000	0.346
L303	106.680	4.445	335.000	0.336	106.680	4.445	335.000	0.336
TRA4	106.680	5.810	335.000	0.143	106.680	5.810	335.000	0.143
TRA2	106.680	5.810	335.000	0.142	106.680	5.810	335.000	0.142
TRA1	106.680	5.810	335.000	0.140	106.680	5.810	335.000	0.140
TRA3	106.680	5.810	335.000	0.139	106.680	5.810	335.000	0.139

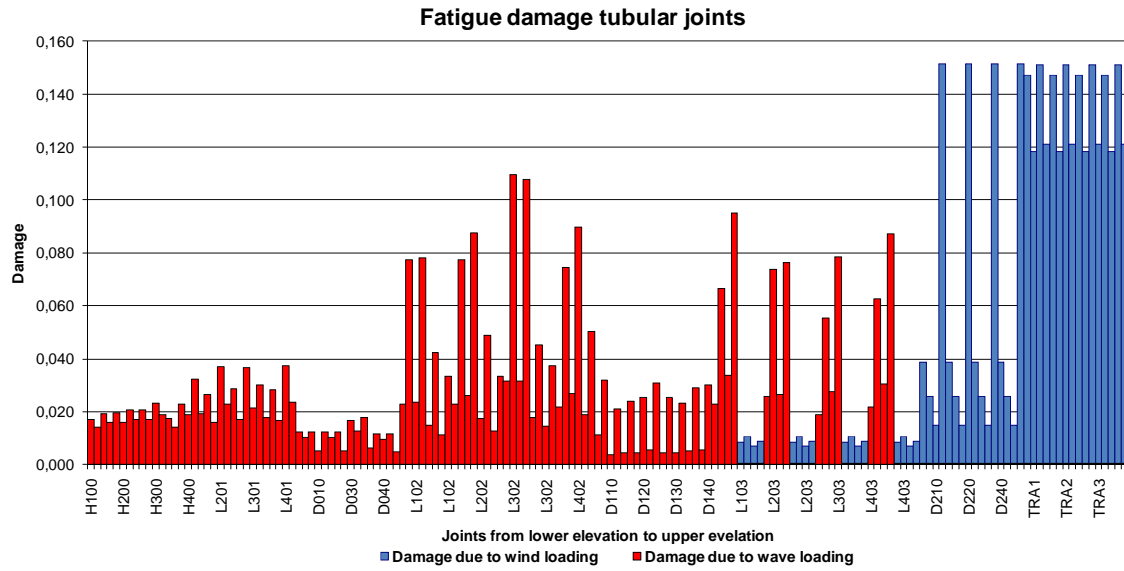


Figure G.9: Fatigue damage tubular joints due to wind and wave

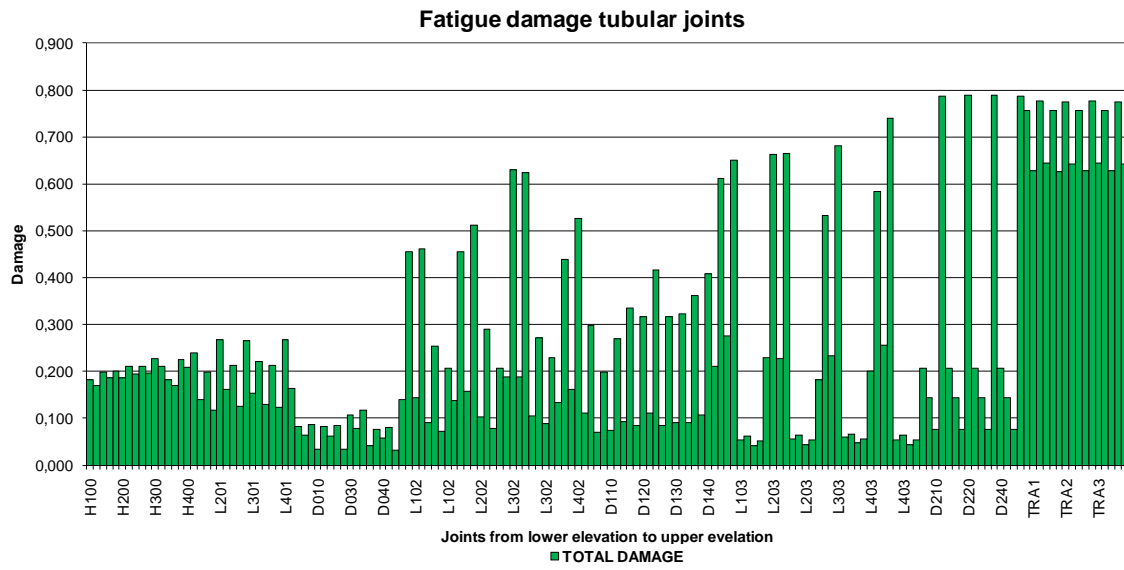


Figure G.10: Total fatigue damage tubular joints

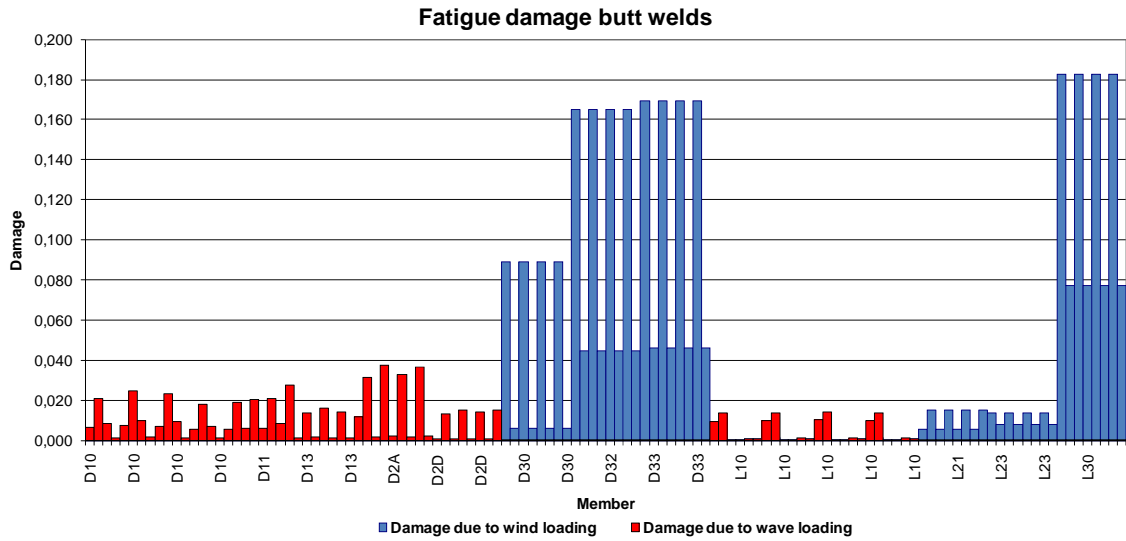


Figure G.11: Fatigue damage butt welds due to wind and wave

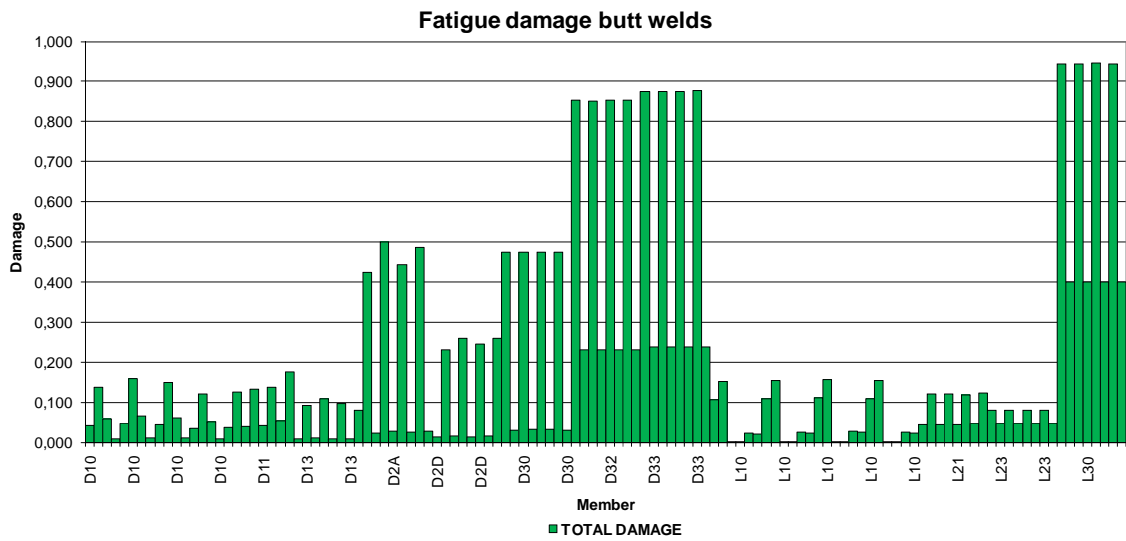


Figure G.12: Total fatigue damage butt welds

G.3 4-leg jacket with K-braces

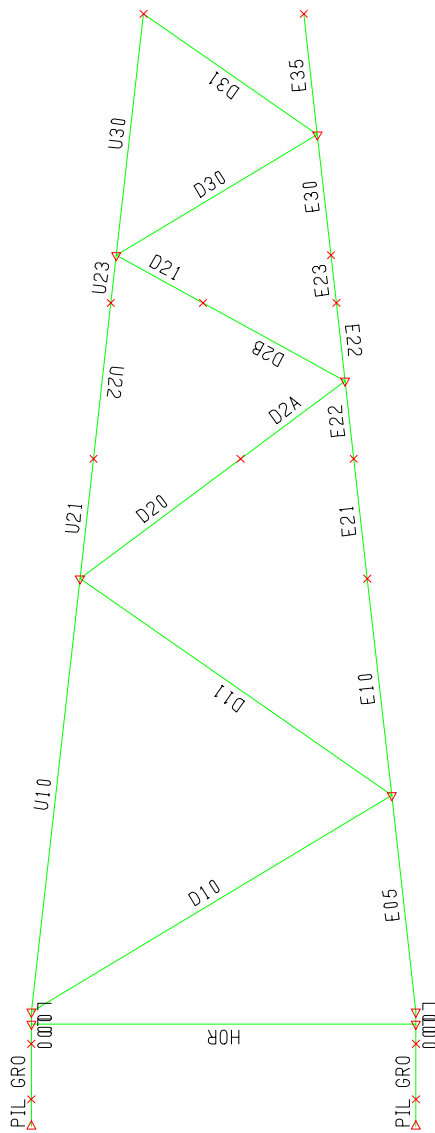


Figure G.13: Member groups in jacket face

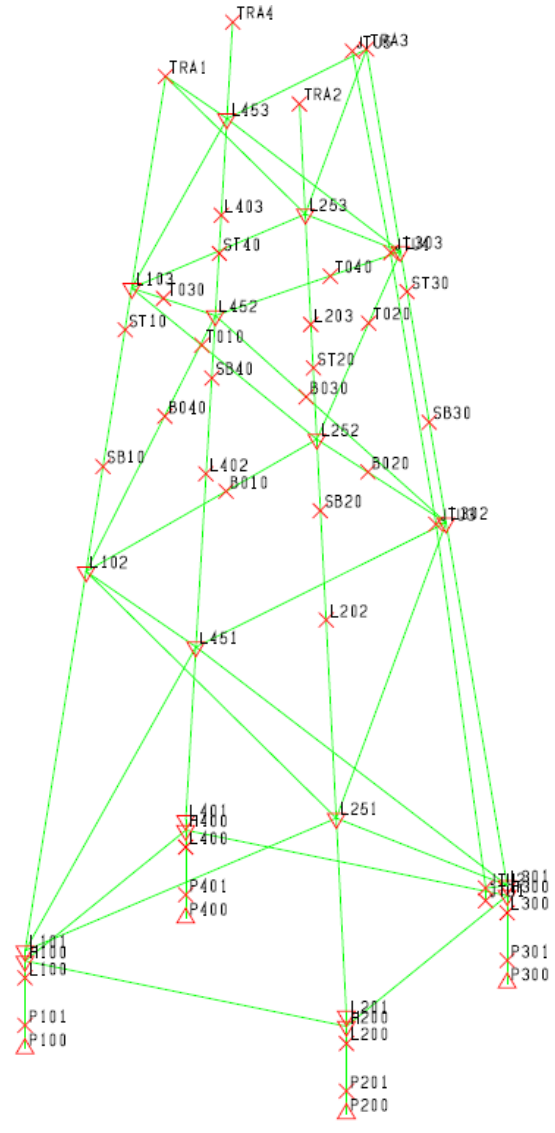


Figure G.14: Joint numbers

Table G.9: Pile maximum axial capacity summary dataset 1

PILE GRP	***** PILE *****	***** COMPRESSION *****					***** TENSION *****					***** *MAXIMUM* *****					
		JT	PILEHEAD O.D.	WEIGHT THK.	PEN.	CAPACITY (INCL. WT)	MAX. LOAD	CRITICAL LOAD	CONDITION SAFETY	CAPACITY (INCL. WT)	MAX. LOAD		CRITICAL LOAD	CONDITION SAFETY			
P100	PL1	213.96	4.45	1419.0	63.0	-39166.0	-27407.9	-27407.9	UL16	1.43	26393.4	20857.4	20857.4	UR32	1.27	1.19	UL32
P200	PL1	213.96	4.45	1419.0	63.0	-39166.0	-27555.8	-27555.8	UL18	1.42	26393.4	21374.8	21374.8	UR34	1.26	1.21	UL34
P300	PL1	213.96	4.45	1419.0	63.0	-39166.0	-27235.6	-27235.6	UR12	1.44	26393.4	20587.6	20587.6	UL36	1.28	1.17	UL36
P400	PL1	213.96	4.45	1419.0	63.0	-39166.0	-27556.0	-27556.0	UR14	1.42	26393.4	21374.9	21374.9	UL38	1.26	1.21	UL38

Table G.10: Pile maximum axial capacity summary dataset 2

PILE GRP	***** PILE *****	***** COMPRESSION *****					***** TENSION *****					***** *MAXIMUM* *****					
		JT	PILEHEAD O.D.	WEIGHT THK.	PEN.	CAPACITY (INCL. WT)	MAX. LOAD	CRITICAL LOAD	CONDITION SAFETY	CAPACITY (INCL. WT)	MAX. LOAD		CRITICAL LOAD	CONDITION SAFETY			
P100	PL1	213.36	4.45	943.3	42.0	-50725.7	-27702.6	-27702.6	UL16	1.83	26214.7	20508.5	20508.5	UR32	1.28	1.17	UL32
P200	PL1	213.36	4.45	943.3	42.0	-50725.7	-27869.9	-27869.9	UL18	1.82	26214.7	21008.7	21008.7	UR34	1.25	1.20	UL34
P300	PL1	213.36	4.45	943.3	42.0	-50725.7	-27483.5	-27483.5	UR12	1.85	26214.7	20220.6	20220.6	UL36	1.30	1.16	UL36
P400	PL1	213.36	4.45	943.3	42.0	-50725.7	-27870.2	-27870.2	UR14	1.82	26214.7	21008.7	21008.7	UL38	1.25	1.20	UL38

Table G.11: Member group summary

GRUP ID	CRITICAL MEMBER	LOAD COND	MAX. UNITY CHECK	DIST FROM END	* APPLIED STRESSES *			*** ALLOWABLE STRESSES ***				CRIT COND	EFFECTIVE LENGTHS		CM * VALUES *	
					AXIAL	BEND-Y	BEND-Z	AXIAL	EULER	BEND-Y	BEND-Z		KLY	KLZ	Y	Z
					N/MM2	N/MM2	N/MM2	N/MM2	N/MM2	N/MM2	N/MM2		N/MM2	M	M	
D10	L301-L251	UR13	0.98	0.0	-100.40	-145.67	-4.74	192.88	249.10	437.04	437.04	ACBI	26.3	26.3	0.85	0.85
D11	L251-L302	UL37	0.86	0.0	-112.32	47.65	-0.56	170.61	210.32	433.45	433.45	ACBI	23.8	23.8	0.85	0.85
D20	L102-B010	UL36	0.47	0.0	-40.90	70.07	-94.97	205.36	277.82	433.45	433.45	ACBI	20.7	20.7	0.85	0.85
D21	L103-T010	UR12	0.42	0.0	-42.43	-9.56	74.93	180.00	225.09	436.89	436.89	ACBI	16.3	16.3	0.85	0.85
D2A	B040-L452	UR18	0.82	8.2	-86.54	-1.49	-122.35	203.60	267.35	389.74	389.74	ACBI	20.7	20.7	0.85	0.85
D2B	L252-T010	UR21	1.00	0.0	-133.98	17.65	36.02	173.28	213.12	396.77	396.77	ACBI	16.3	16.3	0.85	0.85
D30	L303-L453	UL07	0.48	14.7	-53.85	-36.25	84.07	207.78	284.17	427.71	427.71	ACBI	14.7	14.7	0.85	0.85
D31	L453-TRA3	UR12	0.48	11.8	-74.74	77.16	-49.94	319.52	1180.05	368.93	368.93	ACBI	13.3	13.3	0.85	0.85
E05	L401-L451	UR14	0.84	0.0	-80.73	-228.62	22.62	295.45	3706.71	408.74	408.74	ACBI	13.8	13.8	0.85	0.85
E10	L451-L402	UR04	0.66	12.3	-101.72	10.44	-3.11	274.05	930.14	402.56	402.56	LOBU	26.2	26.2	0.85	0.85
E21	L402-SB40	UL04	0.58	6.1	-139.85	-10.67	4.41	255.78	519.88	413.56	413.56	ACBI	26.2	26.2	0.85	0.85
E22	SB40-L452	UL14	0.99	0.0	-222.91	-31.94	7.70	258.85	551.41	365.49	365.49	ACBI	26.2	26.2	0.85	0.85
E23	ST40-L403	UR04	0.61	3.0	-170.73	-4.11	8.34	293.44	1489.47	379.95	379.95	ACBI	15.6	15.6	0.85	0.85
E30	L403-L453	UL04	0.64	6.2	-170.13	10.41	-22.86	294.01	1532.67	379.95	379.95	ACBI	15.6	15.6	0.85	0.85
E35	L453-TRA4	UR04	0.81	7.7	-178.58	-46.99	-76.91	313.64	6300.28	379.95	379.95	ACBI	7.7	7.7	0.85	0.85
GRO	P401-L400	UR14	0.35	3.5	-38.77	-58.27	72.87	313.64	*****	412.28	412.28	ACBI	3.5	3.5	0.85	0.85
HOR	H300-H200	UL37	0.96	0.0	-77.24	222.65	23.63	203.25	272.51	427.69	427.69	ACBI	24.0	24.0	0.85	0.85
L00	H200-L200	UL17	0.73	0.0	-53.25	225.59	-12.15	295.45	*****	411.70	411.70	ACBI	1.2	1.2	0.85	0.85
PIL	P400-P401	UR14	0.65	1.7	-118.30	-62.54	77.81	304.55	*****	377.13	377.13	ACBI	1.7	1.7	0.85	0.85
U10	L101-L102	UL36	0.78	26.1	-118.00	74.38	7.68	281.92	1253.49	402.56	402.56	LOBU	27.5	27.5	0.85	0.85
U21	L102-SB10	UL16	0.71	1.5	-122.14	103.53	13.84	271.45	857.06	403.59	403.59	ACBI	20.6	20.6	0.85	0.85
U22	ST10-SB10	UR06	0.89	9.9	-216.59	33.23	6.81	276.79	822.69	365.49	365.49	ACBI	20.6	20.6	0.85	0.85
U23	ST10-L103	UR06	0.50	1.5	-127.90	16.52	14.07	283.59	1001.29	413.56	413.56	ACBI	20.6	20.6	0.85	0.85
U30	L103-TRA1	UL16	0.42	13.9	-87.49	-30.61	49.60	293.60	1501.66	433.77	433.77	ACBI	15.3	15.3	0.85	0.85

Table G.12: Joint can summary

JOINT	***** ORIGINAL *****				***** DESIGN *****			
	DIAMETER (CM)	THICKNESS (CM)	YLD STRS (N/MM2)	UC	DIAMETER (CM)	THICKNESS (CM)	YLD STRS (N/MM2)	UC
H200	172.720	7.620	325.000	0.704	172.720	7.620	325.000	0.704
H400	172.720	7.620	325.000	0.703	172.720	7.620	325.000	0.703
L301	172.750	7.620	325.000	0.613	172.750	7.620	325.000	0.613
L302	121.920	5.080	335.000	0.596	121.920	5.080	335.000	0.596
L101	172.750	7.620	325.000	0.580	172.750	7.620	325.000	0.580
L102	121.920	5.080	335.000	0.554	121.920	5.080	335.000	0.554
L251	172.720	6.985	325.000	0.519	172.720	6.985	325.000	0.519
L451	172.720	6.985	325.000	0.519	172.720	6.985	325.000	0.519
H300	172.720	7.620	325.000	0.423	172.720	7.620	325.000	0.423
H100	172.720	7.620	325.000	0.392	172.720	7.620	325.000	0.392
L252	119.380	4.445	335.000	0.374	119.380	4.445	345.000	0.374
L452	119.380	4.445	335.000	0.374	119.380	4.445	345.000	0.374
L103	121.920	5.080	335.000	0.271	121.920	5.080	335.000	0.271
L303	121.920	5.080	335.000	0.248	121.920	5.080	335.000	0.248
TRA3	121.920	6.350	325.000	0.191	121.920	6.350	325.000	0.191
TRA1	121.920	6.350	325.000	0.179	121.920	6.350	325.000	0.179
L453	121.920	5.715	335.000	0.160	121.920	5.715	335.000	0.160
L253	121.920	5.715	335.000	0.160	121.920	5.715	335.000	0.160

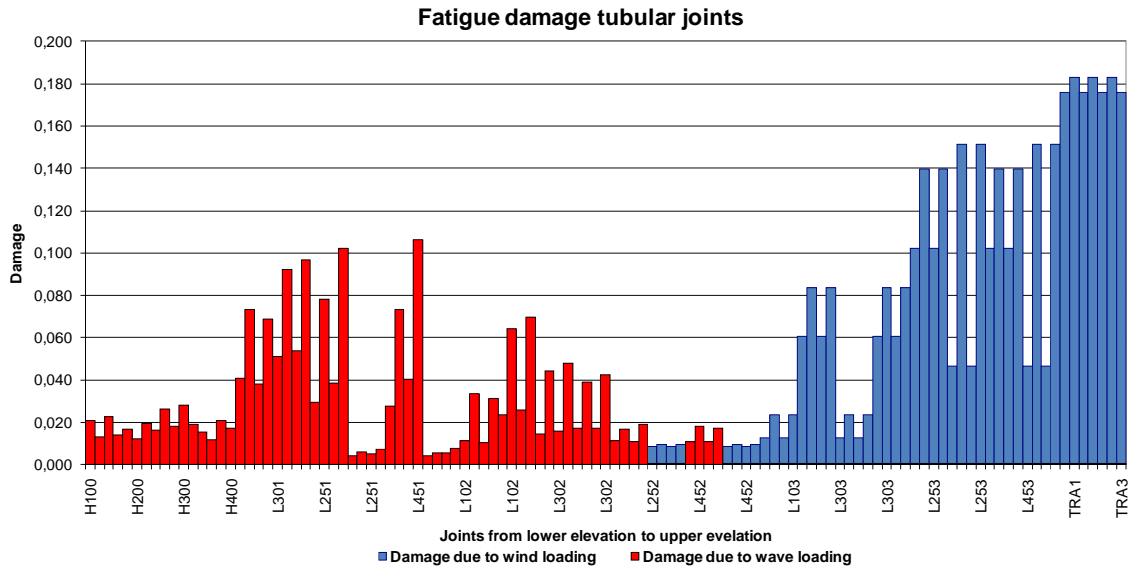


Figure G.15: Fatigue damage tubular joints due to wind and wave

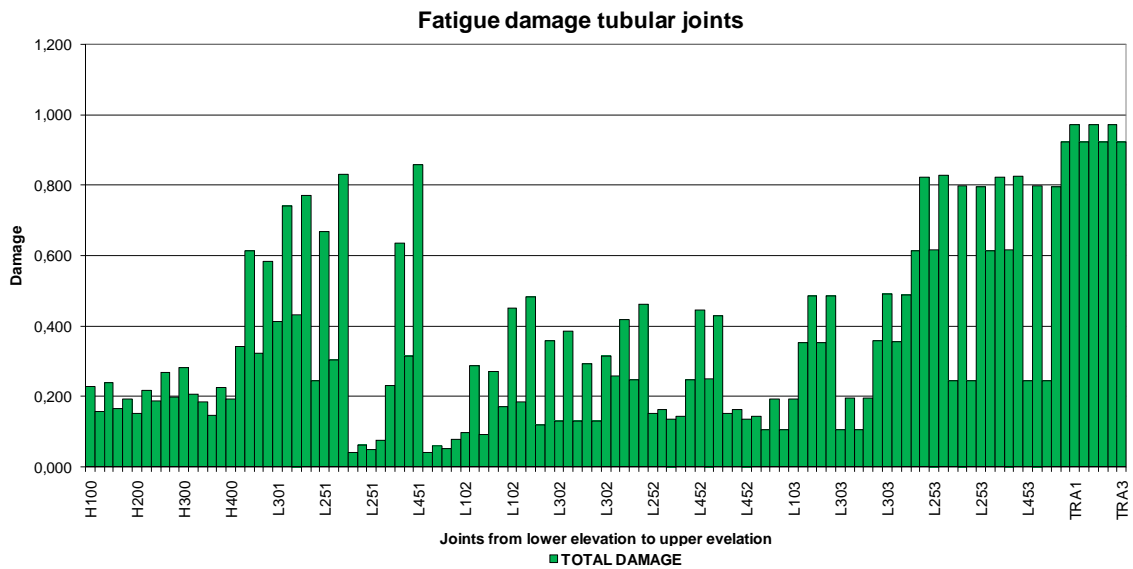


Figure G.16: Total fatigue damage tubular joints

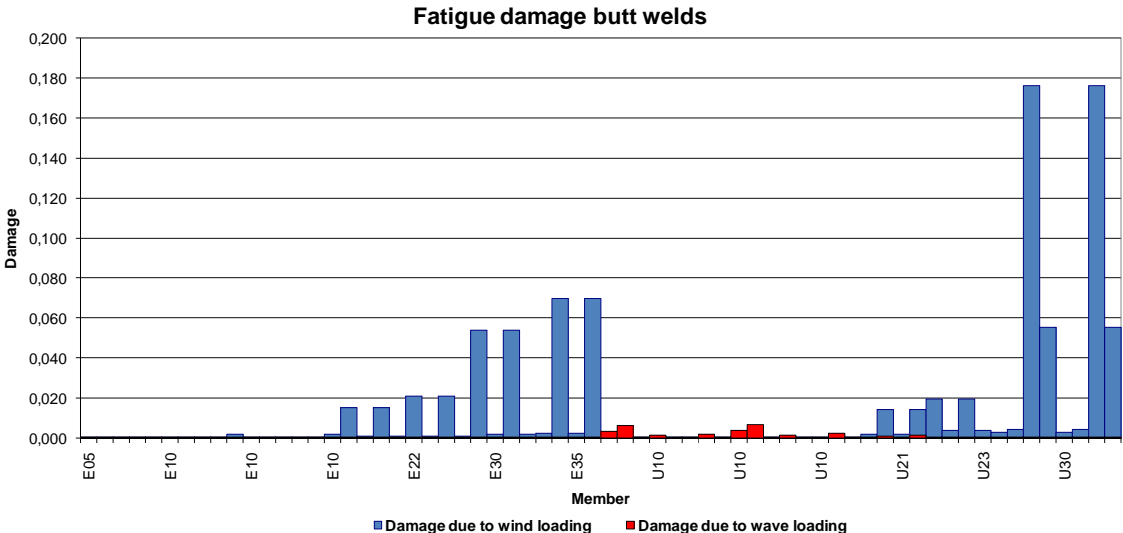


Figure G.17: Fatigue damage butt welds due to wind and wave

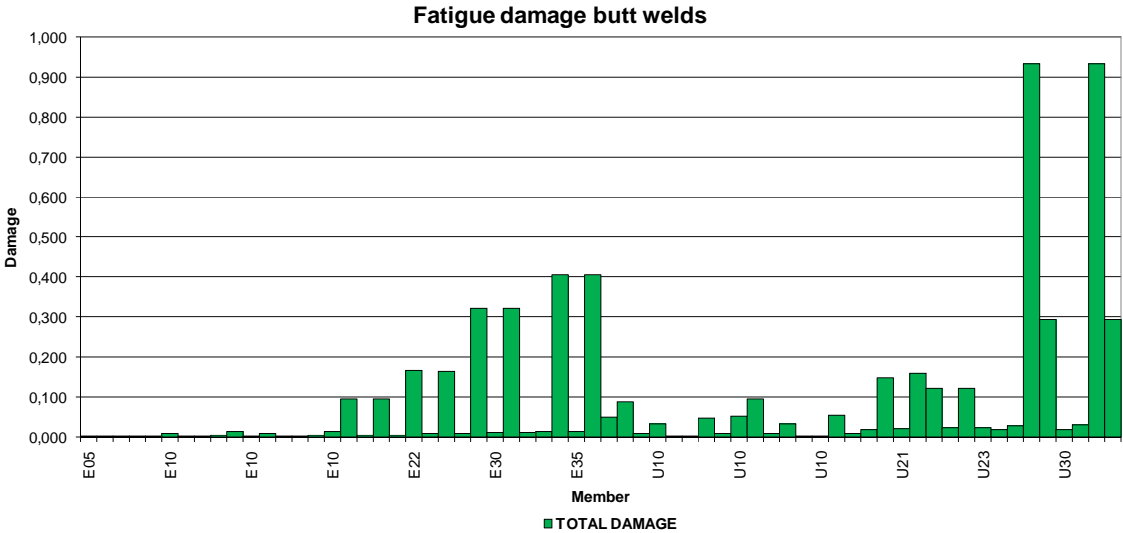


Figure G.18: Total fatigue butt welds

G.4 3-leg jacket

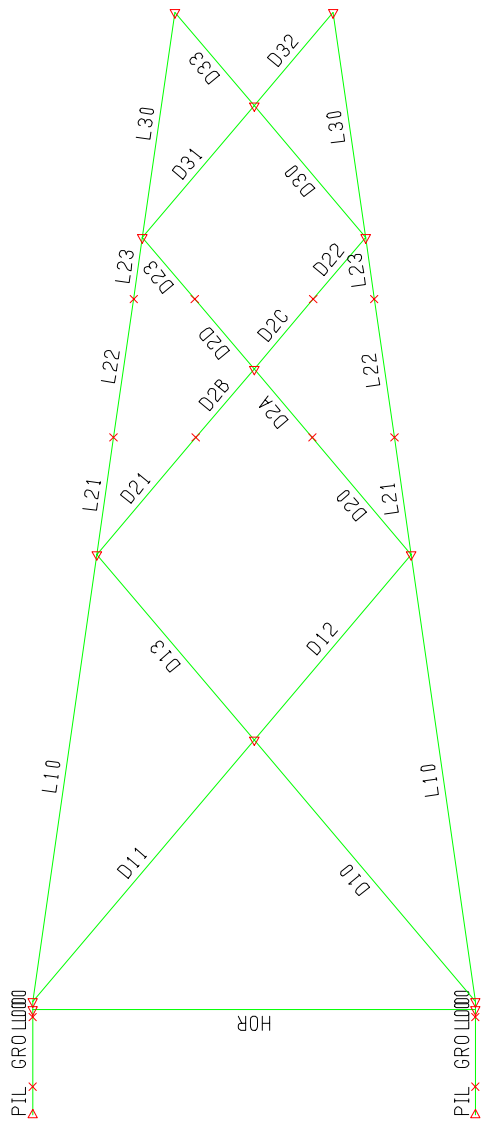


Figure G.19: Member group in jacket face

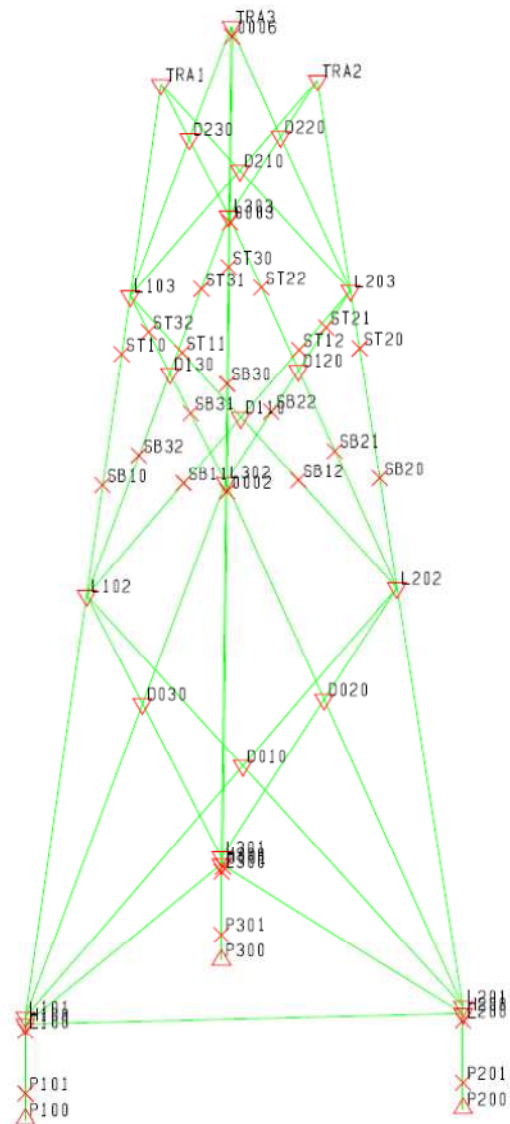


Figure G.20: Joint numbers

Table G.13: Pile maximum axial capacity summary dataset 1

PILE GRP	***** PILE *****				***** COMPRESSION *****				***** TENSION *****				
	JT	PILEHEAD O.D.	WEIGHT THK.	PEN.	CAPACITY (INCL. WT)	MAX. LOAD	CRITICAL LOAD	CONDITION LOAD SAFETY	CAPACITY (INCL. WT)	MAX. LOAD	CRITICAL LOAD	CONDITION LOAD SAFETY	*MAXIMUM* UNITY LOAD CHECK CASE
	CM	CM	KN	M	KN	KN	KN	CASE FACTOR	KN	KN	KN	CASE FACTOR	
P100 PL1	228.60	5.08	2197.4	80.0	-52687.6	-41678.3	-41678.3	R109 1.26	39025.6	30726.6	30726.6	L303 1.27	1.19 R109
P200 PL1	228.60	5.08	2197.4	80.0	-52687.6	-41543.4	-41543.4	R101 1.27	39025.6	30719.6	30719.6	L307 1.27	1.18 R101
P300 PL1	228.60	5.08	2197.4	80.0	-52687.6	-41548.0	-41548.0	L105 1.27	39025.6	30623.7	30623.7	R311 1.27	1.18 L105

Table G.14: Pile maximum axial capacity summary dataset 2

PILE GRP	***** PILE *****				***** COMPRESSION *****				***** TENSION *****				
	JT	PILEHEAD O.D.	WEIGHT THK.	PEN.	CAPACITY (INCL. WT)	MAX. LOAD	CRITICAL LOAD	CONDITION LOAD SAFETY	CAPACITY (INCL. WT)	MAX. LOAD	CRITICAL LOAD	CONDITION LOAD SAFETY	*MAXIMUM* UNITY LOAD CHECK CASE
	CM	CM	KN	M	KN	KN	KN	CASE FACTOR	KN	KN	KN	CASE FACTOR	
P100 PL1	228.60	5.08	1428.0	52.0	-78247.1	-41573.8	-41573.8	R109 1.88	40029.1	30568.9	30568.9	L303 1.31	1.15 L303
P200 PL1	228.60	5.08	1428.0	52.0	-78247.1	-41414.1	-41414.1	R101 1.89	40029.1	30547.5	30547.5	L307 1.31	1.14 L307
P300 PL1	228.60	5.08	1428.0	52.0	-78247.1	-41402.4	-41402.4	L105 1.89	40029.1	30434.3	30434.3	R311 1.32	1.14 R311

Table G.15: Member group summary

GRUP ID	CRITICAL MEMBER	LOAD COND	MAX. UNITY CHECK	DIST FROM END	* APPLIED STRESSES *			*** ALLOWABLE STRESSES ***				CRIT COND	EFFECTIVE LENGTHS		CM * VALUES *	
					AXIAL	BEND-Y	BEND-Z	AXIAL	EULER	BEND-Y	BEND-Z		KLY	KLZ	Y	Z
					N/MM2	N/MM2	N/MM2	N/MM2	N/MM2	N/MM2	N/MM2		M	M		
D10	L201-D020	R101	0.89	6.0	-141.49	-118.66	-7.39	245.69	600.74	423.17	423.17	ACBI	17.4	17.4	0.85	0.85
D11	L101-D030	L109	0.89	6.0	-139.83	-123.59	0.16	245.69	600.71	423.17	423.17	ACBI	17.4	17.4	0.85	0.85
D12	D030-L302	L307	0.85	15.4	-69.53	5.27	170.73	185.75	263.00	412.60	412.60	ACBI	12.4	26.1	0.85	0.85
D13	D020-L302	R303	0.86	15.4	-68.27	5.89	-177.74	186.61	265.14	412.60	412.60	ACBI	12.4	26.1	0.85	0.85
D20	L202-SB21	R103	0.87	0.0	-53.39	31.11	-250.46	199.31	301.32	432.57	432.57	ACBI	12.4	18.5	0.85	0.85
D21	L102-SB32	L107	0.85	0.0	-53.67	28.27	240.59	199.31	301.32	432.57	432.57	ACBI	12.4	18.5	0.85	0.85
D22	ST21-L203	L303	0.75	5.1	-53.75	41.57	199.63	199.31	301.32	432.57	432.57	ACBI	8.8	18.5	0.85	0.85
D23	ST32-L103	R307	0.79	5.1	-52.65	46.45	-215.16	199.31	301.32	432.57	432.57	ACBI	8.8	18.5	0.85	0.85
D2A	SB31-D130	R107	0.85	2.1	-80.15	-25.76	154.25	198.13	297.56	410.18	410.18	ACBI	12.4	18.5	0.85	0.85
D2B	SB22-D120	L103	0.82	2.9	-81.94	-23.19	-136.35	193.44	283.44	410.18	410.18	ACBI	12.4	18.5	0.85	0.85
D2C	D120-ST21	L103	0.77	0.0	-78.77	-50.63	-119.58	193.44	283.44	410.18	410.18	ACBI	8.8	18.5	0.85	0.85
D2D	D130-ST32	R107	0.72	1.5	-77.11	-43.28	114.62	197.92	296.87	410.18	410.18	ACBI	8.8	18.5	0.85	0.85
D30	L203-D220	R307	0.35	9.5	-73.09	-43.27	-16.20	281.901567	330.438	330.438	330.438	ACBI	8.8	8.8	0.85	0.85
D31	L103-D230	L303	0.37	11.0	-70.33	-49.10	20.17	274.301551	330.438	330.438	330.438	ACBI	8.8	8.8	0.85	0.85
D32	D210-TRA1	L209	0.32	7.8	-42.70	73.37	13.51	292.373000	330.438	330.438	330.438	ACBI	6.2	6.2	0.85	0.85
D33	D220-TRA3	R205	0.31	7.8	-43.72	74.30	-14.57	300.853010	330.438	330.438	330.438	ACBI	6.2	6.2	0.85	0.85
GR0	P201-L200	R101	0.42	4.4	-50.19	10.92	-99.65	292.37*****	408.28	408.28	408.28	ACBI	4.4	4.4	0.85	0.85
H0R	H200-H300	L108	0.89	28.0	-55.83	-153.82	31.98	129.01	169.14	439.58	439.58	ACBI	28.0	28.0	0.85	0.85
L00	H200-L201	R101	0.87	0.5	-91.83	24.01	-219.83	275.42*****	412.63	412.63	412.63	ACBI	0.5	0.5	0.85	0.85
L10	L201-L202	R101	0.83	3.0	-84.13	-225.03	-24.10	254.66	904.29	420.88	420.88	ACBI	28.8	28.8	0.85	0.85
L21	L202-SB20	R101	0.86	6.0	-95.81	67.05	9.13	267.411603	327.410	410.46	410.46	LOBU	20.4	20.4	0.85	0.85
L22	SB20-ST20	R001	0.80	0.0	-164.13	76.07	9.72	267.631133	350.401	401.80	401.80	ACBI	20.4	20.4	0.85	0.85
L23	ST20-L203	R001	0.48	2.0	-115.41	-15.69	-13.15	264.051332	310.416	416.98	416.98	ACBI	20.4	20.4	0.85	0.85
L30	L203-TRA2	R101	0.53	13.0	-118.84	5.08	42.97	272.522323	060.416	416.98	416.98	ACBI	14.5	14.5	0.85	0.85

Table G.16: Joint Can summary

JOINT	***** ORIGINAL *****				***** DESIGN *****			
	DIAMETER (CM)	THICKNESS (CM)	YLD STRS (N/MM2)	UC	DIAMETER (CM)	THICKNESS (CM)	YLD STRS (N/MM2)	UC
D030	86.360	4.445	335.000	0.965	86.360	4.445	335.000	0.965
H200	177.800	8.255	325.000	0.911	177.800	8.255	325.000	0.911
D020	86.360	4.445	335.000	0.871	86.360	4.445	335.000	0.871
H100	177.800	8.255	325.000	0.864	177.800	8.255	325.000	0.864
D010	86.360	4.445	335.000	0.839	86.360	4.445	335.000	0.839
H300	177.800	8.255	325.000	0.733	177.800	8.255	325.000	0.733
D120	63.500	3.175	345.000	0.732	63.500	3.175	345.000	0.732
D130	63.500	3.175	345.000	0.706	63.500	3.175	345.000	0.706
D110	63.500	3.175	345.000	0.682	63.500	3.175	345.000	0.682
L201	177.800	7.620	325.000	0.579	177.800	7.620	325.000	0.579
D230	71.120	3.493	345.000	0.571	71.120	3.493	345.000	0.571
L302	177.800	6.985	325.000	0.562	177.800	6.985	325.000	0.562
D210	71.120	3.493	345.000	0.543	71.120	3.493	345.000	0.543
L101	177.800	7.620	325.000	0.533	177.800	7.620	325.000	0.533
L202	177.800	6.985	325.000	0.527	177.800	6.985	325.000	0.527
L102	177.800	6.985	325.000	0.517	177.800	6.985	325.000	0.517
D220	71.120	3.493	345.000	0.488	71.120	3.493	345.000	0.488
L301	177.800	7.620	325.000	0.428	177.800	7.620	325.000	0.428
L103	142.240	6.350	325.000	0.392	142.240	6.350	325.000	0.392
L303	142.240	6.350	325.000	0.378	142.240	6.350	325.000	0.378
L203	142.240	6.350	325.000	0.377	142.240	6.350	325.000	0.377
TRA3	142.340	6.985	325.000	0.183	142.340	6.985	325.000	0.183
TRA1	142.340	6.985	325.000	0.178	142.340	6.985	325.000	0.178
TRA2	142.340	6.985	325.000	0.176	142.340	6.985	325.000	0.176

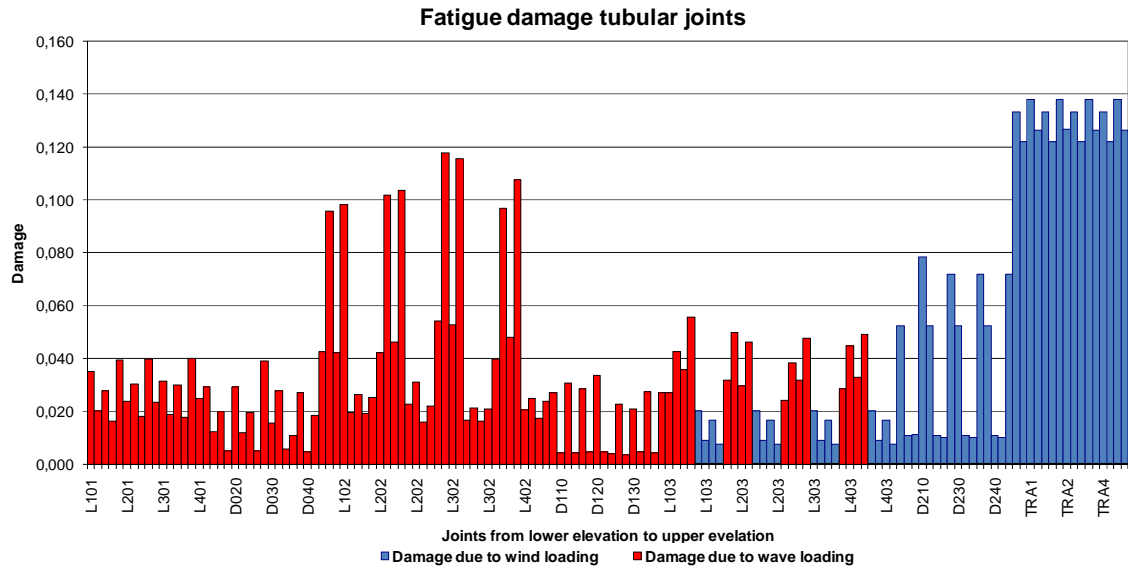


Figure G.21: Fatigue damage tubular joints due to wind and wave

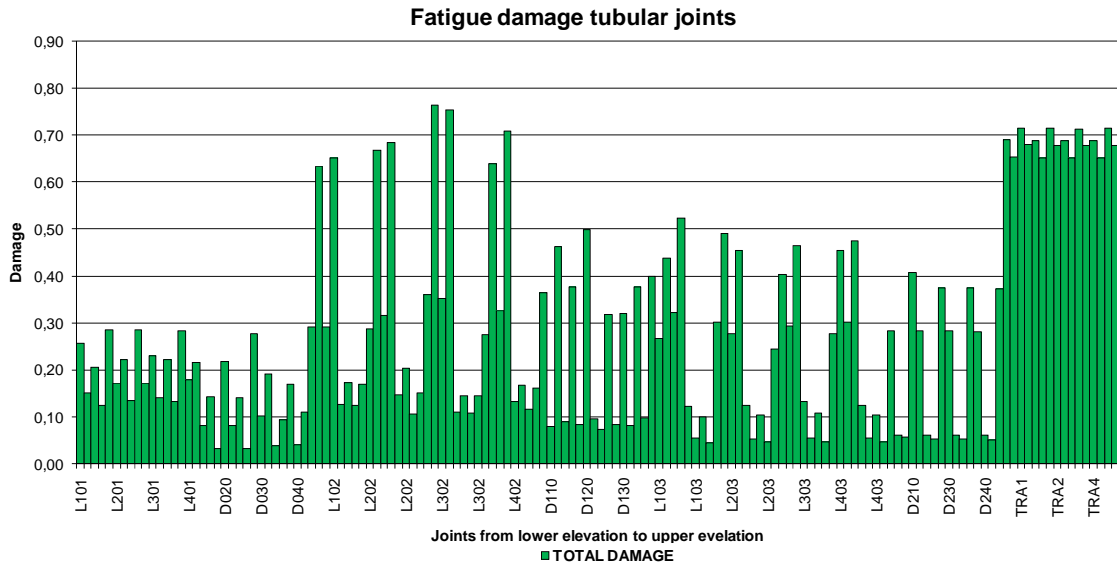


Figure G.22: Total fatigue damage tubular joints

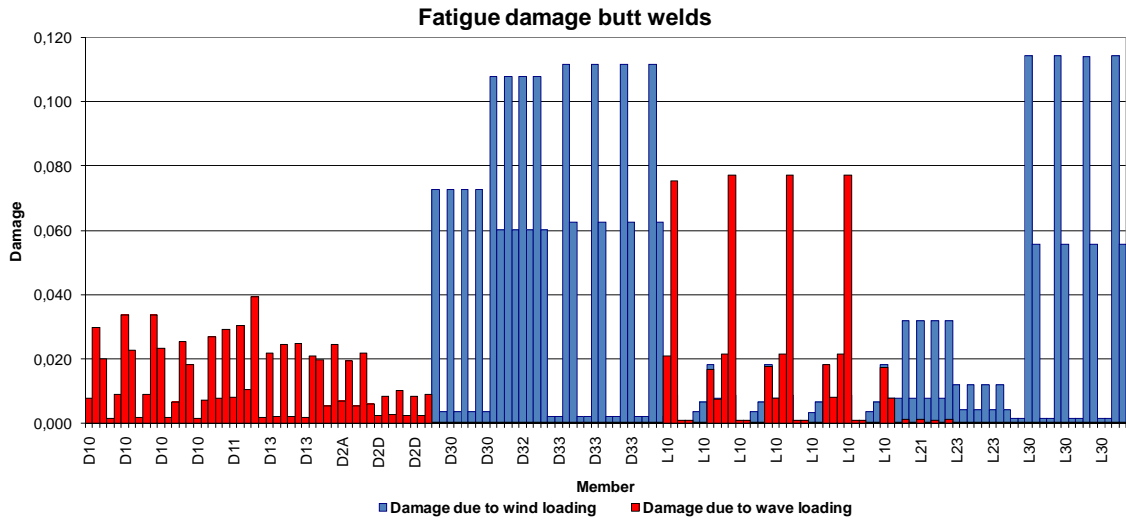


Figure G.23: Fatigue damage butt welds due to wind and wave

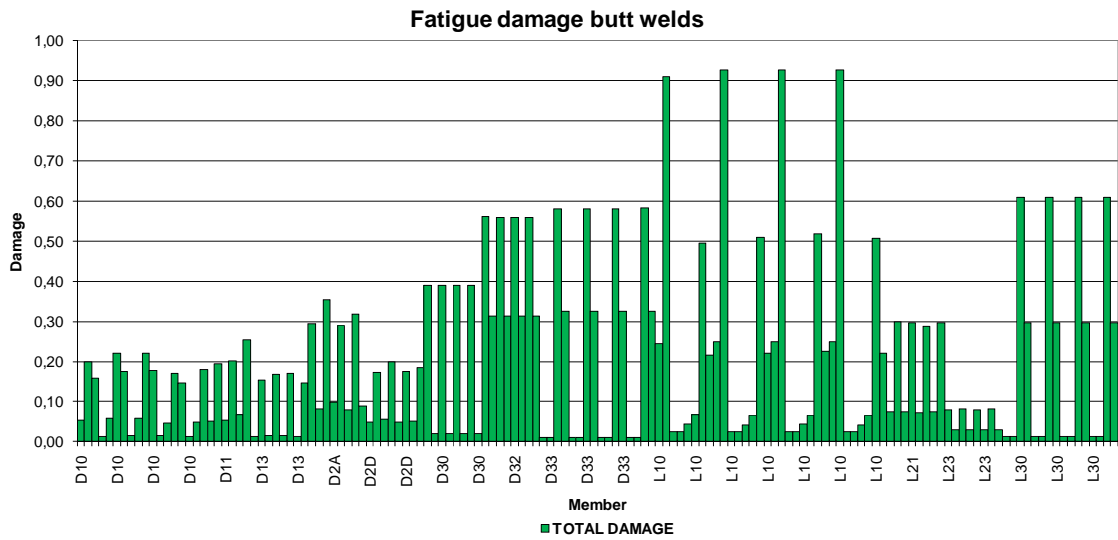


Figure G.24: Total fatigue damage butt welds

Appendix H Grout Connection Check

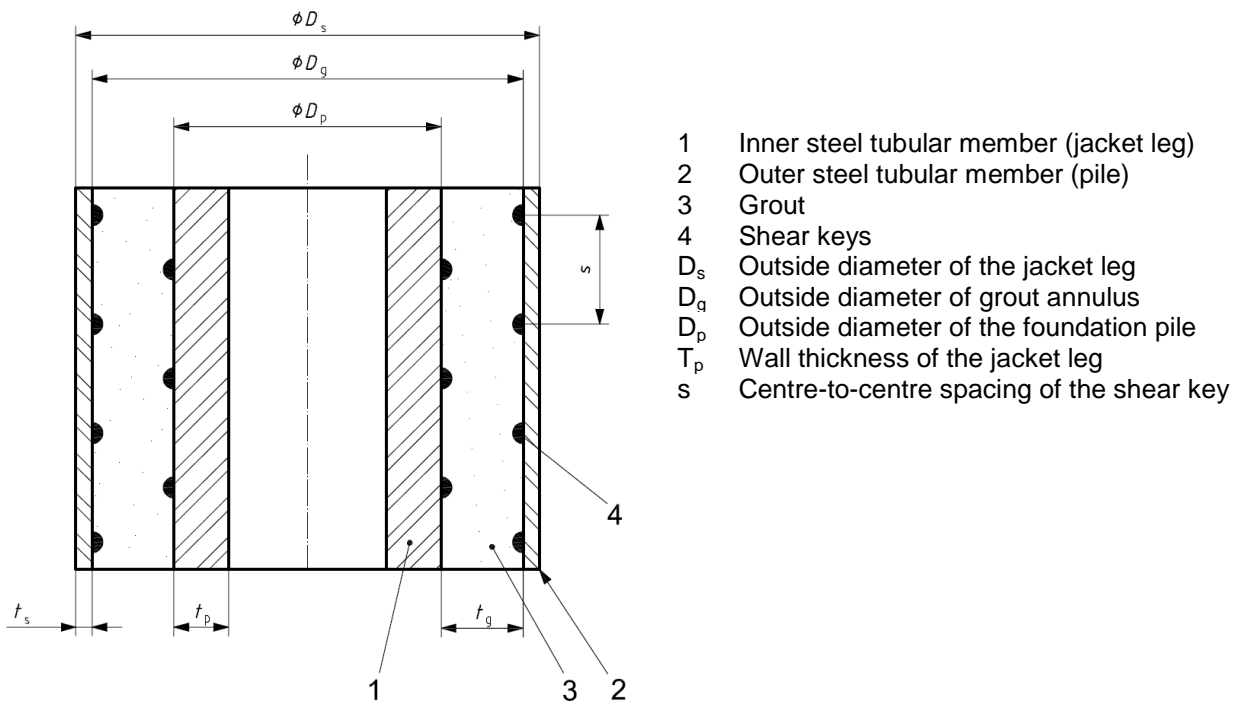


Figure H.1: Grout connection

The component of the interface transfer stress at the inner steel tubular member due to axial force is defined by the equation

$$\sigma_a = \frac{P}{\pi D_p L_e} \quad (H.1)$$

P = axial force on the grouted connection

L_e = effective grouted connection length

$$L_e = L - \max(s; 2t_g) \quad (H.2)$$

The design interface transfer strength f_d for cement-water grouts shall be calculated from the lesser of the representative interface strengths for sliding at grout-steel interface, $f_{g,sliding}$, and the representative interface transfer strength for grout failure, $f_{g, shear}$.

$$f_d = \frac{f_g}{\gamma_{R,g}} \quad (H.3)$$

f_g = representative interface transfer strength and is the lesser of $f_{g,sliding}$ and $f_{g, shear}$.

$\gamma_{R,g}$ = partial resistance factor for interface transfer strength = 2.0

$$f_{g,sliding} = C_p \left[2 + 140 \left(\frac{h}{s} \right)^{0.8} \right] K^{0.6} f_{cu}^{0.3} \quad (H.4)$$

$$f_{g,shear} = \left[0.75 - 1.4 \left(\frac{h}{s} \right) \right] f_{cu}^{0.5} \quad (H.5)$$

- C_p = scale factor for the diameter of the inner steel member (jacket leg) = 1.0
 s = shear key spacing
 h = shear key height
 f_{cu} = unconfined cube strength of the grout = 50 MPa
 K = radial stiffness factor of the grouted connection

$$K = \left[\left(\frac{D_p}{t_p} \right) + \left(\frac{D_s}{t_s} \right) \right]^{-1} + \frac{1}{m} \left(\frac{D_g}{t_g} \right)^{-1} \quad (H.6)$$

- m = ratio of elastic modulus of steel and grout = E_s/E_g , taken as 18

GROUT CONNECTION CHECK

NOTE : Geometries with D/t below the lower bound may conservatively be designed using the lower bound D/t values in the calculations. Not valid for Helical shear keys

SACS showed that the torsional moments are negligible small and therefore not included in this calculation

$F_{op} := 41 \cdot \text{MN}$	Max. axial load		
$D_p := 1778.0 \cdot \text{mm}$	Leg diameter	$t_p := 76.20 \cdot \text{mm}$	Leg thickness
$D_s := 2286.0 \cdot \text{mm}$	Pile diameter	$t_s := 50.8 \cdot \text{mm}$	Pile thickness
$h := 8 \cdot \text{mm}$	Shear key height	$w := 16 \cdot \text{mm}$	Shear key width
$L := 4400 \cdot \text{mm}$	Nominal grouted connection length		
$s := 200 \cdot \text{mm}$	Shear key spacing		
$f_{cu} := 50$	Characteristic cube strength [MPa]		
$\epsilon_g := 0.00\%$	relative axial movement during during grout setting		
$m := 18$			

Calculations:

$D_g := D_s - 2 \cdot t_s$	Outside diameter of grout annulus	$D_g = 2184.4 \cdot \text{mm}$
$t_g := \frac{(D_g - D_p)}{2}$	Thickness of grout annulus	$t_g = 203.2 \cdot \text{mm}$
$L_{red} := \max(2 \cdot t_g, s)$	non-structural length of grouting	$L_{red} = 0.406 \text{ m}$
$L_e := L - L_{red}$		$L_e = 3.994 \text{ m}$
$\sigma_{op} := \frac{F_{op}}{\pi \cdot D_p \cdot L_e}$	Design interface transfer stress operational condition	$\sigma_{op} = 1.838 \cdot \text{MPa}$

$$K := \left[\left(\frac{D_g}{t_g} \right)^{-1} \cdot \frac{1}{m} + \left(\frac{D_p}{t_p} + \frac{D_s}{t_s} \right)^{-1} \right]^{-1} \quad \text{Stiffness factor} \quad K = 0.02$$

$$C_p := \begin{cases} \left(\frac{D_p}{1000\text{mm}} \right)^2 - \left(\frac{D_p}{500\text{mm}} \right) + 2 & \text{if } D_p \leq 1000\text{mm} \\ 1.0 & \text{if } D_p > 1000\text{mm} \end{cases} \quad C_p = 1$$

$$f_{g\text{sliding}} := C_p \cdot \left[2 + 140 \left(\frac{h}{s} \right)^{0.8} \right] K^{0.6} \cdot f_{cu}^{0.3}$$

$$f_{g\text{shear}} := \left[0.75 - 1.4 \left(\frac{h}{s} \right) \right] \cdot f_{cu}^{0.5}$$

$$f_g := \min(f_{g\text{sliding}}, f_{g\text{shear}}) \quad \varepsilon_g = 0 \quad f_g = 3.892$$

$$k_{\text{red}} := \begin{cases} 1.0 & \text{if } \varepsilon_g < 0.035\% \\ \left[1.0 - 0.1 \left(\frac{h}{s} \right) \cdot f_{cu} \right] & \text{if } \left[(0.035\% < \varepsilon_g < 0.35\%) \wedge \left(\frac{h}{s} \leq 0.06 \right) \right] \\ 0 & \text{otherwise} \end{cases} \quad k_{\text{red}} = 1$$

$$\gamma_{Rg} := 2$$

$$f_d := f_g \cdot \frac{k_{\text{red}}}{\gamma_{Rg}} \cdot \text{MPa} = 1.946 \times 10^6 \text{ Pa}$$

$$UC_{\text{op}} := \frac{\sigma_{\text{op}}}{f_d} \quad \boxed{UC_{\text{op}} = 0.94}$$

$$\text{chk} := 0$$

$$\text{chk} := \text{if}(t_g \geq 40\text{mm}, \text{chk} + 1, 0)$$

$$\text{chk} = 0$$

$$\text{chk} := \text{if}\left(1.5 \leq \frac{w}{h} \leq 3, \text{chk} + 1, 0\right)$$

$$\text{chk} = 1$$

$$\text{chk} := \text{if}\left(0.0 \leq \frac{h}{s} \leq 0.10, \text{chk} + 1, 0\right)$$

$$\text{chk} = 2$$

$\text{chk} := \text{if} \left(20 \leq \frac{D_p}{t_p} \leq 40, \text{chk} + 1, 0 \right)$	$\text{chk} = 3$
$\text{chk} := \text{if} \left(10 \leq \frac{D_g}{t_g} \leq 45, \text{chk} + 1, 0 \right)$	$\text{chk} = 4$
$\text{chk} := \text{if} \left(1 \leq \frac{L_e}{D_p} \leq 10, \text{chk} + 1, 0 \right)$	$\text{chk} = 5$
$\text{chk} := \text{if} \left(0.0 \leq \frac{h}{D_p} \leq 0.012, \text{chk} + 1, 0 \right)$	$\text{chk} = 6$
$\text{chk} := \text{if} \left(0 \leq \frac{D_p}{s} \leq 16, \text{chk} + 1, 0 \right)$	$\text{chk} = 7$
$\text{chk} := \text{if} \left(30 \leq \frac{D_s}{t_s} \leq 140, \text{chk} + 1, 0 \right)$	$\text{chk} = 8$
$\text{chk} := \text{if} (C_p \leq 1.5, \text{chk} + 1, 0)$	$\text{chk} = 9$
$\text{chk} := \text{if} (K \leq 0.020, \text{chk} + 1, 0)$	$\text{chk} = 10$
$\text{chk} := \text{if} (UC_{op} \leq 1.0, \text{chk} + 1, 0)$	$\text{chk} = 11$
$\text{CONNECTION} := \text{if} (\text{chk} = 12, \text{"OK"} , \text{"FALSE"})$	$\text{chk} = 12$

$\text{CONNECTION} = \text{"OK"}$

Appendix I Drawing Definitive Designs

1 2 3 4 5 6 7 8

A

A

B

B

C

C

D

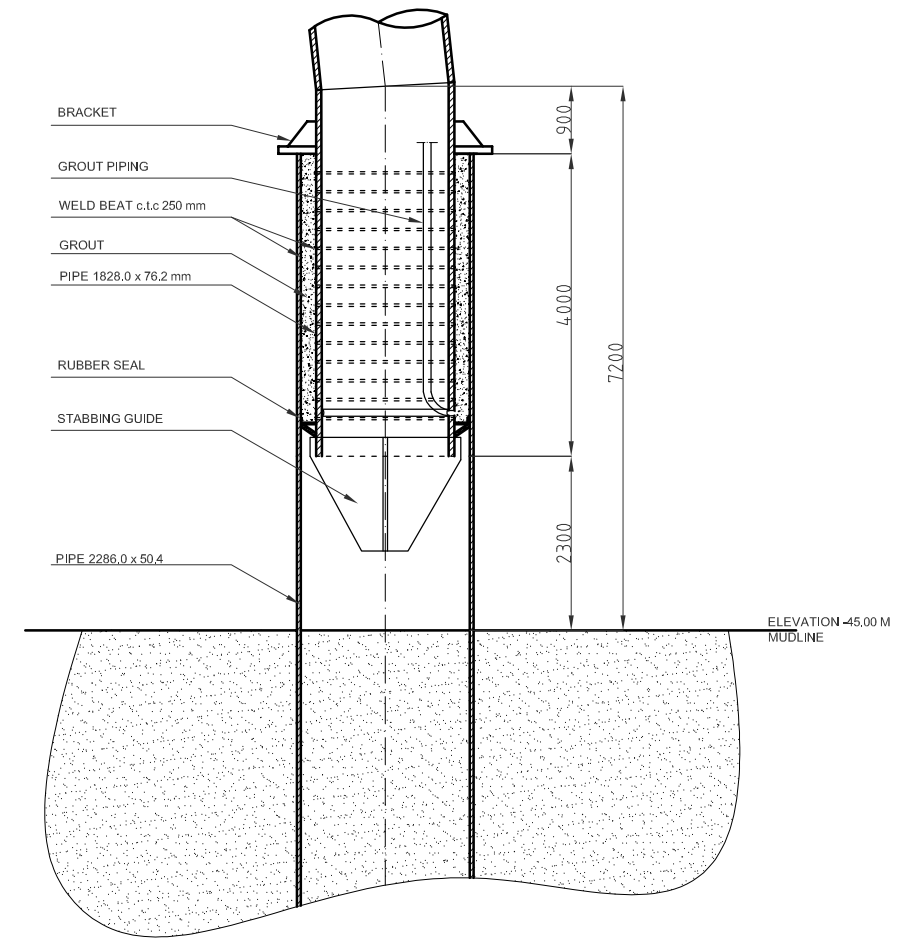
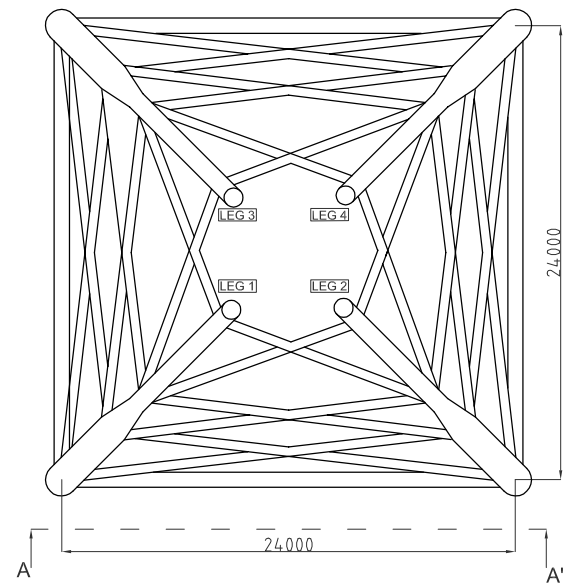
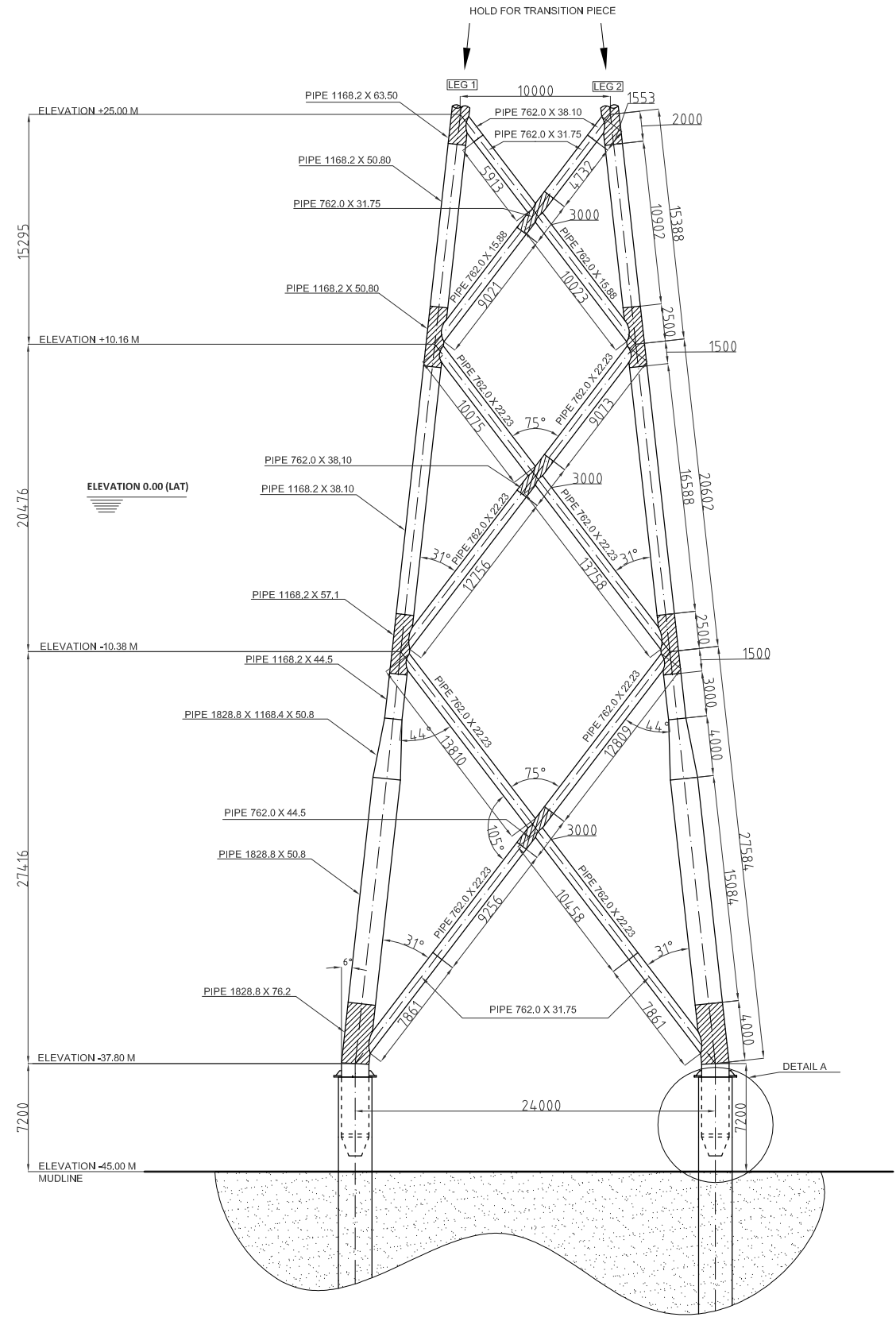
D

E

E

F

F



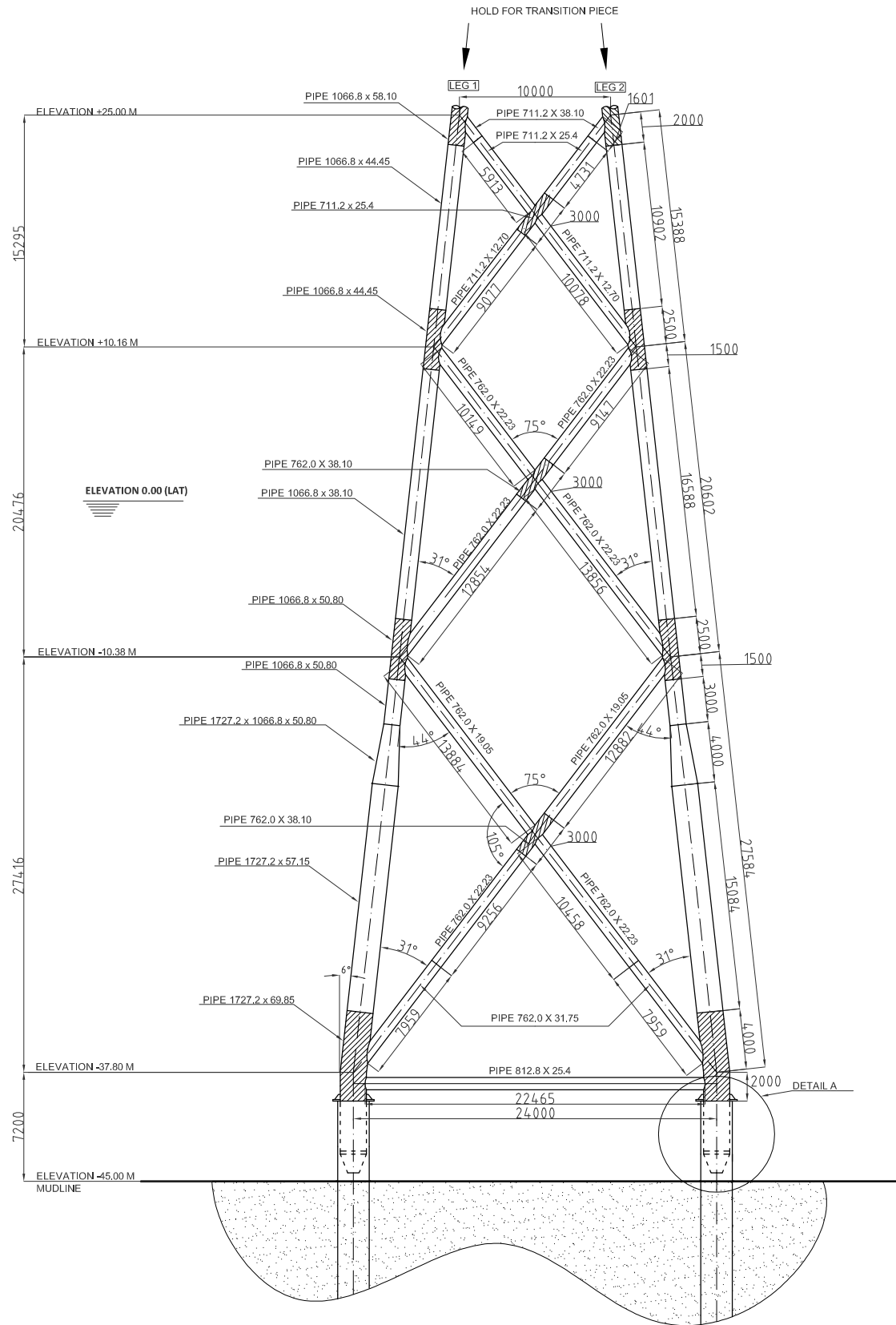
-material type 1 (S355G15)
 -material type 2 (S355G15-through thickness)
 material type 2

Designed by Frank van Gerven	Dimension mm	Date 21/07/2011	Scale 1:400
---------------------------------	-----------------	--------------------	----------------

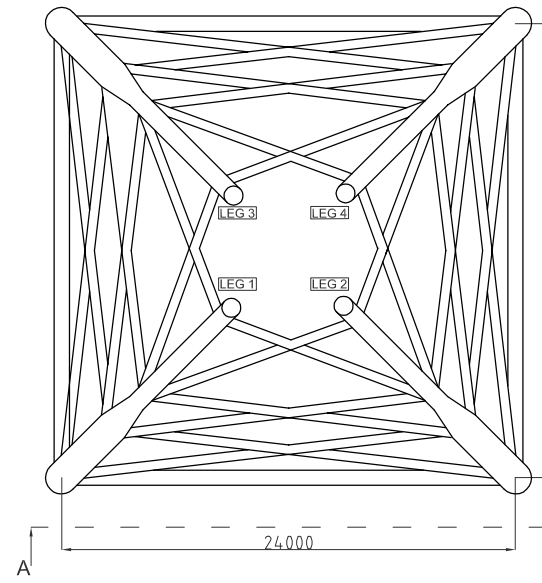
4-leg jacket (reference design)

Optimizing the design of a steel substructure for offshore wind turbines in deeper waters	I01	Edition x	Sheet 1/1
---	-----	--------------	--------------

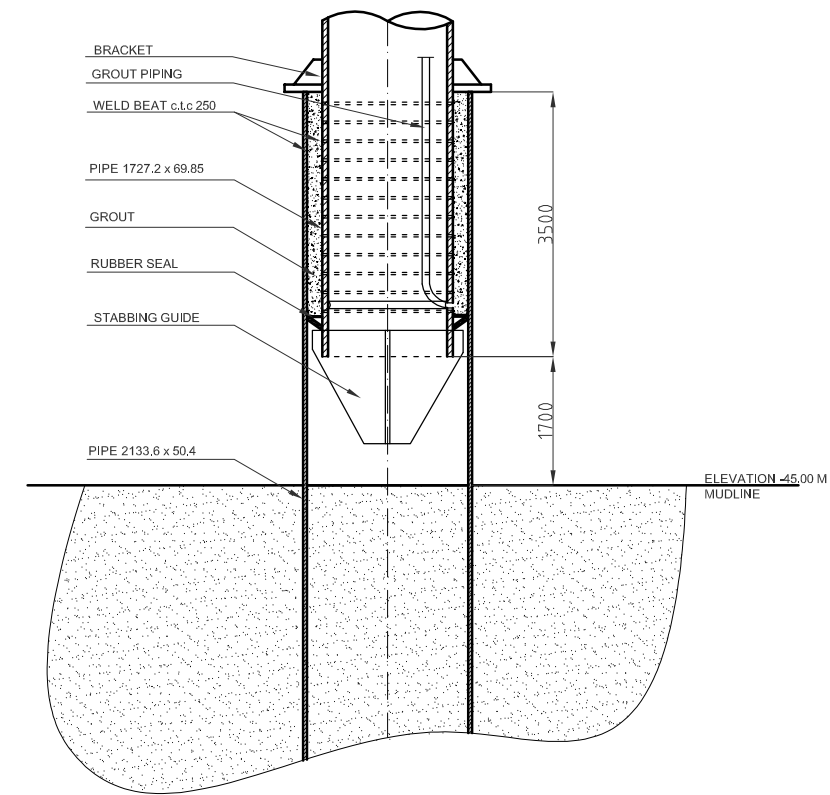
1 2 3 4 5 6 7 8



VIEW VERTICAL PLANE (A-A')



TOP VIEW



DETAIL A

1:100

- material type 1 (S355G15)
- material type 2 (S355G15-through thickness)
- material type 2

Designed by
Frank van Gerven

Dimension
mm

Date
21/07/2011

Scale
1:400

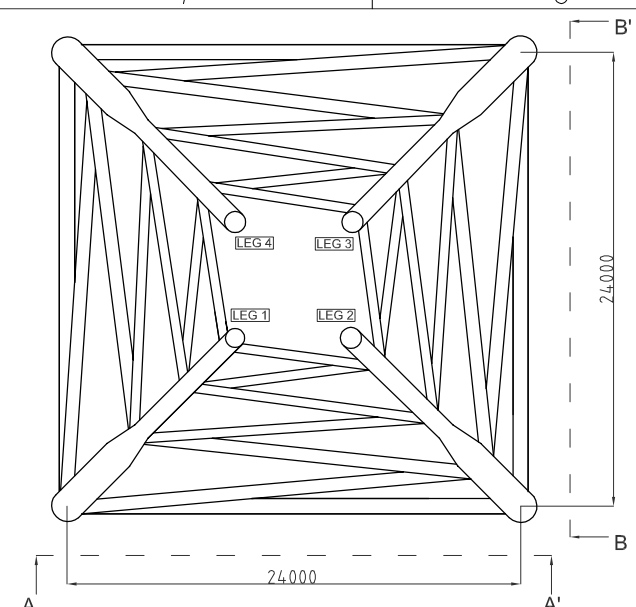
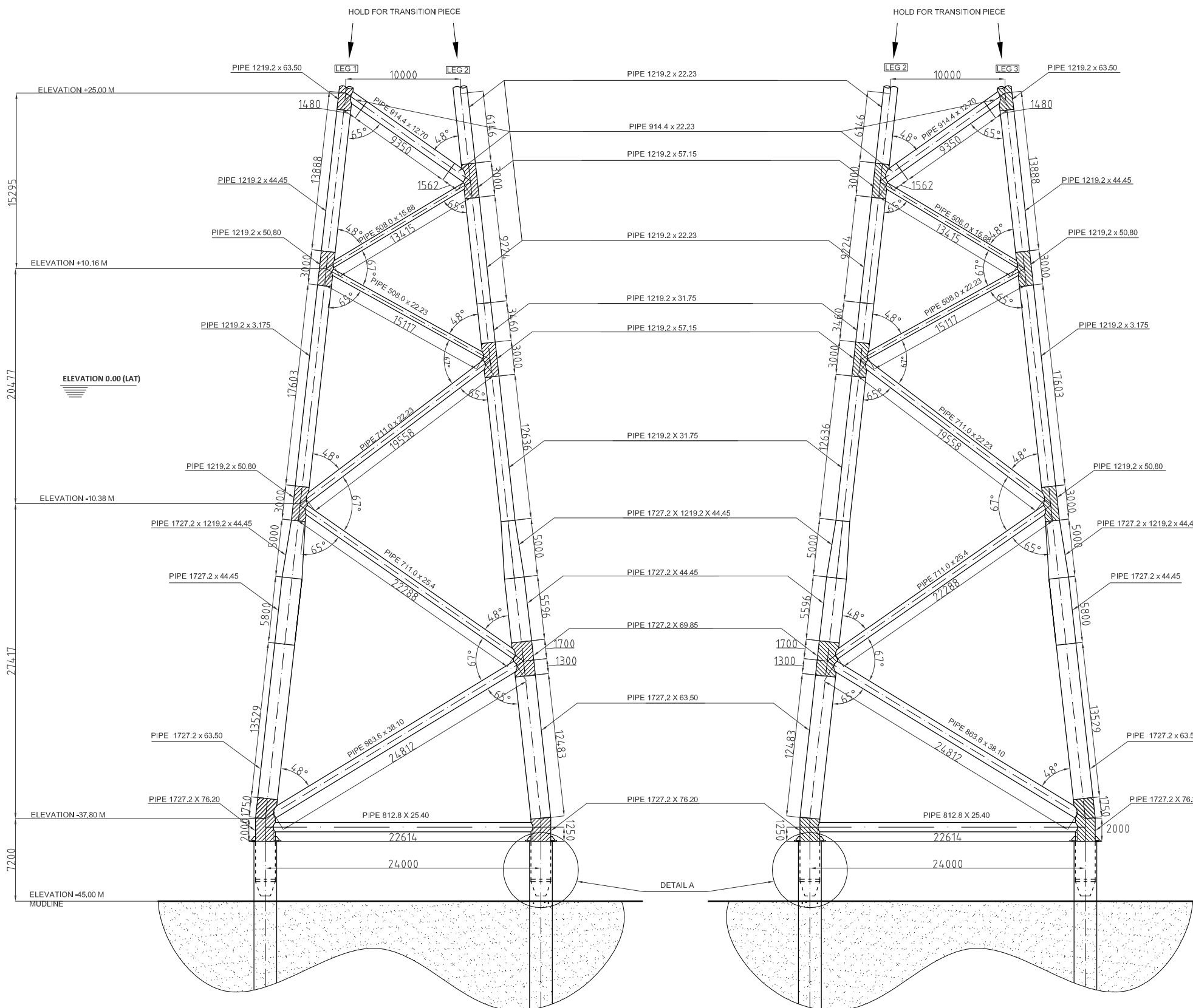
4-leg jacket optimized

Optimizing the design of a steel substructure for offshore wind turbines in deeper waters

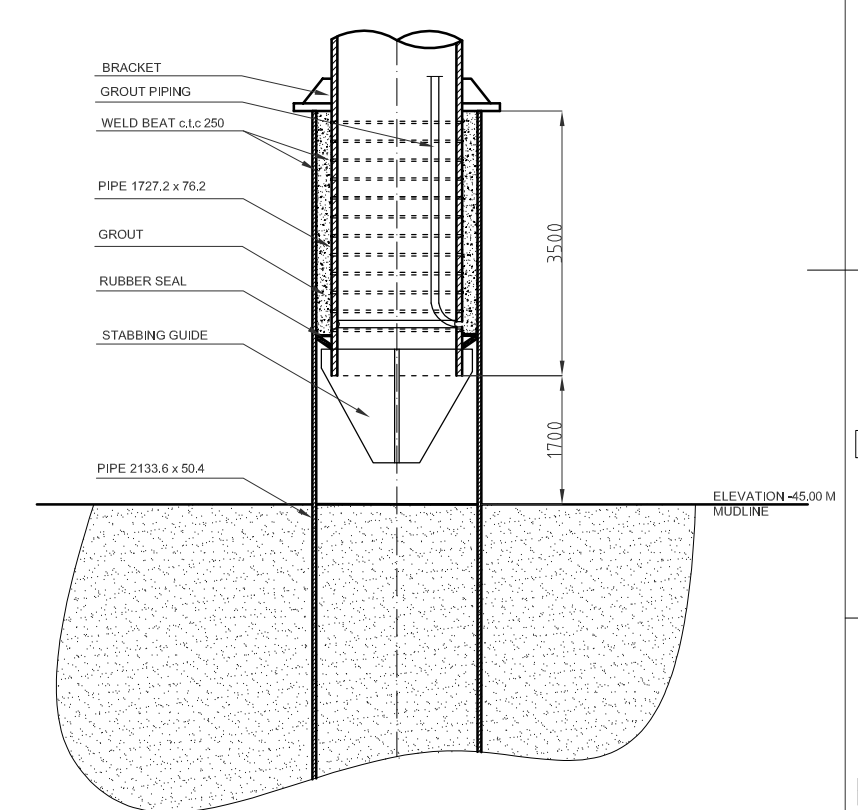
102

Edition
x

Sheet
1/1



TOP VIEW



DETAIL A
1:100

-material type 1 (S355G15)
 -material type 2 (S355G15-through thickness)
 material type 2

Designed by Frank van Gerven	Dimension mm	Date 21/07/2011	Scale 1:400
---------------------------------	-----------------	--------------------	----------------

4-leg jacket K-braces

Optimizing the design of a steel substructure for offshore wind turbines in deeper waters	I03	Edition x	Sheet 1/1
---	-----	--------------	--------------

Appendix J Fabrication Cost Estimation

		Reference Design				4-leg optimized			
Jacket	Weight (kg)	711,281	Material	€ 971,059	688,218	Material	€ 959,211		
			Anodes	€ 196,174		Anodes	€ 193,780		
	Benchworks (hr)	2,311	Beveling	€ 512,601	1,993	Beveling	€ 557,631		
	Welding time (hr)	2,534	Loan	€ 368,501	1,611	Loan	€ 357,854		
	Internal transport (hr)	1,735	Welding Investigation	€ 6,634	1,583	Welding investigation	€ 7,146		
	Subtotal manufacture	6,386		€ 2,054,970		5,187	€ 2,075,623		
		Office	€ 178,660		Office	€ 172,640			
		Scaffolding	€ 150,903		Scaffolding	€ 149,062			
		Engineering	€ 52,816		Engineering	€ 52,172			
		Preservation	€ 66,599		Preservation	€ 66,599			
		Load Out*	€ 61,783		Load Out*	€ 55,833			
		Transport	€ 37,726		Transport	€ 37,265			
Total			€ 2,603,456			€ 2,609,193			
Piles	Weight (kg)	570,193	Material	€ 1,026,347	488,858	Material	€ 935,874		
			Engineering	€ 39,913		Engineering	€ 36,395		
Total			€ 1,066,260			€ 972,269			
Transition Piece	Weight (kg)	125,000	Material	€ 431,314	125,000	Material	€ 437,603		
Total			€ 431,314			€ 437,603			
			€ 4,101,030			€ 4,019,065			

* Including piles

		4-Leg K-braces				3-Leg			
Jacket	Weight (kg)	688,218	Material	€ 885,736	740,758	Material	€ 971,348		
			Anodes	€ 178,937		Anodes	€ 196,232		
	Benchworks (hr)	1,993	Beveling	€ 447,375	3,091	Beveling	€ 497,619		
	Welding time (hr)	1,611	Loan	€ 290,500	2,059	Loan	€ 385,652		
	Internal transport (hr)	1,583	Welding investigation	€ 3,966	1,736	Welding investigation	€ 5,128		
	Subtotal manufacture	5,187		€ 1,806,514		6,887	€ 2,055,979		
		Office	€ 162,490		Office	€ 175,380			
		Scaffolding	€ 137,644		Scaffolding	€ 150,948			
		Engineering	€ 48,175		Engineering	€ 52,832			
		Preservation	€ 68,822		Painting	€ 73,234			
		Load Out*	€ 52,607		Load Out*	€ 51,078			
		Transport	€ 34,411		Transport	€ 37,737			
Total			€ 2,310,662			€ 2,597,187			
Piles	Weight (kg)	488,858	Material	€ 879,945	480,996	Material	€ 865,792		
			Engineering	€ 34,220		Engineering	€ 33,670		
Total			€ 914,165			€ 899,462			
Transition Piece	Weight (kg)	125,000	Material	€ 419,682	125,000	Material	€ 430,147		
Total			€ 425,898			€ 430,147			
			€ 3,650,725			€ 3,926,796			

* Including piles

Appendix K Installation equipment

Jack-Up barge

Besides the crane capacities especially the operating water depth is critical. Because of the big market potential a number of new jack-up barges are developed or being build. The following table shows qualified jack-up barges.

Table K.1: Jack-Up barges

Fleet	Name	Year in service	Operating water depth [m]	Crane Capacity	
				SWL [t]	Radius [m]
A2SEA	SEA INSTALLER	2012	45	900	24
Beluga-Hochtief	Unknown	2012	50	1,500	32
Workfox	Seafox 7	2012	65	1,200	25
MPI	Adventure	2011	40	1,000	25
	Discovery	2011	40	1,000	25
RWE innogy	Unknown (2x)	2011	45	800	25
Jack-up Barge	JB-117	2011	45	1,000	22

Crane vessels

The following overview is a list of possible crane vessels that fulfil the requirements. Some ships are purpose built crane vessels; other ships are combination ships which have the ability to install the substructures.

Table K.2: Crane vessels

Fleet	Name	Crane Capacity	
		SWL [t]	Radius [m]
Jumbo	J1800 class	1,800	28
Seaway heavy lifting	Olev Strashnov	5,000	32
	Stanislav Yudin	2,500	78.3
ADSA	Oceanic 5000	4,400	unknown
Acergy	Borealis	4,500	34
Mc Dermott	DB-50	2,500	boom length 78.3 m *
	DB-27	1,270	boom length 71.6 m *
Saipem	Saipem 3000	2,200	39.6

*relevant radius is not known

